UNIVERSITEIT VAN PRETORIA
UNIVERSITY OF PRETORIA
YUNIBESITHI YA PRETORIA

Proteases and protease inhibitors involved in plant stress response and acclimation

by

Anneke Prins

Submitted in partial fulfilment of the requirements for the degree

Philosophiae Doctor

in the Faculty of Natural and Agricultural Sciences

University of Pretoria

Pretoria

March 2008

Supervisors:

Prof. K.J. Kunert

Prof. C.H. Foyer

The financial assistance of the National Research Foundation (NRF) towards this research is hereby acknowledged. Opinions expressed and conclusions arrived at are those of the author and are not necessarily to be attributed to the NRF.

Declaration

I, the undersigned, hereby declare that the thesis submitted herewith for the degree Philosophiae Doctor to the University of Pretoria, contains my own independent work and has not been submitted for any degree at any other university.

Anneke Prins

March 2008

Acknowledgements

I owe a debt of gratitude to my two supervisors, Prof. Karl Kunert and Prof. Christine Foyer, who have made it possible for me to submit this thesis with confidence, as the first step in a successful career in science. I am extremely grateful for your guidance, support, and advice.

To all my friends and colleagues at the University of Pretoria, Rothamsted Research, and Newcastle University, I would like to express sincere thanks for your helpfulness, friendliness, support in troubleshooting, and company in the lab at all times of the day and night.

I am also very grateful to the Commonwealth Scholarship Commission in the United Kingdom for granting me a Split-Site PhD Scholarship and the National Research Foundation (NRF) for financial assistance towards this research.

UNIVERSITEIT VAN PRETORIA
UNIVERSITY OF PRETORIA
YUNIBESITHI YA PRETORIA

Proteases and protease inhibitors involved in plant stress response and acclimation

(Submitted in partial fulfilment of the requirements for the degree Philosophiae Doctor)

Anneke Prins

Department of Botany, Forestry and Agricultural Biotechnology Institute, University of Pretoria, Hillcrest, Pretoria, 0002, South Africa.

Supervisor: Karl J. Kunert

Department of Botany, Forestry and Agricultural Biotechnology Institute, University of Pretoria, Hillcrest, Pretoria, 0002, South Africa.

Supervisor: Christine H. Foyer

School of Agriculture, Food and Rural Development, Agriculture Building, The University of Newcastle upon Tyne, Newcastle upon Tyne, NE1 7RU, UK.

Abstract

Proteases play a crucial role in plant defence mechanisms as well as acclimation to changing metabolic demands and environmental cues. Proteases regulate the development of a plant from germination through to senescence and plant death. In this thesis the role of proteases and their inhibitors in plant response to cold stress and CO_2 enrichment were investigated.

The activity and inhibition of cysteine proteases (CP), as well as degradation of their potential target proteins was investigated in transgenic tobacco plants expressing the rice cystatin, OC-I. Expression of OC-I caused a longer life span; delayed senescence; significant decrease in *in vitro* CP activity; a concurrent increase in protein content; and protection from chilling-induced decreases in photosynthesis. An initial proteomics study identified altered abundance of a cyclophilin, a histone, a peptidyl-prolyl cis-trans isomerase and two RuBisCO activase isoforms in OC-I expressing leaves. Immunogold labelling studies revealed that RuBisCO and OC-I is present in RuBisCO vesicular bodies (RVB) that appear to be important in RuBisCO degradation in leaves under optimal and stress conditions.

Plants need to respond quickly to changes in the environment that cause changes in the demand for photosynthesis. In this study the effect of CO_2 enrichment on photosynthesis-related genes and novel proteases and protease inhibitors regulated by CO_2 enrichment and/or development, was investigated. Maize plants grown to maturity with CO_2 enrichment showed significant changes in leaf chlorophyll and protein content, increased epidermal cell size, and decreased epidermal cell density. An increased stomatal index in leaves grown at high-CO_2 indicates that leaves adjust their stomatal densities through changes in epidermal cell numbers rather than stomatal numbers. Photosynthesis and carbohydrate metabolism were not significantly affected. Developmental stage affected over 3000 transcripts between leaf ranks 3 and 12, while 142 and 90 transcripts were modified by high CO_2 in the same leaf ranks respectively. Only 18 transcripts were affected by CO_2 enrichment exclusively. Particularly, two novel CO_2-modulated serine protease inhibitors modulated by both sugars and pro-oxidants, were identified. Growth with high CO_2 decreased oxidative damage to leaf proteins.

Abbreviations

ABA	-	abscissic acid
ACC	-	1-aminocyclopropane-1-carboxylate
ADP	-	adenosine diphsophate
AGPase	-	ADP glucose pyrophosphorylase
ANOVA	-	analysis of variance
Asp	-	asparagine
ATP	-	adenosine triphosphate
BBI	-	Bowman Birk Inhibitor
beta-lcy	-	lycopene beta-cyclase
BLAST	-	Basic Local Alignment Search Tool
BS	-	bundle sheath
BSA	-	bovine serum albumin
Bt	-	bacillus thuringiensis
ºC	-	degree Celsius
C_a	-	ambient CO_2 concentration
CA-1-P	-	2-carboxyarabinitol 1-phosphate
CatB	-	cathepsin B
CBF1	-	C promoter-binding factor 1
CE	-	carboxylation efficiency
CHAPS	-	3-[(3-Cholamidopropyl)dimethylammonio]-1-propanesulfonate
CHCA	-	α-cyano-4-hydroxycinnamic acid
C_i	-	intercellular CO_2 concentration
CIN	-	cytoplasmic invertase
CP	-	cysteine protease
CP4 EPSPS	-	5-Enol-pyruvylshikimate-3-phosphate synthase CP4
Ct	-	threshold cycle
CWIN	-	cell wall invertase
dATP	-	2'-deoxyadenosine 5'-triphosphate
dCTP	-	2'-deoxycytosine 5'-triphosphate
DEPC	-	diethyl pyrocarbonate
dGTP	-	2'-deoxyguanosine 5'-triphosphate
DMSO	-	dimethyl sulfoxide

DNA	-	deoxyribonucleic acid
DNAse	-	deoxyribonuclease
dNTP	-	deoxyribonucleotide triphosphate
dTTP	-	2'-deoxythymidine 5'-triphosphate
DREB1A	-	dehydration response element B1A (
DTT	-	dithiotreitol
E	-	efficiency
E1	-	uibiquitin-activating enzyme
E2	-	ubiquitin-conjugating enzyme
E3	-	ubiquitin ligase
E64	-	*trans*-epoxysuccinyl-L-leucylamido(4-guanidino)butane
EDTA	-	ethylenediaminetetraacetic acid
ER	-	endoplasmic reticulum
FACE	-	free-air CO_2 enrichment
G3P	-	glyceraldehyde 3-phosphate
GA	-	gibberellic acid
Gin	-	glucose insensitive
GPCR	-	G-protein coupled receptor
gus	-	β-glucuronidase
h	-	hour(s)
HB	-	hemoglobin
HSP	-	heat shock protein
HXK	-	hexokinase
Incw4	-	cell wall invertase 4
IPM	-	integrated pest management
JA	-	jasmonic acid
J_{max}	-	CO_2 saturated rate of photosynthesis
kDa	-	kilodalton
KV	-	KDEL vesicles
Lhc	-	light harvesting complex
LSU	-	large subunit
M	-	mesophyll
MAP	-	mitogen-activated protein
ME	-	malic enzyme

min	-	minute(s)
MOPS	-	3-(N-Morpholino)propanesulfonic acid
MS	-	mass spectrometry
MW	-	molecular weight
NAD	-	nicotinamide adenine dinucleotide
NADP	-	nicotinamide adenine dinucleotide phosphate
NCBI	-	National Center for Biotechnology Information
NR	-	nitrogen reductase
OC-I	-	oryzacystatin I
OCE	-	OC-I expressing tobacco
PAGE	-	polyacrylamide gel electrophoresis
PAL	-	phosphoammonia lyase
PARP	-	poly (ADP-ribose) polymerase
PBS	-	phosphate buffered saline
PCR	-	polymerase chain reaction
PCD	-	programmed cell death
PEP	-	phosphoenolpyruvate
PEPC	-	phosphoenolpyrvate carboxylase
PGA	-	phosphoglycerate
Pi	-	inorganic phosphate
pI	-	isoelectric point
PMSF	-	phenylmethylsulphonyl fluoride
ppm	-	parts per million
PR	-	phathogenesis-related
psy	-	phytoene synthase
qPCR	-	quantitative realtime PCR
RACE	-	rapid amplification of cDNA ends
RbcL	-	ribulose-1, 5-bisphosphate carboxylase/oxygenase large subunit
Rbcs	-	ribulose-1, 5-bisphosphate carboxylase/oxygenase small subunit
RGS1	-	regulator of G-protein signalling1
RMA	-	Robust Multichip Average
RNA	-	ribonucleic acid
RNAse	-	ribonuclease
ROS	-	reactive oxygen species

Rpm	-	revolutions per minute
RQ	-	relative quantity
RT	-	reverse transcriptase
RuBisCO	-	ribulose-1, 5-bisphosphate carboxylase/oxygenase
RuBP	-	ribulose-1, 5-bisphosphate
RVB	-	RuBisCO vesicular body
s	-	second(s)
SAG	-	senescence-associated gene
SD	-	standard deviation
SDS	-	sodium dodecyl sulphate
SE	-	standard error
SELDI-TOF MS-		surface-enhanced laser desorption ionization - time of flight mass spectrometry
SA	-	salicylic acid
serpin	-	serine protease inhibitor
SnRK	-	SNF-1 related kinase
SPP	-	sucrose phosphate phosphatase
SPS	-	sucrose phosphate synthase
SSU	-	small subunit
SUS	-	sucrose synthase
SuSy	-	sucrose synthase
SUT	-	sucrose transporter
TAE	-	Tris-Acetic acid-EDTA
TBS	-	Tris-buffered saline
TCA	-	trichloroacetic acid
TFA	-	trifluoroacetic acid
TP	-	triose phosphate
T-6-P	-	trehalose-6-phosphate
U	-	units
UV	-	ultraviolet
UDP	-	uridine 5′-diphosphate
UDPG	-	uridine 5′-diphosphoglucose
V	-	volt
VIN	-	vacuolar invertase

VPE	-	vacuolar processing enzyme
v/v	-	volume per volume
WIP	-	wound-induced protein

Index **Page**

CHAPTER 4: Acclimation of maize source leaves to CO_2 enrichment at flowering

CHAPTER 1: Introduction

1.1 Approaches for crop improvement and resistance to biotic and abiotic stress

Since the first transgenic tobacco plants expressing foreign proteins were produced (Horsch et al., 1985), genetic engineering approaches have become a routine in plant science laboratories around the world (Table 1.1). However, the introduction of a useful single well-defined and optimized gene is still a major focus for research in many crop species (Altpeter et al., 1999; Repellin et al., 2001; Langridge et al., 2006). There is also a need for the identification and evaluation of novel DNA sequences that will be useful in increasing the tolerance of plants to the often extreme environmental growth conditions experienced in Africa (Langridge et al., 2006). Factors that increase tolerance to pest species and extreme heat and drought are also critical to the future success of African agriculture. Hence, achieving enhanced resistance to biotic and abiotic stresses is one of the most important challenges to plant scientists in Africa.

Table 1.1 Examples of successful expression of transgenes in plants by genetic engineering.

Genes of plant origin are indicated in bold. (From Babu et al., 2003)

Introduced trait	**Chimeric genes**
Abiotic stress tolerance	***gpat***, ***sod***, *MtID*
Salinity tolerance	*betA*, ***p5cs***, *halI*, *codA*, *afp*, *imtI*
Fungal resistance	Chitinase, ribosome inactivating protein (RIP)
Virus protection	Coat protein genes, antisense-coat protein, satellite RNA
Insect resistance	Bt toxin; *cryIA(a)*, *cryIA(b)*, *cryIA(c)*, *cryIC*, *cryIIIA*, **protease inhibitor (*CpTi*), corn cystatin (CC), oryza cystatin I (OCI), α-AI, *gna***, chicken *avidin* gene
Herbicide tolerance	*aro A* and EPSP (glyphosate), *bar* (phosphinothricin), *bxn* (bromoxynil), *ALS* (sulfonylurea), *tfdA* (2,4-D)

The use of protease inhibitors in the improvement of plant tolerance to insects has received a lot of interest. Since the first successful increase in insect resistance was achieved by introduction of a trypsin inhibitor (Hilder et al., 1987), plant-derived protease inhibitor genes have been viewed as attractive targets in approaches geared to increasing the insect resistance of crop plants (Hilder and Boulter, 1999; Ussuf et al., 2001; Ferry et

al., 2004). Early examples include expression of a potato serine protease inhibitor applied in cowpea and rice (Duan et al., 1996), a Kunitz protease inhibitor in poplar (Colfalonieri et al., 1998) and a trypsin inhibitor in rice (Mochizuki et al., 1999).

Relatively few studies have incorporated more than one transgene. However, the inclusion of protease inhibitors together with other transgenes conferring insect tolerance can enhance the effectiveness of the latter (Sharma et al., 2004). For example, Boulter et al (1990) showed enhanced resistance to *Heliothis virescens* (tobacco budworm) by introduction of both the cowpea trypsin inhibitor and the pea lectin into tobacco plants. In addition, Bt activity can be enhanced in transgenic plants by simultaneous expression of serine protease inhibitors (MacIntosh et al., 1990). The interaction between proteases and protease inhibitors and their enzyme substrates in transgenic plants is therefore important but has been relatively poorly studied to date.

Traditional approaches designed to improve abiotic stress tolerance in crop plants have exploited the natural diversity of more-resistant varieties in breeding programs (Akbar et al., 1986; Yamauchi et al., 1993; Flowers and Yeo, 1995; Moons et al., 1995; McCouch, 2005). However, classic genetic approaches are difficult to implement, largely because of the complex multi-genic nature of the tolerance traits (Jain and Selvaraj, 1997; Nguyen et al., 1997; Khanna-Chopra and Sinha, 1998; Flowers, 2004; Vinocur and Altman, 2005). The abiotic factors that cause stress include sub- and supra-optimal temperatures, excess salt (mainly NaCl) levels, reduced water availability leading to dehydration stress, as well as the cellular oxidative stress caused by sub- and supra-optimal environmental conditions (Grover et al., 1999; Knight and Knight, 2001; Chinnusamy et al., 2004). Many of these stress factors occur simultaneously, resulting in a compound effect. For example, drought is often accompanied by high temperature stress; salt stress often results in water deficits, while low temperature stress is frequently associated with drought stress. In addition, oxidative stress results from exposure to a wide variety of stresses like excess light, excess or shortage of water, and extreme temperatures.

Survival of stressful environments requires extensive acclimation of most if not all of the major metabolic processes including photosynthesis, nitrogen fixation, nitrogen metabolism and respiration (Grime, 1989; Nguyen et al., 1997; Pareek et al., 1997; Khanna-Chopra and Sinha, 1998; Knight and Knight, 2001; Chinnusamy et al., 2004;

Maestre et al., 2005). Since plant growth and development respond to environmental cues, it is perhaps not surprising that exposure to stress causes many physiological and morphological adjustments, and these can effect plant productivity at every developmental stage (Khanna-Chopra and Sinha, 1998; Maestre et al., 2005; Mittler 2006).

Transgenic approaches to the improvement of plant stress tolerance require identification of genes of interest that will not only protect plants but enable them to maintain vigour under abiotic stress conditions. Global expression profiling has identified large numbers of genes involved in plant stress responses (Cheong et al., 2002; Kreps et al., 2002; Jiang and Zhang, 2003). Comparisons of multiple stresses at different time points has allowed the identification of transcript changes that underpin stress-specific and "common" or "shared" responses (Fig. 1.1; Shinozaki and Yamaguchi-Shinozaki, 2000; Knight and Knight, 2001; Kreps et al., 2002; Fujita et al., 2006).

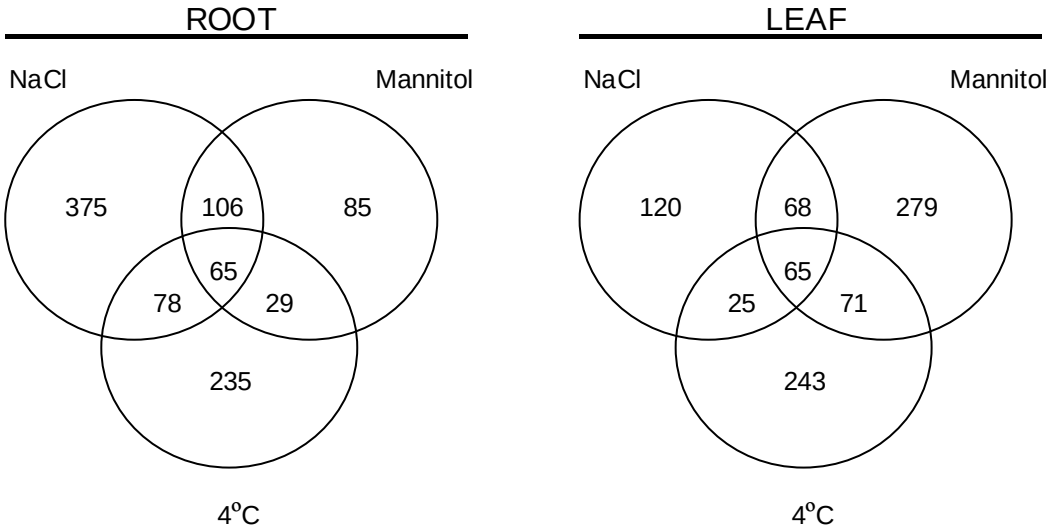

Figure 1.1 Venn diagrams showing the distribution of stimulus-specific and shared stress responses (> 2-fold) in *Arabidopsis thaliana*. These changes were observed after 3 hours of exposure to the stress applied, either NaCl, mannitol, or cold stress (4ºC). (From Kreps et al., 2002).

A rather large number of individual genes are effective in improving abiotic stress tolerance using transgenic approaches. Some of these encode enzymes involved in metabolic pathways that confer stress tolerance, such as glycerol 3-phosphate acyltransferase (Murata et al., 1992; Grover et al., 2000; Iba, 2002) mannitol-1 phosphate dehydrogenase (Tarczynski et al., 1993; Chen and Murata, 2002) and superoxide dismutase (Aono et al., 1995; McKersie et al., 1999; Van Breusegem et al., 1999;

McKersie et al., 2000). A number of studies have involved modified expression of osmolytes (Yancey et al., 1982; Morgan, 1984; Vernon et al., 1993; Kavi Kishor et al., 1995; Hayashi et al., 1997; Romero et al., 1997; Shen et al., 1997). Many of the studies that have focused on the enhancement of the antioxidant defences have met with mixed success (Foyer and Noctor, 2003). The mechanisms by which some selected transgenes confer tolerance to abiotic stresses are more obscure. For example, transgenic plants with decreased poly (ADP-ribose) polymerase (PARP) levels show broad-spectrum stress-resistant phenotypes. This increase in stress tolerance was initially attributed to an improved maintenance of cellular energy homeostasis due to reduced NAD(+) consumption (De Block et al., 2005). However, it has recently been shown that PARP2-deficient *Arabidopsis* plants also have higher leaf abscisic acid contents and this could also explain the observed induction of a wide set of defence-related genes in the transgenic plants (Vanderauwera et al., 2007).

The C promoter-binding factor 1 (CBF1) transcription factor, which controls the cold-regulated *cor* genes has been used to increase the freezing tolerance of plants and dehydration response element B1A (DREB1A), a drought-responsive element binding protein was found to enhance both freezing and dehydration tolerance (Liu et al; 1998; Gong et al., 2002; Pino et al., 2007). However, transgenic plants over expressing DREB1A also showed a dwarfed phenotype (Pellegrineschi et al., 2004). Genes that play a role in signal transduction pathways involved in regulating stress responses have also been used in transgenic approaches to improve stress resistance (Liu and Zhu, 1998). More recent approaches have focused on other signal transducing components, particularly the mitogen-activated protein (MAP) kinase pathways (Lee and Ellis, 2007).

While transgene technologies have greatly improved over the intervening years and many genes that are important in plant stress responses have been identified, there remains a large gap in our current ability to translate information gained in the laboratory into enhanced vigour under stressful environmental conditions. In part this is due to the absence of a comprehensive characterisation of gene function in crop plants. Much work has focused on the analysis of stress responses in model species. Moreover the functions of stress markers and stress-related genes have been studied largely in model plants, such as tobacco and *Arabidopsis* (Vinocur and Altman, 2005). While such studies are vital, it is also important to identify genes that are involved in the stress responses of crop plants and

to study their function in the context of overall yield in the field as well as under controlled environment conditions.

1.2 The use of protease inhibitors for crop improvement

The application of protease inhibitors in plant protection was investigated as early as 1947, when Mickel and Standish observed that the larvae of certain insects were unable to develop normally on soybean products (Mickel and Standish, 1947). Subsequently, it was shown that trypsin inhibitors present in soybean are toxic to the larvae of the flour beetle, *Tribolium confusum* (Lipke et al., 1954). Other investigations revealed that plant protease inhibitors can inhibit insect gut proteases; both *in vitro* (Pannetier et al., 1997; Koiwa et al., 1998) and *in vivo* using artificial diet bioassays (Urwin et al., 1997; Vain et al., 1998; Foissac et al., 2000; De Leo et al., 2001; Ferry et al., 2004). There has been a large amount of interest in the use of plant protease inhibitors in transgenic approaches for the improvement of crop resistance to both biotic and abiotic stresses. In addition to improved stress tolerance, the application of protease inhibitors has three additional advantages. Firstly, transgenic crops expressing plant-derived protease inhibitors are useful in integrated pest management (IPM) systems that aim to minimise pest damage to crops without the application of harmful pesticides (Boulter, 1993). Secondly, protease inhibitors improve the nutritional quality of food as many of them are rich in cysteine and lysine (Ryan, 1989). Thirdly, protease inhibitors can protect heterologous proteins when both are expressed together in transgenic potato (Rivard et al., 2006). Hence, protease inhibitors have great potential in large-scale production systems for recombinant proteins in plants. This transgenic approach is a viable, safe, and useful option, especially when considering the expression of biologically active mammalian proteins that require essential post-translational modifications. It is widely assumed that ectopic protease inhibitor expression has little effect on plant growth and development but this has not been studied intensively in most cases. Furthermore, it is of interest to determine whether ectopically expressed protease inhibitors affect the action of key endogenous proteases involved in essential proteolysis functional during development, stress response, and senescence. Of the wide variety of protease inhibitors that occur in plants, only one family, the cystatins, has been studied in great detail.

1.2.1 Cysteine protease inhibitors (Cystatins)

The cystatin superfamily is composed of cysteine protease inhibitors that bind tightly and reversibly to the papain-like cysteine proteases present throughout the animal and plant kingdoms (Nicklin and Barret, 1984; Margis et al., 1998). All members of the superfamily exhibit similarities in their amino acid sequences and functions (Barret et al., 1986). Three distinct families were originally classified: the cystatin family consisting of groups of small proteins with two disulfide bonds; the stefin family of small proteins (~12 kDa) lacking disulfide bonds; and the kininogen family of large glycoproteins (60-120 kDa) containing three repeats similar to those found the cystatin family (Barret et al., 1986). The plant cystatins have structural peculiarities, genomic arrangements and intrinsic diversity compared to animal cystatins. This led to the creation of a new family, the phytocystatins (Kondo et al., 1991; Margis et al., 1998).

Cystatins are part of an innate plant bio-defence system against insect attack (Michaud et al., 1993b; Matsumoto et al., 1995; Michaud et al., 1995; Edmonds et al., 1996; Kuroda et al., 1996 Matsumoto et al., 1997; Matsumoto et al., 1998). This has lead to research using transgenic approaches involving cystatins in insect control (Benchekroun et al., 1995; Urwin et al., 1995; Irie et al., 1996; Arai et al., 2000). Cystatin expression can have other beneficial effects, for example, expression of the rice phytocystatin Oryzacystatin-I (OC-I; Fig. 1.2) in transformed tobacco improved recovery of photosynthesis following cold stress (Van der Vyver et al., 2003).

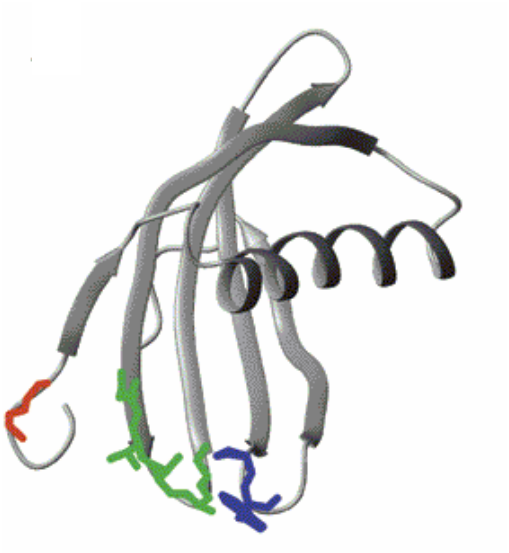

Figure 1.2 Structure of the rice phytocystatin OC-I (Nagata et al., 2000).

A number of investigations concerning cystatin expression have focussed on seeds. (Kondo et al., 1990; Abe et al., 1995; Kuroda et al., 2001). Less information is available on other tissues. A sorghum cystatin was reported in vegetative tissues (Li et al., 1996). The barley cystatin, Hv-CPI, was detected in embryos, developing endosperm, leaves and roots. Hv-CPI expression increased in vegetative tissues in response to stress, particularly anaerobiosis, dark and cold shock (Gaddour et al., 2001). Many phytocystatins are induced upon exposure to abiotic stress (Pernas et al., 2000) and biotic stresses (Leple et al., 1995). Cysteine proteases are key enzymes in animal apoptosis and they may have similar roles in plant programmed cell death (PCD) as ectopic expression of cystatins was found to block H_2O_2-induced cysteine protease activity during PCD (Solomon et al., 1999). In such situations plant cystatins may protect against invasion by viruses, bacteria, and insects as they can inhibit cysteine proteases from a wide range of organisms. The relationships between the expression of cysteine proteases and that of cystatins is poorly characterised. The cathepsin B-like cysteine protease (gene *CatB*) was found to show similar patterns of expression to the *Icy* cystatin in barley vegetative tissues (Martínez et al., 2002). The *Icy* encoded protein is a potential inhibitor of several cysteine proteases including the CatB protease. Leaf *CatB* and *Icy* mRNAs show similar circadian expression patterns of regulation and they are similarly induced by chilling. However, these genes showed different expression patterns in pre and post-germinating embryos and they had different hormonal responses in the aleurone layers.

While protease inhibitors have been used ectopically to improve biotic and abiotic stress resistance, little research has focused on the effect of this ectopically-expressed inhibitor on possible endogenous protease targets. Interaction between an exogenous protease inhibitor and an endogenous protease will potentially affect the mechanism of proteolysis which is very important in the process of metabolic change due to development or stress response. It is important to understand the function of protein degradation as well as the role of important proteases in the plant, in order to understand where exogenous protease inhibitors might affect plant metabolism.

1.3 Protein degradation and proteases

Proteolytic enzymes play a crucial role in plant defence and acclimation to changing metabolic demands and environmental cues, as well as in the orchestration of plant development from regulation of cyclin lifetime in the cell cycle to the programming of

senescence. These important enzymes are responsible for the post-translational modification of the cellular protein network by limited proteolysis at highly specific sites (Vierstra, 1996, Beers et al., 2000). Limited proteolysis participates in the control of enzyme activity as well as the functioning of regulatory proteins and peptides (Callis and Vierstra, 2000). It is used by the cell to control the production, assembly and sub-cellular targeting of mature enzyme forms.

Proteolytic enzymes play a vital role in protein turnover. They are essential components of the cellular protein homeostasis and repair system, removing damaged, mis-folded, or harmful proteins as well as limiting the lifetime of proteins such as the DELLA proteins that control plant growth and development (Vierstra, 1996; Frugis and Chua, 2002). The selective breakdown of regulatory proteins by the ubiquitin-proteasome pathway (Fig. 1.3) controls key aspects of plant growth, development, and defence (Hochstrasser, 1995; Hellman and Estell, 2002; Vierstra, 2003; Dreher and Callis, 2007).

1.3.1 The ubiquitin/proteasome system

Proteins that are targeted for degradation by ubiquitin/proteasome system are first modified by the addition of ubiquitin. The polyubiquitin chains are covalently linked to a lysine residue in the target protein (Pickart, 2001) in a sequential cascade of enzymatic reactions (Fig. 1.3). A uibiquitin-activating enzyme (E1) first binds to the G76 residue of ubiquitin (1). This enzyme transfers the ubiquitin moiety to a ubiquitin-conjugating enzyme (E2) (2), which carries the activated uibiquitin to a ubiquitin ligase (E3) (3), which facilitates the transfer of the ubiquitin to a lysine residue in the target protein (4). This process is repeated for the formation of a polyubiquitin chain on the target protein (5). In *Arabidopsis* two genes encode ubiquitin-activating enzymes, at least 45 genes encode ubiquitin-conjugating enzymes, and almost 1200 genes encode ubiquitin ligases (Vierstra, 2003). The type of chain synthesised determines the fate of the protein that has polyubiquitin chains. Chains formed at the K48 residue of ubiquitin are destined for degradation by the 26S proteasome. The proteasome degrades the target protein and the ubiquitin monomers are reclaimed by the action of de-ubiquitinylating enzymes (Vierstra, 2003).

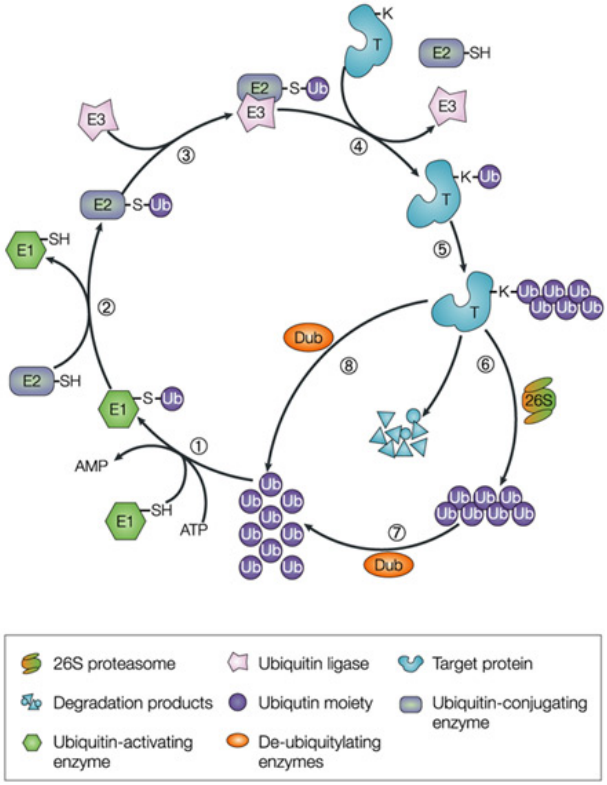

Figure 1.3 The Ubiquitin/Proteasome system. (Sullivan et al., 2003). Process described in text.

The 26S proteasome consists of the 20S core protease and the 19S regulatory particle (Fig. 1.4; Voges et al., 1999). The core protease is a broad-spectrum ATP- and ubiquitin - independent peptidase created by the assembly of four, stacked heptameric rings of related α and β subunits in a $\alpha_{1-7}\beta_{1-7}\beta_{1-7}\alpha_{1-7}$ configuration. The protease-active sites within the β1, β2 and β5 polypeptides are sequestered in a central chamber. Access to this chamber is restricted by a narrow gated channel created by the α-subunit rings that allows only unfolded proteins to enter (Glickman, 2000). Each end of the central protease is capped by a regulatory particle. The regulatory particle confers both ATP-dependence and substrate specificity to the holoenzyme (Voges, 1999; Glickman, 2000). The regulatory protein is able to identify appropriate substrates for breakdown, releasing the attached ubiquitins and opening the α-subunit ring gate. This directs the entry of unfolded proteins into the central protease lumen for degradation.

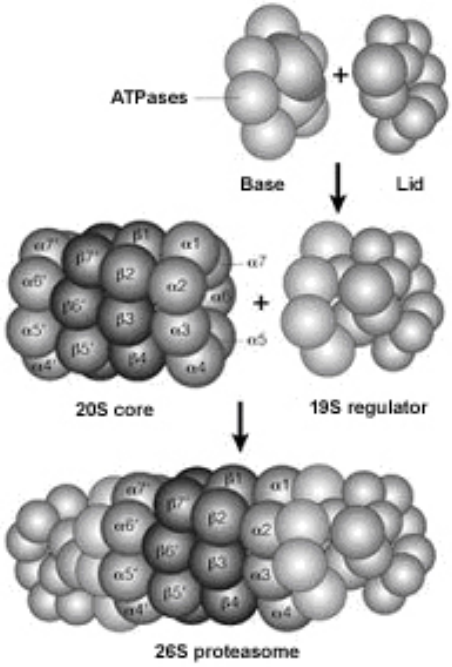

Figure 1.4 The 20S core protease and 19S regulatory protein that constitute the 26S proteasome complex (Kloetzel, 2001).

1.3.2 Proteases

Proteases are responsible for degradation of proteins that are not uibiquitinated. They are divided into four classes according to catalytic mechanism: serine, cysteine, aspartic, and metalloproteases (Fig. 1.5; Fan and Wu, 2005). A further class has been suggested for proteases of unidentified catalytic mechanism. Since the research described in this thesis largely concerns inhibitors of only serine and cysteine proteases, these categories alone are discussed in detail below.

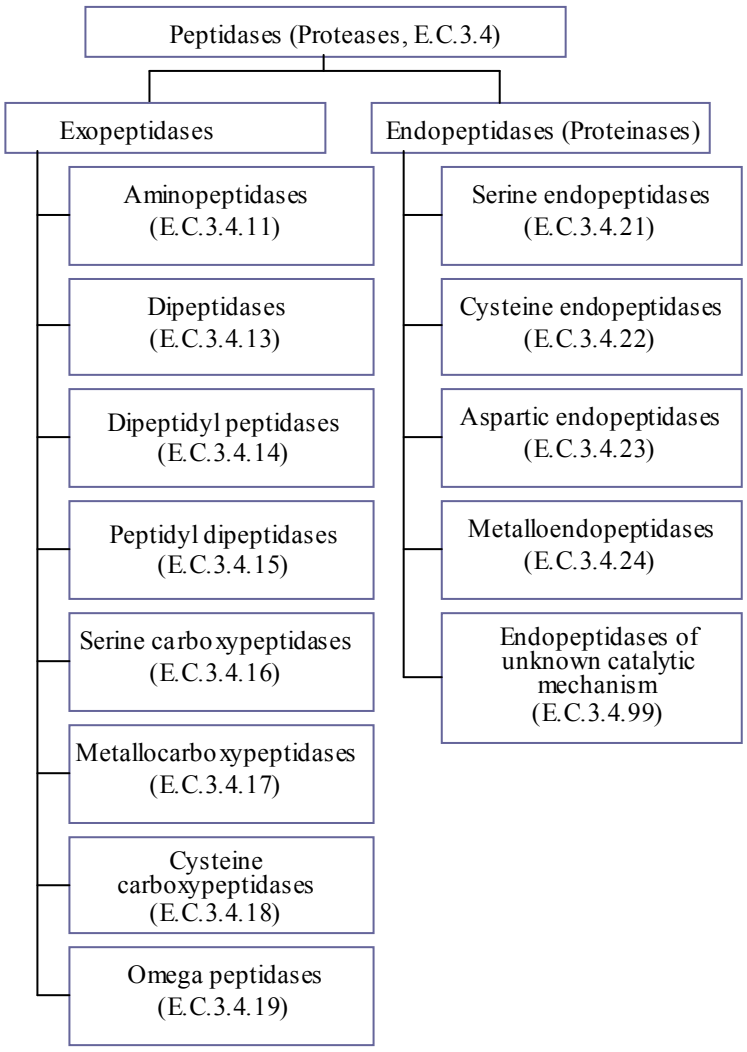

Figure 1.5 The main classes of proteases (peptidases) according to the Nomenclature Committee of the International Union of Biochemistry and Molecular Biology (NC-IUBMB, 1992). NC-IUBMB recommended the term peptidase as the general term for all enzymes that hydrolyse peptide bonds. This is subdivided into exopeptidases cleaving one or a few amino acids from the N- or C-terminus, and endopeptidases cleaving internal peptide bonds of polypeptides. The classification of exopeptidases is based on their actions on substrates while the endopeptidases are divided by their active sites. Proteases are divided into four groups: the serine proteases, the cysteine proteases, the aspartic proteases, and the metalloproteases. (From Fan and Wu, 2005)

Cysteine proteases, senescence, and programmed cell death (PCD)

Cysteine proteases have roles in the resistance of plants to attack by pathogens (Krüger et al., 2002) and insects (Pechan et al., 2000; Konno et al., 2004) and they also have well-characterised functions in senescence and PCD (Solomon et al., 1999; Wagstaff et al., 2002; Belenghi et al., 2003; Okamoto et al., 2003). Their roles in nitrogen remobilisation

have been well characterised, particularly in regard to the degradation of the storage proteins (Kato and Minamikawa, 1996; Tooyoka et al., 2000; Gruis et al., 2002).

Leaf senescence is a complex and highly coordinated developmental process that precedes plant death, and in which proteolysis plays a major part (Smart, 1994; Nooden et al, 1997; Gepstein et al, 2003). Senescence-associated genes (SAGs) are considered to be specifically up-regulated during senescence (Bleecker and Patterson, 1997; Gepstein et al., 2003). These include genes for proteases (Dangl et al., 2000; Lohmann et al., 1994; Thompson et al., 1998, 2000), including those of the cysteine protease family (Chen et al, 2002). It is generally believed that proteases active during senescence function in the remobilization of nitrogen to sink tissue. Two cysteine proteases, SAG2 and SAG12 have proved to be particularly important senescence markers. SAG2 shows senescence-enhanced expression while SAG12 shows senescence-specific expression (Hensel et al. 1993, Lohman et al. 1994; Grbić, 2003). SAG2 shows sequence similarity to cathepsin H and SAG12 to cathepsin L (Hensel et al. 1993, Lohman et al. 1994). The low level of SAG2 expression in young leaves indicates that this protease functions in protein turnover throughout the life of the leaf. In contrast, the specific induction of SAG12 at the onset of leaf senescence indicates that it has a more specialized role in protein breakdown during senescence. Cathepsin cysteine proteases are active at acidic pH, and are therefore assumed to be localised in lysosomes or vacuoles (McGrath 1999; Turk et al., 2001).

The process of PCD in plant cells has been compared to apoptosis in animal cells (Jones and Dangl, 1996; Elbaz et al., 2002; Van Doorn and Woltering, 2005). In animal cells the major regulators of apoptotic cell death are the caspases, a family of cysteine proteases with specificity for asparagine (Asp; Shi, 2002). When an apoptotic signal is perceived, inactive caspases are processed to their active states by oligomerization and subsequent conformational changes (Fuentes-Prior and Salvesen, 2004). This irreversible activation triggers a proteolytic cascade that activates the enzymes involved in apoptosis. While caspase inhibitors can block PCD in plants (Del Pozo and Lam, 1998; Watanabe and Lam, 2004) they have not evolved the apoptotic sequence of activation of canonical caspases or the pro-and anti-apoptotic functions of Bcl-2 family proteins. However, caspase homologs are present in plants based on sequence similarity. These have been designated metacaspases (Uren et al., 2000) but they have no known function. For example, constitutive overexpression or disruption of metacaspase genes in *Arabidopsis* does not

result in an obvious phenotype (Vercammen et al., 2006; Belenghi et al., 2007). However, micro-array analysis on the expression of over 20,000 *Arabidopsis* genes (Zimmermann et al., 2004) showed that metacaspases are induced in response to biotic and abiotic stresses (Sanmartín et al., 2005). Certain metacaspase genes are also strongly induced in senescing flowers (Sanmartín et al., 2005). Moreover, the activity of the *Arabidopsis* metacaspase, AtMC9, is inhibited by AtSerpin1, a serine protease inhibitor that inhibits AtMC9 strongly through binding and cleavage of its reactive center loop (Vercammen et al., 2006).

In contrast to animals, dead cells in plants are never removed by phagocytosis. PCD in plants occurs by autophagasitic processes where the proteins in the dying cell are essentially removed by enzymes in growing lytic vacuoles. Most animal caspases are located in the cytosol where the proteolytic cascade is localised (Nakagawa and Yuan, 2000). However, co-operating pathways involving the vacuoles, chloroplasts, mitochondria and nucleus contribute to plant PCD, together with a repertoire of cell death proteases (Sanmartín et al., 2005). Of these, one group of proteases namely the vacuolar processing enzymes (VPEs) has been suggested to have caspase-like functions in plants (Woltering et al., 2002) particularly in PCD (Hoeberichts et al., 2003; Rojo et al., 2004). VPEs are related in sequence and in tertiary structure to animal caspases (Aravind and Koonin, 2002). VPEs also play a role in the maturation of several seed proteins (Hara-Nishimura et al., 1991, 1993), including a novel membrane protein (Inoue et al., 1995), and vacuolar proteins in leaves (Hara-Nishimura, 1998). VPEs have been identified in seeds and in vegetative tissues (Kinoshita et al., 1995). In vegetative tissues VPEs are localised in the lytic vacuoles (Kinoshita et al., 1999) while seed VPEs are localised in the protein storage vacuoles (Hiraiwa et al., 1993). VPE activities are greatly increased in the lytic vacuoles during senescence and under various stress conditions (Kinoshita et al., 1999). Moreover, VPEs are accumulated in vesicles derived from the endoplasmic reticulum (ER) in the epidermal cells in young seedlings (Hayashi et al., 2001). When seedlings are exposed to stress, these vesicles fuse with the vacuoles and perhaps other organelles and thus assist in stress-induced protein turnover and PCD.

Serine proteases

Serine proteases (carboxypeptidases) function in a wide range of plant defence processes such as PCD (Domínguez and Cejudo, 1998; Domínguez et al., 2002), and response to wounding where they are triggered by brassinosteroid signalling (Li et al., 2001). They are

also important in seed development (Cercos et al., 2003). Like the cysteine proteases, the serine proteases are involved in nitrogen remobilisation and have important functions in processes such as the remobilization of nitrogen reserves during seed germination (Antão and Malcata, 2005). The diversity of serine protease functions has been attributed to differences in substrate specificity (Walker-Simmons and Ryan 1980; Dal Degan et al., 1994; Moura et al., 2001; Granat et al., 2003).

The subtilase class of serine proteases are particularly important during microsporogenessis, where a role in signal peptide production has been suggested (Kobayashi et al., 1994). Relatively little is known about the role of the subtilisin-like serine proteases but they have been shown to function in epidermal structure and patterning. For example, *ALE1* plays a role in epidermal surface formation (Tanaka et al., 2001) and *SDD1* regulates stomatal density and distribution (Berger and Altmann, 2000). Subitilases are also produced in response to PCD triggers and have caspase-like cleavage capabilities.

Proteolysis is an essential element of metabolic change in plants whether it's initiated by development or is triggered by stimulus from the environment. One of the processes that are affected by both development and stress is the process of photosynthesis.

1.4 Photosynthesis as a target for proteolytically-mediated metabolic change

Since photosynthesis drives plant biomass production, knowledge of the responses of this process to different environmental conditions, will be vital in ensuring the success of future crop improvement strategies. As plants grow and respond to external stimuli, the photosynthetic machinery adjusts according to changing demands on photosynthate and energy. The proteins involved in photosynthesis may be controlled on post-translational level by selective proteolytic degradation. It is important to understand the different types of photosynthesis in order to determine how proteins involved in this process will be regulated.

1.4.1 C_3 and C_4 Photosynthesis

Photosynthesis is the process through which plants convert light energy into chemical energy and fix atmospheric CO_2 into organic carbon compounds (Fig. 1.6; Benson and Calvin, 1950; Edwards and Walker, 1983; Furbank and Taylor, 1995). The C_3 pathway

(also called the Calvin cycle, the Calvin-Benson cycle, or the photosynthetic carbon reduction [PCR] cycle) is the only mechanism through which plants fix CO_2 into sugar-phosphates. The C_3 cycle takes its name from the first product of the pathway, which is a three carbon compound, 3-phosphoglycerate (PGA). Two molecules of PGA are produced when CO_2 is introduced into the 5-carbon compound ribulose-1, 5-bisphosphate (RuBP), a reaction that is catalysed by ribulose-1, 5-bisphosphate carboxylase/oxygenase (RuBisCO) (Lorimer, 1981). Phosphoglycerate is then converted to two types of triose phosphate (TP) glyceraldehyde 3-phosphate (G3P) and dihydroxyacetone phosphate by phosphorylation and reduction steps that use ATP and NADPH. For every 6 TP molecules flowing through the PCR cycle, one is produced as net product (Benson and Calvin, 1950). This can either be kept in the chloroplast where it could be used for starch synthesis, or it can be transported to the cytosol where it is used in the synthesis of sucrose or to provide carbon skeletons for the production of a wide range of other molecules including amino acids. Sucrose is then translocated from the green tissues throughout the plant for energy and biomass production.

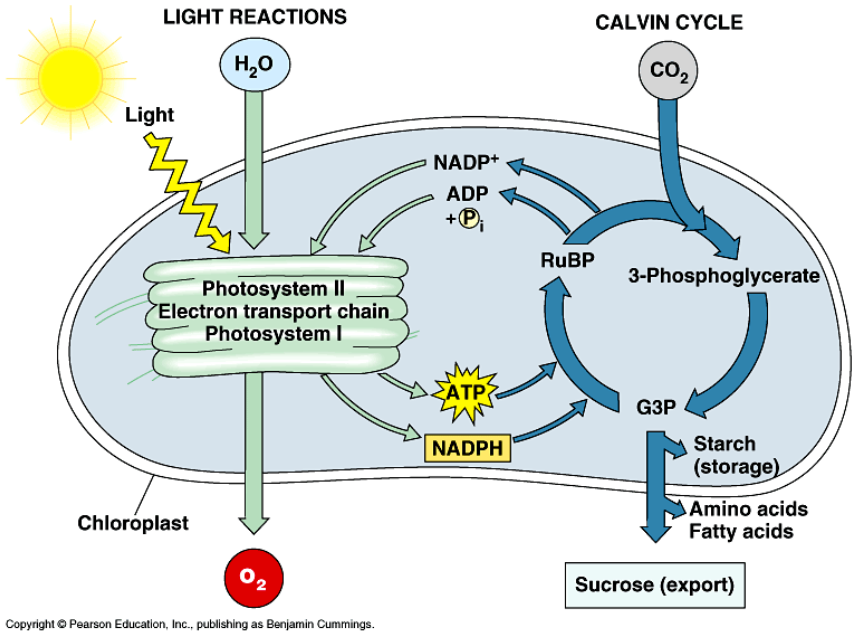

Figure 1.6 A schematic representation of photosynthesis. Light energy absorbed by photosystems I and II in the thylakoid membranes is used to produce ATP and NADPH, which drive the CO_2 assimilation (PCR) pathway in the chloroplast stroma. The PCR pathway liberates ADP and NADP which then return to the thylakoid membranes as the substrates for the light driven electron transport pathways.

RuBisCO also catalyses a second reaction in addition to CO_2 fixation (Lorimer, 1981). Molecular O_2 can replace CO_2 at the enzyme active site and the resultant fixation of O_2 into RuBP initiates a process known as photorespiration. When RuBisCO fixes O_2 it produces one molecule of 3-phosphoglycerate and one molecule of 3-phosphoglycolate rather than two molecules of 3-phosphoglycerate. The present atmospheric CO_2 concentration allows the photorespiratory pathway to operate at high rates in plants that only have the PCR cycle (C_3 plants) as O_2 efficiently competes with CO_2, particularly at higher temperatures. At current atmospheric CO_2 levels, one molecule O_2 is fixed by RuBisCO for every three molecules of CO_2 that are fixed in C_3 plants. Since 3-phosphoglycolate cannot be used in the PCR cycle, it must be recycled to phosphoglycerate through the photorespiratory pathway, which incurs additional energy costs and results in the loss of both CO_2 and nitrogen.

Certain plant species such as maize and sorghum have evolved systems that diminish the flow of carbon through the photorespiratory pathway (Edwards and Walker, 1984; Sage, 2004). In these species (called C_4) a second process has evolved to assist the C_3 pathway in CO_2 assimilation (Fig. 1.7) such that the fixation of CO_2 is a two-step process. Atmospheric CO_2 is first fixed in the cytosol of the mesophyll (M) cells by phosphoenolpyruvate (PEP) carboxylase to form a C_4 metabolite, oxaloacetate. Oxaloacetate is then converted to malate or aspartate, which diffuse into the inner ring of bundle sheath (BS) cells where they are decarboxylated in the chloroplasts. The CO_2 produced by decarboxylation is then refixed by RuBisCO. Hence, two types of photosynthetic cell in the M and BS tissues co-operate in CO_2 fixation in C_4 plants. The leaves of C_4 plants such as maize often show extensive vascularization, with a ring of bundle sheath cells surrounding each vein and an outer ring of M cells surrounding the BS. The development of this “Kranz anatomy” and the cell-specific compartmentalization of C_4 enzymes are important features of C_4 photosynthesis (Hatch, 1992, and references therein).

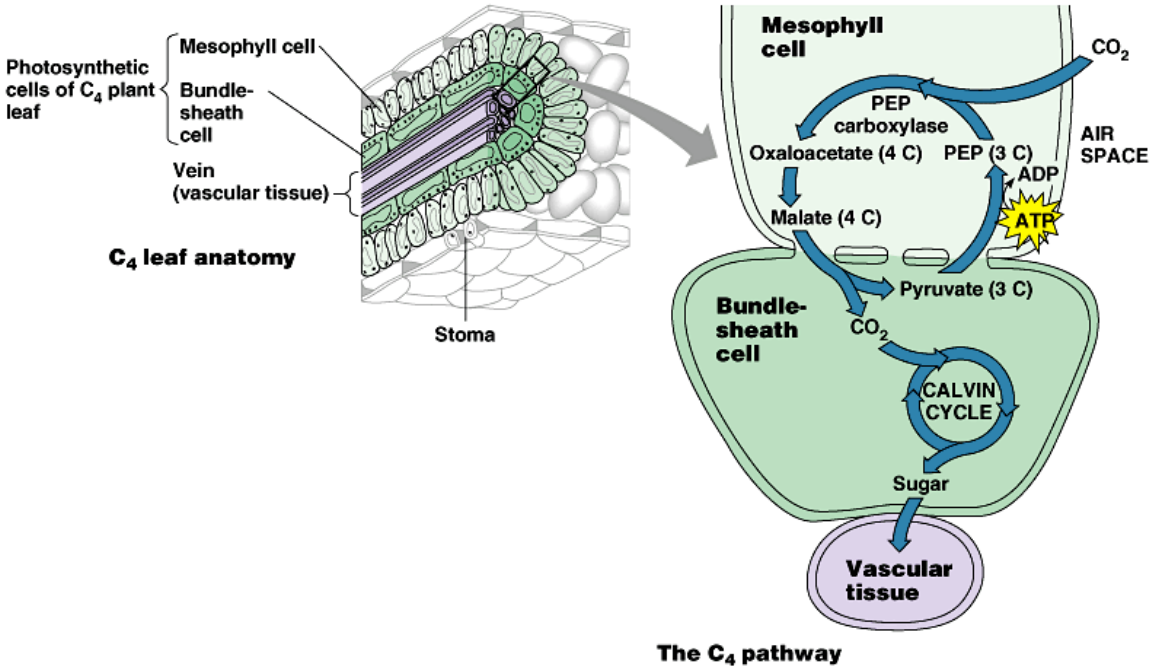

Figure 1.7 The C_4 pathway of photosynthesis. In C_4 plants the mesophyll and bundle sheath cells co-operate in the CO_2-fixing process. In this pathway, the four carbon (4C) acids that are produced by phospho*enol*pyruvate (PEP) carboxylase in the mesophyll are transported to the bundle sheath where CO_2 is liberated and fixed in to 3-phosphoglycerate by the enzymes of the Calvin (PCR) cycle.

The BS cells are separated from the M cells and from the air in the intercellular spaces by a lamella that is highly resistant to the diffusion of CO_2 (Hatch, 1992). Thus, the M-located C_4 cycle acts as an ATP-dependent CO_2 pump that increases the concentration of CO_2 in the BS to approximately 10 times atmospheric concentrations. This high CO_2 level suppresses the RuBisCO oxygenase activity which leads to higher rates of photosynthesis in C_4 plants, particularly at high light intensities and high temperatures due to the increased efficiency of the PCR cycle (Hatch, 1992).

1.4.2 Response of photosynthesis to abiotic stress

Plants need to respond quickly to changes in the environment causing changes in the demand for photosynthesis. This adaptation to environmental change often includes selective and rapid degradation of key proteins. For example, when the amount of incident light is above that which the plant can use for the process of photosynthesis, excess light damages the photosynthetic system causing photoinhibition. Photoinhibition of photo system II requires rapid acclimation with a concomitant degradation of proteins. Photoinactivation of PSII electron transcport is followed by oxidative damage to the D1

protein. The D1 protein is one of the heterodimeric polypeptides of the PSII reaction center complex. Damage to the D1 protein exposes it to an intrinsic protease (Virgin et al., 1991; De Las Rivas et al., 1992) for protein turnover. A proteolytic activity that is involved in the degradation of the major light-harvesting chlorophyll a/b-binding protein of photosystem II (LHCII) has also been identified. Degradation of this protein occurs when the antenna size of photosystem II is reduced upon acclimation of plants from low to high light intensities (Yang et al, 1998). The protease(s) involved in degradation of the major light-harvesting chlorophyll a/b-binding protein is of the serine or cysteine type and is associated with the outer membrane surface of the stroma-exposed thylakoid regions.

1.4.3 Effects of CO_2 enrichment on photosynthesis, RuBisCO, and protein turnover

The effect of increased CO_2 content in the atmosphere has recently been a matter of great interest (Stitt, 1991; Sage, 1994; Drake et al., 1997; Ainsworth et al., 2002; Nowak et al., 2004; Ainsworth and Long, 2005; Matros et al., 2006). In some important crop species a highly beneficial effect was observed. For example, in soybean photosynthesis increased at elevated CO_2 by an average of 39%, leaf area increased by 18%, and plant dry matter increased by 37% (Ainsworth et al., 2002). While increased CO_2 availability leads to a short-term increase in photosynthesis in C_3 species, longer exposures can lead to biochemical and molecular changes that result in a substantial decrease in photosynthetic capacity (Griffin and Seemann, 1996; Van Oosten and Besford, 1996; Ludewig and Sonnewald, 2000). This decrease in photosynthetic capacity has been associated with a decline in the activity of RuBisCO in many species (Sage et al., 1989; Long and Drake, 1992; Nie et al., 1995). In C_3 plants the response of photosynthetic CO_2 assimilation to leaf intercellular CO_2 concentration is governed by two distinct phases when measured under saturating light (Von Caemmerer and Farquhar, 1981). These are the carboxylation efficiency of RuBisCO and the regeneration rate of RuBP. High atmospheric CO_2 levels tend to increase the intercellular CO_2 in C_3 plants, which in turn increases the carboxylation efficiency of RuBisCO as the oxygenase reaction (photorespiration) is decreased. This is due to a greater amount of CO_2 being available as substrate for RuBisCO (Chaves and Pereira, 1992; Wullschleger et al., 1992; Hymus et al., 2001; Arena et al., 2005).

Since CO_2 is the substrate for the process of photosynthesis, it is highly likely that a change in the amount of available CO_2 will cause changes in this process which might

require rapid degradation of unnecessary protein, and/or necessitate post-translational processing of proteins that are required in greater abundance. An increase in the availability of CO_2 changes the control exerted by different enzymes of the Calvin cycle on the overall rate of CO_2 assimilation. This then alters the requirement for different functional proteins. Since increased CO_2 content decreases photorespiration in C3 plants, an increase in CO_2 availability will also decrease the requirement for enzymes and proteins involved in the photorespiratory flux. Furthermore, the decrease in RuBisCO protein at elevated atmospheric CO_2 (Nie et al., 1995) indicates that the expression and turnover of this protein might involve changes in the proteolytic mechanism of the plant cell. This change may be especially evident when plants are switched from an ambient atmosphere to a CO_2-enriched atmosphere, and may involve the selective degradation of RuBisCO protein by RuBisCOlytics. Developmental and environmental signals may cause changes in the quantity and quality of specific proteins in the choloroplast. This could be regulated by proteases and chaperones. Although a limited number of plastid proteases are known (Sakamoto, 2006), a number of ATP-dependent proteases (such as Clp, FtsH and Lon) are considered major enzymes involved in degradation of proteins to oligopeptides and amino acids.

Growth at elevated CO_2 may lead to increased levels of soluble carbohydrate (Bowes, 1993; Drake et al, 1997) which may cause feedback inhibition of photosynthesis (Stitt, 1991). Usually carbohydrate that is synthesised in source tissues are transported to sink tissues. However, when carbohydrate synthesis rate exceeds the rate at which soluble sugars and carbohydrates can be exported, this causes a source-sink imbalance that has to be corrected (Farrar and Williams, 1991). The photosynthetic machinery responds by, amongst other things, altering the quantity and/or activity of RuBisCO (Gesch et al, 1998). A change in the abundance of RuBisCO could be regulated on transcriptional, translational, or protein turnover level (Webber et al., 1994). Increased CO_2 availability causes an earlier peak and then decline of RuBisCO activity and content during leaf expansion compared to controls grown at ambient CO_2 (Winder et al, 1992). While it's known that RuBisCO small subunit transcripts are affected by CO_2 availability (Winder et al., 1992), the level of regulation by translation and posttranslational turnover is complicated by the fact that photosynthetically competent Rubsico has a relatively slow turnover rate (Peterson et al., 1973). However, research has shown that RuBisCO is regulated at the transcriptional, posttranscriptional, translational, and/or posttranslational

levels, depending on developmental factors and environmental signals (Gesch et al., 1998). The response of rice leaves to increased CO_2 availability was shown to be dependent on the developmental stage of the leaf, with mature leaves responding more strongly than expanding leaves where photosynthesis is concerned. In general, photosynthesis was 25% to 30% greater in mature leaves and 20% to 24% greater in expanding leaves of plants grown under high CO_2. Some results illustrate, however, that there is no change in the turnover rate of RuBisCO due to CO_2 availability. The large decline in RuBisCO protein under these circumstances - up to 60% (Sage et al., 1989; Besford et al., 1990; Rowland-Bamford et al., 1991) is therefore not necessarily due to increased proteolysis, but more likely a result of decreased transcription.

Another potential effect of CO_2 enrichment on RuBisCO is a change in the activation state of the enzyme (Crafts-Brandner and Salvucci, 2000; Rogers et al., 2001). RuBisCO activity is regulated by RuBisCO activase and by the binding of inhibitors such as carboxy arabinitol-1-phosphate (CA-1-P; Salvucci and Ogren, 1996; Parry et al., 1997; Portis, 2003). These factors determine the rate of flux through the enzyme in any given time and govern its activation state. The activation state reflects the number of RuBisCO holoenzymes that are actively fixing carbon out of the total pool of RuBisCO present in the plant cell. Decreased RuBisCO activity following CO_2 enrichment may therefore arise from a decline in the activation state of this enzyme (Vu et al., 1983; Sage et al., 1988; Van Oosten et al., 1994; Crafts-Brandner and Salvucci, 2000). This response is rapid as activation state can be regulated within a matter of seconds (Bowes, 1993) and could provide a rapid and regulated switching off of the active sites of RuBisCO in response to CO_2 enrichment. RuBisCO activase is an ATP-dependent AAA+ protein (Neuwald et al, 1999) that facilitates the removal of sugar phosphates (such as CA-1-P or RuBP) from RuBisCO active sites. Since it is dependent on ATP and is inhibited by ADP, the ratio of ATP to ADP in the chloroplast affects activase activity, and hence activation state of RuBisCO (Robinson and Portis, 1989). Furthermore, the level of mRNA abundance and enzyme activity of carbonic anhydrase that facilitates diffusion of CO_2 from intercellular air spaces (Edwards and Walker, 1983) decreases during growth at elevated CO_2 in pea (Majeau and Coleman, 1996), cucumber (Peet et al., 1986), and bean (Porter and Grodzinski, 1984). However, it remains unchanged or even increases in tobacco (Sicher et al., 1994) and *Arabidopsis* (Raines et al., 1992).

1.4.4 Degradation of ribulose-1, 5-bisphosphate carboxylase/oxygenase (RuBisCO)

As described above, it is quite possible that changes in the environment, such as an increase in the amount of available CO_2, will require rapid acclimation by the photosynthetic machinery, including the key enzyme in this process, RuBisCO. Furthermore, the degradation of RuBisCO is often used as a model for the turnover of proteins in plants. While over 50% of the protein content of green leaves is made up of this one enzyme (Fischer and Feller, 1994; Spreitzer and Salvucci, 2002) the nature of the proteolytic enzymes that are involved in RuBisCO degradation has not yet been determined. RuBisCO is an essential component of photosynthesis and it also serves as a reservoir of nitrogen. The RuBisCO holoenzyme consists of 8 large subunits and 8 small subunits (Fig. 1.8). The large subunit is encoded by a single chloroplastic gene (Chan and Wildman, 1972; Ellis, 1981), while the small subunits are encoded by a small family of genes in the nucleus (Manzara and Gruissem, 1988; Rodermel, 1999).

Figure 1.8 A graphical representation of RuBisCO. (Image from Protein Data Bank; http://www.msu.edu/~ngszelin/calvin_cycle_players.htm)

Unassembled small subunit proteins were selectively and rapidly degraded within the chloroplasts of the green alga, *Chlamydomonas reinhardtii*, when pools of large subunit were depleted (Schmidt and Mishkind, 1983). Intensive study has failed to characterise the complex network of processes that control RuBisCO breakdown. The protein can be degraded in intact chloroplasts by stromal proteases (Mitsuhashi et al., 1992; Desimone et al., 1996; Ishida et al., 1998; Adam and Clarke, 2002). A chloroplast-located

metallopeptidase has also been shown to degrade the RuBisCO large subunit (Bushnell et al., 1993; Roulin and Feller, 1998).

RuBisCO degradation can be initiated or accelerated by reactive oxygen species (ROS) in isolated intact chloroplasts (Desimone et al., 1996; Ishida et al., 1997). However, the RuBisCO protein, especially the large subunit, is also sensitive to degradation by vacuolar peptidases (Yoshida and Minamikawa, 1996). Considerable debate remains concerning the occurrence and function of degradation of the RuBisCO protein/peptides outside the chloroplast. A role of vacuolar proteases or other proteases present in cytosolic vesicles such as the ricinosomes or the lytic vacuoles has been postulated (Gietl and Schmid, 2001). During leaf senescence, the photosynthetic machinery is dismantled and chloroplasts are converted into gerontoplasts. Different models have been suggested for the degradation of chloroplast functions in senescing mesophyll cells (Krupinska, 2006): Plastids may be engulfed in the central vacuole by phagocytosis or by membrane fusion of plastid-containing autophagosomes with the vacuole. Considerable evidence suggests that chloroplasts (Minamikawa et al., 2001) and/or chloroplast-derived vesicles (Chiba et al., 2003) interact with the vacuole during senescence and facilitate rapid degradation of chloroplast proteins. Chloroplasts release vesicles from the tips of the stromules (Gunning, 2005; Fig. 1.9). These vesicles contain RuBisCO and other stromal material. These and other types of chloroplast-derived vesicles can also contain thylakoid-derived material. While the release of vesicles was originally considered to occur only during senescence when the plastid envelope is ruptured, recent evidence suggests that they are produced at all stages of development but their production is enhanced during senescence (Gunning, 2005). Accumulating evidence also suggests that RuBisCO and other stromal proteins can be degraded, at least in part, outside the plastid. The chloroplast-derived vesicles may be the vehicle through which this process is facilitated.

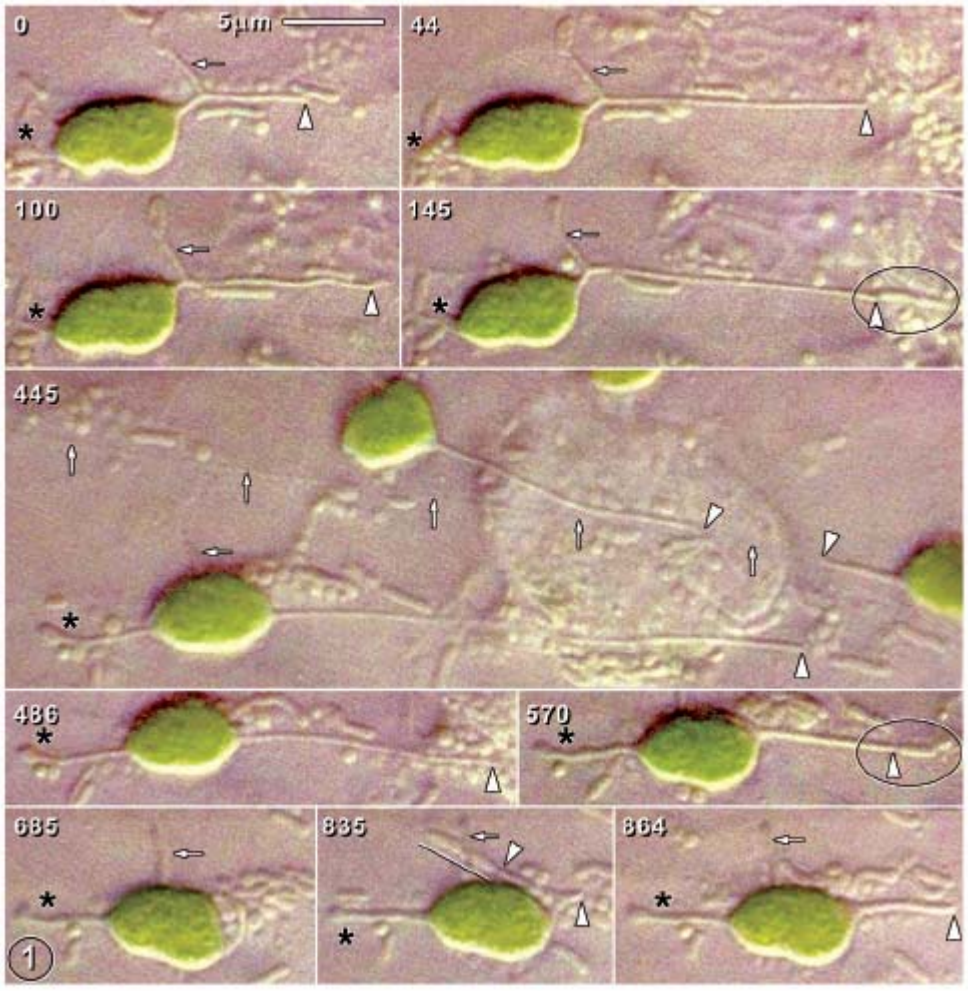

Fig. 1.9 Growth and retraction of stromules on *Iris unguicularia* chloroplasts (Gunning 2005). Elapsed times (seconds) are shown. Time 445 shows stromules on three chloroplasts, with a nucleus in the background. Vertical arrows mark a (presumed) actin cable along which organelles were streaming. The remaining images depict growth and retraction of the lower stromule, which also lay along a track of cytoplasmic streaming. Stromule tips are marked by arrowheads in each image. This chloroplast possessed multiple stromules. In addition to the main one there was a short stromule (asterisk) pointing in the opposite direction, and a branch (horizontal arrows). Both of these had terminal lobes, flattened close to the cell surface.

1.5 Increased CO_2 availability as an environmental signal for plant metabolic change

While high CO_2 can inhibit the maximal rate of photosynthesis (especially in C3 plants), effects are highly variable such that no general single high CO_2 response can be described (Sage et al., 1989). Studies on the effects of CO_2 enrichment on C_4 species has yielded rather mixed results. An enhancement of photosynthesis was found in some studies (Le Cain and Morgan, 1998; Wand et al., 2001) but acclimation and down-regulation were observed in others (Greer et al., 1995; Ghannoum et al., 1997; Walting and Press, 1997).

However, some C_4 species can benefit from CO_2 enrichment in terms of carbon gain (e.g. Ghannoum et al., 1997; 2001; Wand et al., 1999; 2001). For example, while growth at a high CO_2 level had little effect on photosynthetic capacity in *Paspalum dilatatum* leaves (von Caemmerer et al., 2001; Soares et al., 2008), high CO_2 –grown plants had double the total biomass of plants grown in air (Soares et al., 2008).

It is generally accepted that an increased CO_2 content in the atmosphere will have a fertilizing effect on plants (especially C_3 plants), as it will alleviate the CO_2 limitation on photosynthesis. To this effect, increased CO_2 availability is not considered to be an abiotic stress factor. This perspective is supported by results that show increased resource use efficiency in plants grown under elevated CO_2. In particular increased water, light, and nitrogen use efficiencies have been observed in plants grown at elevated CO_2 when compared to plants grown at ambient CO_2 levels (Drake et al., 1997). These plants also showed improved resistance to environmental stresses such as drought, chilling or air pollution (Boese et al., 1997; Hsiao and Jackson, 1999). It has been shown that growth CO_2 concentration can affect stress susceptibility in leaves of poplar trees. Elevated CO_2 levels protected leaves from stress-induced decrease in photosynthesis induced by cold stress or paraquat under hight light conditions (Schwanz and Polle, 2001). Growth under elevated CO_2 concentration improves the internal availability of carbon, thereby, providing better supply of stressed plants with substrates for detoxification and repair (Carlson and Bazzaz, 1982). While enhanced CO_2 increases carbon allocation, especially to roots (Bazzaz, 1990), it also enhances overall plant development and senescence in several species (Rogers et al., 1994). Increased CO_2 availability can also accelerate flowering and increase flower and fruit weight (Bazzaz, 1990; Deng and Woodward, 1998), although the effects of CO_2 on flowering and seed output of wild species vary strongly between species (Jablonski et al., 2002). Even though it was observed that CO_2 enrichment enhances senescence, the decrease of chlorophyll levels general associated with senescence is not always observed under these circumstances, where cholorphyll content increases, decreases or stays unchanged under elevated CO_2 (Vu et al., 1989; Heagle et al., 1993; Mulholland et al., 1997; Lawson et al., 2001; Bindi et al., 2002; Prins et al, 2008). Early senescence (indicated by premature yellowing and a decrease in chlorophyll content) was observed in the leaves of CO_2-enriched sweet chestnut seedlings. However, this response was associated with nutrient dilution caused by the rapid growth of seedlings, and this may have played a role in the early senescence of the plants. It has

been hypothesised that leaf senescence may be triggered earlier due to the different effects of an increase in CO_2 availability, especially during grain filling due to an increased grain nutrient sink capacity (Wingler et al., 2006). In contrast, it has been hypothesised that the increased C/N ratio in species that show increased photosynthesis rate in elevated CO_2 may lead to delayed autumnal senescence (Herrick and Thomas, 2003). Delayed senescence has been observed in populus species grown with CO_2 enrichment (Taylor et al, 2008).

1.6 Effects of CO_2 enrichment on plant morphology and stomatal patterning and function

Besdies changes in photosynthesis on a molecular level, plants grown at high CO_2 can also show changes in whole plant morphology. One example is the decreased shoot/root ratios that result from the acclimation of source-sink processes to increases in carbon gain as a result of higher rates of photosynthesis (Ghannoum et al., 1997; 2001; Walting and Press, 1997). Moreover, CO_2 availability has a strong influence on stomatal patterning and the dorso-ventral organisation of leaf structure and composition/activity (Taylor et al., 1994; Croxdale, 1998; Masle, 2000; Lake et al., 2001; Martin and Glover, 2007). Photosynthetic responses to changes in CO_2 availability may be connected at least in part to changes in stomatal conductance and/or stomatal density (Woodward, 1987; Boetsch et al., 1996). Early studies indicated that stomatal density decreased with increasing CO_2 concentrations (Woodward, 1987; Penuelas and Matamala, 1990; Lin et al., 2001). However, while a comparison of a hundred different species revealed a wide range of stomatal density responses to CO_2 enrichment, there was an average reduction in stomatal density of 14.3% (Woodward and Kelly, 1995). This decrease was independent of taxonomy, growth form, habitat, or stomatal distribution. These authors found that amphistomatous leaves showed greater CO_2–dependent changes in stomatal densities than hypostomatous leaves when grown in controlled environments between 350 and 700 $\mu l\ l^{-1}$ CO_2 (Woodward and Kelly, 1995). In particular, maize plants grown from 340 to 910 $\mu l\ l^{-1}$ CO_2 showed a 26% reduction in stomatal density.

It has been suggested that high CO_2-dependent decreases in stomatal density confer a selective advantage because of improved water use efficiencies (Hetherington and Woodward, 2003). A study on CO_2 enrichment in sorghum, which is a C_4 species like maize, showed that plants grown under Free-Air CO_2 Enrichment (FACE) conditions with

ambient plus 200 µl l^{-1} CO_2 had higher water use efficiencies (Conley et al., 2001). This increase was greater for plants subjected to a drought treatment than those that were well watered. Sorghum plants subjected to drought showed a 19% increase in water use efficiency based on grain yields, compared to 9% in the well-watered plots (Conley et al., 2001). However, whole plant biomass was increased by similar amounts (16% and 17% in wet and dry plots, respectively) suggesting that the increased water use efficiency effect was accompanied by altered assimilate partitioning between organs rather than effects on total carbon gain. These results suggest that C_4 species like sorghum and maize might reap additional benefits from future environments that are CO_2-rich and drought-prone. In contrast, a study looking at 48 accessions of *Arabidopsis thaliana* (a C_3 species) showed no clear trends in these responses (Woodward et al., 2002).

While the nature of the high CO_2 effect varies between species it is widely accepted that CO_2 levels influences stomatal density and patterning (Larkin et al., 1997; Lake et al., 2002). The CO_2-signalling pathways that orchestrate these changes in leaf structure and composition responses remain poorly characterised (Gray et al., 2000; Ferris et al., 2002) but signals transported from mature to developing leaves are considered to be important regulators of such responses (Coupe et al., 2006; Miyazawa et al., 2006). Hence, the CO_2 levels in the atmosphere are considered to be detected primarily by mature leaves. The CO_2 signal, which is then transmitted to the young, developing leaves, modulates stomatal development in a way that is independent of the CO_2 content experienced by the young leaves (Lake et al., 2001).

1.7 Concluding statement and research objectives

The global climate of the future will be much more variable than it is today. To ensure the sustainable production of crops in this future scenario, it is essential to have a much more comprehensive understanding of how plants perceive and respond to changes in their growth environment. The following study was undertaken in order to obtain an improved understanding of plant responses to a changing environment particularly with regard to the role of proteases in metabolic change and senescence triggered by developmental and environmental cues. The first focus of this thesis was the role of cysteine proteases in leaf protein turnover during development and abiotic stress. The effect of constitutive expression of a cysteine protease inhibitor, oryzacystatin I, was studied in tobacco with respect to development and cold stress tolerance. The second focus of this thesis was an

investigation into the effects of CO_2 enrichment on maize leaf transcriptome, physiology, photosynthesis, metabolism, and protein turnover

The hypotheses that formed the foundation for the following study were formulated as follows:

Constitutive expression of the cysteine protease inhibitor OC-I in tobacco alters plant development and protects photosynthesis against dark chilling (Van der Vyver et al, 2003). These plants can therefore be used to explore the stress-induced mechanisms of protein turnover that are regulated by cysteine proteases.
Hypothesis 1: Exogenous OC-I protects RuBisCO from degradation by endogenous proteases that function during development and cold stress.

Atmospheric CO_2 is a major component of climate change that influences plant morphology and metabolism. CO_2 affects many aspects of leaf biology from photosynthesis, sugar metabolism, and the expression of sugar metabolism-related genes to protein content and composition, stomatal density and patterning.
Hypothesis 2: Maize will respond to growth with CO_2 enrichment by acclimation in leaf biology underpinned by changes in gene expression.

Growth with CO_2 enrichment leads to early leaf senescence in some species. Comparisons of the leaf transcriptome at different developmental stages in maize plants grown in air and with CO_2 enrichment might be predicted not only to reveal developmentally regulated proteases and protease inhibitors but also identify those that were preferentially influenced by CO_2-dependent signals.
Hypothesis 3: Changes in plant metabolism due to CO_2 enrichment and development involves changes in the expression and/or activity of proteases and protease inhibitors.

The study was undertaken using two plant species, maize and tobacco. Tobacco was chosen for the analysis of the effects of the OC-I transgene on plant growth and development because OC-I –transgenic tobacco plants had already been generated in the laboratory. While a preliminary characterisation had indicated that plant growth and development were affected by the expression of the transgene, no detailed analysis of

effects on protein composition or turnover had been performed. These plants were therefore an ideal and readily available tool with which to study the role of cystatins.

Maize was chosen as it is the second most important commercial cereal crop world wide and it is grown widely in Southern Africa (Pingali, 2001; Pons, 2003). While there is an extensive literature on maize biology in general, relatively little information is on how maize will be affected by climate change particularly the increased levels of atmospheric CO_2 that will be present in the not too distant future. Maize genomics is well advanced (Keith et al., 1993) cystatin sequences have been identified (Abe et al., 1992; Abe et al., 1995; Abe et al., 1996; Yamada et al., 2000) and maize (corn) micro-array chips are commercially available. Maize also is a C_4 species and as stated previously our current knowledge about the effects of increasing atmospheric CO_2 levels on C_4 plants remains limited and much more information is required in order to be able to accurately predict how the forthcoming change in the earth's atmosphere with regard to greenhouse gases like CO_2 will modify the productivity of C_4 plants. This subject is important as well as extremely topical because it is predicted that maize will be used increasingly in bio-energy production as well as a food crop over the next 50 years. Literature reports on the effects of increased abundance of atmospheric CO_2 on C_4 species show large inter-specific variations. Further characterisation is therefore essential and urgent.

Maize and tobacco are chilling sensitive species. Since exposure to low temperature in the hours of darkness posses a problem to the productivity of both species and it is also a cause of crop losses in Africa, as in other parts of the world, this study focussed on the impact of the OC-I transgene on plant responses to dark chilling. In particular, the experiments focussed on how the expression of the exogenous protease inhibitor effects photosynthesis and RuBisCO turnover and so alters the tolerance of tobacco plants to dark chilling.

In addition to allowing a detailed characterisation of the effects of changes in two key environmental variables, CO_2 and temperature, on plant morphology and metabolism, these analyses also allowed an appraisal of the regulation of protein content and turnover in the natural senescence programme. A further aim was therefore the identification of potential senescence markers that can be used in future studies. The data obtained in the following investigations were used to compare the role of specific proteases and their

inhibitors in plant stress and senescence responses. While the original primary focus was the identification of novel cysteine proteases and their inhibitors, it soon became apparent that other proteases and inhibitors were also important in the plant responses to the variables under study. Two novel CO_2-modulated inhibitors were selected on this basis for further characterisation.

The specific objectives of the following study were:

1) To identify the mechanism through which exogenously expressed OC-I protects photosynthetically important proteins. It is expected that proteins such as RuBisCO might be protected from degradation by endogenous proteases.
2) To study the effect of exogenously expressed OC-I on senescence in tobacco plants. Since cysteine proteases play an important role in senescence, it is expected that constitutive expression of OC-I will delay senescence.
3) To characterize the effects of high CO_2 on whole plant growth, morphology and development in maize and to compare the effects of growth with CO_2 enrichment in young and old source leaves. It is expected that there will be little change in plant morphology since maize already experiences a high CO_2 environment on a molecular level. However, photorespiration might be further minimised in C_4 plants which might affect metabolism.
4) To characterize CO_2-dependent effects on maize leaf epidermal structure, in relation to photosynthesis and metabolism. It is expected that epidermal structure will change, based on previous results (Martin and Glover, 2007).
5) To study the effects of high CO_2 on the transcriptome of leaves at different positions on the stem in order to identify new genes that can be used as markers for senescence. Changes in CO_2 availability will send signals to cell nuclei as the plant acclimates to the different environmental conditions. This will be reflected in changes in transcript abundance between high CO_2-grown maize plants and those grown in air. It is expected that increased CO_2 might lead to early senescence due to increased leaf carbohydrate. This will provide new sequences that are linked to senescence.
6) To identify novel senescence- and high CO_2–regulated proteases and protease inhibitors. Changes in available CO_2 will necessitate changes in the photosynthetic system. It is expected that these changes will partially be effected by selective

proteolysis, which will result in changed expression or activity of proteases and their inhibitors.

CHAPTER 2: Regulation of protein content and composition in tobacco leaves through cysteine proteases

Submitted to Journal of Experimental Botany (in press): Prins, A., Van Heerden, P.D.R., Olmos, E., Kunert, K.J., Foyer, C.H. Cysteine proteases regulate chloroplast protein content and composition in tobacco leaves through interactions with ribulose-1,5-bisphosphate carboxylase/oxygenase (RuBiSCO) vesicular bodies.

2.1 Abstract

In light of previous results indicating that the exogenous expression of a rice cysteine protease inhibitor, OC-I, has a protective effect under low temperature stress (Van der Vyver et al, 2003), the mechanism by which this is affected was investigated in this part of the study. In particular, the roles of cysteine proteases (CP) in leaf protein accumulation and composition were investigated in transgenic tobacco plants expressing OC-I. The OC-I protein was present largely in the cytosol of the leaves of OC-I expressing (OCE) plants with small amounts associated with the chloroplasts and vacuole. Changes in leaf protein composition and turnover caused by OC-I-dependent inhibition of CP activity were assessed in young (6-8 week old) plants in a preliminary proteomic analysis. Seven hundred and sixty five soluble proteins were detected in the controls compared to 860 proteins in the OCE leaves at this stage. A cyclophilin, a histone, a peptidyl-prolyl cis-trans isomerase and two ribulose-, 5-bisphosphate carboxylase/oxygenase (RuBisCO) activase isoforms were markedly altered in abundance in the OCE leaves. Western blot analysis of plants after flowering revealed large increases in the amount of RuBisCO protein in the OCE leaves. The senescence-related decline in photosynthesis was delayed in the OCE leaves. Similarly, OCE leaves maintained higher leaf RuBisCO activities and protein than controls following exposure to dark chilling. Immunogold labelling studies with specific antibodies revealed that RuBisCO was present in RuBisCO vesicular bodies (RVBs) as well as in the chloroplasts of leaves from 8-week old control and OCE plants. The data presented here demonstrate that that CPs are involved in RuBisCO turnover in all leaves under optimal and stress conditions and that this process could involve interactions with RVBs.

2.2 Introduction

Cysteine proteases (CP) are involved with a variety of proteolytic functions in higher plants (Granell et al., 1998), particularly those associated with the processing and degradation of seed storage proteins (Shimada et al., 1994; Toyooka et al., 2000), and fruit ripening (Alonso and Granell, 1995). They are also induced in response to stresses, such as wounding, cold and drought (Schaffer and Fischer, 1988; Koizumi et al., 1993; Linthorst et al., 1993; Harrak et al., 2001), and in programmed cell death (Solomon et al., 1999; Xu and Chye, 1999). Like their CP targets, phytocystatins are regulated by developmental (Lohman et al., 1994) and environmental cues (Botella et al., 1996; Belenghi et al., 2003; Pernas et al., 2000; Diop et al., 2004).

Cysteine proteases have also been identified in tobacco, including a KDEL-type CP *Nt*CP2 (Beyene et al., 2006). The C-terminal KDEL motif, present in some cysteine proteases, is an endoplasmic reticulum retention signal for soluble proteins that allows CP propeptides to be stored either in a special organelle, called the ricinosome (Schmid et al., 1999), or in KDEL vesicles (KV) before transport to vacuoles through a Golgi complex-independent route (Okamoto et al., 2003). The relatively acidic pH optima of many of the endogenous plant CPs indicate that they are localized in the vacuole (Callis, 1995). A papain-like sequence, termed *Nt*CP1, has also been isolated from senescent tobacco leaves (Beyene et al., 2006). Papain-like cysteine proteases are often found in senescing organs particularly leaves (Lohman et al., 1994; Ueda et al., 2000; Gepstein et al., 2003), flowers (Eason et al., 2002), legume nodules (Kardailsky and Brewin, 1996) as well as in germinating seeds (Ling et al., 2003). Senescence -associated genes (SAGs) are up-regulated during leaf senescence (Lohman et al., 1994; Quirino et al., 1999; Swidzinski et al., 2002; Gepstein et al., 2003; Bhalerao et al., 2003; Lin and Wu, 2004). Of these the SAG12 cysteine protease is one of the very few SAGs that are highly senescence-specific (Lohman et al., 1994). While it is known that the major light-harvesting chlorophyll a/b protein of photosystem II as well as RuBisCO large subunit (LSU) is sensitive to degradation by cysteine proteases, the mechanism by which this occurs is unknown. Furthermore, it's unknown whether other chloroplast-located proteins are sensitive to cysteine protease-mediated degradation.

The expression of many photosynthesis genes such as those encoding the chlorophyll a/b binding protein and the ribulose-1, 5-bisphosphate carboxylase-oxygenase (RuBisCO)

subunits decreases during senescence and are hence classed as senescence down-regulated genes (Humbeck et al., 1996). RuBisCO degradation can occur both inside and outside the chloroplast (Irving and Robinson, 2006). Inside the chloroplast, oxidation of critical cysteine residues on the RuBisCO protein modifies the proteolytic susceptibility of these or associated amino acids, causing the protein to adhere to the chloroplast envelope and "marking" the protein for degradation (Garcia-Ferris and Moreno, 1994). Recent evidence suggests that the 26S proteasome is activated by carbonylation and hence this protein degradation pathway is enhanced when the cellular environment becomes even mildly oxidizing (Basset et al., 2002). In the chloroplast RuBisCO is protected against degradation by 2-carboxyarabinitol 1-phosphate (CA-1-P) but how this modulates degradation outside the chloroplast is unknown (Khan et al., 1999).

Little information is further available on the effects of ectopic phytocystatin expression on plant growth and development (Masoud et al., 1993; Guttiérrez-Campos et al., 2001; Van der Vyver et al., 2003) as most studies have concentrated on effects on insect resistance or protein production (Christou et al., 2006; Rivard et al., 2006). The phenotype resulting from expression of the rice cystatin, OC-I, in transformed tobacco plants has been described previously (Masoud et al., 1993; Guttiérrez-Campos et al., 2001; Van der Vyver et al., 2003). However, increased biomass production resulting from cystatin expression under field conditions is often attributed to enhanced insect resistance rather than to direct effects of the cystatin on endogenous protein turnover in the plant tissues. It has been shown that the transgenic OC-I expressing tobacco lines (OCE) grow more slowly with an extended vegetative phase compared to the wild type or empty vector controls (Van der Vyver et al., 2003). They are also more resistant to dark chilling-induced inhibition of photosynthesis (Van der Vyver et al., 2003). The following study was undertaken in order to determine how the constitutive expression of the rice cystatin, OC-I, in the cytosol of tobacco leaves alters leaf protein content and composition and exerts effects on photosynthesis in leaves at different stages of development. Furthermore, the possible sensitivity of RuBisCO to degradation by CP was investigated.

2.3 Materials and Methods

All methods were performed by A. Prins, unless otherwise indicated.

2.3.1 Plant material and growth conditions

Seeds of wild-type non-transformed tobacco (*Nicotiana tabacum* L. cv. Samsun), and a self-fertilized transformed tobacco OCE line (T4/5; Van der Vyver et al., 2003) expressing the gene encoding oryzacystatin-I (OC-I) and the β-glucuronidase coding sequence (*gus* gene) under the control of the 35S promoter, were germinated in trays with commercial peat/loam compost as described for maize plants (Chapter 2). Individual seedlings were transferred to small pots at 4-leaf stage and grown in controlled environment chambers in air. The plants were grown with a 15-h photoperiod at a light intensity of 800 - 1000µmol m^{-2} s^{-1} (at leaf level) with a day/night temperature of 26°C/20°C, and 80% (v/v) relative humidity (Fig. 2.1). When the roots started to appear at the base of the small pots, the plants were transferred to 8.5l volume (25cm diameter) pots. They were then grown to maturity (13 weeks; 20-28 leaf stage depending on the genotype). Plants were irrigated twice daily and maintained in water-replete conditions throughout. Samples were harvested for assay at various stages of development as indicated in the text and figure legends.

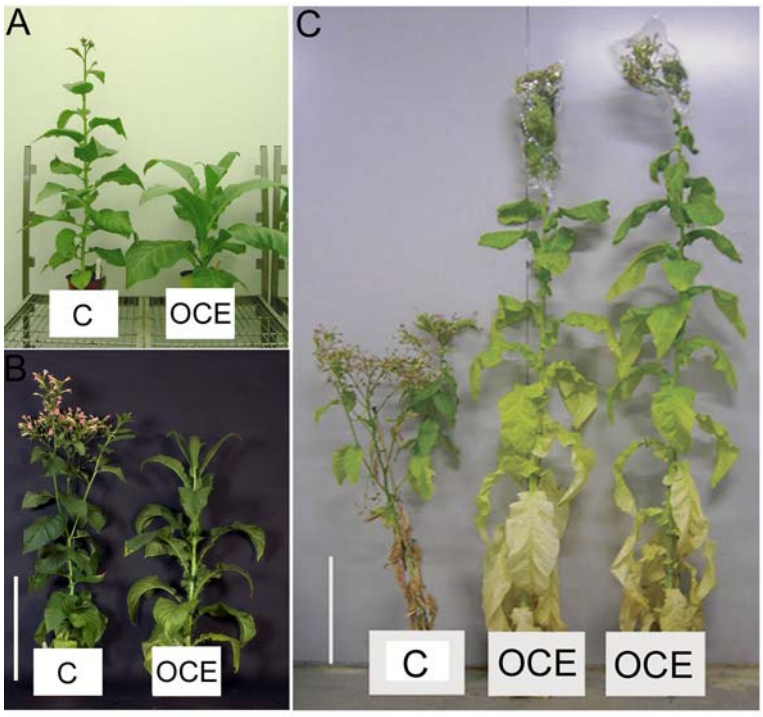

Figure 2.1 Wild type (C) and OC-I expressing (OCE) phenotypes at different developmental stages. Plants are shown at the following stages: A) 8 weeks, B) 10 weeks, and C) 14 weeks. Scale bar represents 0.5m.

2.3.2 Histochemical staining for GUS activity

Young transgenic tobacco plants (approximately 4 weeks old) were screened for transgene expressions using the GUS histochemical assay. Plant leaf tissue was incubated at 37ºC overnight in GUS-staining solution [1mg ml^{-1} 5-bromo-4-chloro-3-indolyl glucoronide in 50mM NaH_2PO_4 buffer, pH7 containing 0.01% (v/v) Tween 80 and 10mM Na_2EDTA]. Transformed plants posess the β-glucuronidase coding sequence (*gus* gene), which produces the hydrolase GUS. This enzyme catalyses the cleavage of 5-bromo-4-chloro-3-indolyl glucoronide, leading to a blue precipitate. Only plants showing expression of the *gus* gene were selected for further investigation.

2.3.3 Chilling treatments

The chilling treatment was performed by P.D.R van Heerden (Potchefstroom University), with leaf samples from plants exposed to chilling treatment being used by A. Prins for further analysis. Six week-old OCE and wild-type plants were subjected to chilling stress (5°C) in darkness for seven consecutive nights. At the end of each photoperiod, six transformed and wild type plants (from batches of 12 each) were transferred to a refrigerated chamber controlled at 5ºC for one entire dark period. The remaining six plants (controls) were kept under normal conditions in the growth chamber at 20ºC and represented the control treatment. Only the shoots and leaves of plants were dark chilled. The roots were kept at 20ºC during dark chilling by inserting the pots into custom designed pot-incubators (Analytical Scientific Instruments, Weltevreden Park, South Africa) that circulated warm air around the pots. This minimised the occurrence of chill-induced drought stress and associated leaf wilting which is a potential artifact that could interfere with interpretations based on the effects of dark chilling *per se* (Allen and Ort, 2001). After nine hours exposure to chilling, the treated plants were returned to the growth chamber where they remained throughout the 15h light period. This process was repeated for seven consecutive dark periods.

2.3.4 Growth analysis

The following measurements were performed at 13-14 weeks. In all experiments leaf phylogeny was classified from the base to the top of the stem, leaf one being at the bottom and leaf twelve at the top. Measurements were performed sequentially as follows:

i) Stem height

Stem height was measured from the base to the top of the stem with a ruler.

ii) Numbers of leaves

Leaves were counted from leaf 1 to 30.

iii) Leaf weight and area

The fresh weight and area of each leaf was measured following excision. Total leaf fresh weights were determined on a standard laboratory balance. Leaf area was measured using a ΔT area meter (Delta-T Devices LTD, England) according to instructions of the manufacturer.

iv) Days to flowering

The flowers were tagged at anthesis. Time to flowering is denoted as time taken for the first flower to open.

2.3.5 Photosynthesis measurements

Photosynthesis measurements were performed by P.D.R. van Heerden (Potchefstroom University). Photosynthetic gas exchange measurements were performed on attached leaves essentially as described in Novitskaya et al. (2002) and Van Heerden et al. (2003). CO_2 assimilation was measured every day after each of the dark chilling treatments on four individual plants of both the control and dark chilling treatments. Measurements were taken with an open circuit infrared gas analysis system (CIRAS-I, PP-systems, Herts, UK) in a 2.5cm^2 cuvette with built-in light and temperature control. Humidity in the cuvette was maintained close to ambient conditions. All measurements were started 3 h after the end of each dark period and conducted at 28°C. CO_2 assimilation at ambient growth conditions was measured at an irradiance of 350µmol m^{-2} s^{-1} and CO_2 (Ca) flow rate of 350µmol mol^{-1}. For the measurement of the relationship between CO_2 assimilation rate (A) and intercellular CO_2 concentration (Ci), irradiance in the leaf cuvette was controlled at 1250µmol m^{-2} s^{-1} and Ca increased with increments from 0 to 1000µmol mol^{-1}.

2.3.6 Protein and chlorophyll quantification

i) Protein

Whole leaves were homogenized with a pestle in a mortar, in liquid nitrogen, and aliquots stored in eppendorf tubes at –80°C until 1ml aliquots of the homogenized powder were assayed for soluble protein content. For protein extraction, leaf tissue (1ml tobacco leaf powder) was ground in ice-cold mortars with pestles, using liquid nitrogen. When leaf tissue had been thoroughly homogenized, 1ml extraction buffer (0.1M citrate phosphate buffer, pH6.5) was added and samples further homogenised with a pestle. Homogenate was poured into an eppendorf tube, and the mortar and pestle rinsed with an additional 1ml extraction buffer which was added to the same tube. Samples were centrifuged at 12 000rpm for 10min at 4ºC, and protein content of supernatant determined.

In general, protein content of extracts was determined according to the method described by Bradford (1976). Plant extracts (5µl) were diluted with water to a volume of 800µl before the addition of Bradford colour reagent (200µl; Bio-Rad, UK) to give a final volume of 1ml. The reaction solution was incubated at room temperature for 30 min, after which the absorbance of the solution was determined on a spectrophotometer at a wavelength of 595nm. Values were compared to a bovine serum albumin (BSA) standard consisting of 0, 1, 2, 5, 10, 15, or 20µg BSA in diluted Bradford colour reagent (20%, v/v), which was also incubated and measured as described above. All measurements were done in duplicate.

ii) Chlorophyll

Whole leaves were homogenized with a pestle in a mortar, in liquid nitrogen, and aliquots stored in eppendorf tubes at –80°C until 1ml aliquots of the homogenized powder were assayed for chlorophyll content. Chlorophyll content was determined according to the method of Lichtenhaler and Wellburn (1983). Leaf tissue (1ml tobacco leaf powder) was first ground in an ice-cold mortar with a pestle, using liquid nitrogen. 1ml ice-cold acetone (80%) was added and leaf tissue further homogenised. Homogenate was decanted into an eppendorf tube, and mortar and pestle rinsed with an additional 1ml ice-cold acetone, which was added to the same tube. All samples were incubated at -20°C over night in the dark for complete chlorophyll extraction, before centrifuging at 14 500rpm for 5min at room temperature. Samples (50µl) were diluted with acetone (80%) before absorbance

was measured using a quartz cuvette in a spectrophotometer at wavelengths of 645nm and 663nm. Chlorophyll (mg l^{-1}) was calculated using the equation: chlorophyll (mg l^{-1}) = 20.2 x A_{645} + 8.02 x A_{663}.

2.3.7 RuBisCO activity and activation state

RuBisCO activity and activation state was measured by P.D.R. van Heerden (University of Pretoria). Leaf discs were collected with a freeze clamp (cooled in liquid nitrogen) from fully expanded leaves of OC-I transformed (OCE) and wild type plants at the start of the experiment (day 0) and again following seven days of growth at 26/20°C or 26/5°C. At the end of the experiment, leaf discs were also collected from young expanding leaves that developed during the 7-day treatment period. Sampling occurred 4h after the start of the light period under full illumination. Initial, total, and maximum RuBisCO activities of collected leaf samples were measured according to Keys and Parry (1990) as described by Van Heerden et al. (2003).

Leaf disks were ground in liquid nitrogen and ice cold extraction buffer (50mM Bicine/NaOH, pH 8.0; 10mM MgCl2; 1mM EDTA; 20mM DTT). RuBisCO activity was measured by incubating extract with reaction buffer containing $^{14}CO_2$ (Fig. 2.2), prepared from $NaH^{14}CO_3$ (Amersham, UK) in 100mM $NaHCO_3$, with a specific activity of 0.5 µci µmol^{-1}, and activating the reaction with Mg^{2+} and CO_2. Initial activity was measured by adding 100 µl of extract to a scintillation vial containing 900 µl reaction buffer consisting of 50mM Bicine (pH 8.0), 10mM $MgCl_2$, 10mM $NaH^{14}CO_3$ (0.5 µci µmol^{-1}), and 33mM ribulose-1,5-bisphosphate (RuBP; Sigma, UK). Reactions were stopped after 1 min by addition of 1ml of formic acid (10M). Total activity was measured after pre-incubation of extract with 1M $NaH^{12}CO_3$ for 10min at room temperature prior to starting the reaction with RuBP. Acidified samples were dried in an oven at 60ºC and resuspended in 5ml of a scintillation fluid (cocktail T, BDH Laboratory Supplies, UK). ^{14}C incorporation was measured by scintillation counting against $^{14}CO_2$ standards.

Initial activity represents the activity of the enzyme under the growth conditions at the time of sampling, without activating all available reactive sites or removing tight-binding inhibitors. Total activity is measured as the activity obtained after all available reactive sites have been activated with bicarbonate, and maximum activity is obtained by

activation of the extracted enzyme with bicarbonate after removal of all known tight-binding inhibitors.

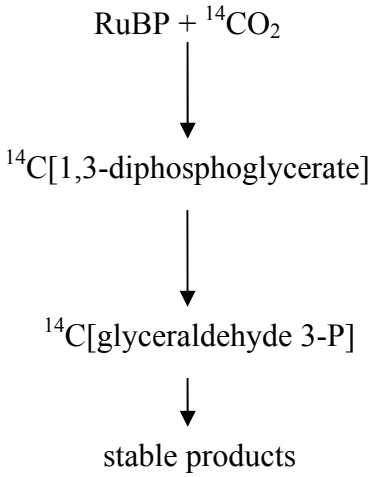

Figure 2.2 Determination of RuBisCO activity by incorporation of ^{14}C into acid stable products.

2.3.8 Western blot analysis

For the immunodetection of OC-I, RuBisCO, and RuBisCO activase in tobacco leaves, leaf discs were extracted in buffer containing 50mM Tris-HCl (pH7.8), 1mM EDTA, 3mM DTT, 6mM PMSF and 30mg insoluble PVPP. Proteins were separated by standard SDS-PAGE procedures according to the method described by Sambrook et al. (1989). Generally, 10-50µg of total soluble protein of crude leaf extracts was separated for analysis. Samples were first incubated at 95°C for 5min in loading buffer containing 62.5mM Tris-HCl (pH 6.8), SDS (2%, w/v), glycerol (10%, v/v), β-mercaptoethanol (5%, v/v) and bromophenol blue (0.001%, w/v), and then loaded onto a precast SDS-PAGE gel (10%) (BioRad, UK). Electrophoresis was performed at 100V through the stacking gel and 120-180V through the resolving gel until the blue front of the loading dye reached the bottom of the gel.

Proteins were transferred to nitrocellulose membranes (Hybond C-extra, Amersham Pharmacia Biotech, UK) in a BioRad Mini protein II transfer apparatus filled with transfer buffer (Sambrook et al., 1989), at 4ºC and 60V for 40min. After transfer, the membrane was incubated in a 5% fat free milk powder/TBS buffer (blocking buffer) over night at 4°C with shaking to prevent non-specific binding of primary antibody. Incubation with

primary antibody occurred in blocking buffer for 2-4h at room temperature with shaking. Concentrations of primary antibodies (polyclonal and raised in rabbit) were as follows: OC-I - 1:5 000, RuBisCO - 1:1 000, RuBisCO activase - 1:250 and glutamine synthetase - 1:500. The membrane was then washed 10-15min three times with blocking buffer before incubation with secondary antibody (1:1000 dilution for 2-4h at room temperature). Secondary antibody was horseradish peroxidase conjugated. After secondary antibody incubation, the membrane was once again washed three times for 10-15min with blocking buffer before signal detection using a buffer containing chloronaphthol (0.04%, w/v) and H_2O_2 (0.05%, v/v) in 50mM Tris (pH7.6). Membranes were incubated in detection buffer until bands could clearly be seen, and then rinsed in distilled water.

2.3.9 In situ localization of RuBisCO

In situ localization was performed by E. Olmos (CEBAS-CSIC, Murcia, Spain). For this procedure leaf samples were fixed at 4ºC in 3% paraformaldehyde and 0.25% glutaraldehyde in 0.1M phosphate buffer (pH 7.2) for 2.5h. The samples were dehydrated with a graded ethanol series and embedded in London Resin White (LR White) acrylic resin. Ultrathin sections (60-70nm) were made on a Leica EM UC6 Ultramicrotome (Leica Microsystems GMBH, Wetzlar). Ultrathin sections on coated nickel grids were incubated for 30min in PBS plus 5% (w/v) BSA to block non-specific protein binding on the sections. They were then incubated for 3h with anti-RbcL (RuBisCO Form I and Form II) antibody raised in rabbit (Agrisera, Vännäs, Sweden) diluted (1:250) in phosphate buffered saline (PBS) plus 5% (w/v) bovine serum albumin (BSA). After washing with PBS plus 1% (w/v) BSA, the sections were incubated for 1.5h with the secondary antibody goat anti-rabbit IgG gold labelled (10nm, British BioCell International) diluted 1:50 with PBS plus 1% (w/v) BSA and 1% (w/v) Goat Serum (Sigma). The sections were washed sequentially with PBS (two washes) and distilled water (five washes). Ultrathin sections were poststained with uranyl acetate followed by lead citrate and observed in Philips Tecnai 12 transmission electron microscope.

2.3.10 Proteolytic activity detection in plant extracts

Cysteine protease activity was detected in plant extracts using a synthetic substrate specific for cysteine proteases (cathepsin B/L) according to a Barret (1980) with slight modifications. In a microtitre plate well, total soluble protein (25µg) was diluted to a final

volume of 100µl by the addition of buffer (0.1M citrate phosphate buffer pH6 with 5mM DTT, 1mM EDTA, 0.01% CHAPS). After adding 1µl substrate (0.5% [w/v] N-CB2-phe-arg-MCA in DMSO), increase in fluorescence due to free 7-amino-4-methylcoumarin in the reaction solution was measured at 360nm for excitation and 460nm for emission in a multiwell plate reader over 30min. A control was measured containing the substrate without protein extract and subtracted from samples containing protein extract.

To measure inhibition of activity by cysteine protease inhibitors in the extracts, samples were preincubated with 100µM E64 (Sigma, UK) for 15min at 37ºC before assaying. E64 is an irreversible, potent, and highly selective inhibitor of cysteine proteases.

2.3.11 Two-dimensional (2-D) gel electrophoresis

The proteome of leaf 16 (as counted from the bottom) from either wild type or OC-I-expressing tobacco was analysed and compared by 2D electrophoresis.

i) Protein extraction and solubilisation

Proteins were extracted essentially as detailed in the handbook "2-D Electrophoresis. Principles and Methods" (GE Healthcare). Freeze-dried leaf material was ground in liquid nitrogen. Approximately 200-250mg leaf powder was incubated over night at –20°C in precipitation buffer (1ml) containing TCA (10%, w/v) and β-mercaptoethanol (0.07% v/v) in acetone (100%, v/v). Precipitated protein was pelleted by centrifuging for 25min at 4°C at 20 000xg and washed 6 times with ice cold washing buffer containing acetone (90%, v/v) and β-mercaptoethanol (0.07% v/v) in Milli-Q water. Proteins were solubilised in sample buffer (1ml) containing urea (8M), CHAPS (2%, w/v), DTT (9.3mg l^{-1}), and IPG buffer pH3-10 (0.5%, v/v) (GE Healthcare) by sonication in an ultrasonic water bath for 1 hour, while vortexing at 15 min intervals. Afterwards, samples were incubated in a heating block for 1.5h at 30°C with vortexing at 15 min intervals. Tubes were further incubated at room temperature overnight for optimal protein solubilisation. Cell debris was removed by centrifugation for 25min at 20 000xg. Solubilised proteins were quantified using the Bradford assay and ovalbumin (Sigma) as standard.

Protein content of samples was determined as described previously (chapters 2-4) except that samples and standards were neutralised with 0.1N HCl to a final concentration of

0.001N (Ramagli, 1999) before measurement. Neutralisation of samples and standards corrects for the effects of basic reagents (8M urea) present in solubilisation buffer that affect the binding of Coomassie G-250 dye to proteins. In this case, ovalbumin (Sigma) was used as standard instead of BSA, since BSA can absorb twice as much dye as most other proteins, which might cause an underestimation of the actual amount of protein being assayed.

ii) First dimension electrophoresis

After protein extraction (as described above), samples were diluted in sample buffer containing a few grains bromophenol blue to a concentration of 0.6µg μl^{-1}. Isoelectric focusing was performed on 150µg protein using Immobiline DryStrip immobilised pH gradient (IPG) strips (13cm) (GE Healthcare) and the Ettan IPGphor apparatus (GE Healthcare), with voltage being increased stepwise as follows: 30V (12h; for rehydration of strip), 100V (1h), 500V (1h), 1000V (1h), 5000V (1h), and 8000V (19 000 Vh) to obtain a total of 26 000Vh. IPG strips were then incubated for 15min each in equilibration buffer (6M urea, 50mM Tris-HCl pH8.8, 30% v/v glycerol, 2% w/v SDS, a few grains bromophenol blue) containing DTT (10mg ml^{-1}) to preserve the fully reduced state of denatured, unalkylated proteins, followed by similar incubation in equilibration buffer containing iodoacetamide (25mg ml^{-1}) for the alkylation of thiol groups on proteins, to prevent their reoxidation during electrophoresis.

iii) Second dimension electrophoresis and protein fixing

Second dimension focusing of proteins was performed by SDS-PAGE on a 1mm, 12% resolving gel with migration at 25mA/gel for 20min followed by 30mA/gel for approximately 4h or until the blue dye front had reached the bottom of the gel. Proteins were fixed in the gel overnight by incubation in fixing solution (50% methanol, v/v, 10% acetic acid, v/v) on a rocking platform at low speed.

iv) Gel staining and image analysis

After fixing of protein, gels were rinsed 3x in Milli-Q water before being stained for 24h in GelCode Blue (Pierce) on a rocking platform at low speed. Gels were rinsed 3x in Milli-Q water before being scanned for image analysis. Images were captured using the

ImageMaster Labscan software, and analysed using Phoretix 2D Expression v2005 software.

2.3.12 Spot identification

Spots of interest were excised from polyacrylamide gels after 2-D electrophoresis for peptide fingerprint analysis by surface-enhanced laser desorption ionization - time of flight mass spectrometry (SELDI-TOF MS) or mass spectrometry mass spectrometry (MS/MS). MS/MS was performed on excised spots at the McGill Proteomics Platform (McGill University, Montreal, Quebec) using an ESI-Quad-TOF mass spectrometer. For SELDI-TOF MS the procedure according to Jensen et al (1999) was followed.

Spots were excised and washed with water/acetonitrile (1:1, v/v) 2x15min. Liquid was removed and replaced with 20µl acetonitrile until gel pieces became white and stuck together. Gel pieces were then rehydrated in 0.1M NH_4HCO_3. An equal volume of acetonitrile was added and the sample incubated for 15min before drying down in a vacuum centrifuge. Gel particles were then swollen in a solution containing 10mM DTT and 0.1M NH_4CO_3 for 45min at 56°C to reduce the protein. The liquid was replaced with 50mM iodoacetamide, 0.1M NH_4CO_3 and the samples incubated for 30min at room temperature in the dark for alkylation of proteins. Liquid was removed and the samples dried in a vacuum centrifuge. In-gel digestion was performed by adding 10µL digestion buffer (50mM NH_4CO_3, 5mM $CaCl_2$) containing trypsin (20ng μl^{-1}) and incubating for 45min on ice. The remaining enzyme supernatant was removed and replaced with digestion buffer (without trypsin, to prevent autodigestion of trypsin).

Samples were then incubated over night at 37°C before peptides were extracted from the gel pieces. For aqueous extraction 20µl NH_4HCO_3 (25mM) was added and samples incubated for 15min in an ultrasonic water bath at 37°C. The same volume of acetonitrile was added, and the incubation step repeated. The supernatant from this step was recovered. For organic extraction 40µl of acetonitrile: TFA (2%) (1:1, v/v) was added to the gel particles. Samples were incubated for 15min in an ultrasonic water bath at 37°C. This step was repeated once and the supernatants pooled. Supernatant was dried down to 1-2µl, after which samples were redissolved in 5µl of a solution containing acetonitrile (5%) and TFA (0.1%).

Samples (1-2µL) were then spotted onto an H4 ProteinChip array (which has a chromatographic surface) (Ciphergen) and mixed with α-cyano-4-hydroxycinnamic acid (CHCA) [20%; in acetonitrile (5%)/TFA (0.1%)]. CHCA is an energy absorbing molecule that allows the efficient laser desorption and ionization of small proteins (< 15kDa). Samples were then analysed by surface-enhanced laser desorption/ionization – time of flight/mass spectrometry (SELDI-TOF/MS) in the Ciphergen SELDI-TOF mass spectrometer (GE Healthcare). Spectra were calibrated against CHCA peaks (643.360Da, 1059.5Da, and 1475.48Da). Peptide peaks with a signal to noise ratio >5 were identified using the Ciphergen ProteinChip Software v3.2.0, and used to identify proteins with the Mascot search engine (www.matrixscience.com; Perkins et al., 1999). The type of search performed was a peptide mass fingerprint search at the NCBInr database as on 15 June 2007 (*Viridiplantae* only), with trypsin as enzyme, carbamidomethyl (C) as fixed modification, oxidation (M) as variable modification, using average mass values, a peptide mass tolerance of ± 1Da, and a maximum of one missed cleavage. MS/MS results were obtained from the McGill proteomics portal online (http://portal.proteomics.mcgill.ca/portal). An MS/MS ion search was performed using the Mascot search engine and a database containing all available nucleotide sequences as on 5 January 2007 in order to find protein homologs, with search specifications of trypsin as enzyme, carbamidomethyl (C) as fixed modification, oxidation (M) as variable modification, using monoisotopic mass values, a peptide mass tolerance and fragment mass tolerance of ± 0.5Da, and maximum of one missed cleavage.

2.3.13 Statistical methods

The data was statistically analysed using parametric tests at a stringency of $P < 0.05$. The significance of variation in mean values for growth parameters and pigment and protein determinations was determined using a T-test. The significance of the data for immuno-gold labelling measurements was analysed using ANOVA and Tukey HSD tests.

2.4 Results

It has previously been shown that expression of OC-I in transgenic tobacco plants decreased plant growth and development rates and protected photosynthesis from chilling-induced inhibition (Van der Vyver et al., 2003). These effects were documented in three independent transgenic lines compared to the wild type and empty vector controls

confirming that the slower developments growth and delayed senescence traits are very likelylinked to the expression of the transgene as was the protection of photosynthesis from chilling induced inhibition (Van der Vyver et al., 2003). Since Van der Vyver et al. (2003) demonstrated unequivocally that the altered traits under investigation are related to the expression of the transgene, the mechanisms by which altered leaf CP activity influences leaf protein composition, photosynthesis, RuBisCO protein content and activity, leaf and plant senescence in one transgenic line (line T4/5) compared to wild type untransformed controls was studied here (with specific focus on proteins involved in photosynthesis).

2.4.1 Leaf protein composition and turnover

To determine whether leaf protein composition was modified in the OCE plants, leaf proteins were extracted from the youngest mature leaves (number 16) of 10 week-old control and OCE plants and separated using 2-D gel electrophoresis (Fig. 2.3). Leaf proteins were extracted and precipitated by standard proteomic procedures, in which the RuBisCO large subunit (LSU) has only limited solubility (Ramagli, 1999). Since RuBisCO generally accounts for 30 to 60% of total soluble proteins in the leaves of C_3 species, it is important to use this selective procedure in order to limit the amount of the RuBisCO LSU on the gels so that other proteins of lower abundance are not obscured. The Phoretix 2D gel analysis software identified 765 protein spots in the extracts prepared from control leaves and 860 protein spots in extracts from OCE leaves. Key parameters (spot volume, pI and MW) were calculated for all spots by the software. Fifty one spots were chosen for more intensive characterisation based on visible differences in spot volume. Of the 51 spots, 13 were not statistically different in volume between C and OCE plants, 7 spots had significantly greater volume in C plants, 26 spots had significantly greater volume in OCE plants, 2 spots were below the level of detection in OCE plants and 3 spots were only detected in OCE plants (Supplementary Table 1 on CD).

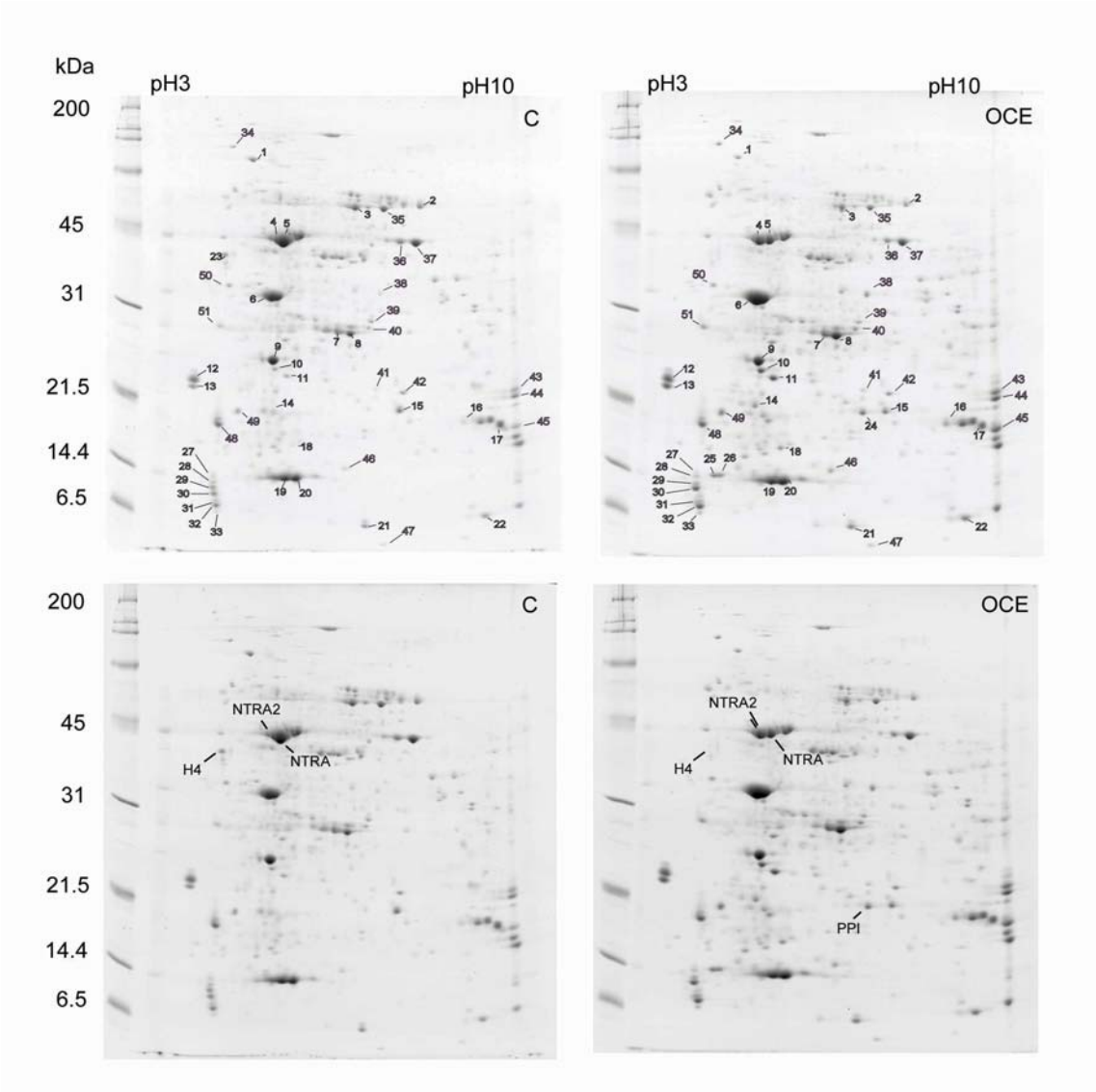

Figure 2.3. The effect of inhibition of CP activity in OCE leaf protein abundance and composition. Proteins were extracted from leaf 16 of control and OCE plants at 8 weeks and were separated on bi-dimensional gels. Proteins with major differences in abundance are indicated (1-51) in upper panels. The position of the proteins with the greatest differences: two rubisco activase forms (NTRA and NTRA2), histone 4 (H4) and putative pepyidylprolyl isomerise (PPI) are indicated in the lower panels.

Two spots showing a difference in volume (Fig. 2.3 upper panels, spots 4 and 5) were identified using SELDI-TOF MS. These proteins were highly homologous to RuBisCO activase 2 (accession Q40565) (spot 4) and RuBisCO activase (accession 1909374A) (spot 5) (Table 1). Spot 4 also showed significant homology to RuBisCO activase (accession 1909374A) and RuBisCO activase 1 (accession Q40460), while spot 5 showed significant homology to RuBisCO activase 1 (accession Q40460) and RuBisCO activase 2 (accession Q40565). The normalised volumes for spots 4 and 5 in OCE extracts were respectively

2.42 and 2.99 times greater than those found in C extracts. In OCE protein extracts, spot 4 had a larger volume than spot 5 (1.3 times).

To further characterise the RuBisCO activase isoforms present in these studies, alignments were performed with three GenBank tobacco RuBisCO activase sequences and two Arabidopsis RuBisCO activase isoforms (Table 1; Supplementary Fig. 1). While the highest scores for spots 4 and 5 were RuBisCO activase 2 and RuBisCO activase from tobacco, the comparison with Arabidopsis revealed the absence of the C-terminal amino acids characteristic of the long isoform of this gene in Arabidopsis. Instead of the final 36 C-terminal amino acids present in the long Arabidopsis isoform, the Arabidopsis short isoform has only 8 amino acids (TEEKEPSK: Werneke et al., 1989), a difference that is considered to result from alternative splicing. The Arabidopsis large isoform has a MW of 46kDa while the small isoform is approximately 43kDa. Spot 4 has the highest homology to NTRA2 (RA2, Supplementary Fig. 1) which lacks the C-terminal amino acids FAS. Spot 5 had the highest homology to another identified tobacco RuBisCO activase (1909374A, RuAct, Supplementary Fig. 1). This form lacks the first 59 amino acids in the N-terminus and also contains 3 additional amino acids at the C-terminal (FAS) when compared to RA2. Spot 5 also shows high homology with NTRA1 (RA1, Supplementary Fig. 1) which has the full-length N-terminal sequence but also has the extra amino acids at the C-terminal. Spot number 23 on Fig. 2.3 upper panels has very low abundance in the OCE proteome (Supplementary Table 1) and was identified by LC-MS/MS analysis as highly homologous to volvox histone H4 (P08436), histone H2A.3 from wheat (HSWT93) and rice H2A protein (AAF07182) (Table 1). Spot number 24 in the OCE proteome, which is below detection in C extracts, was identified by LC-MS/MS and was significantly homologous to rice Os05g0103200 (NP_001054392), which is described as a chloroplast precursor of peptidyl-prolyl cis-trans isomerase TLP20 (EC 5.2.1.8). This protein contains a cyclophilin ABH-like region. Spot 24 is also significantly homologous to an Arabidopsis peptidylprolyl isomerase-like protein (CAC05440), which also has a strong similarity to the chloroplast stromal cyclophilin, ROC4.

Table 2.1. Identification of protein spots showing different abundance in control and OCE lines after 2D electrophoresis. Peptide fingerprint analysis (NTRA2 and NTRA) and/or ion analysis (H4 and PPI) using the Mascot search engine was used to establish protein identities.

Spot	Identification method	Accession	Protein name	Score	e-value	Queries matched	Peptide Sequence (MS/MS)
NTRA2 (4)	SELDI-TOF MS	Q40565	RuBisCO activase 2 (RA 2)	98	6.80E-05	9	
		1909374A	RuBisCO activase	75	1.30E-02	8	
		Q40460	RuBisCO activase 1 (RA 1)	71	3.30E-02	8	
NTRA (5)	SELDI-TOF MS	1909374A	RuBisCO activase	117	7.70E-07	15	
		Q40460	RuBisCO activase 1 (RA 1)	108	6.10E-06	15	
		Q40565	RuBisCO activase 2 (RA 2)	94	1.40E-04	13	
H4 (23)	MS/MS	P08436	Histone H4	195		3	ISGLIYEETR DNIQGITKPAIR TVTAMDVVYALK
		HSWT93	histone H2A.3	48		1	AGLQFPVGR
		AAF07182	H2A protein	48		1	AGIQFPVGR
PPI (24)	MS/MS	NP_001054392	Os05g0103200	357		16	TFKDENFK DFMIQGGDFDK VYFDISIGNPVGK HVVFGQVIEGMDIVK DFMIQGGDFDKGNGTGGK
		CAC05440	peptidylprolyl isomerase-like protein	105		7	TFKDENFK

The relative abundance of the RuBisCO LSU and RuBisCO activase proteins was determined in leaves at different positions on the stem of 14 week-old plants (Fig. 2.4) using western blot analysis.

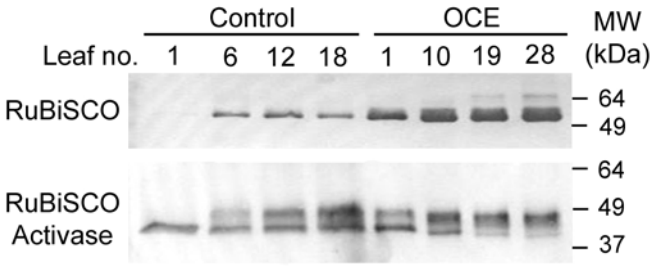

Figure 2.4 Western blot analysis of the abundance of the RuBisCO large subunit, and RuBisCO activase in leaves at different positions on the stem of 14 week-old plants. Soluble proteins were extracted from leaves at the positions on the stems as indicted, with Leaf No 1 being at the bottom of each plant and leaf 18 or 28 being the youngest mature leaf on the control and OCE plants respectively. 10µg and 30µg aliquots of leaf protein were loaded per well for the detection of RuBisCO and RuBisCO activase proteins, respectively.

In the control plants, the amount of RuBisCO LSU protein was highest in the mature source leaves and least abundant in the youngest (18) and oldest (1) leaves (Fig. 2.4). However, the relative abundance of the RuBisCO LSU protein was much higher in the leaves of the OCE plants at all ranks on the stem, even in the oldest leaves (Fig. 2.4). A development-dependent difference in the RuBisCO activase protein bands was also observed (Fig. 2.4). Two distinct bands of RuBisCO activase protein were observed on Western blots using specific antibodies in all but the oldest senescent leaves of the control plants where only the lower band was the dominant band (Fig. 2.4). In marked contrast, the higher molecular weight band of RuBisCO activase protein was more intense than the lower molecular weight band in the young leaves of OCE plants in all leaves except the oldest senescent leaf (Fig. 2.4).

2.4.2 RuBisCO degradation and leaf CP activity

To determine whether tobacco RuBisCO is susceptible to degradation by endogenous tobacco CPs we conducted *in vitro* assays comparing RuBisCO degradation in OCE extracts with that in C extracts in the absence or presence of the CP inhibitor, E64 (Fig. 2.5 A). RuBisCO was protected from degradation by endogenous CPs in OCE extracts compared to control extracts; an effect that could be mimicked by inclusion of the CP inhibitor, E64 in the assays of the control extracts (Fig. 2.5 A).

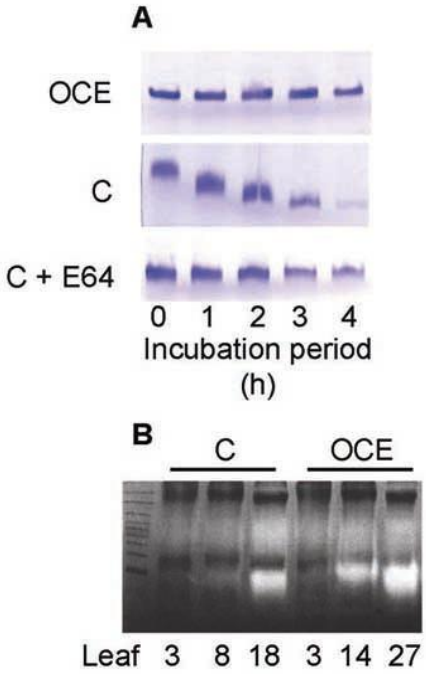

Figure 2.5 Protection of RuBisCO from degradation by OC-I in OCE plants and by E64 in control (C) plants *in vitro* assays. (A) The abundance of the RuBisCO holoenzyme protein was detected in soluble protein extracts from 4-week old control (C) and OCE plants on non-denaturing PAGE gels stained with Commassie brilliant blue. (B) In-gel activity assay showing degradation of the gelatine substrate by endogenous proteases from extracts of leaves of 14 week-old OCE and control (C) plants. Extracts were prepared from leaves at the bottom (3), middle (8, 14), and top (18, 27) leaf ranks. Equal amounts of soluble protein (40 µg per well) extracted from C and OCE plants were compared in all instances.

The protease activities of leaf extracts, scrutinised by activity staining after SDS-PAGE, revealed that the youngest leaves on OCE plants had much higher CP activities than the youngest leaves from controls (Fig. 2.5 B). This increased activity represents unknown proteases, but could include CPs. In this case, increased protease activity observed in OCE plants after separation of OC-I and the proteases they inhibit by SDS-PAGE implicate a possible feedback modulation of CP expression that enhances CP production when activity is impaired by constitutive cystatin expression.

2.4.3 Natural senescence and chilling-dependent inhibition of photosynthesis, decreased RuBisCO content and activity

It was previously shown that chilling dependent effects on photosynthesis were comparable in three independent transgenic lines relative to the wild type and empty vector controls and that effect of constitutive OC-I expression on parameters such as the CO_2 saturated rates of photosynthesis (J_{max}) and carboxylation efficiency (CE) were linked

to expression of the transgene (Van der Vyver et al., 2003). Leaf CE and J_{max} values attained maximal values two weeks after emergence in both OCE and control plants (Table 2.2). To investigate the effect of decreased CP activity on leaf senescence as determined by the age dependent decrease in photosynthesis, leaf CE and J_{max} values were measured on the same leaves from 2 to 6 weeks (Table 2.2). The OCE leaves had greater CE and J_{max} values than controls at equivalent stages of development. Moreover, the senescence-related decline in photosynthesis was delayed in the OCE leaves (Table 2.2).

Table 2.2 Senescence-related decreases in carboxylation efficiency (CE) and CO_2 saturated rates of photosynthesis (J_{max}) in wild type controls (C) and OCE tobacco leaves. Measured CE and J_{max} values, which were highest in both lines two weeks after leaf emergence, were measured in the same leaves for up to six weeks. The values represent the means ± SE of four replicates per experiment.

Time after leaf emergence (weeks)	C plants CE (mol m^{-2} s^{-1})	OCE plants CE (mol m^{-2} s^{-1})	C plants J_{max} (µmol m^{-2} s^{-1})	OCE plants J_{max} (µmol m^{-2} s^{-1})
2	0.078 ± 0.004	0.107 ± 0.007	20.3 ± 1.0	23.2 ± 0.8
3	0.069 ± 0.004	0.110 ± 0.013	15.1 ± 1.0*	21.7 ± 1.1
4	0.040 ± 0.004**	0.064 ± 0.002**	13.6 ± 1.3**	18.5 ± 1.7*
5	0.034 ± 0.004**	0.063 ± 0.005**	9.6 ± 0.6**	16.6 ± 0.6**
6	0.014 ± 0.001**	0.045 ± 0.003**	3.1 ± 0.6**	11.9 ± 0.1**

* and ** indicate significant differences at $P < 0.05$ and $P < 0.01$ respectively

Photosynthesis (Fig. 2.6 A), extractable RuBisCO activities and activation states (Fig. 2.6 B) were compared in the leaves of 6-week old plants maintained at either optimal growth temperatures or exposed to seven consecutive nights of chilling. At the beginning of the experiment (day 0), fully expanded leaves of control (Fig. 2.6 A upper panel) and OCE plants (Fig. 2.6 A lower panel) grown at optimal temperatures had very similar rates of photosynthesis.

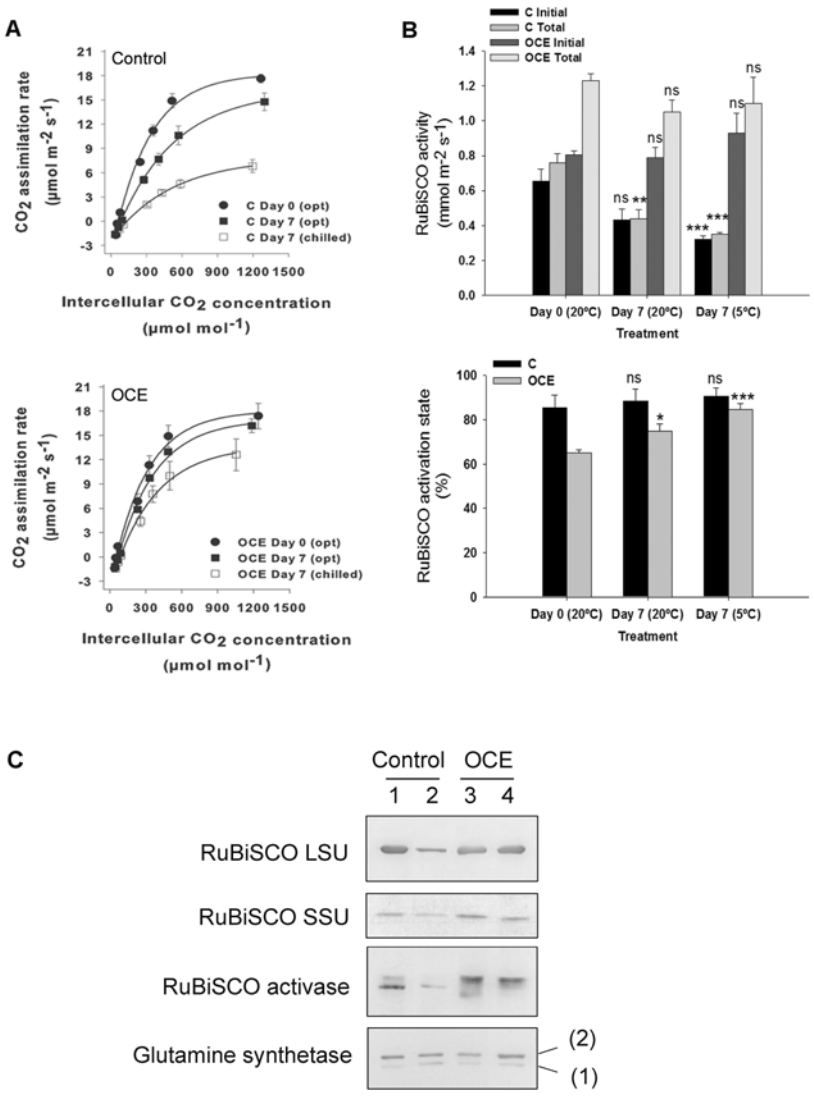

Figure 2.6 Effects of dark chilling on photosynthesis, RuBisCO activity and activation state and relative abundance of RuBisCO, RuBisCO activase and glutamine synthetase in the leaves of 6 week-old OCE and control tobacco plants. CO_2 response curves for photosynthesis (A) in control and OCE leaves were measured at day 1 (closed circle), after 7 days of growth under optimal conditions (Opt: closed square) and after 7 nights of dark chilling (Chilled; open square). Initial and total RuBisCO activities and the RuBisCO activation state in control and OCE leaves measured at day 1, after 7 days of growth under optimal conditions and after 7 nights of dark chilling (B). Immuno-detection of RuBisCO, RuBisCO activase, and glutamine synthetase (C) in soluble protein extracts from control and OCE leaves at the beginning of the experiment (lanes 1 and 3) and after 7 nights of dark chilling (lanes 2 and 4).

At this stage the OCE plants had higher total RuBisCO activities but lower activation states than controls (Fig. 2.6 B). Seven days later, the control leaves maintained at optimal temperatures had about 20% lower photosynthetic rates than the OCE plants (Fig. 2.6 A). Over the same period, total RuBisCO activity in the control leaves maintained at optimal

temperatures had also decreased (Fig. 2.6 B) with significant effect on RuBisCO activation state (Fig. 2.6 B). While RuBisCO activities were similar in OCE plants at both time points the RuBisCO activation state was slightly increased at day 7 (Fig. 2.6 B). The chilling-dependent increase in RuBisCO activation state in the OCE lines is surprising given that the overall rate of photosynthesis declined and that the initial slope of the photosynthesis: intercellular CO_2 response is also slightly decreased. However, these effects are very small compared to the large effect of chilling on photosynthesis rates in the control line, where RuBisCO activation state is unchanged. It was previously shown that the leaves of the different independent OCE lines contain about 20% more total soluble protein than those of controls at 6 weeks old (Van der Vyver et al., 2003). Consistent with this observation, the amounts of RuBisCO LSU and SSU proteins (Fig. 2.6 C) were similar in the leaves 6-week old control and OCE plants at this stage. However, dark chilling stress led to a pronounced decrease in the abundance of RuBisCO LSU and SSU proteins (Fig. 2.6 C) in the leaves of control plants. In contrast, dark chilling had no effect on the amount of detectable RuBisCO LSU and SSU proteins in the OCE plants.

2.4.4 Intracellular localisation of RuBisCO protein in chloroplasts and vesicular bodies in the palisade cells of young leaves

Electron microscopy and immuno-gold labelling with specific polyclonal antibodies to the RuBisCO LSU were used to determine the intracellular distribution of the RuBisCO protein in the youngest mature leaves of control and OCE tobacco at 6 weeks old (Fig. 2.7). Label was detected in the chloroplasts of the palisade cells of control (Fig. 2.7 B) and OCE leaves (Fig. 2.7 C). In addition RuBisCO protein was also observed in vesicular bodies outside the chloroplast (Fig. 2.7 B and C). The relative amounts of label were quantified in the chloroplasts and in the RuBisCO vesicular bodies (RVB) of both control and OCE leave (Table 2.3). No differences were observed in the relative localization of RuBisCO protein in the chloroplasts relative to the RVB's of both control and OCE leaves (Table 2.3).

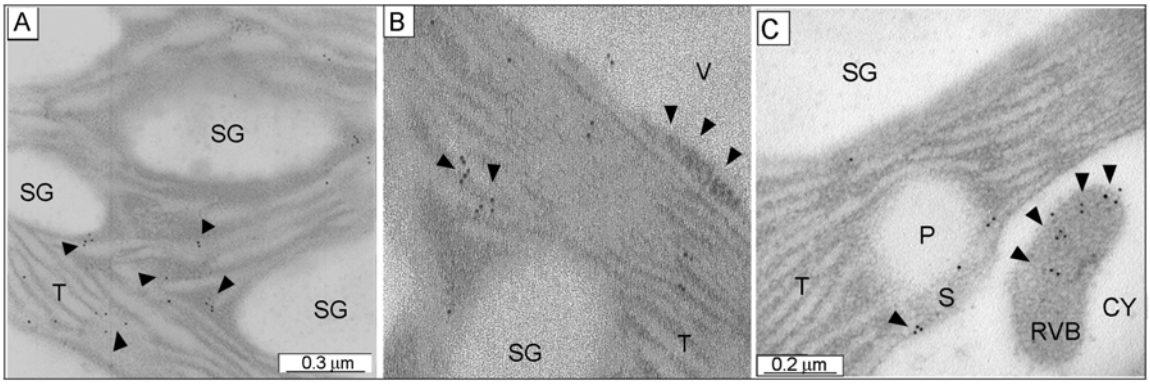

Figure 2.7 Immunogold labelling detection of RuBisCO protein in palisade cells of 6-week old control and OCE tobacco leaves. High magnification of a cross-section of a control leaf showing the structure of the palisade cells with immuno-gold labelling (A), and higher magnification images of the intra-cellular structure showing the compartmention of the label in wild type and OCE leaves (B and C). The presence of RuBisCO protein in chloroplasts and vesicular bodies outside the chloroplast is indicated in B and C Areas of immuno-gold are indicated by black arrows. CY, cytosol, IS, intercellular space; P, plastoglobulus, RVB, RuBisCO vesicle body, S, stroma, SG, starch grain, T, thylakoid membranes, V, vacuole.

Table 2.3. Counts of gold particles (GP) after immunogold labelling of RuBisCO large subunit in ultrathin leaf sections of C and OCE tobacco. Gold particles were counted in chloroplasts, RuBisCO protein vesicles (RVB) and cytosol. Values obtained were compared to controls lacking antibody (Control).

	GP in Chloroplast (μm^{-2})	*GP in RVB* (μm^{-2})	*GP in Cytosol* (μm^{-2})
Control	0.4± 0.2	0.2 ± 0.1	0.4± 0.2
OCE	27.9± 3.3*	31.4 ± 6.5*	1.4 ±0.8
C	26.7± 2.8*	29.1 ± 5.3*	1.4 ± 0.7

Mean values ± SE (n=30). The means were compared by analysis of variance and by using the Tukey multiple range test at $P < 0.05$. Significant differences between treatments are indicated by *.

2.4.5 Intracellular localisation of OC-I protein in the cytosol, chloroplasts and vacuoles in the palisade cells of young leaves

Electron microscopy and immuno-gold labelling with specific polyclonal antibodies to the OC-I protein were used to determine the intracellular distribution of the OC-I protein in the youngest mature leaves of control and OCE tobacco at 6 weeks old (Fig. 2.8). The OC-I protein was mainly located in the cytosol which had the highest relative gold particle concentrations (71 ± 8 μm^{-2}; n=9). However, label was also detected in the vacuole at a much lower gold particle concentration of 5.5 ± 2 μm^{-2} (n=9), and also in the chloroplasts

which had a gold particle concentration of 20.6 ± 4.2 μm^{-2} (n=9). Interestingly, the chloroplasts that showed immuno-gold labelling for the presence of the OC-I protein also had an alteration to the structure at the periphery of the chloroplast either beneath or adjacent to the chloroplast envelope (Fig. 2.8 A and C). A higher magnification of the chloroplast periphery shows that this is possibly fibrillar or membranous. (Fig. 2.8 B and D). Since these samples were not fixed with osmium, lipids are not stained in these images, implying that the changes in the periphery of the chloroplast is not due to changes in the lipid membrane, or that it may have a low lipid content. The chloroplasts containing changes in the structure of their periphery clearly show label (Fig. 2.8 B inset and D inset) but further studies are required to explain the presence and possible function of OC-I in the altered chloroplast periphery. Some of the OCE cells also show the presence of cytosolic inclusion bodies (Fig. 2.8 E and F), which has a crystalline structure that also contains OC-I label (Fig. 2.8 G). The high level of label in the cytosol (Fig. 2.8 H inset and I inset) is consistent with the mode of expression of the OC-I protein in these studies, where the protein lacked sequences for specific organellar targeting. However, presence of OC-I in the vacuole and chloroplast require reconfirmation and further investigation.

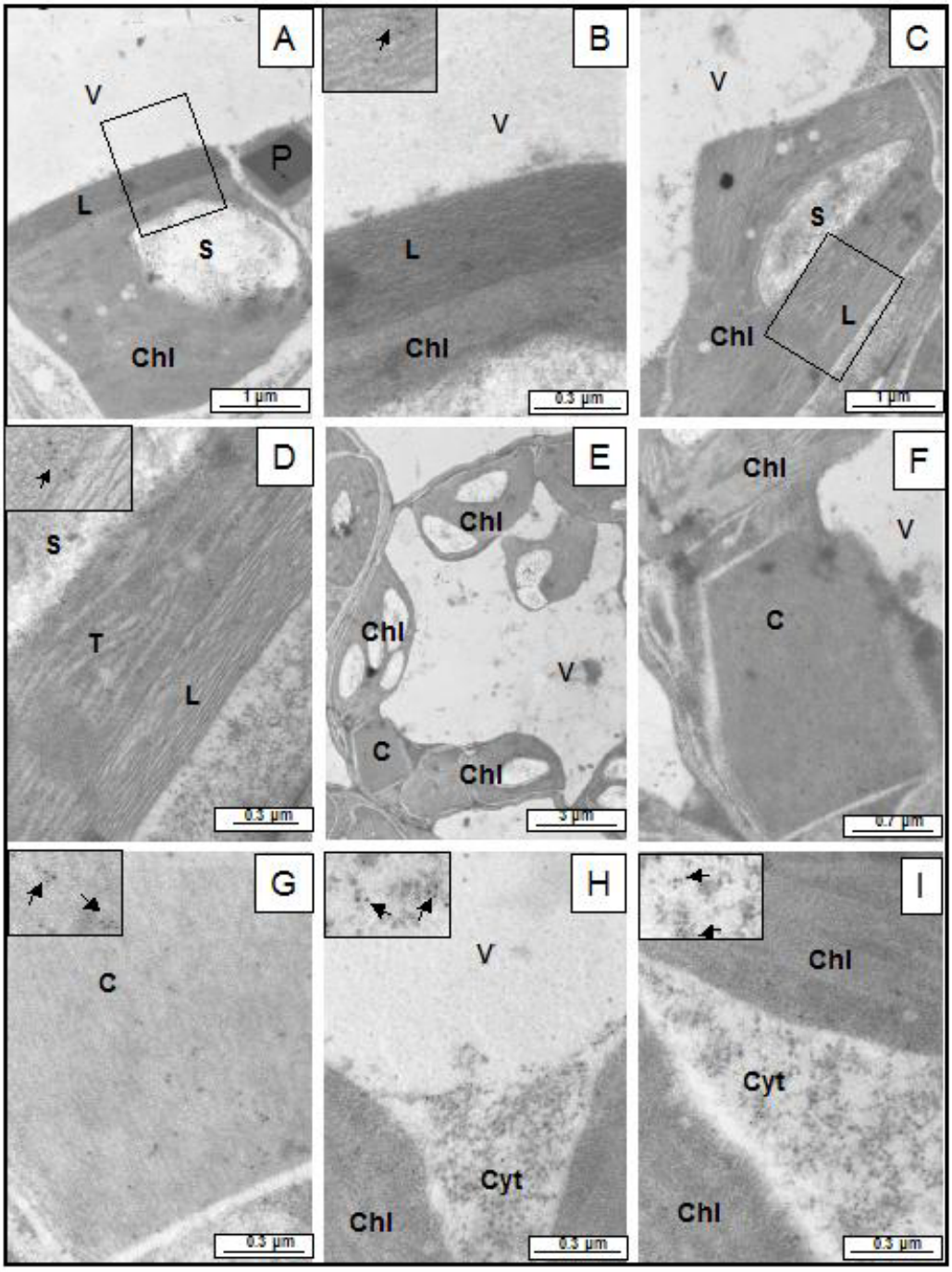

Figure 2.8 Transmission electron micrographs of immuno-gold labelling detection of OC-I protein in the palisade cells of 6-week old control and OCE tobacco leaves. Chloroplasts in OCE leaves with an unusual fibril structure below the chloroplast envelope (A and C); Enhanced images of the unusual structure below the chloroplast envelope (B and D). In both cases the chloroplasts (A and C) show labelling for OC-I protein (B and D). A section of the OCE leaf shows the presence of a cystatin inclusion body (E) together with a higher magnification image showing that the cystatin inclusion body is present in the cytosol (F) and has a crystalline structure with positive labelling for the OC-I protein (G). The presence of immuno-gold label in the cytosol of the OCE leaves (H and I). C= cystatin inclusion body; Chl, chloroplast; Cyt, cytosol; L, unusual chloroplast structure; S, starch; T, thylakoid; V, vacuole.

2.4.6 Inhibition of CP activity effects on lifespan and leaf protein and chlorophyll contents after flowering

The OCE plants have a slow growth phenotype compared to wild type or empty vector controls (Van der Vyver et al., 2003). In the present experiments, the control plants flowered at 58.33 ± 1.20 days, at which point vegetative growth ceased. The OCE plants also sustained vegetative growth until flowering but in this case vegetative development ceased at 80.67 ± 1.45 days (Fig. 2.9). Hence, at the point where the OCE lines reached sexual maturity (14 weeks in the OCE lines) the OCE lines were much taller (Fig. 2.9 A), with greater numbers of larger and heavier leaves than the controls (Fig. 2.9 B-H).

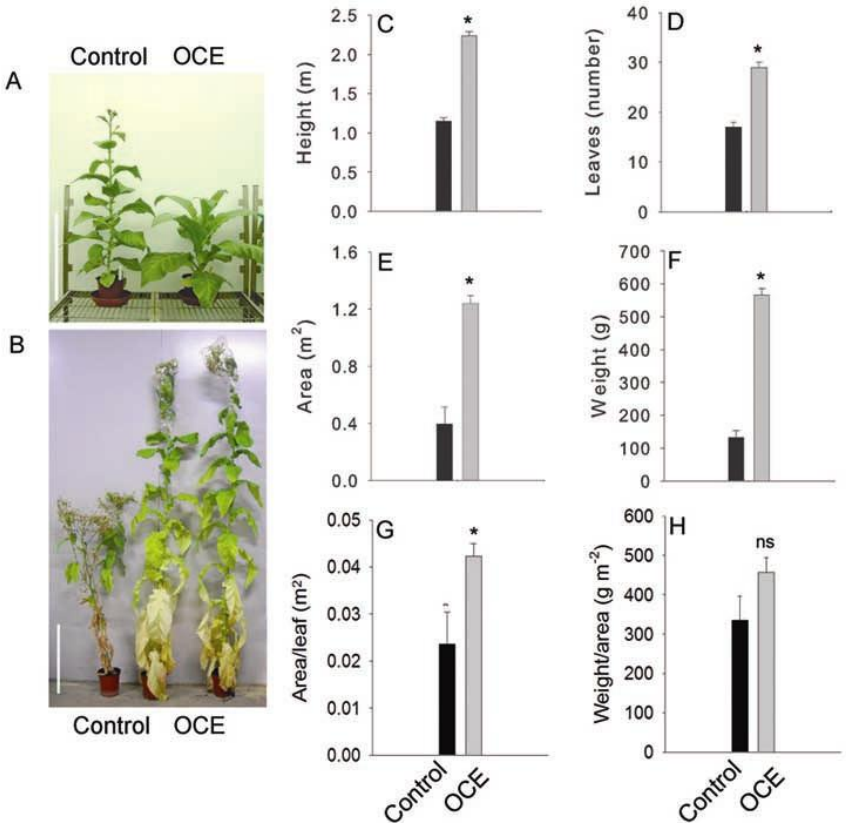

Figure 2.9. A comparison of plant growth and development in OCE and control plants. Plant phenotype at 8 weeks (A) and 14 weeks (B). After both genotypes had flowered at 14 weeks the following parameters were measured: plant height C), leaf number (D), total leaf area (E), leaf weight (F), area per leaf (G), and leaf weight per leaf area (H). Data represent average ± SE of n=6. The size bar indicates 0.5m. Significant differences at $P < 0.05$ indicated by *.

The effects of inhibition of CP activity on leaf protein accumulation were much more pronounced in 14-weeks (Fig. 2.10 A) than they were in 6-8 week-old tobacco plants (Van der Vyver et al., 2003). The increase in leaf protein in OCE plants that had flowered depended on the position on the stem (Fig. 2.10 A). Chlorophyll was also increased but

only in the youngest tobacco leaves (Fig. 2.10 B). Maximal extractable leaf CP activities were greatly decreased in OCE leaves compared to controls at all positions on the stem (Fig. 2.10 C), suggesting that the OC-I remains bound to the CP during the extraction and spectrophotometric assay procedures, whereas it is removed by the in-gel assay methods of used in Fig. 2.5 B.

Figure 8

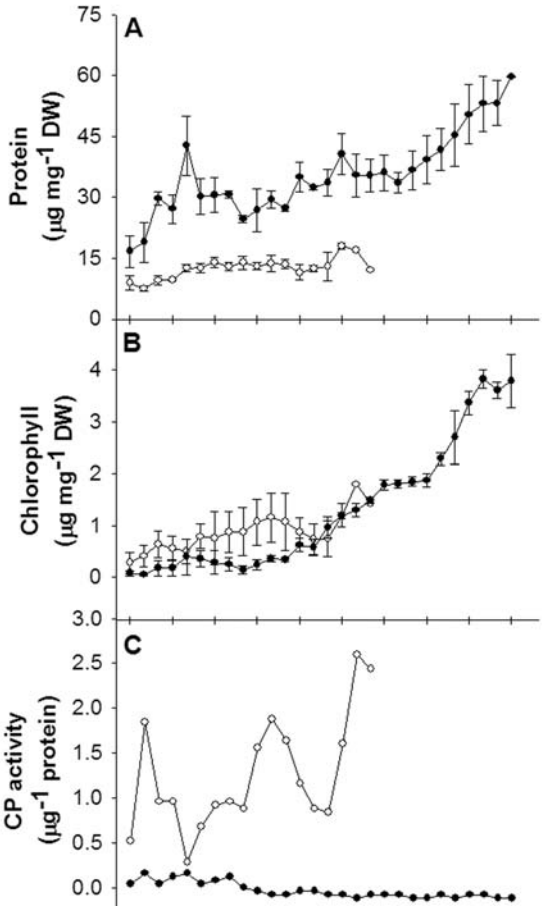

Figure 2.10. Leaf soluble protein and chlorophyll contents and cysteine protease activities in mature OCE and control tobacco plants. Soluble protein content (A). Chlorophyll content (B). Cysteine protease (CP) activity (C). Open and closed symbols represent control and OCE plants respectively.

2.5 Discussion

The results presented here demonstrate that chloroplast proteins particularly RuBisCO and RuBisCO activase are affected by the expression of an exogenous CP inhibitor. This could be due to effects of OC-I on the activity of endogenous CPs, since RuBisCO was found to be sensitive to degradation by proteases *in vitro*, a process that could be inhibited by CP

inhibitors or exogenously expressed OC-I in an in vitro study. However, for RuBisCO to be degraded by CPs *in planta*, a mechanism of interaction between RuBisco and vacuolar or vesicular CPs must exist. This would provide a link between the protein turnover machinery in the chloroplasts, cytosol and vacuoles. A detailed discussion of the results and logic corroborating the above conclusions is provided below.

While there are relatively few reports on tobacco leaf proteomics in the literature (Cooper et al., 2003; Franceschetti et al., 2004; Giri et al., 2006), the technique has been used successfully to study the proteome of leaf plasma membranes (Rouquié et al., 1997), trichomes (Amme et al., 2005) and apoplast (Dani et al., 2005). Proteome information is available for tobacco BY2 cell suspension cultures (Laukens et al., 2004) and for plastids isolated from these cultures **(**Baginsky et al., 2004). RuBisCO activase sequences (Q40565, CAA78703, or 1909374A), have been identified previously in *Nicotiana attenuata* leaves (Giri et al., 2006). In this study concerning proteins elicited by oral secretions from *Manduca sexta* seven spots with homology to RuBisCO activase were identified (Giri et al., 2006). Of these, four spots had kDa/pI values similar to reported RCA proteins, with comparable molecular weights but different pI values. In the present study, spots four and five in Fig. 2.3 occupy similar positions to the RuBisCO activase spots reported by Giri et al. (2006). Differences in the positions of the RuBisCO activase spots on the gels might arise from proteolytic cleavage (Giri et al., 2006). The data presented in Figs. 2.3-2.5 not only implicates CPs in RuBisCO activase degradation but also in the relative abundance of different forms of the protein present in leaves. The relative abundance of the two RuBisCO activase protein bands detected on Western blots was changed by inhibition of CP activity, with greater abundance of the higher molecular weight form. RuBisCO activase is a crucial regulator of RuBisCO activation state (Zhang et al, 2002). This nuclear-encoded chloroplast protein consists of two isoforms in Arabidopsis, produced by alternative splicing (Zhang et al., 2002). In Arabidopsis, the longer isoform houses critical cysteine residues that are modulated by redox changes in the stroma, particularly under limiting light intensities (Zhang et al., 2002). However, the tobacco RuBisCO activase spots examined in the present study lack the critical cysteine residues that characterise the longer isoform sequence in Arabidopsis. In order to clarify this result, further research needs to be done on the sequence of RuBisCO activase protein sequences as well as the mRNAs that encode them, in order to identify whether the two bands observed with the Western blot are isoforms or degradation produts.

While the mechanisms of turnover and degradation of RuBisCO activase remain poorly characterised, there have been a large number of studies on the turnover of RuBisCO and glutamine synthetase. Within the chloroplast oxidation of critical cysteine residues enhances the binding of the RuBisCO protein to the chloroplast envelope membranes, marking the protein for degradation (Marín-Navarro and Moreno, 2006). While chaperone-mediated autophagy pathways for oxidatively modified proteins remain 562 to be demonstrated in plants, stress-induced non-specific autophagasitic pathways of protein degradation have been described (Xiong et al., 2007). Once outside the chloroplast RuBisCO occurs in the vesicular transport system and involves cytoplasmic vacuole-type compartments (Chiba et al., 2003). Thereafter, RuBisCO degradation products appear in the vacuoles (Huffaker, 1990). While this process has only previously been considered to be important in senescing leaves where chloroplast lysis occurs (Mae et al., 1984; Ono et al., 1995; Hörtensteiner and Feller, 2002), the data presented here in Table 2.2 and Fig. 2.7 show that they are present even in young leaves. Our immo-gold labelling results demonstrate the existence of a cytoplasmic vacuole-type compartment that has been called RuBisCO vesicular bodies (RVBs) that are involved in RuBisCO degradation even in young leaves.

Since OC-I is detected both in the cytosol and the chloroplast, interaction between OC-I, endogenous protease, and RuBisCO could occur in either of these compartments. The endogenous protease inhibited by OC-I is most likely a cysteine protease or cysteine proteases that are suggested to be present in the vacuole, or small lytic vacuoles in the cytosol. Therefore a model is proposed for RuBisCO degradation of the type illustrated in Fig. 2.11 where vesicles containing CPs continuously interact with those from functional chloroplasts to remove proteins marked for degradation. RuBisCO protein is present in vesicles as well as in the chloroplasts in both young wild type and OCE leaves (Fig. 2.7, Table 2.3).

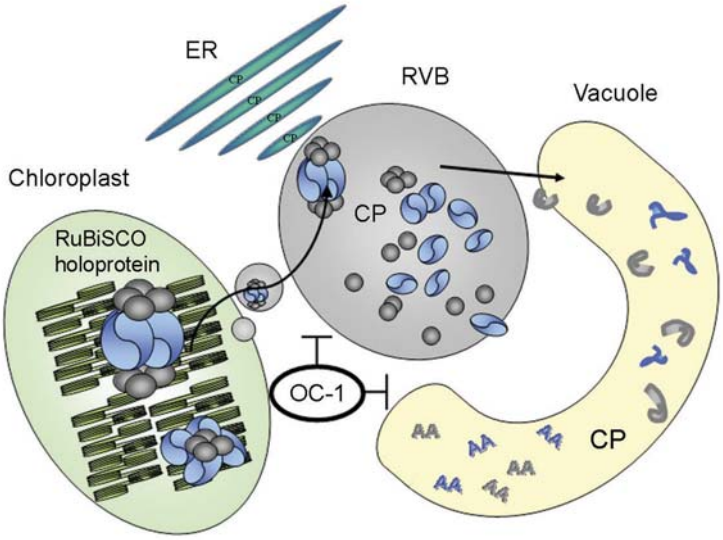

Figure 2.11 A hypothetical model for RuBisCO degradation via autophagy and the plant vesicle trafficking system. AA: amino acids; CP, cysteine protease, ER: endoplasmic reticulum; OC-I, oryzacyctatin-1.

Interestingly, RVBs have been recently shown to arise from the stromules that are continuously produced by chloroplasts even in young leaves (Ishida et al., 2007). While the function of stromules remains a matter of debate (Foyer and Noctor, 2007), available evidence suggests that stromules forge associations between chloroplasts and other organelles including the vacuole. The similar pattern of RuBisCO labelling in the RVBs and chloroplasts observed in the present study is entirely consistent with the chloroplast-stromule origin of RVBs. Furtermore, sjnce the fibrillar structure observed on the chloroplast periphery contains OC-I protein, this may provide a means by which RuBisCO and OC-I proteins are enclosed in vesicles that bud off from the chloroplast, and then fuses with a lytic vacuole in the cytosol. Plant cells contain several different types of vacuole-like compartments with distinct functions (Chrispeels and Herman, 2000). Vesicle trafficking has been traditionally viewed as a housekeeping process, but recent findings in plant, yeast and animal cells show that it can also play an important role in stress responses (Chrispeels and Herman, 2000; Herman and Schmidt, 2004). The physiological and biochemical identity of vacuoles is largely determined by correct targeting of vesicles and their cargo (Vitale and Pedrazzini, 2005).

While the data presented here concerning RVBs are limited to RuBisCO, it may be that other chloroplast proteins such as RuBisCO activase are also present in the RVB's. This aspect is currently under investigation together with the role of CPs and cystatins in the

formation of peripheral structure adjacent to the chloroplast envelope that we have observed when CP activity is inhibited. To date we have only counted the number of RVB's in the leaves of young plants prior to flowering, and values appear to be similar regardless of leaf CP activity. However, the number may increase as the leaf develops and senesces. Despite the absence of this information at present, our data suggest that the RuBisCO turnover cycle involving RVB's must have a feedback interaction with the chloroplast that requires CP activity, as inhibition of CPs by expression of an exogenous cystatin allows the chloroplast to maintain RuBisCO activity and photosynthesis upon exposure to stress. These interactions may be controlled by redox regulation.

The data presented here show that the lifespan of tobacco plants can be extended by the expression of an exogenous phytocystatin. It is unusual for a single transgene to have such a large effect on plants, however, and it is also possible that the observed morphological changes may be due to somaclonal variation. However, the large effect may be caused by OC-I inhibiting endogenous cysteine proteases that play key roles in the synthesis of developmentally important hormones. In order to clarify this, the level of developmentally important hormones in these plants could be measured.

```
RA1             MATSVSTIGAVNKTPLSLNNSVAGT-SVPSTAFFGKTLKKVYGKGVSSPKVTNKSLRIVA
RA2             MATSVSTIGAANKAPLSLNNSVAGT-SVPSTAFFGKTLKKVYGKGVSSPKVTNRSLRIAA
RuAct           ------------------------------------------------------------
AthL            MAAAVSTVGAINRAPLSLNGSGSGAVSAPASTFLGKKVVTV-SRFAQSNKKSNGSFKVLA
AthS            MAAAVSTVGAINRAPLSLNGSGSGAVSAPASTFLGKKVVTV-SRFAQSNKKSNGSFKVLA

RA1             EQIDVDPKKQTDSDRWKGLVQDFSDDQQDITRGKGMVDSLFQAPTGTGTHHAVLQSYEYV
RA2             EEKDADPKKQTYSDRWKGLVQDFSDDQQDIARGKGMVDSLFQAPTGTGTHHAVLQSYEYV
RuAct           EEKDADPKKQTDSDRWKGLVQDFSDDQQDITRGKGMVDSLFQAPTGTGTHHAVLQSYEYV
AthL            VKED----KQTDGDRWRGLAYDTSDDQQDITRGKGMVDSVFQAPMGTGTHHAVLSSYEYV
AthS            VKED----KQTDGDRWRGLAYDTSDDQQDITRGKGMVDSVFQAPMGTGTHHAVLSSYEYV
                 : *    *** .***:**. * *******:********:**** *********.*****

RA1             SQGLRQYNLDNKLDGFYIAPAFMDKLVVHITKNFLKLPNIKVPLILGIWGGKGQGKSFQC
RA2             SQGLRQYNMDNTLDGFYIAPSFMDKLVVHITKNFLKLPNIKVPLILGVWGGKGQGKSFQC
RuAct           SQGLRQYNLDNKLDGFYIAPAFMDKLVVHITKNFLKLPNIKVPLILGIWGGKGQGKSFQC
AthL            SQGLRQYNLDNMMDGFYIAPAFMDKLVVHITKNFLTLPNIKVPLILGIWGGKGQGKSFQC
AthS            SQGLRQYNLDNMMDGFYIAPAFMDKLVVHITKNFLTLPNIKVPLILGIWGGKGQGKSFQC
                ********:** :*******:***************.***********:************

RA1             ELVFRKMGINPIMMSAGELESGNAGEPAKLIRQRYREAAEIIRKGNMCCLFINDLDAGAG
RA2             ELVFRKMGINPIMMSAGELESGNAGEPAKLIRQRYREAAEIIRKGNICCLFINDLDAGAG
RuAct           ELVFRKMGINPIMMSAGELESGNAGEPAKLIRQRYREAAEIIRKGNMCCLFINDLDAGAG
AthL            ELVMAKMGINPIMMSAGELESGNAGEPAKLIRQRYREAADLIKKGKMCCLFINDLDAGAG
AthS            ELVMAKMGINPIMMSAGELESGNAGEPAKLIRQRYREAADLIKKGKMCCLFINDLDAGAG
                ***: ***********************************::*:**::*************

RA1             RMGGTTQYTVNNQMVNATLMNIADNPTNVQLPGMYNKQENARVPIIVTGNDFSTLYAPLI
RA2             RMGGTTQYTVNNQMVNATLMNIADNPTNVQLPGMYNKQENARVPIIVTGNDFSTLYAPLI
RuAct           RMGGTTQYTVNNQMVNATLMNIADNPTNVQLPGMYNKQENARVPIIVTGNDFSTLYAPLI
AthL            RMGGTTQYTVNNQMVNATLMNIADNPTNVQLPGMYNKEENARVPIICTGNDFSTLYAPLI
AthS            RMGGTTQYTVNNQMVNATLMNIADNPTNVQLPGMYNKEENARVPIICTGNDFSTLYAPLI
                ************************************:******** *************

RA1             RDGRMEKFYWAPTREDRIGVCTGIFRTDNVPAEDVVKIVDNFPGQSIDFFGALRARVYDD
RA2             RDGRMEKFYWAPTREDRIGVCKGIFRTDNVPEEAVIKIVDTFPGQSIDFFGALRARVYDD
RuAct           RDGRMEKFYWAPTREDRIGVCTGIFRTDNVPAEDVVKIVDNFPGQSIDFFGALRARVYDD
AthL            RDGRMEKFYWAPTREDRIGVCKGIFRTDKIKDEDIVTLVDQFPGQSIDFFGALRARVYDD
AthS            RDGRMEKFYWAPTREDRIGVCKGIFRTDKIKDEDIVTLVDQFPGQSIDFFGALRARVYDD
                ********************.******::  * ::.:** ******************

RA1             EVRKWVSGTGIEKIGDKLLNSFDGPPTFEQPKMTIEKLLEYGNMLVQEQENVKRVQLADK
RA2             EVRKWVSGTGIEAIGDKLLNSFDGPPTFEQPKMTVEKLLEYGNMLVQEQENVKRVQLAET
RuAct           EVRKWVSGTGIEKIGDKLLNSFDGPPTFEQPKMTIEKLLEYGNMLVQEQENVKRVQLADK
AthL            EVRKFVESLGVEKIGKRLVNSREGPPVFEQPEMTYEKLMEYGNMLVMEQENVKRVQLAET
AthS            EVRKFVESLGVEKIGKRLVNSREGPPVFEQPEMTYEKLMEYGNMLVMEQENVKRVQLAET
                ****:*.. *:* **.:*:** :***.****:** ***:******* ***********:.

RA1             YLKEAALGDANADAINNGSFFAS-----------------------------------
RA2             YLKEAALGDANADAINTGNF-------------------------------------
RuAct           YLKEAALGDANADAINNGSFFAS-----------------------------------
AthL            YLSQAALGDANADAIGRGTFYGKGAQQVNLPVPEGCTDPVAENFDPTARSDDGTCVYNF
AthS            YLSQAALGDANADAIGRGTFYGK----------------TEEKEPSK-----------
                **.:***********. *.*
```

Supplementary Figure 1. Pair-wise alignment of RuBiSCO activase isoforms from Arabidopsis and three RuBiSCO activase proteins identified in tobacco. RA1 - RuBiSCO activase 1 (tobacco), RA2 - RuBiSCO activase 2 (tobacco), RuAct - RuBiSCO activase (tobacco), AthL - RuBiSCO activase long isoform (Arabidopsis), AthS - RuBiSCO activase short isoform (Arabidopsis).

Consensus symbols:
* - all residues in the column are identical in all sequences in the alignment
: - conserved substitutions are observed
. - semi-conserved substitutions are observed

CHAPTER 3: Specification of adaxial and abaxial stomata, epidermal structure and photosynthesis to CO_2 enrichment in maize leaves

Published: Driscoll, S.P., Prins, A., Olmos, E., Kunert, K.J., Foyer, C.H. (2006). Specification of adaxial and abaxial stomata, epidermal structure and photosynthesis to CO_2 enrichment in maize leaves. J. Exp. Bot., 57: 381-390.

3.1 Abstract

The results from Chapter 2 indicated a strong role for cysteine proteases in plant acclimation to cold stress. These proteases are known to play an important role in senescence. Since CO_2 enrichment could both enhance or delay senescence - dependent on species and development stage of plants - the question was asked whether an increase in CO_2 would affect senescence in maize, and hence proteases or protease inhibitors that regulate this process. In order to answer this question acclimation to CO_2 enrichment was studied in maize plants grown to maturity at either 350 or 700µl l^{-1} CO_2. In this part of the study, plants grown with CO_2 enrichment were significantly taller than those grown at 350µl l^{-1} but they had the same number of leaves. High CO_2 concentration led to a marked decrease in whole leaf chlorophyll and protein. The ratio of stomata on the adaxial and abaxial leaf surfaces was similar in all growth conditions, but the stomatal index was considerably increased in plants grown at 700µl l^{-1}. Doubling the atmospheric CO_2 content altered epidermal cell size leading to fewer, much larger cells on both leaf surfaces. The photosynthesis and transpiration rates were always higher on the abaxial surface than the adaxial surface. CO_2 uptake rates increased as atmospheric CO_2 was increased up to the growth concentrations on both leaf surfaces. Above these values, CO_2 uptake on the abaxial surface was either stable or increased as CO_2 concentration increased. In marked contrast, CO_2 uptake rates on the adaxial surface were progressively inhibited at concentrations above the growth CO_2 value, whether light was supplied directly to this or the abaxial surface. These results show that maize leaves adjust their stomatal densities through changes in epidermal cell numbers rather than stomatal numbers. Moreover, the CO_2-response curve of photosynthesis on the adaxial surface is specifically determined by growth CO_2 abundance and tracks transpiration. Conversely, photosynthesis on the abaxial surface is largely independent of CO_2 concentration and rather independent of stomatal function.

3.2 Introduction

Stomata are the portals for gas exchange between the leaf mesophyll cells and the environment. They occupy between 0.5% and 5% of the leaf epidermis and are most abundant on the bottom or abaxial surface. Amphistomatous leaves, such as maize, have stomata on both sides. The pattern of the epidermal cells and abaxial/adaxial polarity of the maize leaf is established in the meristem and is subsequently maintained throughout leaf development (Juarez et al., 2004). It is not surprising, therefore, that the abaxial/adaxial polarity of maize leaves is genetically controlled. The abaxial surface receives and exchanges cell fate-determining signals with the adaxial epidermis. Several mutants involved in the regulation of this development have been described including the rolled leaf1 (Rld1-0), which shows partial reversal of polarity and adaxialization, and the leafbladeless1 (lbl1) mutant that has abaxialized leaves (Nelson et al., 2002). The RLD1 and LBL1 proteins are considered to act in the same genetic pathway to maintain the dorsoventral features of the leaf and to govern adaxial cell fate. These components appear to function upstream of members of the maize yabby family that act only after adaxial/abaxial polarity has been established (Juarez et al., 2004). In *Arabidopsis thaliana*, two related transcription factors, the R2R3 MYB proteins FOUR LIPS and MYB88, jointly restrict divisions late in stomatal cell formation (Lai et al., 2005).

The concept that stomatal structure and function has been honed through evolution to optimize the ratio of CO_2 uptake to water lost through photosynthesis, is now widely accepted. Species with the C_4 pathway of photosynthesis have further optimized CO_2 uptake processes to minimize water loss and photorespiratory CO_2 release. In maize leaves for example, CO_2 is absorbed in photosynthesis and CO_2 released in respiration at a ratio of about 17:1. As such, one hectare of maize in the field can remove about 22 tonnes of CO_2 from the atmosphere in a single growing season.

CO_2 is not only a passive substrate in gas uptake processes, but it is also involved in signal transduction processes that influence leaf structure and function. It is now established that long-distance signalling of information concerning CO_2 concentration is transmitted from mature to developing leaves (Lake et al., 2001) in such a way as to control absolute stomatal numbers and stomatal function (Lake et al., 2002; Woodward, 2002). Relatively few components of this signalling pathway have been identified. The Arabidopsis high

carbon dioxide (HIC) gene, for example, which encodes a putative 3-ketoacyl coenzyme A synthase, is a negative regulator involved in the CO_2-dependent control of stomatal numbers (Gray et al., 2000).

Extensive acclimation of photosynthesis to CO_2 enrichment is observed in plant species with either the C_3 or C_4 pathways of photosynthesis (Nie et al., 1995; Jacob et al., 1995; Tissue et al., 1993; Drake et al., 1997; Watling et al., 2000). Acclimation involves down-regulation of carbon assimilation pathways and up-regulation of processes using assimilate such as carbohydrate synthesis and respiration (Winzeler et al., 1990; Stitt, 1991; McKee and Woodward, 1994; Smart et al., 1994; Tuba et al., 1994; Nie et al., 1995). CO_2 enrichment-dependent carbohydrate accumulation is involved in the orchestration of gene expression (Stitt, 1991; Jang and Sheen, 1994; Van Oosten and Besford, 1996). Since sucrose and hexose-specific signalling mechanisms link source metabolism to nitrogen signalling and to hormone signalling pathways (Finkelstein and Lynch, 2000; Finkelstein and Gibson, 2002; Leon and Sheen, 2003), it is probable that sugar signalling is also involved in long-distance CO_2 signalling from mature to developing leaves. CO_2 enrichment induces changes in cell structure (Robertson and Leech, 1995; Robertson et al., 1995) and in whole plant morphology (Lewis et al., 1999, 2000). In sorghum, the increase in growth CO_2 from 350 to 700µl l^{-1} resulted in a marked decrease in the thickness of the bundle sheath and decreased CO_2-saturated rates of photosynthesis (Watling et al., 2000). There is little information in the literature concerning the effects of long-term CO_2 enrichment on maize leaf stomata structure/function relationships, particularly with regard to the abaxial/adaxial polarity of the leaf. The following experiments were therefore undertaken to investigate the acclimation of abaxial/adaxial morphology and photosynthetic function to CO_2 enrichment in maize

3.3 Materials and Methods

All methods were performed by A. Prins, unless otherwise indicated.

3.3.1 Plant material and growth conditions

Maize seeds (*Zea mays* variety H99) were obtained from Euralis (EURALIS Semences, Blois, France). For all experiments, plants were germinated in air in batches (12-14 plants per batch). The dry seeds were first immersed in deionised water and stirred for 2h at

room temperature. Seeds were placed separately in rows on moistened filter paper and placed in closed plastic containers at 24°C in darkness for 3-4 days to allow germination to occur. The germination rate was 96-100%. Individual germinated seeds were transferred to small pots (one per pot) containing a commercial peat/loam compost blend (Petersfield Products, Cosby, UK). This consisted of 75% medium grade peat, 12% sterilised loam, 3% medium grade vermiculite, 10% grit (5mm screened, lime free) with added nutrients [N (14%), P_2O_5 (16%), K_2O (18%), MgO (0.7%), B (0.03%), Mo (0.2%), Cu (0.12%), Mn (0.16%), Zn (0.04%), Fe (chelated) (0.09%)]. Pots were transferred to controlled environment cabinets (Sanyo 970, Sanyo, Osaka) or controlled environment rooms (Sanyo, Osaka) as illustrated in Figures 3.1 and 3.2, where atmospheric CO_2 levels were strictly maintained at either 350µl l^{-1} or at 700µl l^{-1} (Fig. 3.4). The plants were grown with a 16-h photoperiod at a light intensity of 800µmol m^{-2} s^{-1} (at leaf level) with a day/night temperature of 25ºC /19ºC, and 80% (v/v) relative humidity. When the roots started to appear at the base of the small pots, the plants were transferred to 8.5l volume (25cm diameter) pots. They were then grown to maturity (8 weeks; 12-13 leaf stage). Plants were irrigated twice daily and maintained in water-replete conditions throughout. Samples were harvested for assay at various stages of development as indicated in the text and figure legends.

Certain batches of plants were grown at 350µl l^{-1} until the 5th leaf had reached the mid-emergence stage, at which point they were transferred to 700µl l^{-1} CO_2. Just prior to transfer, the base of the 5th leaf was marked with tippex to identify the portion which had emerged at 350µl l^{-1} CO_2.

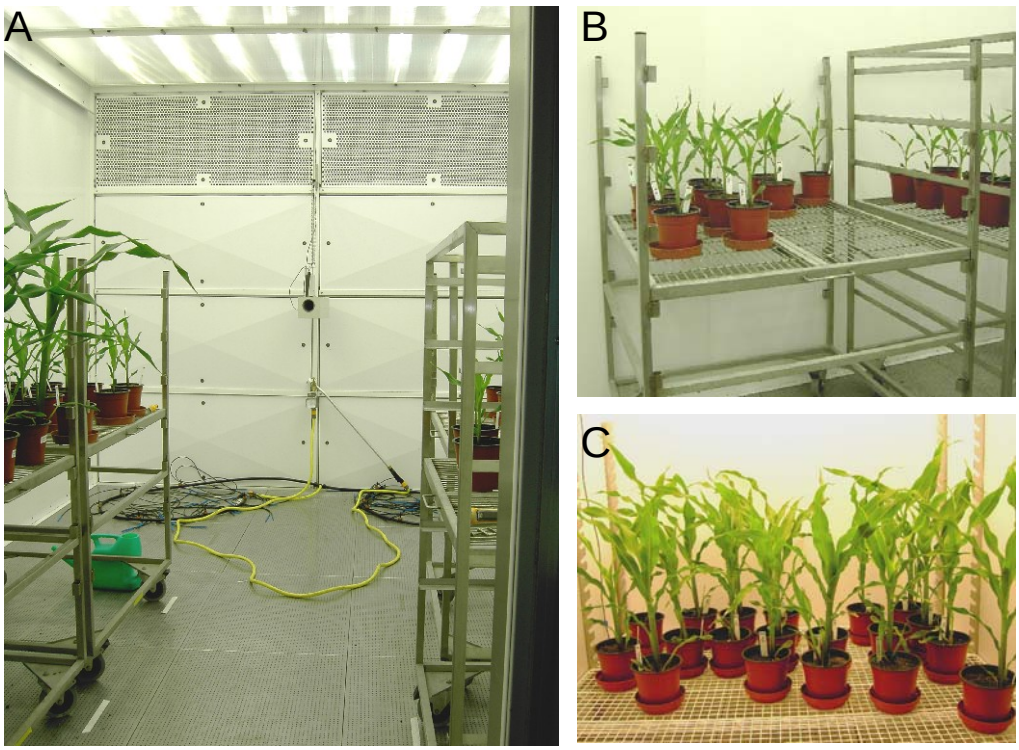

Figure 3.1 The controlled environment growth rooms and cabinets used in this study. Maize plants were grown either on trolleys in the controlled environment growth rooms (A, B) or on racks in the controlled environment cabinets (C), so that plant height could be adjusted to ensure uniform irradiance throughout development.

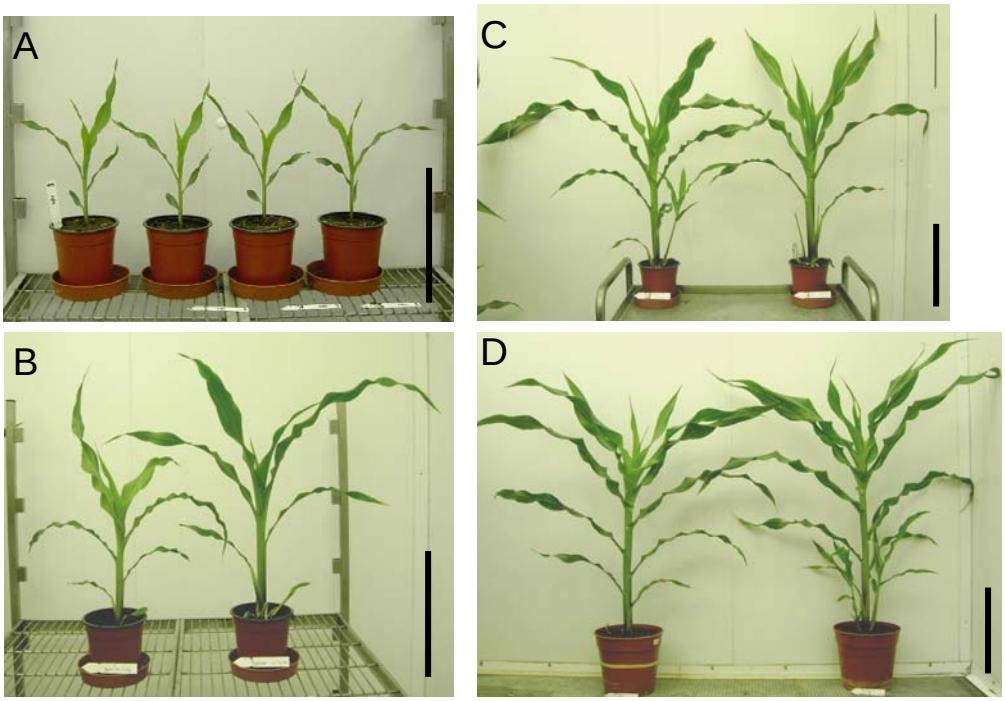

Figure 3.2 Relative low (350µl l^{-1}) and high (700µl l^{-1}) CO_2 phenotypes at different developmental stages. Plants are shown at the following stages: A) 9 days, B) 18 days, C) 25 days, and D) 32 days. In A, the first two plants (left) had been grown in air while the second two plants (right) had been grown with CO_2 enrichment. In B, C and D the plant

on the left had been grown in air while the plant on the right had been grown with CO_2 enrichment. (Scale bar = 24 cm).

3.3.2 Growth analysis

The following measurements were performed at the 12-13 leaf stage (8 weeks) from plants grown either in air or at high CO_2 (Fig. 3.4). In all experiments leaf phylogeny was classified from the base to the top of the stem, leaf one being at the bottom and leaf twelve at the top. Measurements were performed sequentially as follows:

i) Stem height

Stem height was measured from the base to the top of the stem with a ruler.

ii) Numbers of leaves, cobs, and tillers

Leaves were counted from leaf 1 to 12 as above. Although no standard fertilization procedures were applied, numbers of cobs and tillers were counted.

iii) Leaf weight

The fresh weight of each leaf was measured following excision. Total leaf fresh weights were determined on a standard laboratory balance.

3.3.3 Photosynthesis and related parameters

The following experiments were conducted on the 6^{th} or 7^{th} leaves of eight week-old plants. The same leaf segments were used for gas exchange and structural analysis. Measurements were made on either side of the mid-rib of individual leaves where the width was approximately 4cm, 24 and half cm from the leaf tip i.e. about half way from base to tip. Where plants had been exposed to a single CO_2 concentration during growth, the leaf area used for gas exchange measurements was also used for stomatal and epidermal characterisation. In leaves that had experienced growth in air for 18 days and then moved to a high CO_2 environment, two samples were taken (Fig. 3.3). The leaf part exposed to 350µl l^{-1} CO_2 was sampled by taking a 7.5x3.5cm piece on the leaf tip-side, right next to the mark indicating the area of leaf that emerged in air. The leaf part exposed to 700µl l^{-1} CO_2 was sampled by measuring 15cm from the mark (measured towards the leaf base), and taking a 7.5x3.5cm piece at this point on the leaf.

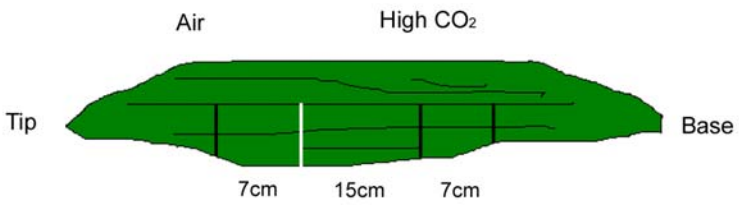

Figure 3.3 Leaf sampling to observe stomatal and epidermal characteristics in leaves exposed to air for 18 days and thereafter to high CO_2. Samples were taken next to the white mark, which indicates the leaf tip that emerged in air, and 15cm from this mark towards the leaf base, where the leaf had emerged in a high CO_2 environment.

i) Epidermal structure and stomatal patterning

Leaf pieces (7cm x 3.5cm) were harvested and epidermal tissue was stripped from the adaxial and abaxial surfaces using forceps. The epidermal peels were mounted in citrate phosphate buffer (0.1M sodium citrate, 0.1M sodium phosphate, pH6.5) and examined by light microscopy (Olympus BH-2, Olympus Optical Co. Ltd, Tokyo, Japan). The total area and numbers of stomata and epidermal cells were counted. At least 90 cells were measured from each of the digitised images from six sections using Sigma ScanPro photographic analysis software Version 5 (Sigma Chemical Co.). The digitised images were sent to E. Olmos (CEBAS-CSIC, Murcia, Spain) who performed the cell area and density measurements. The stomatal index was calculated as the number of stomata/ (number of epidermal cells + number of stomata) times 100, according to Salisbury (1927)

ii) Gas exchange, transpiration, and stomatal conductance

Gas exchange measurements were performed by S.P. Driscoll (Rothamsted Research) with assistance by A. Prins. Photosynthetic gas exchange, transpiration, and stomatal conductance was measured on attached leaves using an Infra Red Gas Analyser (model wa-225-mk3, ADC, Hoddesdon, Hertfordshire, UK). In these experiments specialized leaf chambers were used that allow simultaneous measurements of CO_2 assimilation and transpiration on each leaf surface independently. All experiments were conducted at 20°C with 50% relative humidity. The gas composition was controlled on each half of the chamber by a gas mixer supplying CO_2 and 20% O_2 and with the balance made up with N_2. The CO_2 response curves for photosynthesis were measured at 900–1000µmol m^{-2} s^{-1} irradiance. Steady-state rates of CO_2 uptake were attained at each CO_2 concentration. The CO_2 level in the chambers was increased step-wise from 50 to1000µl l^{-1}.

3.3.4 Protein and chlorophyll quantification

i) Protein

For the leaf protein profile, a disk (9.62cm^2) was cut from each leaf at a distance 12-21cm from the leaf tip (where the leaf blade could accommodate the disk diameter of 3.5cm), frozen in liquid nitrogen and stored at –80°C until protein content was determined. Leaf disks were ground in ice-cold mortars with pestles, using liquid nitrogen. When leaf tissue had been thoroughly homogenized, 1ml extraction buffer (0.1M citrate phosphate buffer, pH6.5) was added (per leaf disk) and samples further homogenised with a pestle. Homogenate was poured into an Eppendorf tube, and the mortar and pestle rinsed with an additional 1ml extraction buffer which was added to the same tube. Samples were centrifuged at 12 000rpm for 10min at 4ºC, and protein content of supernatant determined.

In general, protein content of extracts was determined according to the method described by Bradford (1976). Plant extracts (5µl) were diluted with water to a volume of 800µl before the addition of Bradford colour reagent (200µl; Bio-Rad, UK) to give a final volume of 1ml. The reaction solution was incubated at room temperature for 30 min, after which the absorbance of the solution was determined on a spectrophotometer at a wavelength of 595nm. Values were compared to a bovine serum albumin (BSA) standard consisting of 0, 1, 2, 5, 10, 15, or 20 µg BSA in diluted Bradford colour reagent (20%, v/v; Bio-Rad, UK), which was also incubated and measured as described above. All measurements were done in duplicate.

ii) Chlorophyll

For the leaf chlorophyll profile, a disk (9.62cm^2) was cut at a distance approximately 13.5-24.5cm from the leaf tip. Disks were frozen in liquid nitrogen and stored at –80°C until chlorophyll content was determined.

Chlorophyll content was determined according to the method of Lichtenhaler and Wellburn (1983). Leaf tissue was first ground in an ice-cold mortar with a pestle, using liquid nitrogen. Each leaf disk was extracted in 1ml ice-cold acetone (80%). Homogenate was decanted into an Eppendorf tube, and mortar and pestle rinsed with an additional 1ml ice-cold acetone, which was added to the same tube. All samples were incubated at -20°C over night in the dark for complete chlorophyll extraction, before centrifuging at

14500rpm for 5min at room temperature. Samples (50µl) were diluted with acetone (80%) before absorbance was measured using a quartz cuvette in a spectrophotometer at wavelengths of 645nm and 663nm. Chlorophyll (mg l^{-1}) was calculated using the equation: chlorophyll (mg l^{-1}) = 20.2 x A_{645} + 8.02 x A_{663}.

3.3.5 Statistical methods

The analysis of variance between mean values was compared using the Duncan multiple range test at $P< 0.05$.

3.4 Results

3.4.1 Effects of CO_2 enrichment on epidermal cell structure and stomatal densities on adaxial and abaxial leaf surfaces

Maize plants grown with CO_2 enrichment were significantly taller (23%; Fig. 3.4) than those grown at 350µl l^{-1} CO_2 although they had the same number of leaves (Table 3.1). The plants grown at 700µl l^{-1} had similar numbers of tillers and cobs to those grown at 350µl l^{-1} (Table 3.1).

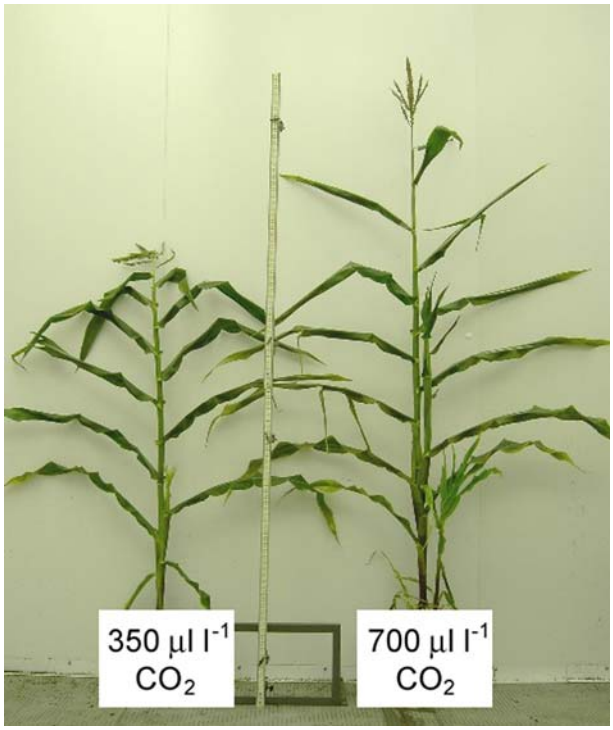

Fig. 3.4 The effect of doubling the concentration of atmospheric CO_2 from 350µl l^{-1} to 700µl l^{-1} on maize plants.

Table 3.1 The effect of growth CO_2 on the growth of maize plants. Plants were grown for 2 months at either 350µl l^{-1} CO_2 or 350µl l^{-1} CO_2. Each data point represents the mean ± SD of 13 plants per treatment, with an average of three experiments. The different letters represent statistical differences at $P < 0.05$.

CO_2 (µl l^{-1})	Height (cm)	Number of Leaves	Cobs	Tillers
350	122 ± 6^b	13 ± 1^a	2 ± 0^a	0 ± 0^a
700	150 ± 8^a	13 ± 1^a	2 ± 0^a	1 ± 1^a

The epidermal cells were arranged in parallel rows with stomata in every third or fourth row (Fig. 3.5). This pattern was similar on the adaxial (Fig. 3.5 A and C) and abaxial (Fig. 3.5 B and D) surfaces of plants grown either at 350µl l^{-1} or 700µl l^{-1} CO_2. However, the epidermal cells on both adaxial and abaxial surfaces were larger in the plants grown at 700µl l^{-1} (Fig. 3.5 C and D) than in those grown at 350µl l^{-1} CO_2. (Fig. 3.5 A and B).

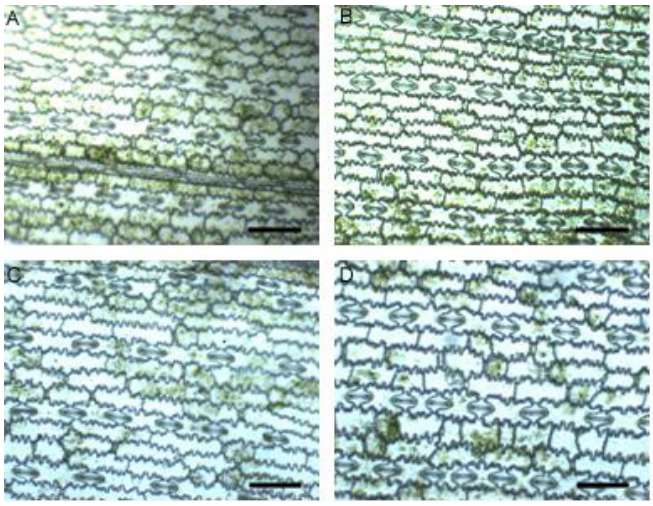

Figure 3.5 The effect of growth CO_2 on maize leaf epidermal structure. The light micrographs are representative of the structures of the adaxial surfaces of the fifth leaves of plants grown at either 350µl l^{-1} CO_2 (A) or 700µl l^{-1} CO_2 (C) and the abaxial surfaces of the leaves grown at 350µl l^{-1} CO_2 (B) or 700µl l^{-1} CO_2 (D). The bar scale is: 100µm.

The average epidermal cell area was significantly greater in 700µl l^{-1} CO_2 -grown leaves than those grown at 350µl l^{-1} CO_2 (Table 3.2). The smallest epidermal cells were observed on the abaxial surface of leaves grown at 350µl l^{-1} CO_2 while the largest were on the adaxial surface of leaves grown at 700µl l^{-1} CO2 (Table 3.2). In contrast to epidermal cell area, which increased by about 40%, epidermal cell numbers decreased by about 30% in leaves grown at 700µl l^{-1} CO_2. While the number of stomata was unaffected by CO_2 concentration, the size of the stomata was increased by growth at 700µl l^{-1} CO_2 compared with 350µl l^{-1} CO_2. The stomatal index increased as a result of doubling the CO_2

concentration on both leaf surfaces (Table 3.2). The area occupied by stomata was greater on the abaxial surface than the adaxial surface of the leaves under both growth CO_2 conditions. However, while doubling CO_2 concentration increased this parameter by over 30% on the adaxial surface, the effect was much less pronounced on the abaxial side of the leaf where stomatal area was increased by less than 20%.

Table 3.2 The structure of the adaxial and abaxial epidermis of maize leaves grown to maturity in either low (350µl l^{-1}) or high (700µl l^{-1}) CO_2.

	350µl l^{-1} CO_2		700µl l^{-1} CO_2	
	Adaxial	Abaxial	Adaxial	Abaxial
Epidermal cell area (µm^2)	2501 ± 341 ^{c}	2140 ± 285 ^{d}	3488 ± 504 ^{a}	3066 ± 615 ^{b}
Epidermal cells (number mm^{-2})	467 ± 23 ^{a}	493 ± 15 ^{a}	315 ± 36 ^{b}	341 ± 33 ^{b}
Stomatal area (µm^2)	753 ± 146 ^{c}	918 ± 69 ^{b}	1006 ± 81 ^{a}	1072 ± 139 ^{a}
Stomata (number mm^{-2})	71 ± 15 ^{b}	100 ± 19 ^{a}	67 ± 15 ^{b}	97 ± 15 ^{a}
Stomatal index	13.2 ^{c}	16.9 ^{b}	17.5 ^{b}	22.1 ^{a}
Ratio of stomata (adaxial/abaxial)	0.71		0.69	

Data represents the average ± SD for three different leaves per experiment. The different letters represent statistical differences at $P < 0.05$.

To explore acclimation of leaf structure to CO_2 concentration further, a second series of experiments was performed where all plants were grown at 350µl l^{-1} CO_2 until a point where leaf 5 had emerged from the leaf sheath. Leaf 5 was then marked at the leaf base to indicate the amount of the leaf lamina that had developed and emerged into low CO_2 at this point. Half of the plants were then transferred to an environment containing 700µl l^{-1} CO_2 and all plants were then grown for a further 6 weeks until all plants had reached maturity and leaf 5 had doubled in size with sections that emerged either into either 350µl l^{-1} or700µl l^{-1} CO_2 as illustrated in Fig. 3.6.

Figure 3.6. Acclimation of the 5th leaf to CO_2 enrichment. Maize plants were transferred from 350µl l^{-1} CO_2 to 700µl l^{-1} CO_2 at a point where half the leaf had developed and emerged into low CO_2 and plants were then grown with CO_2 enrichment to maturity. The epidermis was sampled from two different areas: one that had developed and emerged into low CO_2 and was then allowed to acclimate to high CO_2 (A) and one that had developed for 2.5 weeks at low CO_2 and thereafter (6 weeks) at 700µl l^{-1} CO_2 (B). The scale bar is 4cm.

At this point, the section of the leaf that had emerged in air (Fig. 3A) had fewer larger epidermal cells (Table 3.3) than the part of the leaf that had emerged into high CO_2 (Fig. 3.6 B). However, the epidermal cells were large on both parts of the leaf, resembling those present on high CO_2-grown leaves rather than those grown at 350µl l^{-1} CO_2 alone. In particular, while the epidermal cells in the part of the leaf that had emerged into 700 µl l^{-1} CO_2, were similar in both types of experiments (compare the data for 700µl l^{-1} in Tables 3.2 and 3.3) the cells on the parts of the leaves that had emerged into air and were then transferred to 700µl l^{-1} CO_2 tended to be even larger than those that had emerged from the leaf sheath directly into 700µl l^{-1} CO_2 (Table 3.2).

Table 3.3 A comparison of acclimation effects on the structure of the adaxial and abaxial epidermis. Samples from the 5th maize leaf that had emerged and grown at 350µl l^{-1} CO_2 for 2.5 weeks and thereafter at 700µl l^{-1} CO_2 (A) are compared with sections that had emerged and grown at 700µl l^{-1} CO_2 (B). Data represents average ± SD for three different leaves per experiment. The different letters represent statistical differences at $P < 0.05$.

	(A) Emerged in 350µl l^{-1} CO_2		(B) Emerged in 700µl l^{-1} CO_2	
	Adaxial	Abaxial	Adaxial	Abaxial
Epidermal cell area (μm^2)	3755 ± 430 ^{a}	3842 ± 589 ^{a}	3169 ± 772 ^{b}	2913 ± 458 ^{b}
Epidermal cells (number μm^{-2})	234 ± 33 ^{b}	269 ± 77 ^{ab}	284 ± 71 ^{ab}	322 ± 60 ^{a}
Stomata (number μm^{-2})	57 ± 10 ^{b}	82 ± 16 ^{a}	60 ± 13 ^{b}	82 ± 15 ^{a}
Ratio of stomata (adaxial/abaxial)	0.7		0.73	

While the adaxial surface always had fewer stomata than the abaxial surface regardless of growth CO_2 concentration, there was no statistically significant difference in epidermal cell area, number of epidermal cells per μm^2, number of stomata per μm^2 or stomatal ratio of either the adaxial or abaxial epidermis between parts of the leaf grown at 350µl l^{-1} CO_2 for 2.5 weeks and subsequently transferred to 700µl l^{-1} CO_2 and those that had only been exposed to 700µl l^{-1} CO_2 (Table 3.3). It is concluded that the section of leaf that had emerged into air had fully acclimated to higher CO_2 concentration in terms of structure during the 6 weeks growth at 700µl l^{-1} CO_2.

3.4.2 Acclimation of leaf chlorophyll and protein to CO_2 enrichment

Chlorophyll (Fig. 3.7 A) and protein (Fig. 3.7 B)contents were determined in leaves of mature plants grown either at 350µl l^{-1} CO_2 or 700µl l^{-1} CO_2 and in those grown at 350µl l^{-}

^{1} CO_2 for 2.5 weeks (to the leaf 5 stage) and transferred to an environment containing 700µl l^{-1} CO_2 (Fig. 3.7).

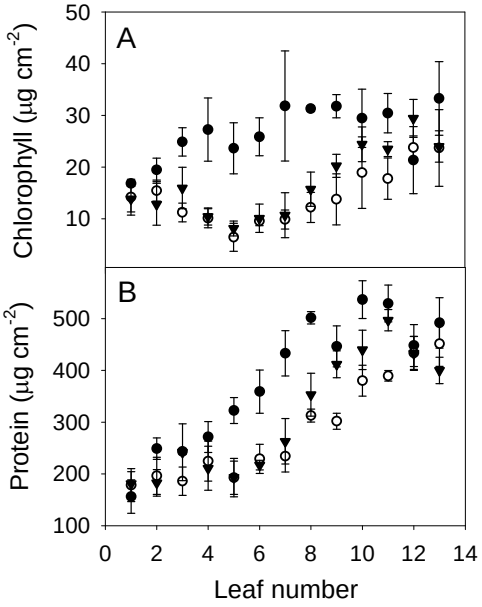

Figure 3.7 The effect of CO_2 enrichment on the chlorophyll (A) and protein (B) content of the leaves on fully mature maize plants (as shown in Fig. 3.4). Measurements were made from the lowest leaf (1) to uppermost mature leaf (13) in plants grown at either 350µl l^{-1} CO_2 (filled circles), 700µl l^{-1} CO_2 (open circles), or at 350µl l^{-1} CO_2 for 2.5 weeks and thereafter at 700µl l^{-1} CO_2 (inverted triangles). The complete experiment involving 12-14 plants was repeated three times. Data show the mean values ± SE in each case (n=3).

The youngest (leaves 12 and 13) had similar amounts of leaf chlorophyll and protein regardless of growth CO_2 as did the oldest leaves (leaves 1 and 2). All other leaves on the plants, particularly the middle leaves, had markedly lower chlorophyll and protein at 700µl l^{-1} CO_2 compared with 350µl l^{-1} CO_2. Similarly, leaves of plants transferred after 2.5 weeks from350µl l^{-1} CO_2 to700µl l^{-1} CO_2 showed lower levels of chlorophyll and leaf protein comparable to values measured in plants that had continuously experienced only 700µl l^{-1} CO_2 (Fig. 3.7). These data support the conclusion that the leaves that had originally emerged into air had fully acclimated to higher CO_2 concentration during the 6 weeks growth at 700µl l^{-1} CO_2.

3.4.3 Photosynthesis rates in mature source leaves

As shown in Fig. 3.7, mature source leaves of plants grown at 350µl l^{-1} CO_2 had a total chlorophyll content of 26.71 ± 5.24µg cm^{-2} and a protein content of 383.12 ± 124.64µg cm^{-2}, whereas those from plants grown at 700µl l^{-1} CO_2 had a total chlorophyll content of

14.38 ± 5.39µg cm^{-2} and a protein content of 286.71 ± 97.30µg cm^{-2}. Similarly, plants that were grown at 350µl l^{-1} CO_2 2.5 weeks, and subsequently transferred to 700µl l^{-1} CO_2 had a total chlorophyll content of 16.9 ± 6.8µg cm^{-2} and a protein content of 312.2 ± 113.1µg cm^{-2}.

While the whole leaves of plants grown at 700µl l^{-1} CO_2 had lower photosynthesis rates on a surface area basis compared with plants that were grown at 350µl l^{-1} CO_2 they had higher photosynthesis rates on a chlorophyll basis (Fig. 3.8; Table 3.4). The average rate of CO_2 assimilation for whole leaves, measured at 350 µl l^{-1} CO_2, in plants grown at 350µl l^{-1} CO_2 was 394 ± 168µmol h^{-1} mg^{-1} chl whereas the rate in leaves grown at 700µl l^{-1} CO_2 at 350µl l^{-1} CO_2 was 810 ± 258µmol h^{-1} mg^{-1} chl.

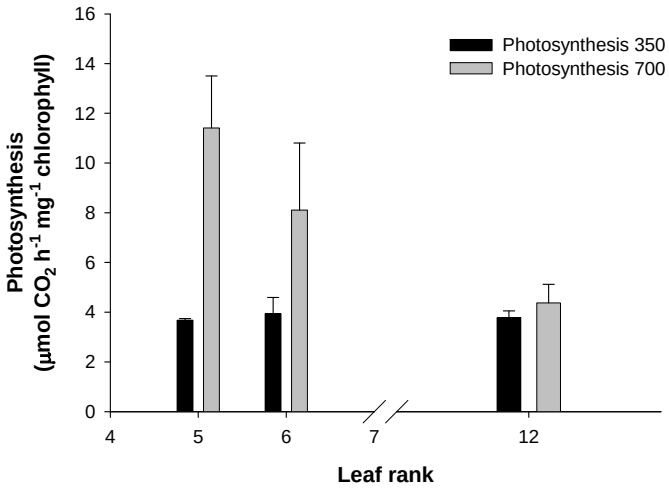

Figure 3.8 Photosynthesis rates measured in leaves 5, 6, and 12 of mature maize plants grown in air (350µl l^{-1} CO_2, "350") or with CO_2 enrichment (700µl l^{-1} CO_2, "700").

Table 3.4 Comparison of photosynthesis rates in leaves grown in air or with CO_2 enrichment, based on leaf surface area or chlorophyll (Chl) content.

Growth CO_2 (µl l^{-1})	Leaf rank	Photosynthesis measured on	Total leaf chlorophyll content (mg m^{-2})	Photosynthesis (per area) (µmol m^{-2} h^{-1})	Photosynthesis (per Chl) (µmol mg^{-1} h^{-1})
350	12	whole leaf	332.72	1257.60	3.78
350	6	abaxial side	258.50	1020.00	3.95
350	5	whole leaf	236.31	868.80	3.68
700	12	whole leaf	236.96	1036.80	4.38
700	6	abaxial side	95.48	774.00	8.11
700	5	whole leaf	64.33	734.40	11.42

3.4.4 CO_2 response curves for photosynthesis on the adaxial and abaxial leaf surfaces

Increasing ambient CO_2 (C_a) caused different responses in gas exchange on the adaxial and abaxial surfaces of maize leaves. This effect was examined in two maize hybrids: H99 (Fig. 3.9) and Hudson (Fig. 3.10), which had different absolute photosynthetic capacities, rates in Hudson being about twice those measured in H99. These hybrids were grown to maturity at either 350µl l^{-1} CO_2 or 700µl l^{-1} CO_2. Photosynthetic CO_2 assimilation rates were consistently higher on the abaxial surfaces than the adaxial surfaces in both H99 (Fig. 3.9 A and B) and Hudson (Fig. 3.10 A and B), regardless of the growth CO_2. Photosynthetic rates on both surfaces were lower in plants grown at 700µl l^{-1} CO_2. However, the kinetics of the CO_2 response curve for photosynthesis was very different on the two leaf surfaces. On the abaxial surface, photosynthesis increases with CO_2 concentration until maximal assimilation rates are reached and rates thereafter remain stable as ambient CO_2 concentration is increased. This is not the case on the adaxial surface where maximal assimilation rates are much lower than on the abaxial surface. Moreover, while maximal photosynthetic rates are attained at about the ambient CO_2 concentration sat which plants had been grown, higher CO_2 concentrations inhibited photosynthesis.

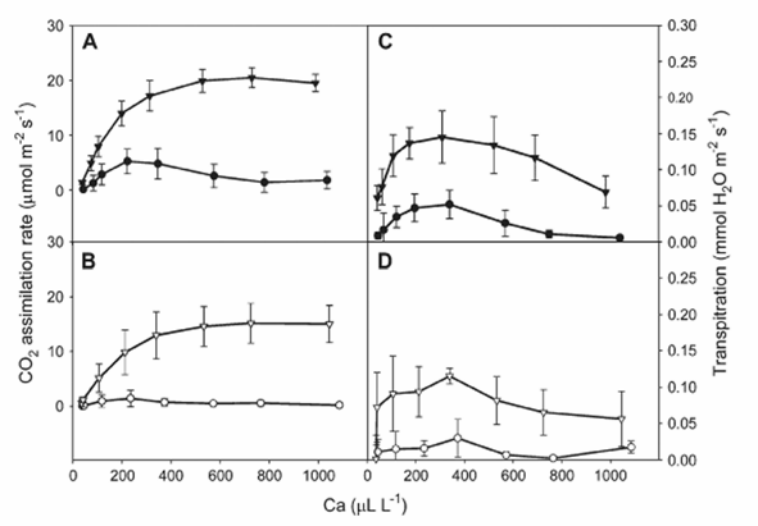

Figure 3.9 CO_2 response curves for photosynthesis (A, B) and transpiration rates (C and D) on the adaxial (filled/open circles) and abaxial (filled/open inverted triangles) surface of *Zea mays* hybrid H99 leaves. Plants were grown at either 350µl l^{-1} CO_2 (A and C) or 700µl l^{-1} CO_2 (B and D). The experiment was repeated three times with leaves from six plants measured in each experiment. Data show the mean values ± SE in each case (n=3).

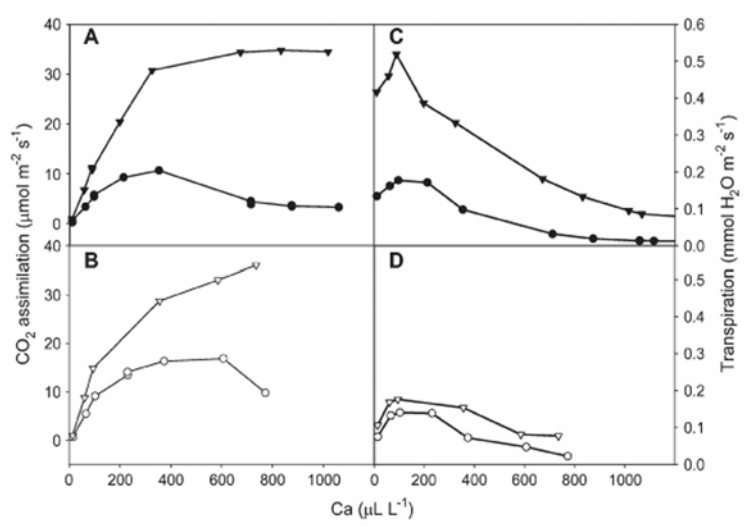

Figure 3.10 CO_2 response curves for photosynthesis (A and B) and transpiration rates (C and D) on the adaxial (filled/open circles) and abaxial (filled/open inverted triangles) surface of *Zea mays* hybrid Hudson leaves. Plants were grown at either 350µl l^{-1} CO_2 (A and C) or 700µl l^{-1} CO_2 (B and D). The complete experiment was repeated three times but the figure shows a single representative curve in each case.

The stomatal index was considerably increased in plants grown at 700µl l^{-1} CO_2. The stomatal index was lowest on the adaxial (Fig. 3.11, i) surfaces of maize leaves grown at 350µl l^{-1} CO_2. Calculated values were higher on the abaxial (Fig. 3.11, ii) surfaces in both growth conditions. Increasing the growth CO_2 concentration affected the relationship between stomatal index and CO_2 assimilation rate (Fig. 3.11 A) in a similar manner to that observed with regard to transpiration rates (Fig. 3.11 B).

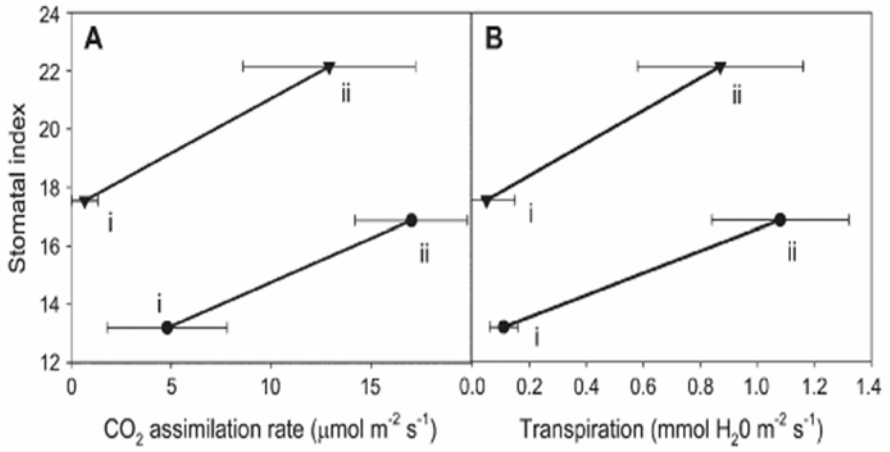

Figure 3.11 Relationships between photosynthesis, transpiration rates and stomatal index on the adaxial (i) and the abaxial (ii) surfaces of maize leaves grown either at 350µl l^{-1} CO_2 (closed circles) or 700µl l^{-1} CO_2 (filled inverted triangles).

3.4.5 The effect of light orientation on photosynthetic CO_2 responses

In the above experiments irradiance had been supplied only on the upper adaxial surface. To test whether the direction of the irradiance had a direct effect on CO_2 uptake from each surface, CO_2 assimilation was measured with irradiance supplied first to the adaxial side of the leaf until a steady rate of photosynthesis was observed, and then with irradiance supplied to the abaxial side of the leaf.

Steady-state CO_2 assimilation rates were established by incubating the leaves for 30 min at 780µl l^{-1} CO_2 with light on the adaxial surface (Fig. 3.12 i). The leaves were then inverted so that the light entered the leaves via the abaxial surfaces (Fig. 3.12 ii). The low CO_2 uptake rates observed on the adaxial surfaces in the standard orientation did not recover once the leaves were inverted and light was applied directly to the abaxial surfaces (Fig. 3.12 i). Moreover, while leaf inversion caused an initial transient decrease in the photosynthesis rate on the abaxial surface this rapidly recovered (Fig. 3.12 ii). Even after several h in this condition no subsequent changes in CO_2 uptake rates were observed.

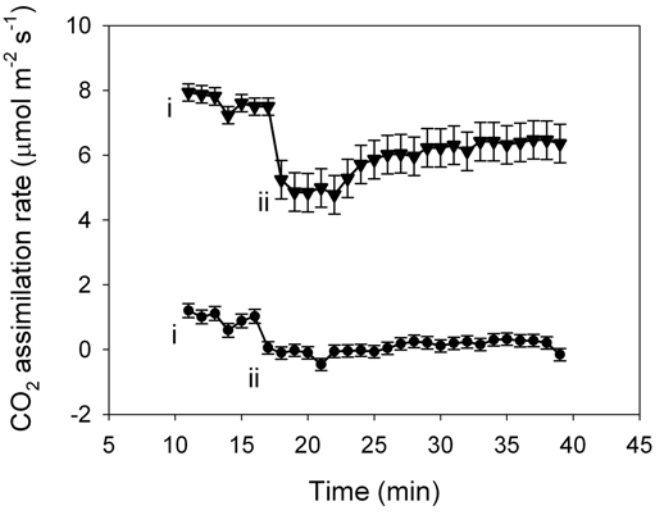

Figure 3.12 The effect of irradiance on CO_2 assimilation rates when applied directly either to the adaxial or the abaxial leaf surfaces. The light input was orientated first from the adaxial side (i) until steady-state rates of photosynthesis had been attained (30 min after the onset of illumination). Then the light source was switched to the abaxial surface (ii). CO_2 assimilation rates on the adaxial surface (filled circles) and abaxial surface (filled inverted triangles) were measured simultaneously at 780µl l^{-1} CO_2 in plants grown at 780µl l^{-1} CO_2. The experiment was repeated three times with leaves from six plants measured in each experiment. Data show the mean values ± SE in each case.

3.5 Discussion

The developmental and physiological consequences of elevated CO_2 concentration on leaf structure and function are of particular relevance in maize as it is a major food crop. The effects of climate change occasioned by anthropogenic release of CO_2 has been considered many times in relation to crops, with C_4 plants predicted to respond only marginally to future elevated CO_2 concentrations (Poorter and Navas, 2003). The results presented here indicate that maize plants show a very significant positive response to doubling ambient growth CO_2 concentrations. While early studies on the effects of CO_2 enrichment on C_4 photosynthesis had led to the prediction that maize photosynthesis would not be enhanced by elevated atmospheric CO_2, recent work in Free-Air CO_2 enrichment (FACE) experiments has established that maize leaf photosynthesis can be increased by elevated CO_2 (Leakey et al., 2004; Long et al., 2004). Similarly, the FACE studies have provided little evidence of the photosynthetic acclimation observed in C_4 species in controlled environment chamber and glasshouse studies (Long et al., 2004). In the present study conducted on plants grown in controlled environment cabinets and rooms, CO_2 assimilation rates measured on a surface area basis were decreased as a result of growth at high CO_2, but the plants were much taller as a consequence of CO_2 enrichment.

Mature leaves detect and regulate the CO_2 response of stomatal initiation in developing leaves (Lake et al., 2001 and 2002) with stomatal densities decreasing by about 20–30% for a doubling of atmospheric CO_2 (Woodward, 2002). Moreover, CO_2 signalling from mature leaves determines the photosynthetic potential of the developing leaves (Lake et al., 2002; Woodward, 2002). The presence of stomata on the upper adaxial surface increases maximum leaf conductance to CO_2 and the overall value of varying stomatal densities on the upper and lower leaf surfaces has been discussed in terms of decreasing diffusion limitations to photosynthesis in thick leaves with high photosynthetic capacities (Mott et al., 1982; Mott and Michaelson, 1991). Gas exchange characteristics from the surfaces of amphistomatous leaves have previously been described in detail particularly in relation to light intensity (Mott and O'Leary, 1984; Mott and Michaelson, 1991; Mott et al., 1982, 1993; Anderson et al., 2001) but little information is available on responses to CO_2 enrichment. Stomata on the upper and lower surfaces on amphistomatous leaves respond differently to environmental factors, but this response is not an adaptation to

different CO_2 exchange characteristics on the two surfaces (Mott and O'Leary, 1984). The results presented here allow the following conclusions to be drawn.

CO_2 enrichment modifies epidermal cell expansion in maize leaves

The adaxial surface of the maize leaves always had fewer stomata than the abaxial surface regardless of growth CO_2 concentration. However, increasing the atmospheric CO_2 resulted in fewer, larger epidermal cells in which a similar number of larger stomata are interspersed. Thus, the stomatal index increased as a result of CO_2 enrichment. The transfer experiments from low to high CO_2 confirmed that the maize leaf epidermal cells rapidly acclimate to CO_2 enrichment. Six weeks after transfer to 700µl l^{-1} CO_2 the epidermal cells on both parts of the leaf were large and resembled those present on high CO_2-grown leaves rather than those grown at 350µl l^{-1} CO_2. Moreover, the cells on the parts of the leaves that had developed and emerged into air and then been transferred to 700µl l^{-1} CO_2 were even larger than those that had developed and emerged from the leaf sheath directly into 700µl l^{-1} CO_2. This would suggest that stimulation of cell expansion and cell enlargement is a primary acclimatory response to CO_2 enrichment.

There was no statistically significant difference in the number of stomata per unit surface (mm^2) or stomatal/epidermal cell ratio in parts of the leaf that had emerged into 350µl l^{-1} CO_2 and had then been transferred to high CO_2 and those that had emerged into high CO_2 alone. These data confirm that, unlike epidermal cell area that shows an acclimatory response to prevailing CO_2, stomatal patterns are fixed prior to emergence. In Arabidopsis, local high CO_2 in the developing leaf environment negated the signal for increased density arising from mature leaves maintained at a low CO_2 (Lake et al., 2002). In maize, the epidermal cell numbers and epidermal and stomatal cell sizes are highly responsive to environmental CO_2 concentration. Hence, changes in epidermal cell numbers are largely responsible for CO_2-induced increases in stomatal index rather than a CO_2 effect on stomatal numbers *per se*.

CO_2 enrichment causes acclimation of maize leaf photosynthesis

Maize, like sorghum (Watling et al., 2000), showed extensive acclimation to growth at high CO_2. While plants with higher stomatal densities generally have high stomatal conductance and photosynthetic rates (Lake et al., 2002), the stomatal area measured here in the 700µl l^{-1} CO_2-grown maize was slightly higher than that of plants grown at 350µl l^{-1}

CO_2 despite similar rates of photosynthesis. However, acclimation of leaf chlorophyll and protein was evident in plants grown at 700µl l^{-1} CO_2, which had much lower levels of both parameters than plants grown at 350µl l^{-1} CO_2. On average, plants grown at 350µl l^{-1} CO_2 had 58% more chlorophyll and 29% more protein than plants grown at 700µl l^{-1} CO_2. Lower levels of chlorophyll and leaf protein were also observed in plants transferred to 700µl l^{-1} CO_2 after 2.5 weeks growth at 350µl l^{-1} CO_2. Hence, all leaves rapidly acclimated to CO_2 enrichment after transfer. While growth at high CO_2 led to a slight decrease in leaf photosynthesis on a surface area basis, acclimation was associated with a large increase in the efficiency of photosynthesis, which was doubled on a chlorophyll basis in plants grown at the higher CO_2 concentration. These results show that maize leaves acclimate well to growth at high CO_2 and benefit from CO_2 enrichment.

CO_2 enrichment has a different effect on photosynthesis of the adaxial and abaxial leaf surfaces

The amphistomatous nature of maize leaves means that they have the capacity to open and close their stomata on both sides independently, with transpiration rates being more sensitive to changes in stomatal aperture on the abaxial surface. The data presented here shows that atmospheric CO_2 has a pronounced differential effect on photosynthetic CO_2 uptake rates on the adaxial and abaxial leaf surfaces. The CO_2 response curves for photosynthesis on the adaxial and abaxial surfaces showed that in both cases uptake increased with increasing CO_2 concentration up to growth CO_2. Above these values, CO_2 assimilation rates showed different responses to ambient CO_2 on the adaxial and abaxial surfaces. While assimilation on the abaxial surface was stable or increased as CO_2 concentration increased, assimilation on the adaxial surface decreased as CO_2 concentration increased. The physiological significance of the observed stomatal polarity with regard to the regulation of CO_2 uptake rates is unknown and it is surprising given that the C_4 maize leaf is essentially non-polar with similar distances for light and CO_2 to travel on either side of the leaf. Further work is required to determine the structural mechanisms contributing to this marked functional polarity, for example, perhaps the chloroplasts are arranged somewhat differently in the photosynthetic cells beneath the adaxial and abaxial epidermal surfaces. However, it may be that this phenomenon is a specific feature of C_4 leaves as such differential controls of photosynthesis have been observed on the adaxial and abaxial surfaces of another C4 species, *Paspalum*, but not in the leaves of the C3 species, wheat (Soares et al., 2008).

The decrease in photosynthesis on the adaxial leaf surfaces in response to high CO_2 is not necessarily related to water use efficiency

The differential photosynthetic assimilation rates observed on the adaxial and abaxial surfaces in response to ambient CO_2 were not influenced by the direction of light entry to the leaf. Improved plant water status is considered to be the primary basis for higher CO_2 assimilation rates in C_4 plants under elevated CO_2. However, the results presented here suggest that the function of stomata with regard to control of photosynthesis is genetically programmed to be different on the leaf surfaces. Given that transpiration rates are more sensitive to changes in stomatal aperture on the abaxial surface, it is surprising that this population has a much higher threshold for closure in response to high CO_2 and high light than the adaxial surface population. This has important implications for the control of plant water loss even though the maize plants studied here were well watered. These results would argue against a simple stomata-based strategy for optimizing water-use efficiency in maize and indicate that the stomata on the upper leaf surface are programmed to be a much more sensitive barometer for changes in ambient CO_2 than those on the lower surface, which remain open even at excessively high CO_2 levels.

Overall, this part of the study has shown that maize acclimates substantially to an increased availability of CO_2 by decreasing protein and chlorophyll content, and increasing stomatal index. In order to identify changes in the maize transcriptome and possible signalling molecules that might underpin these acclamatory responses, a microarray study was undertaken which is discussed in the following chapter.

CHAPTER 4: Acclimation of maize source leaves to CO_2 enrichment at flowering

In preparation for re-submission to The Plant Cell: Prins, A., Muchwezi, J., Verrier, P., Pellny, T., Beyene, G., Kunert, K.J., Foyer, C.H. Acclimation of maize source leaves to CO_2 enrichment involves regulation of serine protease inhibitors by redox and hexose-signaling.

4.1 Abstract

As an extension of the study on maize acclimation to high CO2 initiated in Chapter 3, a further study was launched to identify additional morphological and photosynthetic changes, and, in particular, the effect of CO2 ennrichment on the maize transcriptome. To this end maize plants grown for 8 weeks under either air (350µl l^{-1} CO_2) or high CO_2 (700µl l^{-1} CO_2) were studied. Whole plant morphology was unaffected by high CO_2 under the growth conditions used in this part of the study in contrast to previous results. Photosynthesis was decreased on a surface area basis as a result of CO_2 enrichment but relatively few changes in transcripts involved in photosynthesis and related metabolism were observed. Transcriptome comparisons revealed over 3000 transcripts modified between leaf ranks 3 (old source leaves) and 12 (young source leaves) but only 142 and 90 transcripts respectively were modified as a result of high growth CO_2 availability. The high CO_2 leaf transcriptome displayed a decreased oxidative stress signature with effects on primary metabolism largely restricted to the youngest source leaves. Among the up-regulated transcripts two novel CO_2-modulated putative serine protease inhibitors (a serpin and a Bowman-Birk-type inhibitor) were identified, which were modulated by both sugars and pro-oxidants. High CO_2 decreased leaf protein carbonyls, which were most abundant in the young source leaves. The oldest source leaves were virtually free of protein carbonyls in air but were rich in hexoses. Growth with high CO_2 decreased protein carbonyl formation and eliminated development-dependent changes in the leaf hexose accumulation. It's concluded that the control of leaf hexose accumulation during leaf development is the most important factor modulating the two putative serpin and Bowman-Birk inhibitor transcripts in response to CO_2 enrichment *in planta*.

4.2 Introduction

The on-going substantial rise in atmospheric CO_2 levels presents multiple challenges for the sustainable management of agricultural ecosystems. While photosynthesis is considered to play a crucial role in ecosystem sustainability (Millennium Ecosystem Assessment, 2005) major uncertainties remain concerning high atmospheric CO_2-dependent effects on the relative competitiveness of plants using the C_3 and C_4 pathways of photosynthesis (Ward et al., 1999: Wand et al., 1999; Zhu et al., 1999). The CO_2-concentrating mechanism employed by C_4 plants diminishes CO_2-limitations at the active sites of RuBisCO, leading to suggest that C_4 plants will not respond positively to rising levels of atmospheric CO_2. However, the acclimation of photosynthesis involving down-regulation of RuBisCO and the Benson-Calvin cycle that has often been observed when C_3 species are grown with atmospheric CO_2 enrichment may be absent from C_4 plants, where these enzymes have already acclimated to functioning under high CO_2 conditions. Literature evidence suggests that different C_4 plants such as *Amaranthus retroflexus*, maize, *Sorghum bicolour,* and *Paspalum dilatatum* can benefit from increased atmospheric CO_2 availability, showing enhanced rates of photosynthesis (Maroco et al., 1999; Ziska and Bunce, 1999; Ward et al., 1999; Cousins et al., 2001) and carbon gain (Driscoll et al., 2006; Soares et al., 2008). However, the degree of the response of photosynthesis to CO_2 enrichment varies between species and conditions such that often little or no effect is observed (Sage, 1994; Ghannoum et al., 1997 and 2001; von Caemmerer et al., 2001, Wand et al., 2001; Leakey et al., 2006).

Atmospheric CO_2 availability exerts a strong influence on leaf structure and composition as well as stomatal density and patterning (Larkin et al., 1997; Croxdale, 1998; Taylor et al., 1994; Masle, 2000; Lake et al., 2001; 2002; Poorter and Navas, 2003; Martin and Glover, 2007). The stomatal index increased in response to CO_2 in maize (Chapter 2) and *P. dilatatum* (Soares et al., 2008), two monocotyledonous C_4 species, implying that fewer epidermal cells surround each stomatal aperture. The CO_2-signalling pathways that orchestrate these changes in leaf structure and composition responses remain poorly characterised (Gray et al., 2000; Ferris et al., 2002) but signals transported from mature to developing leaves are considered to be important regulators of such responses (Coupe et al., 2006; Miyazawa et al., 2006).

While the regulation of photosynthesis and related gene expression has been extensively characterized with respect to CO_2 availability in dicotyledonous C_3 leaves, little information is available on the effects of CO_2 enrichment in C_4 plants. The focus of this research has therefore been to elucidate how metabolism and gene expression in the different leaf ranks of maize at anthesis, a point where all the leaves are source leaves, respond to growth with CO_2 enrichment. Maize leaves are monocotyledonous species and employ the NADP-malic enzyme (ME) decarboxylation pathway of C_4 photosynthesis. In the present study, a classic whole plant physiology approach has been combined with molecular genetic techniques to resolve the genetic basis for the responses of maize to the rise in atmospheric CO_2, which could be almost double the 2006 figure of 381µl l^{-1} in 2050. Any estimation of the role of C_4 photosynthesis in sustaining both cultivated and natural ecosystems (Millennium Ecosystem Assessment, 2005), necessitates an improved understanding of how leaf metabolism and gene expression are controlled in C_4 plants, particularly at flowering, a stage which is very sensitive to water deprivation and other environmental stresses.

Since very little information is available in the literature on the components that regulate leaf protein turnover in response to CO_2 enrichment, the effect of development and CO_2 enrichment on maize plants was investigated, focusing on the leaf transcriptome and leaf metabolism. A further aspect of this study was to investigate if CO_2 enrichment also affects the function of proteases and their inhibitors in maize plants. In order to characterize the metabolic components that are important in the regulation of leaf proteases and protease inhibitors, the respective roles of carbohydrate status and cellular oxidation state in the regulation of gene expression and protein turnover with respect to growth CO_2 level were investigated.

4.3 Materials and Methods

All methods were performed by A. Prins, unless otherwise indicated.

4.3.1 Plant material and growth conditions

Zea mays L. hybrid H99 plants were grown for eight weeks in compost (Driscoll et al., 2006) in duplicate controlled environment rooms (Sanyo 970, SANYO, Osaka) where the atmospheric CO_2 was maintained at either 350µl l^{-1} or at 700µl l^{-1}. The plants were

exposed to 16h photoperiod (700µmol m^{-2} s^{-1}) and the temperature was maintained at 25ºC (day) and 19ºC (night) with 80% relative humidity. The CO_2 was supplied from a bulk container, transmitted via a Vaisala GMT220 CO_2 transmitter (VAISALA OYJ, Helsinki, Finland), and maintained by a Eurotherm 2704 controller (EUROTHERM LTD., Worthing, U.K.) that kept CO_2 levels at 350 ± 20µl l^{-1} or 700 ± 20µl l^{-1}. All plants were watered everyday throughout development in order to avoid a water stress, especially in plants grown at 700µl l^{-1}.

4.3.2 Growth analysis

The following measurements were performed at the 12-13 leaf stage (8 weeks) from plants grown either in air or at high CO_2 (Fig. 4.1). In all experiments leaf phylogeny was classified from the base to the top of the stem, leaf one being at the bottom and leaf twelve at the top. Measurements were performed sequentially as follows:

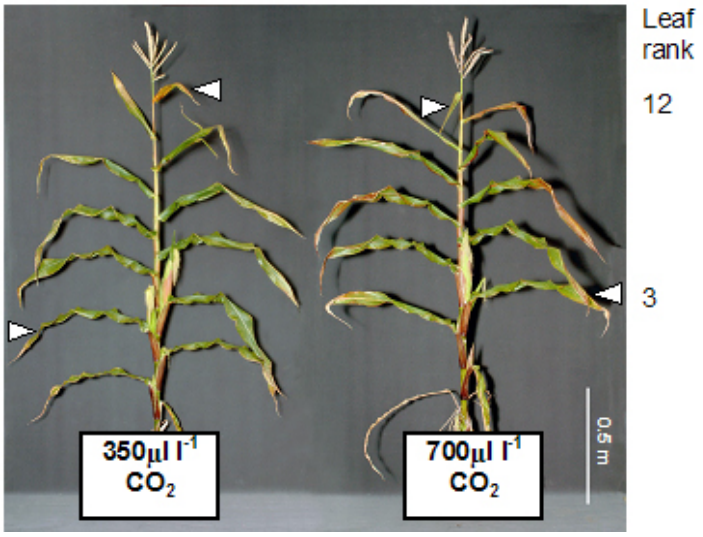

Figure 4.1 A comparison for the air (350µl l^{-1}) and high CO_2 (700µl l^{-1}) maize phenotypes at 8 weeks. The leaf ranks sampled for microarray analysis are indicated by arrows.

i) Leaf weight and area

The fresh weight and area of each leaf was measured following excision. Total leaf fresh weights were determined on a standard laboratory balance. Leaf area was measured using a ΔT area meter (Delta-T Devices LTD, England) according to instructions of the manufacturer.

ii) Tissue water content

Tissue water contents were determined from the relative fresh weight and dry weights of 8cm^2 leaf disks. Discs were harvested from the centre of every second leaf, midway between leaf tip and base. Fresh weights were determined as above. The discs were then placed in an oven at 60°C for 3 days, after which time the discs were weighed again. Tissue water content was calculated according to the equation: tissue water content (TWC) = (fresh weight – dry weight) / dry weight.

4.3.3 Leaf tissue anthocyanin pheophytin, and chlorophyll contents

Anthocyanin was measured in maize samples according to Sims and Gamon (2002). Whole leaves from three biological replicates were pooled and ground until homogeneity with a pestle in a mortar, under liquid nitrogen, after which samples were stored in 50ml Falcon tubes at –80°C. Samples representing each leaf on the stem of maize plants grown either at 350µl l^{-1} or 700µl l^{-1} CO_2 were analysed. Aliquots of the pooled, homogenised leaf material (approximately 100mg) was crushed with liquid nitrogen in extraction solution (1ml; methanol/HCl/water [90:1:1, vol:vol:vol]) and ground until homogenised. Mortars were rinsed with an additional 1ml extraction solution which was added to the same tube, to ensure complete recovery of tissue. Due to the interference of pheophytin, which has an overlapping tail that absorbs light at A_{529}, an adjusted absorbance was calculated to obtain a corrected value from which anthocyanin content was calculated. Corrected absorbance was calculated using the following equation: corrected anthocyanin absorbance = A_{529} – (0.288 A_{650}). The corrected anthocyanin absorbance was used to calculate total anthocyanin content using a molar absorbance coefficient for anthocyanin at 529nm of 30,000 M^{-1} cm^{-1} and using the Beer-Lambert equation: $A = \varepsilon.C.L$, where A – absorbance, ε - molar absorbance coefficient (M^{-1} cm^{-1}), C – concentration (M), and L – path length (cm). Anthocyanin content was expressed as nmol anthocyanin mg^{-1} pheophytin.

In acidified solutions used for measuring anthocyanin content the chlorophyll degradation product pheophytin was measured according to Vernon (1960). Absorbance of extracts prepared as described above was measured in a spectrophotometer at wavelengths of 655nm and 666nm. Pheophytin content of these solutions was calculated using the equation: pheophytin (mg l^{-1}) = 26.03 x A_{655} + 6.75 x A_{666}. Absorbance measurements for

pheophytin were taken in the same solutions in which anthocyanin content was determined, where pigments were extracted in a solution consisting of methanol/HCl/water (90:1:1, vol:vol:vol), and also after re-extraction of pelleted plant material collected after measurement of anthocyanin. For re-extraction, pelleted plant material was resuspended in 80% acetone and incubated overnight at -20°C in the dark. The values obtained in both solutions at 655nm and 666nm were added before calculating the final amount of pheophytin in the extract.

4.3.4 Quantification of leaf sucrose, hexose and starch

Quantification of leaf sucrose, hexose, and starch was performed by J. Muchwezi (University of Pretoria). Whole leaves were harvested and immediately frozen in liquid nitrogen in the growth cabinets. Hexose content was measured in frozen, crushed tissue pooled from three biological replicates, representing each leaf of the plant profile, according to Jones et al. (1977). Starch was extracted and assayed in the same samples according to the method of Paul and Stitt (1993). Sugar and starch content was expressed per µg chlorophyll.

4.3.5 Protein carbonylation

Protein carbonylation was determined by J. Muchwezi (University of Pretoria). Whole leaves were harvested and immediately frozen in liquid nitrogen in the growth cabinets. The composition and extent of protein carbonyl group formation was measured using the OxyBlot™ Oxidized Protein Detection Kit (Chemicon International, UK). Oxidative modification of proteins introduces carbonyl groups into the side chains of these proteins. Carbonyl groups can be derivatised with 2,4-dinitrophenylhydrazine (DNPH) and then detected by antibodies specific to the attached DNP moiety of the proteins. In brief, protein extracts (15-20µg) were first denatured by the addition of 6% SDS (v/v; total volume of 10µl) and then incubated in an equal volume of 1xDNPH for 15min at room temperature. Samples were neutralised by the addition of 7.5µl neturalisation buffer before being separated by SDS-PAGE. Proteins separated on the PA gel were transferred to a nitrocellulose membrane which was then incubated for 1h in blocking/dilution buffer. The membrane was then incubated for 1h in primary antibody diluted in blocking/dilution buffer to a concentration of 1:150. After washing the membrane three times in 1x phosphate buffered saline (PBS) it was incubated for 1h in secondary antibody diluted in

blocking/dilution buffer to a concentration of 1:300. The membrane was again washed three times with 1xPBS before being treated with chemiluminescent reagents and exposing the resultant membranes to X-ray film.

4.3.6 RNA extraction, purification, and analysis

Total RNA was extracted using Trizol reagent (Invitrogen, UK). This is a mono-phasic solution of phenol and guanidine isothiocyanate which protects RNA from degradation by inhibiting RNAse activity while disrupting cells and dissolving cell components. All solutions used throughout the procedure were treated with 1mM diethyl pyrocarbonate (DEPC) and autoclaved for 20min to remove RNase activity. In general, 300mg leaf tissue was ground to a fine powder in a mortar with pestle, in the presence of liquid nitrogen and then further homogenized with 3mL Trizol reagent. The sample was ground continuously until it had completely thawed. After 5min at room temperature the sample was centrifuged at 12000xg for 15min. The supernatant was extracted twice in chloroform (first in 0.2 volumes chloroform and then in an equal volume chloroform) by vortexing for 15 seconds after addition of chloroform, leaving samples at room temperature for 5min and then centrifuging at 8000xg for 10min. Addition of chloroform followed by centrifugation separates the solution into an aqueous phase and an organic phase. RNA is present exclusively in the aqueous phase. After transfer of the aqueous phase, the RNA was precipitated by the addition of 0.5 volumes isopropyl alcohol and incubation at room temperature for 30min. Precipitated RNA was sedimented by centrifuging at 12000xg for 10min and then washed in absolute ethanol (75%). The supernatant was discarded and the RNA pellet evaporated to dryness in a dessicator before re-suspension in DEPC treated water (100µl).

RNA concentration and purity was quantified by applying 2µl of dissolved RNA to the column of a NanoDrop ND-1000 spectrophotometer (NanoDrop Technologies, UK) and measuring the absorbance at 230nm, 260nm, and 280nm. An A_{260}/A_{280} ratio of ~2.0 and A_{260}/A_{230} ratio of 1.8-2.2 indicates RNA mostly free from contaminating substances. A ratio that is appreciably lower indicates the presence of proteins, phenol, or other contaminants in the former and co-purified contaminants in the latter. After spectrophotometric analysis, 40 - 100µg RNA from each sample was purified with RNeasy Mini Spin Columns (Qiagen) according to the manufacturers' instructions. After

purification, concentration and purity was again determined on the Nanodrop spectrophotometer. Quality of RNA samples was also determined by electrophoresis on agarose gels and staining with ethidium bromide, which allows the visualisation of the 18S and 28S ribosomal RNA (rRNA) subunits. A theoretical ratio of 1.7-2.0 between 28S and 18S indicates intact RNA, however, this ratio is difficult to attain in standard RNA isolation procedures. For electrophoresis, RNA samples (2µg) were heated to 65°C for 5min in a loading buffer containing 50% (v/v) glycerol, 1xTAE buffer, 1% (w/v) bromophenol blue and 60% (v/v) formamide before being cooled and then separated on a 1.5% non-denaturing agarose gel according to the method of Sambrook et al. (1986). Formamide is a denaturing agent that stabilizes RNA and ensures RNA molecules migrate according to size even in non-denaturing electophoresis. Agarose gels were run at 180V and 100mA to separate the RNA. RNA was visualised by including the fluorescent, intercalating agent, ethidium bromide in the gel and illuminating the gel with UV light after electrophoresis.

For the microarray study, leaf 12 (young leaf) and leaf 3 (old leaf) of 8 week-old maize plants grown at 350µl l^{-1} or 700µl l^{-1} CO_2 were used. Eight plants from each treatment were sampled, with equal amounts of RNA from 2-3 plants being pooled to obtain 3 replicate samples. For qPCR, RNA was extracted from pooled samples (n=3) of plants grown in either air or with CO_2 enrichment, representing each leaf on the stem (Fig. 4.2 A). For the feeding study, total RNA was extracted from 400mg of frozen tissue (Fig. 4.2 B).

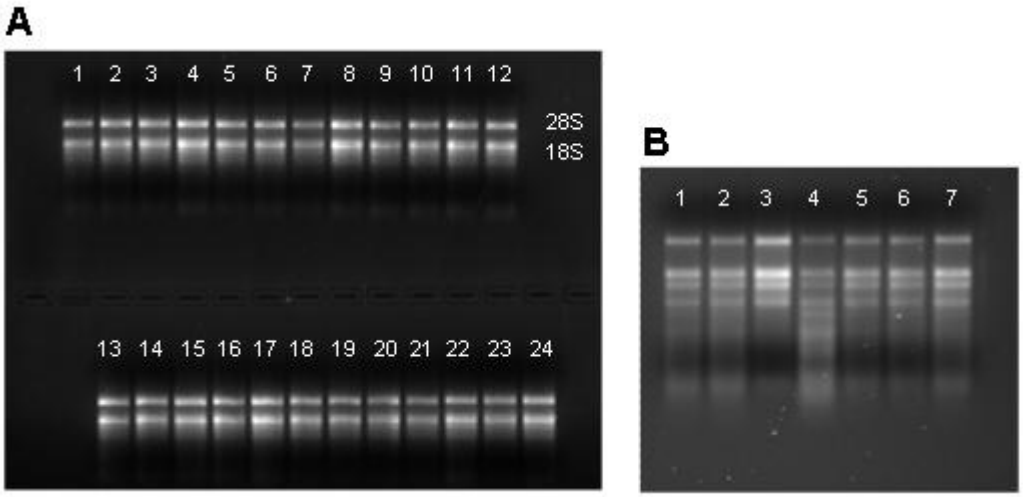

Figure 4.2 Electrophoresis of total RNA (2µg) on a 1.5% non-denaturing agarose gel visualized under UV after staining with ethidium bromide. RNA extracted from leaf 1 to leaf 12 for qPCR (A) of plants grown at 350µl l^{-1} CO_2 (1-12) or 700µl l^{-1} CO_2 (13-24), and RNA extracted from leaves after 16h of feeding (B) with 1) 10mM Hepes (pH7), 2) 1mM methyl viologen, 3) 20mM H_2O_2, 4) 20mM DTT, 5) 50mM glucose, 6) 50mM fructose, and 7) 50mM sucrose as detailed in section 4.6.

4.3.7 Micorarray hybridization

Three replicate samples of purified RNA from 8 biological replicates (2-3 biological replicates being pooled into a single sample) were used for microarray analysis. RNA was extracted from young (leaf 12 of 13) or old leaves (leaf 3 of 13) of maize plants grown either in air or with CO_2 enrichment, and sent to ArosAB, Denmark for microarray analysis. There, samples were converted to cDNA with Superscript (Invitrogen) and used to synthesise biotin-labelled cRNA (BioArray High Yield RNA Transcript Labeling Kit, Enzo). Labelled cRNA was fragmented before being hybridised to microarray chips (Affymetrix). This was done in triplicate for each sample. Each array was washed and scanned in a GeneChip Scanner 3000 (Affymetrix). The Affymetrix maize microarray chip provides comprehensive coverage of over 100 cultivars present in NCBI's UniGene data set with sequence information being selected from NCBI's GenBank © (up to September 29, 2004) and *Zea mays* UniGene Build 42 (July 23, 2004) databases. The array includes 17 555 probe sets for approximately 14 850 *Zea mays* transcripts which in turn represent 13 339 genes (12 113 of which are presented in distinct UniGene clusters).

4.3.8 Microarray analysis

Raw intensity values from the scanned array were analysed by P. Verrier (Rothamsted Research, UK) using the Robust Multichip Average method (RMA) (Bolstad et al., 2003)

as implemented in RMAExpress (http://rmaexpress.bmbolstad.com/). Normalised intensity values expressed as $\log_2$ values were compared as ratios, where a ratio of ±0.5 was selected as significant for further study. The putative identity of unknown or uncharacterised differentially expressed transcripts was determined by A. Prins. Putative transcript identity was determined from annotation available for probes at the NetAffx website (https://www.affymetrix.com/analysis/netaffx/index.affx),according to the Unigene cluster they fall into (http://www.ncbi.nlm.nih.gov/UniGene; Pontius et al., 2003), or by translated homology search. Homology search was done by translating the differentially expressed transcript sequence into amino acids (in all possible reading frames) and comparing it to known protein sequences (tblastx) on the NCBI protein refseq database (as on 17 March 2006) and the trembl (EBI) data set (as on 16 May 2006) with a criteria of minimum homology of 50% and e value of ≤-7 for significance.

4.3.9 Modulation of tissue sugars and redox state by exogenous supply of sugars and pro-oxidants

Leaf 3 (n=10) was removed from 3 week-old maize plants (seventh leaf emergent), cut into ~1cm^2 pieces under 10mM Hepes, pH7 and mixed well. Thirty of these pieces were placed into separate feeding solutions consisting of 50mM fructose, 50mM glucose, 50mM sucrose, 20mM DTT, 20mM H_2O_2, or 1mM methyl viologen in 10mM Hepes buffer, pH 7, and left for 16h in the dark. Feeding solutions were then drained, leaf pieces briefly dried by touching to paper towel, and RNA extracted (Fig. 4.2) for qPCR to quantify relative expression of selected transcripts. Controls consisted of leaf pieces incubated in 10mM Hepes buffer, pH 7 without addition of an extra solute.

4.3.10 Quantitative realtime PCR (qPCR) analysis

i) Selection of sequences for analysis and primer design

Transcripts were selected for further analysis by qPCR based on microarray results that revealed an effect of CO_2 enrichment or developmental stage on them (Table 4.1). Two transcripts specifically modified by CO_2 (Zm.3332.1.A1_at and Zm.4270.2.A1_a_at) and 5 transcripts specifically modified by developmental stage (Zm.13430.1.S1_at; Zm.231.1.S1_at; Zm.3478.1.S1_a_at; Zm.6977.1.S1_at; Zm.26.1.A1_at) were analysed. Quantitative PCR was done, firstly, in each leaf of the maize plant profile and, secondly, after feeding leaves as detailed in section 4.3.9. Primers targeting a 50-53bp region on

Table 4.2. Expression values of endogenous controls based on microarray results. Probe sets with a raw expression intensity of >10 000 (log_2 value = 13.288) were selected as endogenous controls.

	log_2 raw expression values					
Probe set and gene identity	**Old-Air**	**Young-Air**	**Old-CO_2**	**Young-CO_2**	**Forward primer**	**Reverse primer**
Zm.12132.3.S1_a_at Ubiquitin	14.070	14.013	14.074	14.025	GTGCCTGCGTCGTC TGG	AACAGCAGATACT TTGACAACCTCC
Zm.719.1.A1_at Thioredoxin M	13.306	13.329	13.328	13.305	CATGCATCGACGAC TAAACACA	TGATCATATCCCGT ATGCAAAGG
AFFX-Zm_Cyph_3_at Cyclophilin	13.786	13.812	13.795	13.775	TCCGTTCCTTTGGA TCTGAATAA	AACTAAGACCACC ACTCAGATCACC

ii) Sequence amplification

Purified total RNA was extracted from samples pooled from three biological replicates for qPCR on the plant profile, and from 400mg frozen leaf tissue obtained from ten biological replicates for the feeding study using Trizol reagent (Invitrogen) as detailed in section 2.5.1. The purified RNA (2µg) was treated with DNAse I (2U; amplification grade) (Invitrogen) according to the instructions provided by the supplier, for removal of any remaining genomic DNA. DNAse I was inactivated by incubation at 65ºC for 10min, after which first strand cDNA was prepared in the same tube using SuperScript II (Invitrogen) according to instructions provided by the supplier. Oligo dT_{12-18} primers (1µg), dNTP mix (12.5nmol each of dATP, dGTP, dCTP, and dTTP), first strand buffer (1x, as supplied by manufacturer), and 11.4mM DTT were added to DNAse treated RNA and incubated at room temperature for 2min before adding 200U SuperScript II and incubating the reaction at 42°C for 90min. Samples were stored at –20°C. Oligo dT primers amplify mRNA molecules by binding to 3' poly-A tails.

Primer stock solutions (100µM) for individual primers were first prepared, after which stock solutions containing both forward (5µM) and reverse (5µM) primers were prepared in autoclaved distilled H_2O, for use in amplification reactions. First-strand RNA template was diluted 2-fold and stored in aliquots. Quantitative PCR was done at least in triplicate on this template using the Applied Biosystems 7500 Real Time PCR System and SYBR green as intercalating dye. The SYBR® Green JumpStart™ Taq ReadyMix™ for Quantitative PCR (Sigma, UK) was used for amplification. The ReadyMix solution contains 20mM Tris-HCl, pH8.3, 100mM KCl, 7mM MgCl2, 0.4mM each dNTP (dATP,

dCTP, dGTP, TTP), stabilizers, 0.05unit/ml Taq DNA Polymerase, JumpStart Taq antibody, and SYBR Green I. SYBR Green is a fluorescent DNA binding dye with excitation and emission maxima of 494nm and 521nm respectively. It binds all double-stranded DNA causing an increase in fluorescence throughout cycling as DNA is amplified. An Internal Reference Dye (Sigma) that is similar to 6-Carboxy-X-rhodamine (ROX) was included as internal reference dye. Each amplification reaction consisted of 50% (v/v) SYBR Green JumpStart Taq ReadyMix, 1% (v/v) Internal Reference Dye, 200nM each forward and reverse primers and 4µl template in a total volume of 25µl. A mastermix containing all ingredients except template was prepared and aliquoted into the wells of a 96-well PCR plate, after which template was added to each well. Negative controls consisted of reaction solution not containing template.

In order to determine the concentration of template RNA to use in amplification reactions, as well as to monitor the efficiency of the amplification reaction with the different primer pairs, optimisation was performed on template as prepared after first strand amplification in a dilution series consisting of 1x, 0.1x, 0.01x and 0.001x solutions of template. It was decided that template diluted 10x would be used for all amplification reactions and final calculations (Fig. 2.6). All amplifications were done at least in triplicate, including a water control reaction for each primer set.

The following thermal cycler profile was used:

Stage	Repetitions	Temperature	Time
1	1	50°C	02:00
2	1	95°C	10:00
3	40	95°C	00:15
		60°C	01:00

iii) Amplicon abundance analysis

Relative quantitative analysis of transcripts was performed with the Applied Biosystems Detection Software (SDS) v1.2.1 (Fig. 4.3 and 4.4). For analysis, a baseline was firstly selected to exclude the initial cycles of amplification in which little change in fluorescence can be detected (Fig. 4.3). Secondly, a threshold level in the detected increase of fluorescence was selected above the baseline and within the exponential growth region of the amplification curve. The point at which the threshold level intersects the amplification

plot defines the threshold cycle (Ct). The Ct is the key value in qPCR analysis and is defined as the fractional cycle number at which the fluorescence detected by the system passes the threshold level as determined by the user. This value is used to calculate relative abundance of transcripts.

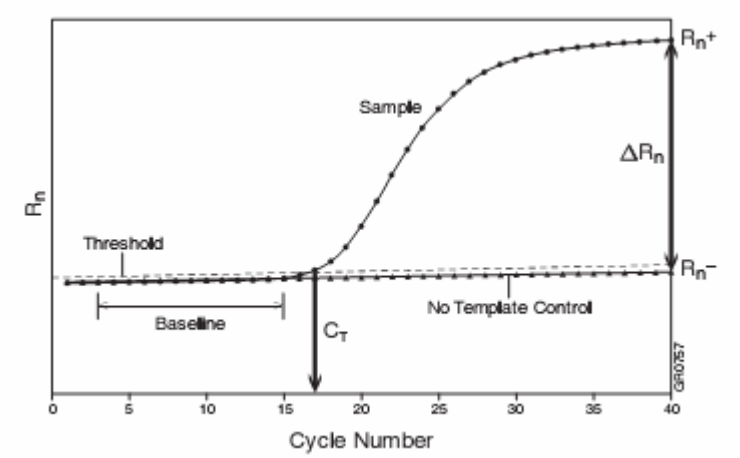

Figure 4.3 A representative amplification plot illustrating important parameters measured during qPCR (ABI7500 user manual).

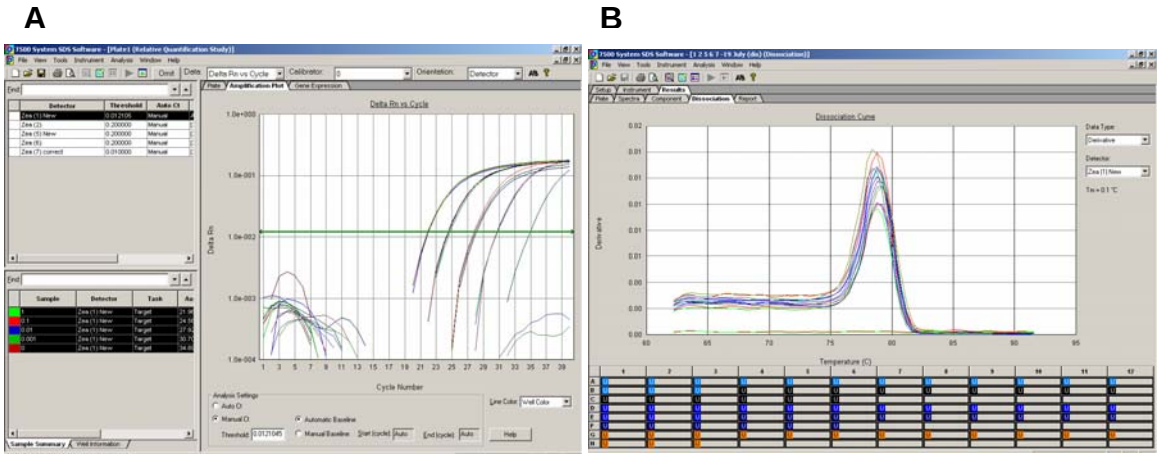

Figure 4.4 Example of amplification plot of a dilution series (A) showing change in fluorescence vs cycle number for template at 1x, 0.1x, 0.01x, and 0.001x concentration (represented from left to right on plot), and dissociation curve (B) of this reaction showing a single amplification product in a reaction where a putative serine protease inhibitor sequence was amplified.

Specificity of amplicons was confirmed by melting curve analysis (Fig. 4.4 B), where a single peak indicated a single amplification product, but multiple peaks indicated non-specific binding or contamination of reaction solution. Efficiency of individual amplification reactions was determined by first calculating the slope generated when graphing the Ct value of individual amplification reactions against a concentration series

of the template (expressed as a logarithm), and then using the equation Efficiency (E) = $10^{(-1/slope)}$. An efficiency of ≥2 represents acceptable amplification of template (Fig. 4.5) since it indiactes that each template strand produces two product strands during each amplification cycle.

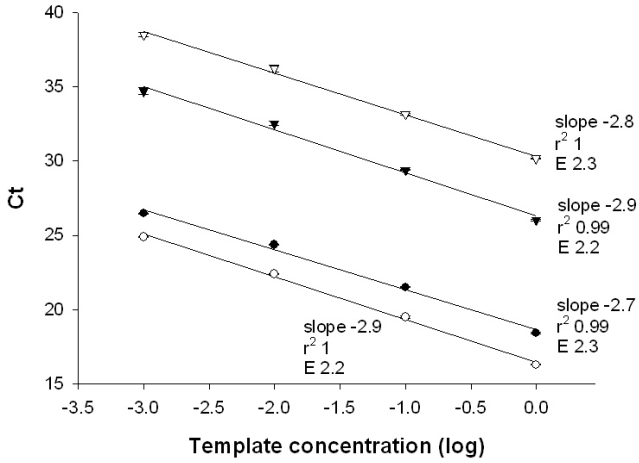

Figure 4.5 Example of amplification efficiencies obtained with primers designed to amplify invertase (open triangle), cell wall invertase (closed triangle), ubiquitin (closed circle), and thioredoxin (open circle) amplicons, showing the slope, r^2 value of regression line, and efficiency (E) calculated for each.

Relative abundance of qPCR amplicons were confirmed by comparison to the abundance of at least two endogenous controls. During qPCR analysis of transcript abundance in the maize leaf profile, leaf 1 (lowest on the stem) from air-grown plants was chosen as calibrator, and assigned a relative quantity (RQ) value of 1. The abundance of transcripts in other leaves was compared relative to this value. If a specific transcript was more abundant in a leaf relative to the abundance of that transcript in leaf 1, the RQ would be represented with a calculated value higher than 1. If a specific transcript was less abundant in a leaf relative to the abundance of that transcrtip in leaf 1, the RQ would be represented with a calculated value lower than 1. During analysis of transcript abundance after feeding of maize leaf pieces, leaf pieces fed only on 10mM Hepes, pH7 (with no added solute) was employed as calibrator, and assigned a RQ of 1.

4.3.11 Isolation and analysis of gene sequences of two novel protease inhibitors

i) Isolation of full-length protease inhibitor sequences

G. Beyene (University of Pretoria) performed determination of full-length gene sequences of two transcripts affected by CO_2 enrichment. Total RNA was extracted from leaf 3

pooled from seedlings (n=6) at five-leaf stage using the TriPure total RNA isolation kit according to the manufacturer's recommendation (Roche, Germany) and contaminant genomic DNA was digested by RNase-free DNase. Two µg of total RNA was reverse transcribed using superscript III™ Reverse Transcriptase (RT) (Invitrogen, USA) according to the manufactuer's instruction and used as a template in PCR reaction. Full-length cDNA clones for *Zea mays* putative serine-type endopeptidase inhibitor and putative Bowman-Birk-type serine protease inhibitor (accession numbers EF406275 and EF406276 respectively) were obtained by performing 5' and 3' rapid amplification of cDNA ends (RACE) using the GeneRacer™ kit according to the manufacturer's instruction (Invitrogen, USA) along with gene-specific primers. Gene-specific primers forward 5'-tactcagctcaaggttgaaggcatgg–3' and reverse 5'-cgaatcacgcacactttggttcagag-3' were used for isolation of a full-length serine-type endopeptidase inhibitor and primers forward 5'-cctcagctgatactcgtcggcact-3' and reverse 5'-gaacgtcgtcacagcggtaggtga-3' were used for isolation of a full-length Bowman-Birk-type serine protease inhibitor. The 5' RACE, 5' nested, 3' RACE and 3' nested primers were provided with the GeneRacer™ kit (Invitrogen, USA) that were used together with the gene specific primers. All amplified PCR products were T/A cloned into PCR4-TOPO (which was also provided with GeneRacer Kit) and sequenced in both direction using M13 forward and reverse primers.

Sequencing of the inserts were performed by using the BigDye® Terminator Cycle Sequencing FS Ready Reaction Kit, v 3.1 on ABI PRISM® 3100 automatic DNA-Sequencer (Applied Biosystems, USA). The BLASTn and BLASTp programs (Altschul et al., 1997) were used for gene sequence homology search.

ii) Analysis of protease inhibitor sequences

The cDNA sequences of EF406275 (putative serpin) and EF406276 (putative BBI) as determined by RACE were analysed by A. Prins using the following online tools: BLASTn and BLASTx at GenBank (Altschul et al., 1997), WU-blastn V2.0 (http://blast.wustl.edu/; Gish, W., 1996-2006) on the EMBL database, ORF finder (http://www.ncbi.nlm.nih.gov/gorf/gorf.html), BLASTx (Gish and States, 1993), ProtParam (Gasteiger et al., 2005), TargetP (http://www.cbs.dtu.dk/services/TargetP/; Emanuelsson et al., 2000), and Eukaryotic Linear Motif Resource (ELM) (http://elm.eu.org/; Puntervoll et al., 2003). After identification of their respective coding

sequences, protein homologs of the putative serpin and putative BBI genes were identified by translated homology search (BLASTx) at GenBank. This algorithm translates the query from nucleotide codons to amino acid sequence and compares this to known protein sequences in the GenBank database. Amino acid sequences were aligned using ClustalW (1.83: http://www.ebi.ac.uk/Tools/clustalw/) (Chenna et al., 2003).

4.3.12 Phylogenetic analysis of putative serpin and BBI sequence

Phylogentic analysis of the putative serpin and putative BBI was performed by P. Verrier (Rothamsted Research). Translated gene sequences were compared to protein homologs by phylogenetic comparison, the alignments being determined by ClustalW (in VectorNTI), and the best unrooted tree was generated with PAUP4* in default parameter configuration and the resultant trees were displayed using the PhyloDraw package.

4.3.13 Analysis of photosynthesis-related transcript abundance

To compare expression of photosynthesis-related transcripts in maize leaves grown in air or with CO_2 enrichment, raw intensity levels of photosynthesis-related probes as detected by microarray analysis were compared. To do this, a keyword search was first done at the NetAffx website to identify all probes on the maize microarray identified under the keywords “RuBisCO”, “ribulose”, “photosynthesis”, and “carbonic anhydrase”. The effect of CO_2 enrichment on transcript abundance as detected by microarray study was determined by comparing expression intensity levels of transcripts obtained from leaves grown either with CO_2 enrichment or in air. Difference in expression level was expressed as a percentage for analysis.

4.3.14 Photosynthesis and related parameters

Photosynthesis, transpiration, and stomatal conductance rates were measured on leaves 5-6 and leaves 11-12 of 9 week-old maize plants, using a portable Infra Red Gas Analyser (CIRAS-I; PP systems, UK). The flow rate was 300ml min^{-1}, the CO_2 concentration in the chamber was 350 ±20µl l^{-1} and light intensity was 800µmol m^{-2} s^{-1}.

4.3.15 Sugar metabolism enzyme activity

i) Sucrose phosphate synthase

SPS activities were measured in maize leaves according to Guy et al. (1992) with minor changes. Frozen leaf tissue (approximately 0.25g) was crushed in a mortar with liquid nitrogen in extraction buffer (1:20 [w/v]) containing 100mM Tricine (pH7.5), 200mM KCl, 5mM DTT, 5mM $MgCl_2$, 1.3mM EDTA, 4% (w/v) Polyclar AT, and 1% (v/v) protease inhibitor cocktail (Sigma). The homogenates were centrifuged at 15 000rpm for 3min and the supernatants were desalted on a Sephadex G-25 column (PD-10, GE Healthcare) using an elution buffer containing 100mM Tricine (pH 7.5), 200mM KCl, 5mM $MgCl_2$, and 1.3mM EDTA. Samples were diluted 1:1 (v/v) before use. SPS activities were measured under V_{max} conditions in a buffer containing 50mM MOPS-NaOH (pH 7.5), 15mM $MgCl_2$, 1.3mM EDTA, 10mM uridine 5'-diphosphoglucose, 40mM glucose-6-phosphate, and 10mM fructose-6-phosphate (reaction buffer). Desalted, diluted extract (35µl) was incubated with 35µl reaction buffer at 25ºC for 15min before the reaction was terminated by the addition of 70µl NaOH (7.5M). Samples were then incubated in a water bath at 100ºC for 10min and allowed to cool before sucrose content in the solution was measured. To quantify the amount of sucrose formed in the reaction solution, 1mL anthrone reagent (0.14% anthrone in 74% HCl) was added to each reaction tube and incubated at 40ºC for 20min. The absorbance of the solution was then measured at a wavelength of 620nm. Sucrose in the extract produced by SPS activity was calculated from a sucrose standard curve containing 0, 1, 2, 3, 4, 5, 10, or 14µg sucrose in deionised water. For the standard curve, sucrose was dissolved in water (70µl), after which 70µl NaOH (7.5M) was added, and solutions were incubated in a water bath at 100ºC for 10min before adding anthrone reagent as described above. Control reactions were performed using a buffer lacking uridine 5'-diphosphoglucose. Values obtained from control reactions were subtracted from values obtained with samples. Two independent extractions were done for each measurement from tissue pooled from 3 plants, and all measurements were done in duplicate.

The reactions that the sucrose phosphate assay is based on is:

1) Fructose-6-phosphate + UDP-glucose $\xrightarrow{\text{SPS (EC 2.4.1.14)}}$ Sucrose-6-phosphate + UDP

$$\text{2) Sucrose-6-phosphate} + H_2O \xrightarrow[(EC\ 3.1.3.24)]{SPP} \text{Sucrose} + P_i$$

Glucose-6-phosphate acts as an activator compound in this reaction since it favours the dephosphorylation of phospho-SPS (less active) to active SPS by SPS protein phosphatase (SPSPP) and also increases catalytic activity *in situ* as a result of allosteric regulation (Huber and Huber, 1992). This assay is a colorimetric method to measures the amount of sucrose formed in reaction 2, since sugars react with the anthrone reagent under acidic conditions to yield a blue-green color. There is a linear relationship between the absorbance and the amount of sugar that is present in the sample. This method determines both reducing and non-reducing sugars because of the presence of the strongly oxidizing sulfuric acid. It is a non-stoichiometric quantification method and therefore it is necessary to prepare a calibration curve using a series of standards of known carbohydrate concentration.

ii) Sucrose synthase

Sucrose synthase activities were measured according to Guy et al. (1992) in desalted extract prepared as for the SPS assay. SuSy activities were measured in the sucrose synthesis direction, using the same buffer as for SPS, except that 10mM fructose replaced the fructose-6-phosphate. Reactions were set up and treated as for SPS in order to measure sucrose in the reaction solution by employing the anthrone method as described above. Control reactions were performed using a buffer lacking uridine 5'-diphosphoglucose. Values obtained from control reactions were subtracted from values obtained with samples. Two independent extractions were done for each measurement from tissue pooled from 3 plants, and all measurements were done in duplicate. The reaction that the sucrose phosphate assay is based on is:

$$\text{3) Fructose} + \text{UDP-glucose} \underset{(EC\ 2.4.1.13)}{\overset{SuSy}{\rightleftharpoons}} \text{Sucrose} + \text{UDP}$$

While *in vivo* the sucrose cleavage reaction is favoured (Huber and Huber, 1996; Kruger, 1990), in this assay UDP-glucose is added to the desalted extract, which pushes the balance of the reversible reaction in the direction of sucrose synthesis. The amount of

sucrose formed in reaction 3 is determined colorimetrically through the anthrone method as detailed in section 4.3.16 I).

iii) Invertase

Invertase activities were measured in the same desalted extracts as for SPS and SuSy activities. Samples (100µl) were incubated in a 3-fold excess of buffer containing 100mM sodium citrate, 100mM NaH_2PO_4, and 100mM sucrose at either pH4.8 (to measure acid invertase activity), or pH7.0 (to measure neutral invertase activity) for 2h at 25ºC after which the reaction was stopped by incubating at 100°C for 5min. Two independent extractions were done for each measurement, and all measurements were done in duplicate. For the quantification of acid and neutral invertase activities respectively, 10-20µl and 20-40µl was added to 100µl 2x assay buffer [200mM imidazole, 10mM $MgCl_2$, 3mM ATP, 1mM NADP, 0.04% (w/v) BSA] and made up to a final reaction volume of 200µl with deionised water, in separate wells in a 96-well plate. To measure the amount of hexose formed by hydrolysis of sucrose by invertase (reaction 4), the method of Jones et al. (1977) was followed. Coupling enzymes (0.1U each of hexokinase, phosphoglucose isomerise, and G6P dehydrogenase, Roche, UK) were added to reaction solutions and the resultant production of NADPH was observed as the increase in absorption at 340nm measured on a plate reader (Spectramax, Molecular Devices, UK). The molar extinction coefficient of NADPH (6220 M^{-1} cm^{-1}) at 340nm was used to measure the amount formed, taking into account that a 200µl volume represents a path-length of 0.5cm.

Invertase catalyses the following reaction:

$$4)\ \text{Sucrose} + H_2O \xrightarrow[\text{(EC 3.2.1.26)}]{\text{Invertase}} \text{Glucose} + \text{Fructose}$$

In the reaction solutions incubated with an excess of substrate (sucrose), the sucrose is hydrolysed to glucose and fructose (hexoses) by maize endogenous invertases. Hexose content of samples was measured according to Jones et al (1977) where the addition of the coupling enzymes hexokinase, glucose-6-phosphate dehydrogenase, and phosphoglucose isomerise catalyse the following reactions:

$$5)\ \text{Glucose} + \text{ATP} \xrightarrow[\text{(EC 2.7.1.1)}]{\text{Hexokinase}} \text{Glucose-6-phosphate} + \text{ADP}$$

6) Fructose + ATP $\xrightarrow{\text{Hexokinase (EC 2.7.1.1)}}$ Fructose-6-phosphate + ADP

7) Fructose-6-phosphate $\xrightarrow{\text{Phosphoglucose isomerase (EC 5.3.1.9)}}$ Glucose-6-phosphate

8) Glucose-6-phosphate + $NADP^+$ $\xrightarrow{\text{G6P dehydrogenase (EC 1.1.1.49)}}$ 6-Phosphogluconate + NADPH

For this assay, a mixture of all three coupling enzymes was added to the reaction solution in order to catalyze reactions 5-8 concurrently. For the quantification of acid and neutral invertase activities in extract, 10-20µl and 20-40µl was respectively added to a final volume of 200µl in a 96-well plate. After addition of coupling enzymes to this solution, the resultant production of NADPH was observed as the increase in absorption at 340nm. The molar extinction coefficient of NADPH (6220 M^{-1} cm^{-1}) at 340nm was used to measure the amount formed, taking into account that a 200µl volume represents a path-length of 0.5cm. Therefore, since in a 1cm path length 1AU = 1/6.22 µM, it can be calculated that in a 200µl volume (0.5cm path length) NADPH formed (µmol) = ΔA_{340}/6.22x0.5. Since one molecule NADPH is formed for each molecule hexose, the amount of hexose is directly equivalent to the amount of NADPH.

4.3.16 Statistical methods

The gas exchange data was analyzed by ANOVA. Data for all other physiological parameters was analyzed by Student's t-test. Correlation analysis between transcript abundance and hexose and sucrose content of leaves was done with the Statistica software (v 7.1; StatSoft Inc).

4.4 Results

4.4.1 High CO_2 effects on whole plant morphology and photosynthesis

Maize plants were grown eight weeks in either air (350µl l^{-1} CO_2) or with CO_2 enrichment (700µl l^{-1} CO_2) (Fig. 4.6 A). The anthers were present at this growth stage and cobs were starting to form. Hence, all the leaves can be classed as source leaves at this growth stage.

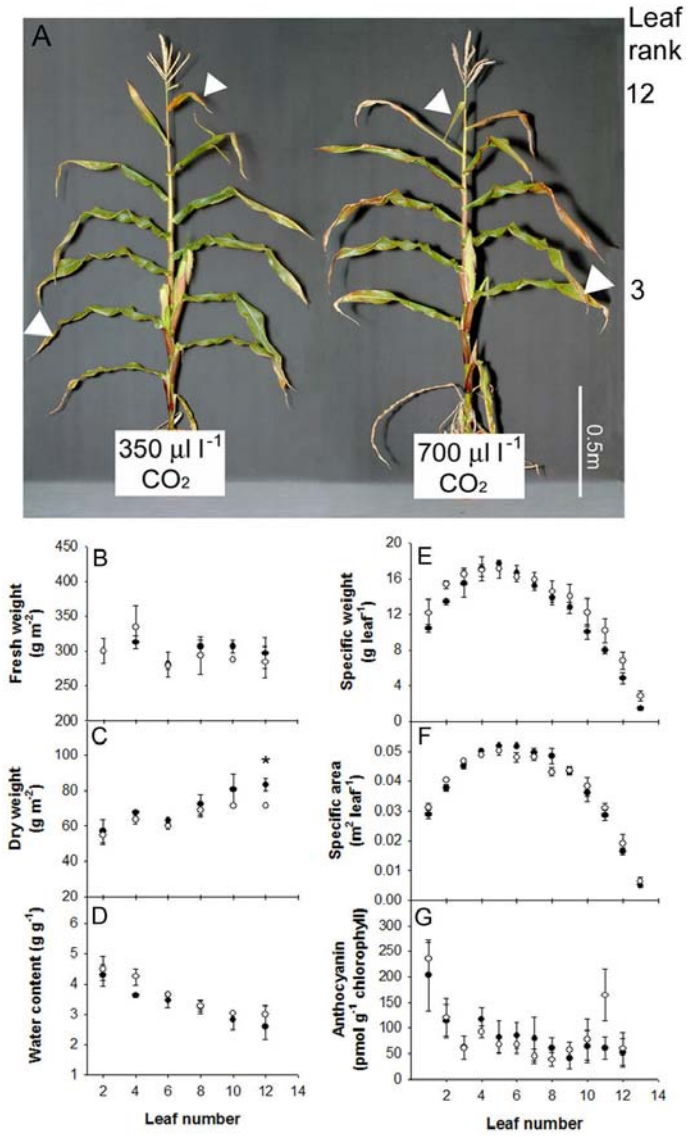

Figure 4.6. The growth CO_2 phenoytpe in maize. Maize phenotype at the point of harvest and analysis (A). Arrows indicate leaf ranks sampled for trancriptome analysis. Leaves harvested from air-grown plants (closed circle) or plants grown with CO_2 enrichment (open circle) were analysed for fresh weight (B) and dry weight (C) values that were used to calculate tissue water content (D); Specific leaf weight (E); Specific leaf area (F); leaf anthocyanin content (G). Significant differences at $P < 0.05$ indicated by the symbol (*).

All the leaves had high rates of photosynthesis regardless of the position of the stem (Table 4.4). However, values obtained for the oldest mature leaves i.e. leaf ranks 3-5, were significantly lower than those measured in leaf rank 12, suggesting that these leaves were only in the early stages of senescence. The development-dependent decreases in CO_2 assimilation rates were of the same order (29-31%) in both air and high CO_2 –grown plants (Table 4.4). While no significant decreases in photosynthetic CO_2 assimilation rates

(expressed on a surface area basis) resulted from growth with CO_2 enrichment, transpiration rates were significantly decreased in the high CO_2 –grown plants (Table 4.4).

Table 4.4 Acclimation of photosynthesis, transpiration, and stomatal conductance to CO_2 enrichment in young source leaves (leaf rank 12) and old source leaves (leaf rank 5) of 8 week-old plants. Values represent mean ± SE; n=4.

CO_2 ($\mu l\ l^{-1}$)	**Leaf rank**	**Photosynthesis ($\mu mol\ m^{-2}\ s^{-1}$)**	**Transpiration ($mmol\ m^{-2}\ s^{-1}$)**	**Stomatal conductance ($mmol\ m^{-2}\ s^{-1}$)**
350	12	20.96 ± 1.50	3.10 ± 0.37	119.0 ± 15.8
350	5	14.48 ± 0.25	2.69 ± 0.14	101.25 ± 8.9
700	12	17.28 ± 2.93	2.95 ± 0.42	83.48 ± 13.8
700	5	12.24 ± 2.24	2.14 ± 0.31	58.6 ± 2.2

ANOVA analysis:
Significant difference at $P < 0.05$ indicated by *

Parameter	Leaf Rank	CO_2 level	Interaction
Photosynthesis	0.014*	0.163	no
Transpiration	0.087	0.305	no
Stomatal conductance	0.105	0.007*	no

No differences in phenotype were observed between air and high CO_2–grown plants at this stage (Fig. 4.6 A). There were no significant differences in the fresh weights (Fig. 4.6 B), the dry weights (Fig. 4.6 C), or tissue water contents (Fig. 4.6 D) of leaves at equivalent positions on the stem. The leaf fresh weight values were similar regardless of ontogeny, but the dry weight values were greatest in the young leaves and decreased with leaf position on the stem (1 to 12). The oldest source leaves had the lowest dry weight values (Fig. 4.6 C). Similarly, the tissue water content was greatest in oldest source leaves and decreased gradually with the leaf position on the stem, the young leaves having the lowest tissue water contents (Fig. 4.6 D). The leaves were at their maximum size and weight at leaf rank 5 (Fig. 4.6 E and 4.6 F) regardless of whether the plants had been grown in air or with CO_2 enrichment. The total anthocyanin contents, which have been taken as an indicator of stress, increased progressively as the leaves aged being highest in leaf rank 1, but values were similar in plants grown in air or with CO_2 enrichment (Fig. 4.6 G).

4.4.2 CO_2 –dependent effects on the leaf transcriptome

The transcriptome of leaf ranks 3 and 12 was compared in air-grown and high CO_2-grown plants (Web Table 1-7; PDF files on CD). Leaf developmental stage/ontogeny had a much greater effect on the leaf transcriptome than growth CO_2 level (Fig. 4.7 A and B).

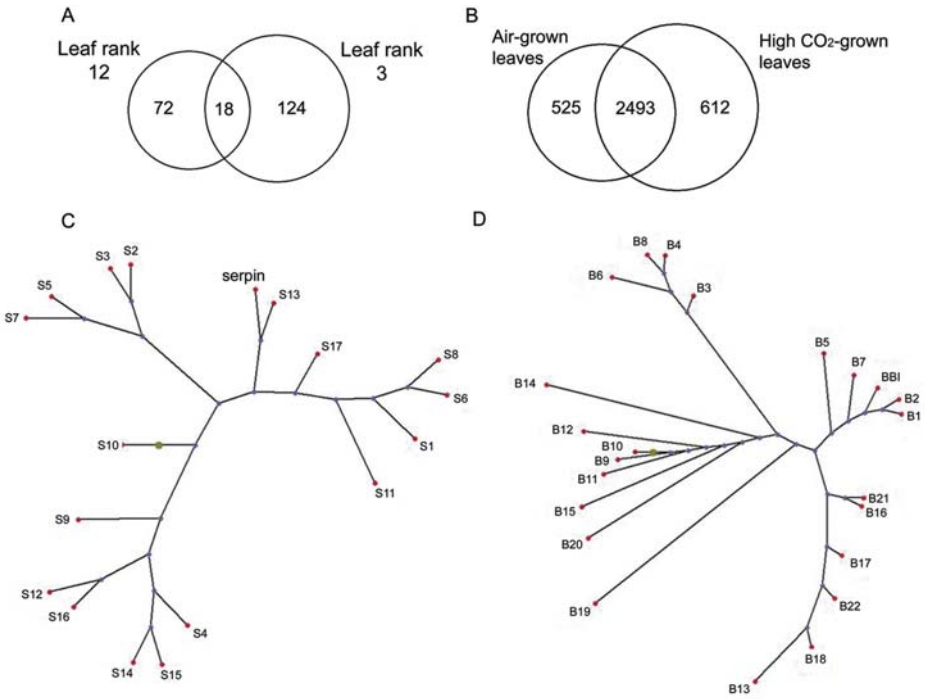

Figure 4.7 Transcriptome analysis of young and old source leaves from air-grown plants or plants grown with CO_2 enrichment. Comparisons of the numbers of CO_2 enrichment-modulated transcripts at the different leaf ranks (A) and the numbers of transcripts that were differentially expressed as a result of leaf position on the stem (B). Phylogenetic trees showing the relationships between putative serpin and known serine protease inhibitor protein sequences (S1-S17; C) and putative BBI and known Bowman-Birk serine protease inhibitor protein sequences (B1-B22, D).

Table 4.5 Sequences used in phylogenetic analysis (Fig. 4.7 C and D).

Sequence	Accession	Definition	Sequence	Accession	Definition
serpin	EF406275.1	Zea mays putative serine type endopeptidase inhibitor	BBI	EF406276.1	Zea mays putative Bowman-Birk serine protease inhibitor
S1	Q43502	Protease inhibitor type-2 CEVI57 precursor	B1	ABL63911.1	Bowman-Birk serine protease inhibitor [Musa acuminata]
S2	AAF18450.1	Protease inhibitor type II precursor NGPI-1 [Nicotiana glutinosa]	B2	P81713	Bowman-Birk type trypsin inhibitor (WTI)
S3	AAF18451.1	Protease inhibitor type II precursor NGPI-2 [Nicotiana glutinosa]	B3	AAO89510.1	Bowman-Birk protease inhibitor [Glycine microphylla]
S4	ABA42892.1	Trypsin protease inhibitor precursor [Nicotiana benthamiana]	B4	BAB86783.1	Bowman-Birk type protease isoinhibitor A1 [Glycine soja]
S5	ABA42904.1	Trypsin protease inhibitor precursor [Nicotiana acuminata]	B5	P16343	Bowman-Birk type protease inhibitor DE-4 (DE4)
S6	AAL54921.2	Protease inhibitor IIb [Solanum americanum]	B6	BAB86784.1	Bowman-Birk type protease isoinhibitor A2 [Glycine soja]
S7	AAR84197.1	Putative 6 repeat protease inhibitor [Nicotiana attenuata]	B7	P82469	Bowman-Birk type protease inhibitor 1
S8	AAR37362.1	Protease inhibitor 2b precursor [Solanum nigrum]	B8	P01055	Bowman-Birk type protease inhibitor precursor (BBI)
S9	AAQ56588.1	6-domain trypsin inhibitor precursor [Nicotiana attenuata]	B9	P81484	Bowman-Birk type protease inhibitor PVI-3(2)
S10	AAO85558.1	7-domain trypsin inhibitor precursor [Nicotiana attenuata]	B10	P81483	Bowman-Birk type protease inhibitor PVI-4
S11	Q40561	Protease inhibitor type-2 precursor	B11	CAD32699.1	double-headed trypsin inhibitor [Phaseolus vulgaris]
S12	ABA86556.1	Six domain protease inhibitor [Nicotiana tabacum]	B12	CAD32698.1	double-headed trypsin inhibitor [Phaseolus vulgaris]
S13	BAA95792.1	Protease inhibitor II [Nicotiana tabacum]	B13	S09415	protease inhibitor - cowpea
S14	AAZ20771.1	Insect injury-induced protease inhibitor [Nicotiana tabacum]	B14	Q9S9E3	Horsegram inhibitor 1
S15	AAF14181.1	Protease inhibitor precursor [Nicotiana alata]	B15	CAL69237.1	double-headed trypsin inhibitor [Phaseolus parvulus]
S16	AAA17739.1	Protease inhibitor precursor	B16	ABD91575.1	trypsin inhibitor [Vigna radiata var. sublobata]
S17	P01080	Protease inhibitor type-2 K precursor	B17	AAW84292.1	trypsin inhibitor [Lens culinaris]
			B18	AAO43982.1	trypsin inhibitor [Vigna unguiculata subsp. sesquipedalis]
			B19	P01059	Bowman-Birk type protease inhibitor DE-4
			B20	P01056	Bowman-Birk type protease inhibitor
			B21	ABD91574.1	trypsin inhibitor [Vigna trilobata]
			B22	CAC81081.1	trypsin inhibitor [Vigna unguiculata]

Growth with CO_2 enrichment resulted in the differential expression of only 90 transcripts (Web Table 1) in the young (leaf 12) source leaves, while 142 transcripts were differentially expressed in the old (leaf 3) source leaves (Web Table 2). The high CO_2 signature of young source leaves (leaf 12) included transcripts involved in carbohydrate and amino acid metabolism (Web Table 1). Putative ADPglucose pyrophosphorylase and starch synthase transcripts were significantly higher in the young source leaves in air compared to high CO_2. Similarly, putative glutamine synthetase, aspargine synthetase and tryptophan synthase transcripts were significantly higher in leaf 12 in air compared to high CO_2. In contrast, while the older leaves lacked high CO_2–dependent effects on these transcripts, they showed a marked decrease in the abundance of nitrate reductase and methionine synthase transcripts at high CO_2.

Relatively few photosynthesis-related sequences were significantly affected by CO_2 enrichment at the chosen cut off point in this study (above the 50% level). To detect any possible CO_2 enrichment-dependent effects on transcripts associated with photosynthesis, the cut-off point for significance was decreased to 10% (Web Table 3). At this level, carbonic anhydrase transcripts were decreased and phosphoenolpyruvate carboxylase and phytase transcripts were increased by CO_2 enrichment. RuBisCO large subunit expression was not significantly affected by the growth CO_2 level, showing air/CO_2 enrichment ratios of 1.00 in young source leaves and 0.97 in old source leaves, respectively. However, RuBisCO SSU transcripts were increased more in air than in high CO_2, an effect that was greatest in the young source leaves. A RuBisCO activase precursor transcript was slightly increased in the older source leaves compared to those grown in air.

While the expression of chlorophyll a/b-binding proteins CP29 (Lhcb4) and CP26 (Lhcb5) was unaffected by CO_2 enrichment, transcripts encoding CP24 (Lhcb6) and a magnesium chelatase subunit I precursor, which plays a role in chlorophyll biosynthesis, were induced in young source leaves grown in air compared to those with CO_2 enrichment. In addition, transcripts encoding PGR5, which has been linked to ferredoxin:plastoquinone oxidoreductase-mediated cyclic electron flow and ferredoxin transcripts were induced more in the old source leaves than the young leaves in air compared to similar leaves grown with CO_2 enrichment.

In contrast to the transcripts associated with photosynthesis that showed relatively minor CO_2 enrichment-dependent effects, all of the following transcripts were significantly affected by high CO_2 above the 50% threshold. While several transcripts involving signaling, DNA-binding and the cell cycle including a putative ethylene responsive element binding factor were differentially expressed as a result of growth with CO_2 enrichment, the most noticeable changes were in transcripts involved in cell rescue and defense responses and in secondary metabolism, which were differentially modified in plants grown in air (Web Tables 1 and 2). In particular, the abundance of ACC oxidase transcripts was higher in both young and old source leaves in air compared to high CO_2 suggesting that the capacity for ethylene production is decreased at high CO_2. Relatively few antioxidant defense transcripts were differentially regulated in response to CO_2 enrichment. Of these, it is notable that *cat*1 transcripts were higher in air than with CO_2 enrichment, but this was restricted to the young source leaves. In contrast, three glutathione S-transferases and three putative peroxidase transcripts were highly expressed in air in the older but not the young source leaves. Hemoglobin (HB2) transcripts were significantly increased in air in both young and old source leaves. Similarly, a number of chitinase and glucanase transcripts were increased in air compared to CO_2 enrichment, in either or both young and old source leaves. Two maize heat shock proteins (HSP22 and HSP26) were much lower in the young and old source leaves in air than with CO_2 enrichment (Web Tables 1 and 2).

Eighteen high CO_2–modulated transcripts were identical (based on probe identity) in leaf ranks 3 and 12 (Table 4.6). Of these, pathogenesis-related protein 10 and two putative peroxidases were decreased in young source leaves but increased in the old source leaves (Table 4.6). The 18S and 23S ribosomal subunit transcripts were decreased in air-grown leaves. Of the ten transcripts that are more abundant in air-grown young and old source leaves, two sequences that were identified as a putative serine protease inhibitor and a putative Bowman-Birk (BBI) serine protease inhibitor were selected for further analysis as they are associated with protein turnover and stress response, which was of major interest in this study.

these transcripts were designed using the Primer Express software (v2.0, Applied Biosystems, UK) and synthesised by Sigma Genosys (Sigma, UK) (Table 2.2). Ubiquitin (MUB3; Zm.12132.3.S1_a_at), thioredoxin M (Zm.719.1.A1_at), and cyclophilin (Cyp; AFFX-Zm_Cyph_3_at) were selected as endogenous controls based on similar microarray expression values higher than 10 000 (Table 4.2).

Table 4.1. Probe sets used to design primers for qPCR, expression levels and primer sequences.

Probe set used for primer design	Maize gene title or description	Log_2 (air / high CO_2)		Forward primer	Reverse primer
		Young leaves	Old leaves		
Zm.3332.1.A1_at	putative serpin	0.541	0.728	TCGATCTGGACAAAGACCAACC	ACAGGCGCCAAAGTTTTA
Zm.4270.2.A1_a_at	putative BBI	1.919	0.622	AGTGCCAGTGCAATGACGTGT	AATTCCTGCACCGACCTTGAC
		Log_2 (young / senescent)			
		Air	High CO_2		
Zm.13430.1.S1_at	Cell wall invertase Incw4	0.625	0.805	GAGGAGCACGAGACCATCAATT	TCCACCACCGAGTGATCAATC
Zm.231.1.S1_at	Invertase	-0.575	-0.626	ATACAACCACGACTACATGGCG	GCATTGCATCGATCAGATGTCT
Zm.3478.1.S1_a_at	sucrose synthase 3	0.800	0.968	TTCTGGAAGTACGTGTCGAAGC	CTCAAGGTAGCGCCTCGTCT
Zm.6977.1.S1_at	sucrose synthase (EC 2.4.1.13)	-1.220	-1.209	TGAAGTACCGTAGCCTGGCAA	CGTACTAATCGAAGGACAGCGG
Zm.6977.5.S1_a_at	sucrose synthase (EC 2.4.1.13)	-1.031	-0.990	-	-
Zm.26.1.A1_at	sucrose phosphate synthase	1.109	1.453	TTCCAGCGGCATGTGAATTT	ATACACACCCGCGGTACTGTTC

Table 4.6 CO_2-modulated transcripts in leaf rank 3 (Young leaves) and 12 (Old leaves)

Probe ID	Genbank accession of probe target	Log_2 (air / high CO_2) Young leaves	Log_2 (air / high CO_2) Old leaves	Maize gene name or function	Best BLASTx hit accession	Protein description	% identity	e-value	bitscore
Zm.11586.1.A1_at	BM379136	0.844	0.561	Transcribed locus	no hit	-	-	-	-
Zm.11985.1.A1_at	CF636772	0.783	0.608	Hb2: Hemoglobin 2 (Hb2)	NP_179204.1	AHB1 [A. thaliana]	67.5	6E-11	63.5
Zm.1419.1.S1_at	CO527884	1.393	0.548	PCO072275 mRNA sequence	NP_914960.1	putative dermal glycoprotein precursor [O. sativa]	55.96	5E-29	124
Zm.1595.1.S1_at	CD967190	1.890	0.918	PCO155066 mRNA sequence	NP_191010.1	ATEP3; chitinase [A. thaliana]	67.86	5E-28	120
Zm.3332.1.A1_at	**BM379802**	**0.541**	**0.728**	**PCO129929 mRNA sequence**	**NP_177351.1**	**serine-type endopeptidase inhibitor [A. thaliana]**	**68**	**8E-18**	**86.3**
Zm.4270.2.A1_a_at	**CF628998**	**1.919**	**0.622**	**PCO107455 mRNA sequence**	**NP_910046.1**	**putative Bowman-Birk serine protease inhibitor [O. sativa]**	**48**	**6E-16**	**80.1**
Zm.6689.1.A1_at	BM381797	0.991	0.807	Transcribed locus, weakly similar to XP_463709.1 putative glucan endo-1,3-beta-D-glucosidase [O. sativa]	NP_914603.1	putative beta 1,3-glucanase [O. sativa]	82.35	1E-36	149
Zm.6689.1.A1_s_at	BM381797	0.707	0.634	Transcribed locus, weakly similar to XP_463709.1 putative glucan endo-1,3-beta-D-glucosidase [O. sativa]	NP_914603.1	putative beta 1,3-glucanase [O. sativa]	82.35	1E-36	87
Zm.8130.1.A1_at	CK369071	0.735	0.579	Transcribed locus, moderately similar to XP_467491.1 unknown protein [O. sativa]	no hit	-	-	-	-
ZmAffx.1198.1.A1_at	BE056195	1.273	1.047	CL3918_1 mRNA sequence	XP_469149.1	putative antifungal zeamatin-like protein [O. sativa]	77.5	1E-14	75.9
Zm.4510.1.A1_a_at	CF636202	0.555	-0.606	PCO135232 mRNA sequence	no hit	-	-	-	-
Zm.17997.1.A1_at	CK369019	-0.658	0.712	PCO129777 mRNA sequence	NP_917067.1	putative phosphoethanolamine N-methyltransferase [O. sativa]	84.26	2E-49	192
Zm.1967.1.A1_at	BG836522	-0.681	0.892	PCO091453 mRNA sequence	Q29SB6	pathogenesis-related protein 10. [Z. mays]	97.81	3E-68	251
Zm.2707.1.S1_at	BG842199	-0.558	1.276	PCO104850 mRNA sequence	XP_479513.1	peroxidase [O. sativa]	81.08	7E-41	164
Zm.3630.1.A1_at	BM380179	-2.577	1.078	Transcribed locus, strongly similar to XP_473863.1 OSJNBa0070C17.11 [O. sativa]	XP_550375.1	putative proline rich protein [O. sativa]	60.71	4E-26	115
Zm.369.1.A1_at	AF035460.1	-0.873	-0.599	Zea mays low molecular weight heat shock protein precursor (hsp22)	XP_467890.1	putative low molecular weight heat shock protein [O. sativa]	89.04	8E-23	103
ZmAffx.1215.1.S1_s_at	6273844	-0.505	-0.585	Zea mays 18S small subunit ribosomal RNA gene	XP_466329.1	18S small subunit ribosomal RNA	38.460	0.980	29.6
ZmAffx.1221.1.S1_at	11990232-113	-1.113	-1.223	Zea mays 23S rRNA	YP_358637.1	23S ribosomal RNA	92.680	0.000	88.6

4.4.3 Characterization of two CO_2 –modulated serine protease inhibitors

The full-length gene sequences of these inhibitors were obtained by RACE and compared to those of known similar inhibitors in the databases (Fig. 4.8). The putative serine protease inhibitor EF406275 (serpin) is 48% homologous to an *Arabidopsis* serine-type endopeptidase inhibitor (NP_177351.1; bit score 86.3; E=6e-16) that aligns to the *Arabidopsis* protein in the +2 frame (Fig. 4.8 A). The putative Bowman-Birk inhibitor (BBI) sequence has a 68% sequence similarity to a patented maize sequence, which is described as a maize protease inhibitor-like polynucleotide (AR494954; patent number US6720480-A/1, 13-APR-2004) (Fig. 4.8 B).

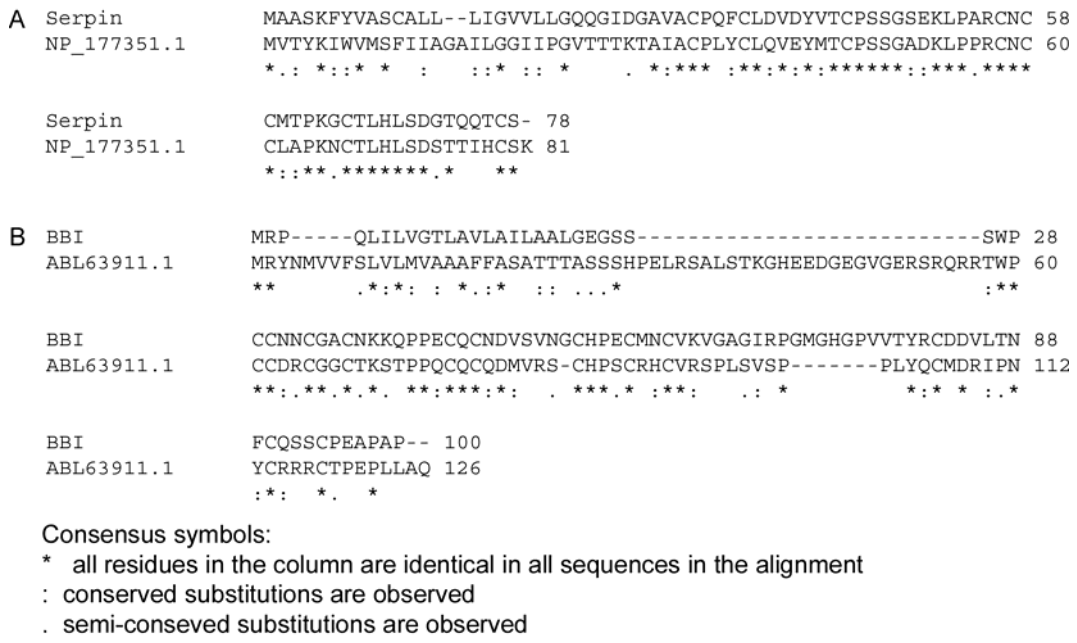

Figure 4.8 Pairwise alignments of two putative serine protease inhibitor protein sequences affected by CO_2 enrichment. The putative serpin is aligned with the closest protein homolog (NP177351.1; A) and the putative BBI is also aligned with the closest protein homolog (ABL6391.1; B).

Analysis of the putative serine protease inhibitor with the Eukaryotic Linear Motif Resource (ELM) (http://elm.eu.org) revealed the presence of a potato type II protease inhibitor (pin2) domain from residue 29 to 73 (Fig. 4.9). Members of the pin2 family are protease inhibitors that contain eight cysteines that form four disulphide bridges, and that inhibit serine proteases. Eight such cysteine residues were identified in the putative serpin (Fig. 4.9). A potential signal peptide was also identified from residue 1 to 28 consistent with other pin2 inhibitors (Barta et al., 2002).

```
                      1 ↓↓2        3           4 56      7           8
Maize_putserpin   -VACPQFCLD-VDYVTCPSSGSEKLPARCNCCMTP-KGCTLHLSDGTQQTCS 49
Maize_pin2        -VACPQFCLD-VDYVTCPSSGSEKLPERCNCCMTP-KGCTLHLSDGTQQTC- 48
Sorghum_pin2      AVPCPQYCLE-VDYVTCPSSGSEKLPARCNCCLAP-KGCTLHLSDGTQQTC- 49
Rice_pin2         -KFCPQFCYDGLEYMTCPSTG-QHLKPACNCCIAGEKGCVLYLNNGOVINC- 49
                     ***:* : ::*:****:* ::*   ****::  ***.*:*.:*   .*
```

Figure 4.9 Pairwise alignment of the putative serpin (Maize_putserpin) with three serpin sequences identified in maize (Maize_pin2; accession AI947362), sorghum (Sorghum_pin2; accession AI724716), and rice (Rice_pin2; accession AU163886). Conserved cysteine residues that participate in disulphide bridges are in bold and numbered. Arrows indicate the putative protease-contact residues (Barta et al, 2002). Consensus symbols are as in Fig. 4.8.

Analysis of the putative BBI revealed the presence of conserved cysteine residues characteristic of those present in Bowman-Birk inhibitors (Mello et al., 2003). These residues were identified at the 9 conserved positions in the two putative reactive sites of the putative maize BBI. The first two conserved cysteine residues (C1 and C2) were identified at residue 29 in the putative protein when compared to known sequences (Fig. 4.10; Mello et al., 2003).

```
                         12  3  4 ↓     5 6       7   8  9   ↓
Maize_putBBI          SWPCCNNCGACNKKQPPECQCNDVSVNGCHPECMNCVKVGAGIRPG 46
Maize_WIP_P31862      --KCCTNC---NFSFSGLYTCDDVKKD-CDPVCKKCVVAVHASY-- 38
Suc_AY093810          SWPCCDNCGACNKKFPPECQCQDISARGCHPECKKCVKIGGGIPPG 46
Suc_AY093809          SWPCCDNCGVCNKKFPPDCQCSDVSVHGCHPECKKCVKQGAGIPPG 46
                         ** **   * . .    *.*:.   *.* * :**    .
```

Figure 4.10 Pairwise alignment of the putative BBI (Maize_putBBI), two BBI sequences identified in *S. officinarum* (Suc_AY093810 and Suc_AY093809), and a wound-induced protein from maize (Maize_WIP_P31862). Conserved cysteine residues that participate in disulphide bridges are in bold and numbered. Arrows indicate the putative reactive binding sites (Mello et al, 2003). Consensus symbols are as in Fig. 4.8.

4.4.4 Development-related effects on the transcriptome of source leaves in air and high CO_2-grown plants

In air-grown plants, 3018 transcripts were differentially expressed between young and old source leaves (Web Table 4), while 3105 transcripts showed differential expression between leaf 12 and leaf 3 on plants grown with CO_2 enrichment (Web Table 5). A comparison of the leaf 12 and leaf 3 transcriptomes in air (Web Table 4) and high CO_2 (Web Table 5) revealed that 2493 transcripts were common based on probe set identity (Fig. 4.7 B). Of the transcripts specifically affected by leaf ontogeny/development irrespective of the CO_2 enrichment (Web Table 6), 1336 transcripts were up-regulated and

1157 transcripts were down-regulated in young compared to old source leaves. Transcripts that could not be identified by translated homology search were assigned as "unknown" and totaled 953 sequences. The remaining transcripts were assigned to the 15 functional categories as previously. For the purposes of the present description and discussion we will focus on transcripts in only three categories that are of interest in relation to the focus of this study: carbon metabolism, redox metabolism and protein turnover. However, it is important to note that transcripts associated with storage proteins were only up-regulated in young leaves. Conversely, transcripts associated with vesicle trafficking, signaling, and transposons were decreased in young rather than old source leaves. Sixteen of the 17 transposon-related transcripts that were identified in this study were lower in abundance in the young source leaves.

Re-adjustments in cellular redox metabolism were observed in response to leaf rank (Web Tables 4 and 5). However, there were no clear trends with regard to indications of enhanced oxidation in either young or old source leaves. For examples, while ascorbate oxidase, dehydroascorbate reductase and three putative peroxidases were lower in the older source leaves, monodehydroascorbate reductase, an NADH dehydrogenase and three other peroxidases were enhanced in the older leaves. A number of sequences involved peroxisomal metabolism were modulated by leaf development. Peroxisomal biogenesis factor 11 and catalase 1 transcripts were increased in the old source leaves whereas catalase 2 transcripts were decreased. Similarly, transcripts encoding four ferredoxins, a thioredoxin m, a glutathione (thioredoxin) peroxidase and three rubredoxins were decreased whereas another glutathione (thioredoxin) peroxidase, a ferredoxin-NADP reductase and two protein disulphide isomerases were increased in the old source leaves. A total of 16 glutathione S-transferases were differentially modulated by leaf development with four more abundant in young leaves and twelve predominating in the older leaves.

A distinct differential orchestration of carbohydrate metabolism transcripts was observed between the young and old source leaves with transcripts encoding ribose-5-phosphate isomerise, fructose bisphosphatase, fructose bisphosphate aldolase, triose phosphate isomerise, phosphoglucomutase, UDP-glucose pyrophosphorylase, glyceraldehyde 3-phosphate dehydrogenase, malate dehydrogense, a glucose 6-phosphate dehydrogenase, UDP-glucosyl transferase, beta glucosidase, glucan 1,3-beta glucosidase, ADP-glucose pyrophosphorylase, sucose phosphate synthase, sucose phosphorylase, predominating in

the younger leaves, together with sucrose and other sugar transporters and glucose 6-phosphate transporter, which were much higher in the younger than the older source leaves. Similarly, transcripts encoding starch metabolism enzymes such as beta amylase, phosphorylase, starch synthase and starch branching enzyme were highest in the young source leaves. While transcripts encoding trehalose 6-phosphatase were highest in young source leaves in both air and high CO_2 transcripts encoding trehalose 6-phosphate synthase were only higher in the young source leaves in air. While sucrose synthase 3 was predominant in young source leaves a different sucrose synthase sequence predominated in the older source leaves. Similarly, neutral invertase and a cell wall invertase (incw4) were highest in the young source leaves; transcripts encoding acid invertase were highest in the old source leaves. Transcripts encoding the glucose 6-P/Pi transporter, several glycosyl transferases, beta-fructofuranosidase, mannosidase, a fructose bisphosphate aldolase, a glucose 6-phosphate dehydrogenase were also highest in the oldest leaves, which tended to be richer in transcripts associated with sugar/carbohydrate signaling than the younger source leaves. These included snf7, SNF-1 related protein kinase, SnRK1-interacting protein 1 and hexokinase (Table 4.7). Hexokinase-catalysed phosphorylation of glucose is essential for the repression of photosynthesis-related genes (Moore et al., 2003).

Table 4.7 Abundance of hexokinase transcripts in young mature leaves (rank 12) and old mature leaves (rank 3) compared as a log_2 ratio in leaves grown at 350µl l^{-1} CO_2 or 700µl l^{-1} CO_2.

Probe ID	Description	log_2 (rank 12/rank3)	
		350 µl l^{-1}	700 µl l^{-1}
Zm.5206.1.S1_x_at	Hexokinase	-0.571	-
Zm.5206.2.S1_a_at	Hexokinase	-0.710	-0.512
Zm.5206.3.A1_a_at	Hexokinase	-0.799	-0.525
Zm.8365.1.A1_at	putative hexokinase 1	-	-0.608

With regard to protein turnover, a large number of proteases (36 transcripts), protease inhibitors (11 transcripts), and proteolysis-related sequences (28 transcripts) were differentially expressed as a result of leaf development/ontogeny (Web Table 7). However, CO_2 enrichment had no significant effects on the abundance of these transcripts. Amongst the protease transcripts, eighteen were higher in young compared to old source leaves, and a further eighteen were higher in old compared to young source leaves. Seven of the eleven protease inhibitor sequences were enhanced and four were decreased in young compared to old source leaves. Other related transcripts particularly those involved

in the ubiquitin-proteosome were mainly lower (25 transcripts out of 28) in young than old source leaves.

4.4.5 The effect of leaf position on the response to growth CO_2 levels for the serpin and BBI inhibitor transcripts and transcripts associated with sugar metabolism

To investigate the relationships between effects of growth CO_2 and leaf development on the abundance of transcripts encoding the two putative serine protease inhibitors identified as CO_2–modulated in both young and old source leaves, qPCR analysis of these transcripts on all the leaves on the stem was conducted. For comparison, the abundance of the four invertase and sucrose synthase sequences associated with carbohydrate metabolism identified in the transcriptome analysis as differentially modulated by development were also analysed. These were cell wall invertase, acid invertase, sucrose synthase 3, sucrose synthase, and sucrose phosphate synthase. The abundance of the putative serpin transcripts in air varied according to the position of the leaves and the highest levels were measured in the leaves 1-3 (Fig. 4.11 A). In contrast, no clear trend in putative BBI transcript abundance could be detected at any positions on the stem (Fig. 4.11 B). However, the response of both the putative serpin and BBI transcripts to growth with CO_2 enrichment was dependant on the position of the leaf on the stem (Fig. 4.11 A and B). While putative serpin transcripts were increased as a result of growth with CO_2 enrichment only in the youngest source leaves (Fig. 4.11 A), putative BBI transcripts showed a marked increase in abundance only in the oldest source leaves in response to high CO_2 (Fig. 4.11 B). Growth with CO_2 enrichment had no effect on the abundance of any of transcripts associated with sugar metabolism that were measured (Fig. 4.11 C-G), except for invertase (Fig. 4.11 C). While the abundance of the sugar-associated transcripts varied with the position on the stem the only clear effect of leaf position was observed with SPS transcripts (Fig. 4.11 G), the abundance of which was highest in the young source leaves and decreased progressively in the leaf ranks down the stem and reaching a lowest expression level in the oldest source leaves.

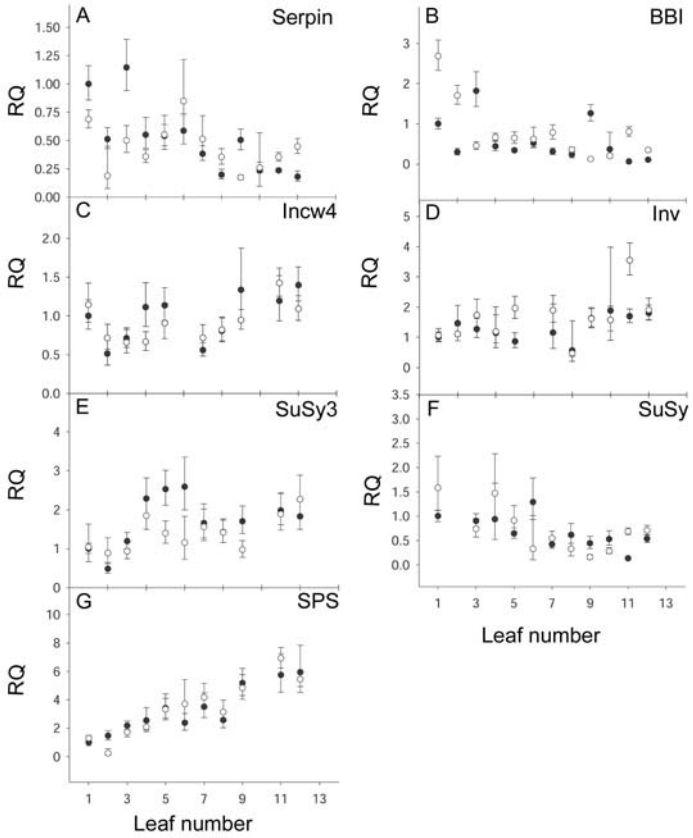

Figure 4.11 Effects of CO_2 enrichment on the abundance of transcripts encoding the two putative serine protease inhibitors and selected transcripts encoding enzymes of sugar metabolism in young and old source leaves. The abundance of transcripts encoding putative seprin (A) putative BBI (B) cell wall invertase (C), invertase (D), sucrose synthase 3 (E), sucrose synthase (F), and sucrose phosphate synthase (G) were determined in all the leaves of air-grown plants (closed circles) or plants grown with CO_2 enrichment (open circles). Values ± max/min were normalised to leaf 1 grown in air (relative quantity, RQ = 1) and expressed relative to thioredoxin transcripts, which were used as the endogenous control.

4.4.6 The effect of leaf position on the response to growth CO_2 levels for tissue carbohydrate contents and invertase and sucrose phosphate synthase activities

The amounts of glucose, fructose, sucrose and starch were measured in all the leaves on the stem (Fig. 4.12 A-D).

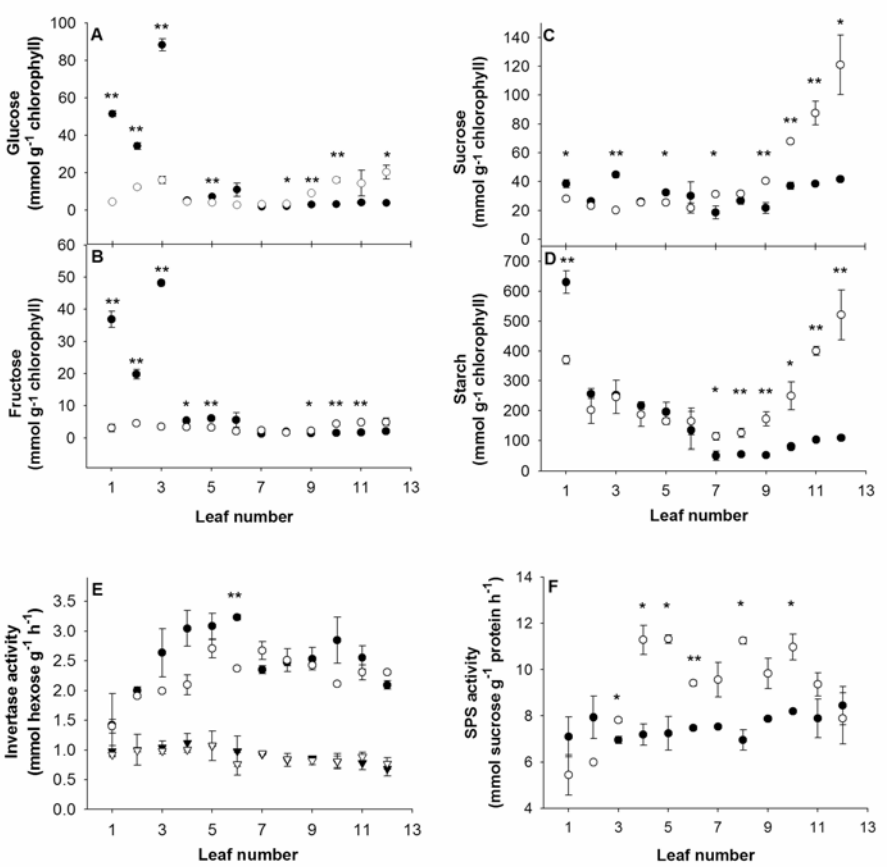

Figure 4.12 Effects of CO_2 enrichment on the abundance of leaf hexoses, sucrose and starch together with the activities of sucrose phosphate synthase and invertase in young and old source leaves. Leaf contents of glucose (A) fructose (B) sucrose (C) and starch (D) and activities of sucrose phosphate synthase (D) and acid invertase (E) were determined in all the leaves of air-grown plants (closed circles) or plants grown with CO_2 enrichment (open circles). Activities of neutral invertase were also determined (E) in all the leaves of air-grown plants (closed triangles) or plants grown with CO_2 enrichment (open triangles). Significant differences at $P < 0.05$ indicated by * and at $P < 0.01$ by **.

Glucose and fructose were greatly increased in the oldest source leaves compared to all other leaves on the stem, which had very low hexose contents when plants were grown in air (Fig. 4.12 A and B). Growth with CO_2 enrichment completely suppressed the age-dependent rise in leaf hexoses such that all the leaves had similar low amounts of glucose and fructose (Fig. 4.12 A). In contrast, while leaf sucrose (Fig. 4.12 C), and starch contents (Fig. 4.12 D) were not greatly affected by leaf rank in plants grown in air, there was a sharp increase in both of these carbohydrates in the youngest source leaves (leaf 7-13) in plants grown with CO_2 enrichment. Soluble acid invertase activities were much higher than those of neutral invertase in all but the oldest leaves on the stem (Fig. 4.12 E). While neutral and acid invertase activities were unaffected by growth CO_2 level (Fig. 4.12

E), SPS activities were markedly increased as a result of growth with CO_2 enrichment, in all but the youngest and oldest leaves (Fig. 4.12 F).

A significant correlation was found between transcript abundance of serpin and hexose content in leaves grown at 350µl l^{-1} CO_2 (Fig. 4.13), with an r^2 value of 0.77 ($p < 0.01$) for glucose, and 0.81 ($p < 0.01$) for fructose. There was a very weak correlation between putative BBI transcript abundance and hexoses, with r^2 values of 0.57 and 0.54 for glucose and fructose respectively. No correlation was found between sucrose content and transcript abundance of either putative serpin or BBI. There was no correlation between transcript abundance of putative serpin or BBI and hexose or sucrose content of leaves grown at 700µl l^{-1} CO_2 (data not shown).

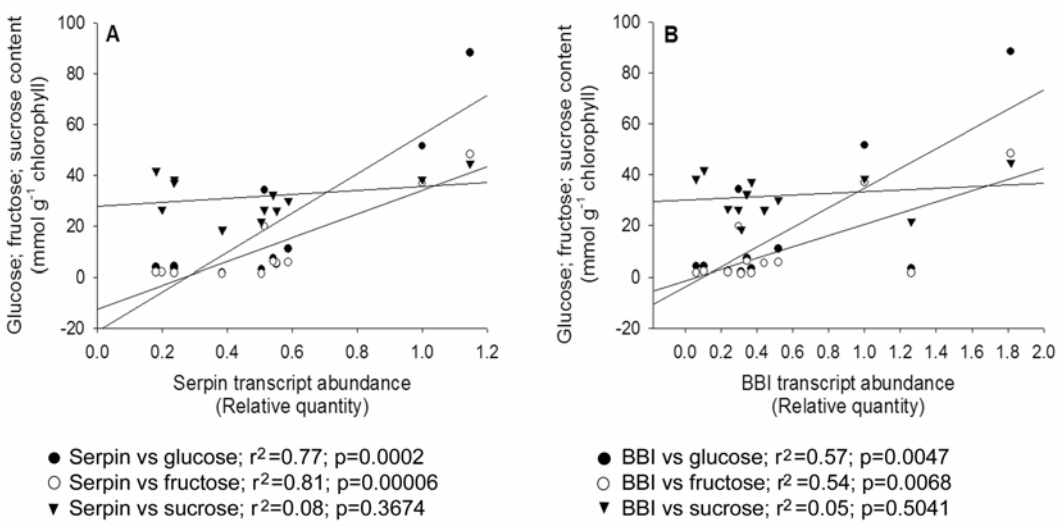

Figure 4.13 Correlation between glucose, fructose, and sucrose content and abundance of putative serpin and BBI transcripts. A significant correlation between hexose level and putative serpin transcript abundance was observed (A). A weak correlation between hexose level and putative BBI transcript abundance was observed (B). There was no correlation in either case between sucrose content and transcript abundance.

4.4.7 Modulation of serpin and BBI inhibitor transcripts and transcripts associated with sugar metabolism by sugars and cellular redox modulators

In order to determine the effects of sugars and redox modulators on the expression of the putative serpin and BBI inhibitors, the abundance of putative serpin and BBI transcripts was measured in leaf pieces that had been incubated in solutions containing either sugars (sucrose, glucose or fructose) or pro-oxidants (hydrogen peroxide or methyl viologen; MV; Table 4.8).

Table 4.8 Effects of sugars and pro-oxidants on the abundance of putative serpin and BBI transcripts relative to selected transcripts encoding enzymes of sugar metabolism. Data represent relative minimum-maximum values calculated from at least 3 technical replicates normalised to values obtained from leaves incubated with buffer alone and relative to cyclophilin and ubiquitin as endogenous controls.

		Treatment				
		Sucrose	**Fructose**	**Glucose**	**H_2O_2**	**MV**
Transcript	**Serpin**	1.83 (1.64-2.04)	1.59 (1.19-2.12)	1.44 (1.34-1.54)	**2.91** (2.51-3.38)	**7.56** (6.05-9.47)
	BBI	**0.54** (0.48-0.61)	**0.52** (0.32-0.85)	**0.44** (0.38-0.51)	**1.97** (1.71-2.27)	1.32 (1.15-1.52)
	Incw4	0.96 (0.86-1.07)	0.95 (0.79-1.13)	0.72 (0.67-0.78)	0.78 (0.66-0.92)	0.91 (0.76-1.10)
	Inv	0.82 (0.54-1.24)	1.31 (0.96-1.80)	1.04 (0.89-1.21)	**0.32** (0.24-0.42)	0.66 (0.56-0.78)
	SuSy3	1.12 (0.94-1.33)	1.29 (1.07-1.55)	1.17 (1.03-1.34)	**0.45** (0.32-0.64)	1.70 (1.52-1.89)
	SuSy	1.22 (0.99-1.49)	1.07 (0.72-1.60)	0.72 (0.67-0.77)	1.81 (1.44-2.28)	0.78 (0.62-0.98)
	SPS	0.91 (0.74-1.11)	1.18 (1.00-1.40)	0.76 (0.72-0.81)	**0.30** (0.25-0.35)	0.77 (0.67-0.87)

Sucrose, fructose, and glucose increased the abundance of serpin transcript and decreased the levels of putative BBI transcripts. Treatment with H_2O_2 and methyl viologen increased the levels of putative serpin transcripts to a similar extent as that observed in the presence of sucrose, fructose or glucose (Table 4.8). However, these pro-oxidants caused a large increase in the abundance of putative BBI transcripts. In contrast, treatment with sugars had very little effect on the abundance of the transcripts associated with sugar metabolism but H_2O_2 and methyl viologen tended to decrease the abundance of these transcripts (Table 4.8).

4.4.8 The effect of leaf position and growth CO_2 level on the abundance of protein carbonyl groups

Using the extent of protein carbonyl group formation as a measure of cellular oxidation, the relationship between leaf rank and cellular redox state was examined (Fig. 4.14).

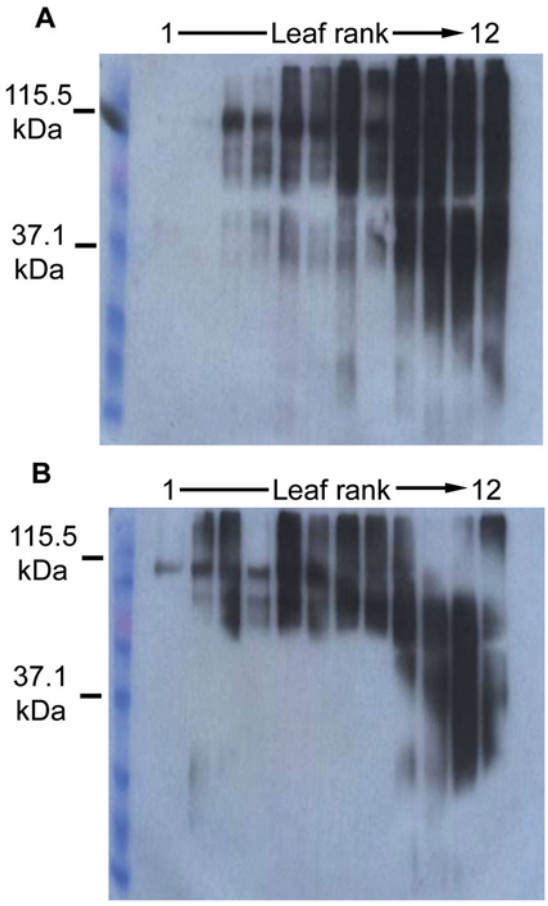

Figure 4.14 Effects of CO_2 enrichment on the abundance of carbonyl groups on the leaf proteins at different positions on the stem of plants grown in air (A) or with CO_2 enrichment (B). The abundance of protein carbonyl groups is compared for all leaves on the stem from the oldest source leaf (leaf rank 1) to the youngest source leaf (leaf rank 12).

Protein carbonyls were most abundant in the youngest source leaves in plants had been grown in air, the number of proteins showing carbonyl group formation and intensity of staining decreasing from the youngest to the oldest source leaves (Fig. 4.14 A). Only one carbonyl-stained protein band was detected in leaf ranks 1 and 2 in air-grown plants (Fig. 4.14 A). Growth with CO_2 enrichment had a dramatic effect on the profile of leaf carbonyl abundance and composition that was particularly marked in the youngest source leaves (Fig. 4.14 B). There was a marked decrease in the number of high molecular weight proteins showing carbonyl group formation in the youngest source leaves at high CO_2 (Fig. 4.14). The level of protein carbonyls was also decreased in other leaf ranks except leaf ranks 1-4 which showed a slight increase compared to the air-grown plants (Fig. 4.14).

4.5 Discussion

The impact of steadily increasing atmospheric CO_2 availability as the major driving force for photosynthesis, carbon gain and whole plant biomass production has become an increasingly important consideration in agriculture for food and bio-fuel production (Long et al., 2004 and 2006). C_4 species are crucial to food security as well as bio-energy applications but their responses to enhanced atmospheric CO_2 availability remains poorly characterized. The data presented here show that growth with CO_2 enrichment did not enhance biomass production or morphology in maize, consistent with other observations (Leakey et al., 2006). These results, however, are in contrast to those observed in Chapter 3, where increased CO_2 availability enhanced plant height. It is likely that the difference in plant height observed in Chapter 3 is due to air-grown maize being grown in cabinets, while high CO_2-grown maize were grown in rooms. This prevented air-grown maize to reach their full height. Growth at the higher CO_2 level furthermore had no significant effects on photosynthesis rates, consistent with previous observations (Leakey et al., 2006). In agreement with these observations, very few transcripts encoding enzymes involved with photosynthesis and primary metabolism were altered by growth at the higher CO_2 level. However, the impact of growth with CO_2 enrichment was dependent on the leaf rank on the stem. Strong development-dependent interactions in the response to CO_2 enrichment involved changes in both leaf carbohydrate status and redox state. We identified two putative serine protease inhibitors that were modulated in response to both of these key regulators of gene expression. We show here that the abundance of transcripts encoding two putative serine protease inhibitors is regulated in response to CO_2 enrichment and that their expression is differentially regulated by sugars, such that putative serpin transcripts were increased in the presence of sucrose, fructose, and glucose while putative BBI transcripts were repressed in the presence of these regulators. The putative serpin (EF406275) that is homologous to an *Arabidopsis* serine-type endopeptidase inhibitor (NP_177351.1) has a theoretical molecular weight of 8.09 kDa and pI of 5.45. The BBI protein has a theoretical molecular weight of 10.4 kDa and pI of 6.01. The putative serpin has a signal peptide and a pin2 domain, while the putative BBI inhibitor has a putative signal peptide and a BB leg domain. The signal peptides suggest that both proteins are targeted to secretary pathways and therefore may be involved in autophagasitic pathways of protein degradation associated with the vesicular transport system.

Entry of proteins into vesicular transport system for degradation from different cellular compartments, such as the chloroplasts and cytosol, was until recently thought only to occur in senescent leaves (Prins et al., submitted for publication to The Plant Cell), is linked to the oxidation of critical amino acids on proteins. The abundance of protein carbonyls on critical amino acids (a measure of cellular oxidation) was highest in the young maize source leaves in air and decreased with leaf position on the stem, such that the oldest source leaves had few detectable carbonyl-containing proteins. This situation appears to be similar to that observed in *Arabidopsis*, where the abundance of protein carbonyl levels progressively increased during vegetative development and then decreased dramatically just prior to bolting and reproductive development (Johansson et al., 2004). While the significance of this development-dependent decrease in protein carbonyl formation remains to be fully elucidated, the data demonstrate that in maize like *Arabidopsis*, protein oxidation is developmentally controlled. Most of the carbonyl groups in young maize leaves were found to be associated with bundle sheath proteins (Kingston-Smith and Foyer, 2000), such as RuBisCO, which is a major target for carbonyl formation upon exposure to oxidative stress (Marin-Navarro and Moreno, 2006). A number of important soluble proteins in leaves, such as RuBisCO and glutamine synthetase, are highly susceptible to oxidation, a process which enhances the cleavage of these proteins (Garcia-Ferris and Moreno, 1994). Within the chloroplast, oxidation of critical cysteine residues enhances the binding of the RuBisCO protein to the chloroplast envelope membranes, marking the protein for degradation (Marín-Navarro and Moreno, 2006). The presence of specific serine protease inhibitors may serve to protect important proteins from turnover in response to appropriate environmental or metabolic cues. A clear correlation between putative serpin transcript abundance and hexose content of leaves grown at 350 µl l^{-1} CO_2 was observed. This supports the role of glucose as signalling molecule, while providing novel evidence for hexoses as possible regulators of serine protease inhibitor expression in maize.

There is no evidence to support the view that oxidative stress was increased in the old source leaves compared to the young source leaves, as the antioxidant transcript profile in the old source leaves reflected adjustments in the defence network rather than a depletion of antioxidant defense. Similarly, the carbonyl groups were lowest in the oldest source leaves and the amounts of leaf anthocyanins were similar in all leaf ranks on the stem and were unaffected by the growth CO_2 environment. However, both the transcriptome profile

and the measured abundance of soluble sugars and starch suggests that there is a massive redeployment of carbohydrate pathways between the young and old source leaves in a manner that was responsive to atmospheric CO_2 availability. Rates of photosynthetic CO_2 assimilation were highest in the young source leaves, where sucrose photosphate synthase transcripts and activity were most abundant. This is consistent with a direct role of the youngest source leaves in carbon gain. Only these leaves accumulated sucrose and starch when plants were grown with CO_2 enrichment. By contrast, the older source leaves, which still maintained high rates of photosynthesis, but showed a high abundance of acid invertase and sugar signaling transcripts, accumulated only hexose when grown with high CO_2. Given the well documented roles of hexoses, hexokinases and the SnRK signaling pathways in controlling gene expression in response to both external environmental and metabolic cues (Baena-González et al., 2007), it can be concluded that the transcriptome signature of the older leaves is consistent with the operation of the sugar-mediated hexokinase signally pathway in the control of the two high CO_2-modulated putative serine protease inhibitors identified in this study.

In this part of the study it was demonstrated that high CO_2–dependent and hexose-dependent control of two putative serine protease inhibitors that participate in the network controlling protein stability and turnover underpins the acclimatory responses to growth CO_2 availability. Similarly, the enhanced operation of sugar signaling pathways in the older source leaves observed in this study is entirely consistent with observations of long distance signaling of information regarding CO_2 availability from mature to developing leaves (Lake et al., 2001). While long-distance CO_2 signaling systems involve sugars and similar molecules (Coupe et al., 2006; Miyazawa et al., 2006), the CO_2 signaling pathways that influence key parameters, such as absolute stomatal numbers and stomatal function (Lake et al., 2002; Woodward, 2002), remain poorly characterized with few identified regulators (Gray et al., 2000).

CHAPTER 5: CO_2 enrichment influences both protease and protease inhibitor expression in maize

In press: Prins, A., Verrier, P., Kunert, K.J., Foyer, C.H. (2008) CO_2 enrichment modulates both proteases and protease inhibitors in maize. In: Allen, J.F., Gantt, E., Golbeck, J.H., Osmond, B. (eds) Photosynthesis. Energy from the Sun: 14th International Congress on Photosynthesis. Springer. Chapter 3: 1379-1382.

5.1 Abstract

Proteolytic enzymes are essential for protein turnover and hence the ability of cells to respond to changing environmental conditions. Since one of the focuses of this study was to identify changes in the expression and activity of proteases and their inhibitors in response to development or CO_2 enrichment, the following studies were performed. Expression of protease inhibitor and protease-related transcripts were studied, and protease activities were investigated using biochemical techniques. Shoots contain high activities of both serine and cysteine proteases. Leaf protease activities were greatly increased by growth with CO_2 enrichment. Transcriptome analysis was performed on young and old source leaves of maize plants that had been grown for 8 weeks under either 350µl l^{-1} (low) or 700µl l^{-1} (high) CO_2. However, relatively few protease transcripts were modified by CO_2 in young and old source leaves. Growth at high CO_2 favours decreased source leaf cysteine proteases and increased cystatins.

5.2 Introduction

Growth with CO_2 enrichment causes extensive acclimation of photosynthesis involving down-regulation of carbon assimilation and up-regulation of carbohydrate synthesis and respiration. This massive reorganization of metabolism requires specific expression and regulation of proteases (Schaller, 2004; Trobacher et al., 2006). These are involved in the selective breakdown of regulatory proteins and enzymes by the ubiquitin/proteasome pathway and also in the post-translational modification of proteins by limited proteolysis for protein assembly and subcellular targeting. However, while it is widely recognized that the serine, cysteine, aspartic, metalloproteases and metacaspases are intricately involved in many aspects of plant growth and development (Mitsuhashi and Oaks, 1994; Xu and Cye, 1999; Bozhkov et al., 2005; Sanmartín et al., 2005), little attention has been paid to the

responses and regulation of these major proteolytic enzymes by high CO_2. CO_2 enrichment may lead to early senescence and changes in the later stages of programmed cell death through accumulation of sugars (Paul and Pellny, 2003). Since senescence is regulated by proteases (especially cysteine proteases) and their inhibitors (Solomon et al., 1999; Wagstaff et al., 2002; Belenghi et al., 2003; Okamoto et al., 2003), this study aimed to identify high CO_2–responsive proteases and protease inhibitors. To this effect, the transcriptome of young and old source leaves in maize plants grown to maturity at either 350 or 700µl l^{-1} CO_2 was studied.

5.3 Materials and Methods

All methods were performed by A. Prins, unless otherwise indicated.

5.3.1 Plant material and growth conditions

Maize (*Zea mays* hybrid H99) seeds were germinated on moistened filter paper. Batches of seedlings were harvested at 6 days for analysis at this point. Each seedling was separated into seed, shoot and root for analysis. Other batches of seedlings were transferred to compost in 8.5l volume (25cm diameter) pots, in controlled environment rooms (Sanyo, Osaka) where atmospheric CO_2 was strictly maintained at either 350µl l^{-1} or at 700µl l^{-1}, with a 16-h photoperiod with light intensity of 800µmol m^{-2} s^{-1}, temperature of 25ºC (day)/19 ºC (night), and 80% relative humidity as described by Driscoll et al. (2006). At 8 weeks the following parameters were measured in leaf 5.

5.3.2 Protein quantification

Protein was quantified as described in Chapter 2 using Bradford reagent.

5.3.3 Proteolytic detection in plant extracts

i) Azocasein assay

Cysteine protease activity was measured according to Reichard et al. (2000) and Michaud et al. (1995) with modifications.

The assay was optimised for use with maize plant extracts prepared from seeds (dry, imbibed and germinated), seedlings (3-6 days post imbibition), young shoots and mature leaves. The assay was tested for linearity with increasing time (Fig. 2.4 A), substrate (Fig.

2.4 B), and extract (Fig. 2.4 C). In general, fresh plant material was extracted by grinding it in a mortar with a pestle on ice, in cold extraction buffer (0.1M citrate phosphate buffer pH 5.5, 0.1% Triton X-100) at a ratio of 1:2 (w/v), with the addition of a small amount of acid washed sand (Sigma, UK). Dry seeds were first ground in a coffee grind (Krups model 203-42 coffee grind) before extraction over ice. A small weight to extraction buffer ratio was used in order to obtain highly concentrated samples. Samples were centrifuged at 12 000rpm for 10min at 4°C and the supernatant transferred to a fresh tube for use in the assay. Protein concentration was determined as described, using Bradford reagent, and in general approximately 500µg protein was used to assay extract obtained from seeds, while approximately 300µg protein was used to assay extract obtained from seedlings. Reactions were set up in duplicate by adding 100µl sample (containing 300-500µg) protein to 10µl extraction buffer and 90µl reaction buffer containing azocasein (1%) in 0.1M citrate-phosphate buffer pH 5.5 and 5mM DTT. Samples were incubated for 0-10min at 37ºC, after which the reaction was stopped by adding 60µl TCA (20%). The tubes were allowed to stand for 30min at room temperature after which they were centrifuged at 14 500 rpm for 5min. The supernatant (150µl) was mixed with 1 volume (150µl) of 1N NaOH and the absorbance of the released dye measured at 436nm in a microplate reader. Values obtained at 0min were subtracted from values obtained at 10min to obtain the change in A_{436} caused by cysteine protease activity.

The contribution of specific proteases to the detected protease activities was determined by pre-incubating samples for 10min at 37°C with specific protease inhibitors. To test for serine protease activity, 2µl extraction buffer was replaced with 2µl 100mM PMSF (final concentration 1mM); to test for cysteine protease activity, 10µl extraction buffer was replaced with 10µl 1mM E64 (final concentration 100µM); to test for metalloprotease activity, 4µl extraction buffer was replaced with 4µl 100mM EDTA (final concentration 2mM).

To test the linearity of the assay over time, the increase in A_{436} obtained by incubating extract obtained from seedlings 3 days post imbibition (380µg soluble protein) at 15min intervals over one hour was determined (Fig. 5.1 A). To test the linearity of the assay with increasing amount of substrate (Fig. 5.1 B), extract obtained from seedlings 5 days post imbibition (340µg protein) was incubated with 0-0.8mg azocasein for 20h to obtain

complete hydrolysis. To test the linearity of the assay with increasing amount of extract (Fig. 5.1 C), extract obtained from seedlings 7 days post imbibition was diluted to obtain total soluble protein content of 20-100µg protein and assayed as described above.

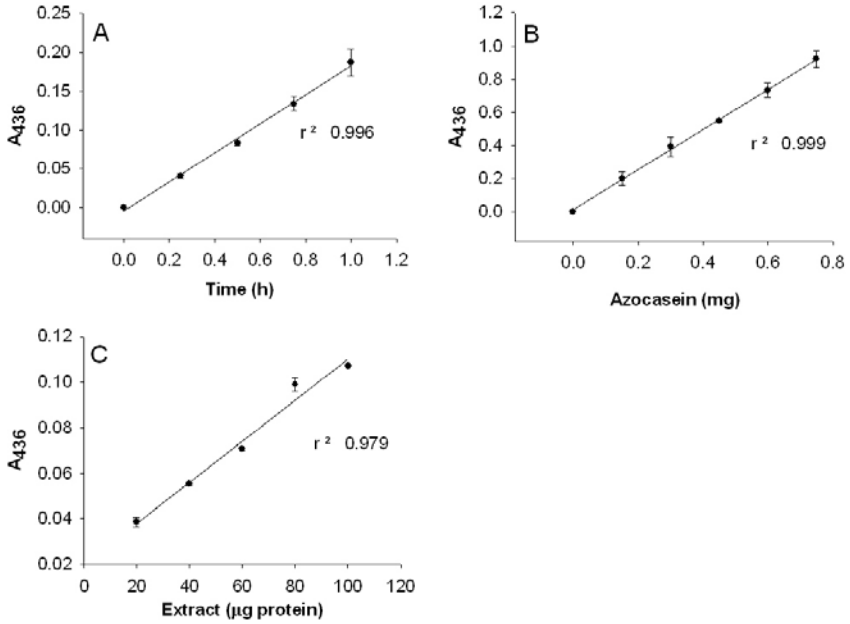

Figure 5.1 Optimisation of azocasein assay with respect to time (A), substrate (B) and extract (C).

ii) In-gel protease assay

In-gel detection of protease activity was done according to Michaud et al. (1993a). Protein samples were extracted in extraction buffer [0.1M citrate phosphate, 5mM DTT, 0.1% (v/v) Triton X-100] and centrifuged at 12 000 rpm for 10min at 4°C before determining protein concentration as described above. Extracts (containing 30µg protein) were then added to SDS PAGE loading buffer containing 62.5mM Tris-HCl (pH 6.8), SDS (2%, w/v), glycerol (10%, v/v), and bromophenol blue (0.001%, w/v). Samples were not boiled prior to gel electrophoresis and loading buffer did not contain β-mercaptoethanol to prevent destruction of secondary structure of proteins. Protein samples were separated on a 10% SDS gel containing gelatine (0.2%) in the resolving gel at 4ºC in 1x SDS PAGE buffer (Sambrook et al., 1989) until the blue front had reached the bottom of the gel. After electrophoresis, gels were placed for 30min in a 2.5% aqueous Triton X-100 solution to remove SDS and renature proteins. Gels were then rinsed with distilled water before being placed for 2-5h in a reaction solution consisting of 0.1M citrate phosphate buffer pH 5.5, 5mM DTT, and 0.1% Triton X-100 at 37ºC, with gentle shaking. After incubation, gels

were stained overnight in staining solution containing 0.25% Coomassie R-250 (w/v), 50% methanol (v/v), and 10% acetic acid (v/v). Gels were then destained in staining solution without Coomassie R-250 until white bands became visible.

To determine specific proteolytic activity, the protein extracts were preincubated in the presence of either 100µM *trans*-epoxysuccinyl-L-leucylamido(4-guanidino)butane (E64; Sigma, UK) or 1mM phenylmethanesulfonyl fluoride (PMSF; Sigma, UK) at 37°C for 15min prior to the addition of sample buffer. E64 is an irreversible, potent, and highly selective inhibitor of cysteine proteases, while PMSF inhibits serine proteases, such as trypsin and chymotrypsin as well as some cysteine proteases (such as papain), although the inhibition of cysteine proteases is reversible by adding reducing agents such as DTT.

5.3.4 RNA extraction, purification, and analysis

RNA was extracted, purified, and analysed as described in Chapter 4 using Trizol reagent.

5.3.5 Micorarray hybridization

Microarray hybridization was performed using commercially available microarray chips (Affymetrix) at ArosAB in Denmark, as described in Chapter 4.

5.3.6 Microarray analysis

Microarray data analysis was performed by P. Verrier (Rothamsted Research, UK) as described in Chapter 4. Probesets were identified by translated homology search as described in Chapter 4.

5.4 Results

5.4.1 Protease activities

The tissue-specific protease activities of seeds, shoots and roots were examined in 6 day-old maize seedlings as well as in leaf 5 of 8 week-old plants (Fig. 5.2). Four well-defined activity bands were identified in the seed extracts (Fig. 5.2 B). These ranged in size from a high molecular weight (band i) to very low molecular weight (band iv). Band (i) was also present in the root, which additionally showed a large but very diffuse band of activity between bands (ii) and (iii). This diffuse band in roots may represent a single protease with high activity, or a number of proteases that all have similar molecular weights. The shoot and mature source leaf

both also showed a large diffuse area of activity between bands (ii) and (iii; Fig. 5.2 B), that, upon inspection, seemed to consist of a large number of distinct bands. The intensity of this diffuse area between bands (ii) and (iii) (Fig. 5.2 B) was greater in mature leaves than in shoots per µg protein, showing comparatively greater protease activity in mature leaves than young, developing leaves. This diffuse area was also enhanced in the leaves of the plants grown with high CO_2 compared to those grown in air (Fig. 5.2 C).

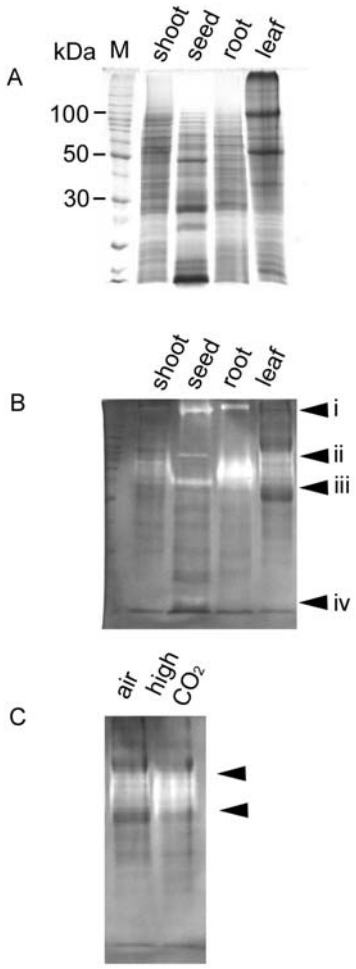

Figure 5.2. Protease activities in different maize organs. Tissue soluble proteins were identified on Commassie-stained gels loaded with equal protein (30 µg; A) and protease activities were detected by the in-gel assay (B and C). The gels in (B) had been loaded with different amounts of protein according to band intensity. The protein loadings were: 30µg shoot; 50µg seed; 15µg root; 30µg leaf. The gels in (C) had been loaded with equal leaf protein (30µg).

The inhibitory effect of PMSF on activity band (i), in shoot and seed extracts from 6 day-old seedlings, suggests that it comprises largely of serine proteases but the presence of PMSF plus DTT caused less suppression of band (i) activity in roots (Fig. 5.3 B) indicating that this band is represented by both serine and cysteine proteases. Seed

protease bands (ii) and (iv) were faint. They were absent in the presence of E64 but present in PSMF (Fig. 5.3 B), which implies that these bands could represent cysteine proteases, but not serine proteases. In contrast seed protease band (iii) was unaffected by E64 or PMSF. Similarly, neither E64 nor PMSF had any effect on the intensity of the diffuse zone of activity between bands (ii) and (iii) in roots, suggesting that this activity in roots arises largely from activity of proteases other than cysteine or serine proteases.

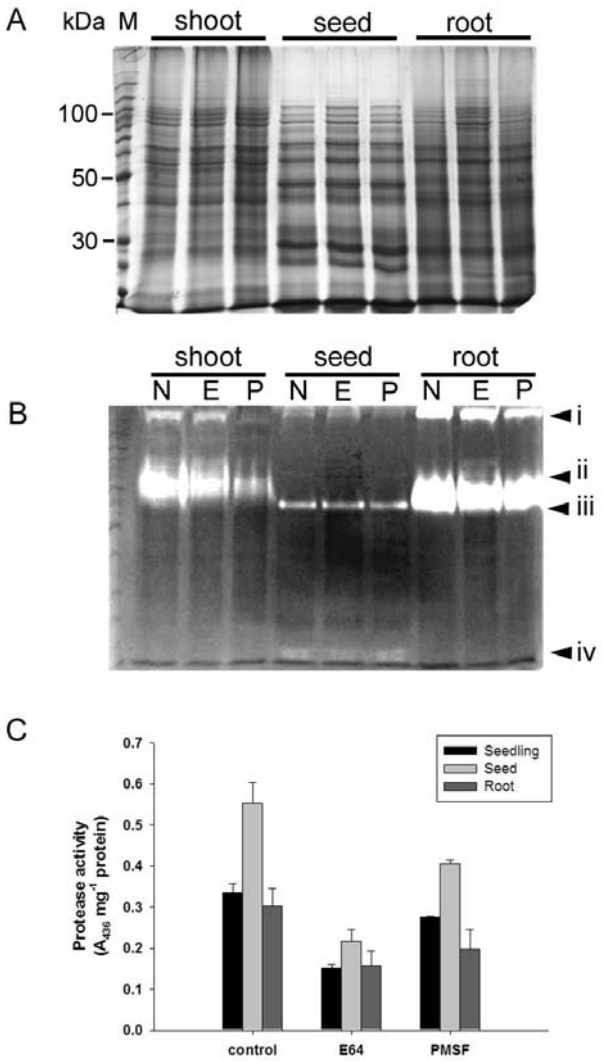

Figure 5.3 Characterization of protease activities in seed shoot and root. Tissue soluble proteins were identified on Commassie-stained gels loaded with equal protein (30µg; A) and protease activities were detected by the in-gel assay (B). The samples in (B) had been pre-incubated either in the absence of inhibitor (N) or in the presence of E64 (E) or PMSF (P). Gels had been loaded with 30µg protein in each case. Spectrophotometric analysis of protease activity (C) was performed on replicate samples to those in A and B.

The diffuse band of activity between bands (ii) and (iii) in shoots was diminished in the presence of E64 and PMSF, suggesting that this activity arises from a complex mixture of

different proteases (cysteine, serine, aspartic proteases and possibly others Fig. 5.3 B). Since this area also corresponds to the area affected by CO_2 enrichment in mature leaves, it is possible that the proteases up-regulated by CO_2 enrichment represent a mixture of different classes of protease.

Quantification of the protease activities, measured on a protein basis in the different tissues of germinating 6 day-old seedlings showed that seeds had the highest protease activities (Fig. 5.3 C). A substantial proportion (61%) of the seed protease activity was inhibited by E64. Similarly, about half of the total root protease activity was inhibited by E64 (Fig. 5.3 C).

5.4.2 Transcriptomic analysis

A preliminary analysis of the transcriptome data (Table 5.1) revealed that the abundance of two cysteine proteases and a chloroplast protease was decreased in the young source leaves of high CO_2 grown maize plants, although only by 21.5%, 18.1%, and 11.3% respectively. An aspartic protease was repressed by high CO_2 in the older source leaves by 17.7%. In contrast to the rather modest effect of CO_2 enrichment on protease transcripts, a large number of cysteine protease inhibitor (cystatin) transcripts were differentially regulated in the leaves of high CO_2-grown plants (Table 5.1). None of these transcripts differed in abundance by more than 25%. Hoever, a trend was observed whereby cystatins are induced in young mature leaves by CO_2 enrichment, while in old mature leaves they are repressed. Trypsin inhibitor transcripts were 31.9% higher in air-grown leaves than high CO_2-grown leaves. In contrast, transcripts encoding corn cystatin 1 were much higher in the leaves at elevated CO_2. Surprisingly, a wound-induced protein (WIP1) transcript, encoding a serine-type endopeptidase inhibitor, showed the greatest overall response to growth with CO_2 enrichment in young source leaves but not in old source leaves. The response of ubiquitin transcripts to CO_2 enrichment also varied with the stage of development, showing the greatest response in the old source leaves (Table 5.1).

Table 5.1 Protease and protease inhibitor transcripts that were differentially modified in response to CO_2 enrichment in maize source leaves. Transcript abundance was measured by microarray.

		(%change)	
Probe set	Gene title	Young source leaf	Old source leaf
Proteases			
Zm.7736.1.S1_at	Cysteine protease Mir2	-21.5%	3.0%
Zm.5987.1.A1_at	Cysteine protease	-18.1%	-10.5%
Zm.18435.1.A1_at	Protease Do-like 8, chloroplast precursor	-11.3%	1.3%
Zm.10845.1.A1_at	Nucellin-like aspartic protease	2.1%	-17.7%
Zm.5987.2.A1_at	Cysteine protease Mir3	-1.3%	9.9%
Protease inhibitors			
Zm.6656.1.A1_at	Trypsin inhibitor	-31.9%	-10.4%
Zm.14272.4.S1_x_at	Corn cystatin I	22.2%	-17.6%
Zm.14272.2.A1_a_at	corn cystatin I	20.2%	-8.5%
Zm.14272.5.S1_x_at	Corn cystatin I	20.0%	-13.5%
Zm.14795.1.A1_at	Putative cystatin	-15.2%	-6.9%
Zm.15278.1.S1_at	Protease inhibitor	12.8%	-1.2%
Zm.3347.1.A1_at	Putative cystatin	-10.0%	3.4%
Other			
Zm.186.1.S1_at	Wound induced protein	-120.3%	3.4%
Zm.3830.1.S1_at	Ubiquitin	1.6%	11.7%

5.5 Discussion

Growth with CO_2 enrichment had a pronounced effect on both source leaf protease activities and transcripts. However, high CO_2 also had a marked effect on the abundance of transcripts encoding protease inhibitors, particularly cystatins. Interestingly, high CO_2 led not only to marked decrease in the abundance of transcripts encoding a number of cysteine proteases but also to an increase in abundance of endogenous cystatin transcripts, particularly in young leaves. While the abundance of different proteases was not changed by a large percentage, there was a distinctive increase in observable protease activity due to CO_2 enrichment, as observed on activity gels. If the observed protease activity observed in leaves and shoots include, amongst other proteases, cysteine protease, this would suggest that high CO_2 causes modulation of cysteine protease activity at the level of translation or interaction with endogenous inhibitors. The protease inhibitor most significantly affected by CO_2 enrichment is a trypsin inhibitor, where the trypsin inhibitor was down-regulated by 31.9% in young source leaves. Trypsin inhibitors not only regulate endogenous proteases, but are regularly induced upon insect attack and therefore are characteristic of a biotic stress response. These results are in agreement with the results obtained in Chapter 3 where high CO_2-grown leaves had a lower abundance of stress-related transcripts, including two putative protease inhibitors.

In addition, there was a large decrease (120.3%) in the serine protease inhibitor, WIP1, in young source leaves due to CO_2 enrichment, which further confirms results obtained in Chapter 3, especially with respect to the specific regulation of serine protease inhibitors by CO_2. Regulation of protease activity in addition to abundance might be a key feature of this response.

This study is the first to identify the regulation of proteases and inhibitors by CO_2 enrichment. While protease transcripts are decreased (although in general, not significantly), protease activity is increased in leaves grown at high CO_2. In addition, the abundance of transcripts encoding protease inhibitors is generally differentially affected by CO_2 enrichment. However, the strong down-regulation of two stress-related protease inhibitors suggest that leaves grown in air experience a stronger stress-related signal than those grown with CO_2 enrichment.

CHAPTER 6:Discussion

The studies described in this thesis contribute to our current knowledge of the role that proteases and protease inhibitors play in plant growth, acclimation, and senescence. Firstly, a characterisation of the effects of an exogenous protease inhibitor (OC-I) expressed in tobacco showed that this inhibitor can effect plant morphology, senescence, and cold stress-induced proteolysis. Results of this part of the study show that a single transgene can possibly have multiple effects on development and stress tolerance, and also provide evidence for a mechanism of RuBiSCO proteolysis outside the chloroplast. Furthermore, the responses of maize to CO_2 enrichment were studied by analysing changes in gene expression, physiology, photosynthesis, and carbon metabolism in plants grown at 700 µl l^{-1} CO_2 compared to those grown in air. This part of the study furthermore characterised the effect of CO_2 enrichment on proteases and protease inhibitors by studying changes in gene expression as well as activity of proteases. The results support a role for sugar and redox signalling cascades in maize response to high CO_2.

6.1 The effect of OC-I expression on development and abiotic stress tolerance in tobacco (Chapter 2)

Previous results showing a protection of photosynthesis by exogenous OC-I expressed in tobacco plants (Van der Vyver et al., 2003) was the basis for the first chapter of this thesis. The objective of this chapter was to elucidate the possible mechanism by which the photosynthetic machinery is protected. The particular plants used in the previous study were already available in my research group and were used for these experiments. Endogenous phytocystatins perform a defensive role against biotic stress, such as insect and nematode attack (Liang et al., 1991; Zhao et al., 1996), and are also induced by abiotic signals, such as wounding or methyl jasmonate (Bolter 1993; Botella et al., 1996). The potential of exogenous OC-I to improve stress tolerance by protecting chloroplastic proteins was studied here. This study is the first to identify a novel role for the protection of RuBisCO and RuBisCO activase by the (presumably) cytosolic OC-I. This is an important result, since RuBisCO is the most abundant protein on earth, and an increase in protein content of crops will make them potentially more nutritious. Furthermore, this protection of photosynthetically important proteins may play a role in the observed tolerance of photosynthesis in OC-I expressing plants to cold stress. In this study an attempt was made to explain the protection of RuBisCO by suggesting a new model of

RuBisCO degradation. The degradation of RuBisCO is a controversial subject, with the main theories suggesting that RuBisCO is either mainly degraded inside the chloroplast with oligopeptides being exported for further degradation in the vacuole, or that RuBisCO is exported whole and degraded in vacuolar vesicles containing RuBisCO-degrading proteases (Feller et al., 2007). In this study immuno-localisation studies provides evidence that RuBisCO is exported from the chloroplast in vesicles for degradation in the cytosol. Any action of cysteine proteases in these vesicles and the protective effect of exogenously expressed OC-I still needs to be characterised. In particular, a follow-up study is being performed in order to identify the mechanism through which RuBisCO, OC-I, and the protease(s) it inhibits interacts. Preliminary results suggest that OC-I is present in vesicles in the cytosol. Furthermore, identification of the endogenous proteases that are inhibited by OC-I will be pursued.

6.2 The effect of CO_2 enrichment on photosynthesis and plant physiology (Chapter 3)

While the increasing concentration of CO_2 in the earth's atmosphere could have a positive effect on photosynthesis in C_3 plants, it was illustrated in this study that increased CO_2 availability does not alter photosynthesis in maize, a C_4 species. Photosynthesis and RuBisCO activity in C_4 species are not limited by CO_2 availability as it is in C_3 plants, due to the CO_2-concentrating mechanism employed by C_4 species. In addition to the lack of CO_2-induced changes in photosynthesis in maize plants grown at high CO_2, there was little or no significant change in the expression of photosynthesis-related transcripts. In *Arabidopsis*, increased availability of CO_2 is associated with an increased level of sugars, which leads to a hexokinase-mediated decrease in the expression of RuBisco SSU (Sun et al., 2002). In this study only a single probe set representing RuBisCO SSU was affected by CO_2 enrichment (by 30%), and only in young leaves. RuBiSCO SSUs are encoded by a multi-gene family that are expressed differentially at ambient CO_2 (Dean et al., 1989) and also respond differentially to CO_2 enrichment (Cheng et al., 1998), which could explain why only a single probe-set was identified. In agreement with the lack of observed changes in RuBiSCO SSU transcripts, there was no significant effect of CO_2 enrichment on the expression of hexokinase, which regulates the expression of this protein. While RuBisCO contributes only up to 30% of total soluble proteins in C_4 plants (Sugiyama et al., 1984), it represents, along with phosphoenolpyruvate (PEP) carboxylase, and pyruvate orthophosphate dikinase, nearly 50% of the soluble leaf proteins in C_4 plants (Sugiyama et

al., 1984; Sage et al., 1987; Makino et al., 2003). These proteins (PEP carboxylase and pyruvate orthophosphate dikinase), that also play important roles in photosynthesis, were similarly unaffected by CO_2 enrichment in young and old mature leaves (rank 12 and rank 3 respectively). Photosynthetic acclimation to elevated CO_2 in C_3 plants generally varies with leaf age, with mature leaves showing a large amount of acclimation (Bowes 1991; Stitt, 1991) while young leaves lack an acclimatory response (Nie et al., 1995). This lack of acclimation may in part be due to young leaves not yet being sufficiently developed as source leaves, and therefore not able to redistribute nitrogen away from RuBisCO until further development has occurred (Moore et al., 1999). However, since RuBisCO is not CO_2-limited in maize, and since all leaves used in this study were mature source leaves, this did not play a role. While CO_2 had no significant effect on the photosynthetic system, leaf rank had a significant effect with old mature leaves (rank 3) having a much lower rate of photosynthesis than young mature leaves (rank 12). This decrease in photosynthesis could be mediated by, amongst other systems, a hexokinase-dependent signal leading to the decreased expression of RuBiSCO SSU as indicated by a higher abundance of hexokinase transcripts in old mature leaves.

While increased CO_2 availability leads to increased crop yield and biomass, and decreased stomatal density in C_3 species, this was not observed in this study on maize, a C_4 species. Since maize grown at high CO_2 did not have significantly different rates of photosynthesis or carbohydrate content, this could be expected. Furthermore, while stomatal density did not decrease, stomatal area and epidermal cell density did. This is a novel finding that contrasts with previous research in which maize plants showed a reduction in stomatal density (Woodward and Kelly, 1995). Furthermore, maize grown at high CO_2 showed a significant decrease in protein and chlorophyll content in the leaves on the mid-section of the stem. This was not observed in the leaves towards the bottom or top of the stem. It is unknown which proteins are affected by CO_2 enrichment in the leaves on the mid-section of the stem, a question that requires further investigation. The old mature leaves (rank 3) also had a significantly lower soluble protein content compared to the young mature leaves (rank 12) despite CO_2 level at which plants were grown. This is possibly a decrease in the amount of RuBisCO, PEPcase, and pyruvate orthophosphate dikinase in these leaves which constitute the bulk of soluble protein in maize cells. A decrease in these proteins would support the observed decrease in photosynthesis in the old mature leaves. While photosynthesis measured per surface area was not significantly affected by CO_2

enrichment, photosynthesis rates measured on leaves on the mid-section of the stem were significantly higher per mg chlorophyll in leaves grown at high CO_2. Plants do not synthesise RuBisCO in excess of that which is required to maintain photosynthesis. In addition to this, plants do not synthesise chlorophyll in excess of that which is required for light absorption in order to drive CO_2 fixation by RuBisCO. If the decreased protein content of leaves grown at high CO_2 represents a decreased amount of photosynthesis-related proteins, such as RuBiSCO, this would explain the decrease in chlorophyll - the major pigment that absorbs light. The amount of light absorbed by the chlorophyll should not exceed the capacity of the plant to use the energy for the fixing of CO_2. However, since photosynthesis rates per leaf area is similar in leaves grown in air or with CO_2 enrichment; this suggests that another rate-limiting process has been affected. While C_4 plants employ a form of photosynthesis that decreases photorespiration, it is possible that maize leaves grown at high CO_2 experience even less photorespiration than those grown in air. This could possibly account for the more efficient photosynthesis rates measured per mg chlorophyll in maize leaves grown with CO_2 enrichment.

6.3 The effect of CO_2 enrichment on the maize transcriptome (Chapter 4)

While other studies on maize and CO_2 enrichment have identified major effects on signalling and metabolism-related sequences, this study identified a number of stress-related sequences which are affected by CO_2 enrichment. This is a new result not reported before. A lower abundance of oxidative stress-related sequences in leaves grown at high CO_2 was observed. This result was complemented by oxyblot analysis which showed that proteins extracted from leaves grown at high CO_2 experience less oxidative marking. Furthermore, two novel protease inhibitors, a putative serine protease inhibitor and putative Bowman-Birk inhibitor, were identified as being specifically controlled by changes in CO_2 availability. These sequences were more abundant in air-grown leaves than high CO_2-grown leaves – a result that has not been reported previously. Serine protease inhibitors (including the BBI-type proteins) not only play a role in the regulation of endogenous trypsin and chymotrypsin activity, but are also induced upon wounding and attack by pathogens and insects (Bowler and Fluhr, 2000; Budai-Hadrian et al., 2006). While the microarray study performed here shows that protease transcripts are not increased by CO_2 enrichment, protease activity (including serine protease activity) were enhanced in leaves grown at high CO_2. Decreased expression of serine protease inhibitors in leaves grown at high CO_2 could result in increased protease activity. Alternatively, the

increased abundance of a putative serpin and putative BBI in air-grown leaves might be a part of the apparent stress-related pattern of transcripts observed. This hypothesis is supported by the observation that pro-oxidants induce transcription of both these sequences, showing that the putative serpin and BBI may be regulated by an oxidative signal. In addition, transcript abundance of both putative serpin and putative BBI showed a positive correlation with the glucose content of leaves, suggesting that these sequences may also be regulated by hexose content. This finding also implies cross-talk between the hexose and oxidative stress signalling pathways – a process that has been illustrated previously (Roitsch et al., 2003; Tajima and Koizumi, 2006). However, only the putative serpin (which contains a pin2 domain) was induced by glucose, a result that has been observed in pin2 proteins (Johnson and Ryan, 1990). These results support previous evidence that an increase in atmospheric CO_2 can increase plant tolerance to biotic (Idso et al., 2000; Matros et al., 2006) and abiotic (Miller et al., 1998) stress.

6.4 The effect of developmental stage on the maize transcriptome (Chapter 5)

Developmental stage affected a large number of proteases, protease inhibitors, and uibiquitin-related sequences as measured by microarray analysis. In particular, ubiquitin-related proteolysis seems to be favoured in old mature leaves based on expression of sequences involved in this system of proteolysis. Seven serine protease-type sequences were affected by developmental stage, including subtilases, serine carboxypeptidases, and a LON protease. The subtilase transcripts were more abundant in young mature leaves, indicating a possible role for these proteins in maize leaf development or regulation of stomatal density. The LON protease mRNA was more abundant in old mature leaves than young mature leaves, where it presumably functions in the regulation of protein fidelity in mitochondria based on this function ascribed to LON proteases (Janska, 2005). All cysteine proteases identified by microarray study as differentially expressed due to differences in leaf rank were more highly abundant in young mature leaves than old mature leaves. However, two cysteine protease inhibitor sequences were differentially regulated between young and old mature leaves, with one probe set being more highly abundant in young leaves, and another being more highly abundant in old leaves. In addition, a subtilase inhibitor sequence was less abundant in young mature leaves compared to old mature leaves. These sequences together provide a pool of potential markers for developmental change. In particular, subtilase and subtilase inhibitor sequences might prove valuable to this effect.

Changes in transcript abundance associated with phytohormone response or synthesis in maize leaves of different ranks on the stem showed that there is a differential response, but that CO_2 enrichment does not necessarily affect this developmentally regulated response. Transcripts associated with the synthesis of ABA (terpene synthase) was especially highly abundant in rank 12 leaves compared to rank 3. As ABA plays a role in the induction of stress-related genes (especially protease inhibitors) this may indicate a signalling role for ABA in this capacity. A further phytohormone that showed differential regulation based on leaf rank was auxin. Transcripts associated with this hormone was, in general, higher in rank 12 than rank 3, indicating a possible role in cell elongation and division and the delay of senescence in young, mature leaves (rank 12).

6.5 Conclusion

In conclusion, the original hypotheses as stated in Chapter 1 can be evaluated as follows:

Hypothesis 1: Exogenous OC-I protects RuBisCO from degradation by endogenous proteases that function during development and cold stress.

In this study it was observed that OC-I expression in tobacco alters development and protects photosynthesis by interacting with unknown endogenous proteases. Expression of the transgene leads to changes in the degradation of RuBisCO and, possibly, RuBisCO activase. RuBisCO was identified in vesicular bodies in the cytosol, supporting a new hypothetical mechanism for RuBisCO degradation outside the chloroplast. These results support the hypothesis and address objectives 1 and 2 as stated in Chapter 1

Hypothesis 2: Maize will respond to growth with CO_2 enrichment by acclimation in leaf biology underpinned by changes in gene expression.

In this study it was observed that increased CO_2 availability causes acclimation of photosynthesis in maize leaves so that photosynthesis rates are not significantly different from those measured in air-grown leaves. Carbohydrate metabolism is also not significantly affected. Transcripts related to photosynthesis and sugar metabolism are, accordingly, not significantly affected. However, epidermal characteristics, protein content, and chlorophyll content are significantly changed. These results support the stated hypothesis and address objectives 3, 4, and 5 as listed in Chapter 1.

Hypothesis 3: Changes in plant metabolism due to CO_2 enrichment and development involves changes in the expression and/or activity of proteases and protease inhibitors

In this study it was observed that growth with CO_2 enrichment does not affect the time of flowering. Since flowering and fruit development is used as an indicator of the onset of senescence (Noode´n et al., 1997), this shows that CO_2 enrichment does not enhance senescence in maize. While protease activity is enhanced in leaves grown at high CO_2 based on in-gel activity assays, expression of protease genes are not affected according to microarray results. Furthermore, the expression of a large number of proteases and protease inhibitors are affected by developmental stage. Two putative serine protease inhibitors (a serpin and a BBI) were specifically affected by CO_2 enrichment, and appear to be regulated by oxidative and hexose signals. These results support hypothesis 3 and address objective 6 as stated in Chapter 1.

6.6 Future work

The study on the protection of photosynthetic proteins by exogenously expressed OC-I provide exciting results that pave the way for further investigation. The mechanism by which RuBisCO is degraded *in planta* is of particular interest. Most importantly, the interaction between OC-I and the endogenous protease(s) that it inhibits, must be characterised. For this co-immunoprecipitation may be performed. Antibodies that recognise the OC-I protein can be included in plant extract prepared from OC-I-expressing tobacco. The antibody binds to the OC-I protein and can be precipitated using protein-G or protein-A sepharose which binds most antibodies. Any proteins or proteases that interact with OC-I will be co-immunoprecipitated in this way. The precipitated complex can then be studied by electrophoresis, mass spectrometry, or sequencing. Furthermore, the cellular localisation of the interaction between OC-I and endogenous proteins is currently being studied by *in situ* immunolocalisation studies.

This also study paves the way for further research to elucidate the effect of increased CO_2 availability on C_4 plants. More specifically, the effect of CO_2 enrichment on the maize proteome is being studied at present to determine regulation of the high CO_2-response on translational level. Differences in the quantity of a number of proteins have already been identified. These proteins will be identified by mass spectrometry or sequencing. Furthermore, the effect of CO_2 enrichment on RuBisCO and RuBisCO activase should be studied by Western blot analysis to determine whether these proteins are decreased in

leaves on the mid-section of the plant stem. Measurement of RuBisCO activity in these leaves could also provide insight into the acclimation of maize photosynthesis to high CO_2. Rubisco activity can be measured using the radioactive method described in this thesis. The putative serpin and BBI identified as being specifically affected by CO_2 enrichment have to be characterised with respect to function, in order to confirm their identity. These proteins should be expressed as fusion proteins and used in activity assays such as zymograms or biochemical assays such as those described in this thesis. Furthermore, the effect of constitutive expression of these genes in a model plant, such as tobacco or Arabidopsis might provide further insight into their function during stress.

References

Abe, M., Abe, K., Kuroda, M., and Arai, S. (1992) Corn kernel cystein protease inhibitor as a novel cystatin superfamily member of plant origin. Eur. J. Biochem., 209: 933-937.

Abe, M., Abe, K., Domoto, C., and Arai, S. (1995) Two distinct species of corn cystatin in corn kernels. Biosci. Biotech. Biochem., 59: 756-758.

Abe, M., Domoto, C., Watanabe, H., Abe, K. and Arai, S. (1996) Structural organization of the gene encoding corn cystatin. Biosci. Biotech. Biochem., 60: 1173-1175.

Adam, Z. and Clarke, A.K. (2002) Cutting edge of chloroplast proteolysis. Trends Plant Sci., 7: 451-456.

Ainsworth, E.A., Davey, P.A., Bernacchi, C.J., Dermody, O.C., Heaton, E.A., Moore, D.J., Morgan, P.B., Naidu, S.L., Yoo Ra, H-S., Zhu, X-G., Peters, C., Long, S.P. (2002) A meta-analysis of elevated [CO_2] effects on soybean (Glycine max) physiology, growth and yield. Glob. Change Biol., 8: 695-709.

Ainsworth, E.A. and Long, S.P. (2005) What have we learned from 15 years of free-air CO_2 enrichment (FACE)? A meta-analytic review of the responses of photosynthesis, canopy properties and plant production to rising CO_2. New Phytol., 165: 351-371.

Akbar, M., Khush, G.S., and Hillerislambers, D. (1986) Genetics of salt tolerance in rice, in: Rice Genetics, International Rice Research Institute, Manila, Philippines, pp. 399-409.

Allen, D.J. and Ort, D.R. (2001) Impacts of chilling temperatures on photosynthesis in warm-climate plants. Trends Plant Sci., 6: 36-42.

Alonso, J.M. and Granell, A**.** (1995) A putative vacuolar processing protease is regulated by ethylene and also during fruit ripening in *citrus* fruit. Plant Physiol., 109: 541-547.

Altpeter, F.; Diaz, I.; McAuslane, H.; Gaddour, K.; Carbonero, P. and Vasil, I.K. (1999). Increased insect resistance in transgenic wheat stably expressing trypsin inhibitor CMe. Mol. Breeding, 5:53-63.

Altschul, S.F., Gish, W., Miller, W., Myers, E.W., Lipman, D.J. (1990) Basic local alignment search tool. J. Mol. Biol., 215: 403-410

Amme, S., Rutten, T., Melzer, M., Sonsmann, G., Vissers, J.P.C., Schlesier, B., Mock, H-P. (2005) A proteome approach defines protective functions of tobacco leaf trichomes. Proteomics, 5: 2508-2518.

Anderson, L.J., Maherali, H., Johnson, H.B., Polley, H.W., Jackson, R.B. (2001) Gas exchange and photosynthetic acclimation over sub-ambient to elevated CO_2 in a C_3–C_4 grassland. Glob. Change Biol., 7: 693–707.

Antão, C.M. and Malcata, F.X. (2005) Plant serine proteases: biochemical, physiological and molecular features. Plant Physiol. Bioch., 43: 637-650.

Aono, M., Saji, H., Sakamoto, A., Tanaka, K., Kondo, N., Tanaka, K. (1995) Paraquat tolerance of transgenic *Nicotiana tabacum* with enhanced activities of glutathione reductase and superoxide dismutase. Plant Cell Physiol., 36: 1687-1691.

Arai, S., Abe, K. (2000) Cystatin-based control of insects with special reference to the efficacy of oryzacystatin. In *Recombinant Protease Inhibitors in Plants*; Michaud, D., Ed.; Landes: Georgetown, TX; pp. 27-42.

Aravind, L. and Koonin, E.V. (2002) Classification of the caspase-hemoglobinase fold: detection of new families and implications for the origin of the eukaryotic separins. Proteins, 46: 355-367.

Arena, C., Vitale, L., Virzo de Santo, A. (2005) Photosynthetic response of *Quercus ilex* L. plants grown on compost and exposed to increasing photon flux densities and elevated CO_2. Photosynthetica, 43: 615-619.

Babu, R.M., Sajeena, A., Seetharaman, K., and Reddy, M.S. (2003) Advances in genetically engingeered (transgenic) plants in pest management – an over view. Crop Prot., 22: 1071-1086.

Baena-González, E., Rolland, F., Thevelein, J.M., Sheen, J. (2007) A central integrator of transcription networks in plant stress and energy signalling. Nature, 448: 938-943.

Baginsky, S., Siddique, A., Gruissem, W. (2004) Proteome analysis of tobacco bright yellow-2 (BY-2) cell culture plastids as a model for undifferentiated heterotrophic plastids. J. Proteome Res., 3: 1128 – 1137.

Barrett, A.J. (1980) Fluorimetric assays for cathepsin B and cathepsin H with methylcoumarylamide substrates. Biochem. J., 187: 909-912.

Barret, A.J., Rawlings, N.D., Cavies, M.E. Machleidt, W., Salvesen, G. and Turk, V. (1986). Cysteine protease inhibitors of the cystatin super family. In: Protease inhibitors (Barrett, A.J. and Salvesen, G., eds.) pp. 515-569. Elsevier. Amsterdam

Barta, E., Pintar, A., Pongor, S. (2002) Repeats with variations: accelerated evolution of the *Pin2* family of proteinase inhibitors. Trends Genet., 18: 600-603.

Basset, G., Raymond, P., Malek, L. and Brouquisse, R. (2002) Changes in the expression and the enzymatic properties of the 20S proteosome in sugar-starved maize roots. Evidence for an in vivo oxidation of the proteosome. Plant Physiol., 128: 1149-1162.

Bazzaz, F.A. (1990) The response of natural ecosystems to the rising global CO_2 levels. Annu. Rev. Ecol. Syst., 21: 167-196.

Beers, E.P., Woffenden, B.J., Zhao, C. (2000) Plant proteolytic enzymes: possible roles during programmed cell death. Plant Mol. Biol., 44: 399-415.

Belenghi, B., Acconcia, F., Trovato, M., Perazzolli, M., Bocedi, A., Polticelli, F., Ascenzi, P., and Delledonne, M. (2003) AtCYS1, a cystatin from *Arabidopsis thaliana*, suppresses hypersensitive cell death. Eur. J. Biochem., 270: 2593-2604.

Belenghi, B., Romero-Puertas, M.C., Vercammen, D., Brackenier, A, Inzé, D., Delledonne, M., Van Breusegem, F. (2007) Metacaspase activity of Arabidopsis thaliana is regulated by S-nitrosylation of a critical cysteine residue. J. Biol. Chem., 282: 1352-1358.

Benchekroun, A., Michaud, D., Nguyen-Quoc, B., Overney, S., Desjardins, Y., Yelle, S. (1995) Synthesis of active oryzacystatin I in transgenic potato plants. Plant Cell Rep., 14: 585-588.

Benson, A.A. and Calvin, M. (1950) Carbon dioxide fixation by green plants. Ann. Rev. Plant Physio., 1: 25–40.

Berger, D. and Altmann, T. (2000). A subtilisin-like serine protease involved in the regulation of stomatal density and distribution in *Arabidopsis thaliana*. Gene Dev., 14: 1119-1131.

Besford, R.T. (1990) The Greenhouse Effect: Acclimation of tomato plants growing in high CO_2, relative changes in Calvin cycle enzymes. Journal of Plant Physiol., 136: 458-463.

Beyene, G., Foyer, C.H. and Kunert, K.J. (2006) Two new cysteine proteases with specific expression patterns in mature and senescent tobacco (Nicotina tabacum L.) leaves. J. Exp. Bot., 57: 1431-1443.

Bhalerao, R., Keskitalo, J., Sterky, F., Erlandsson, R., Bjorkbacka, H., Birve, S.J., Karlsson, J., Gardestrom, P., Gustafsson, P., Lundeberg, J. and Jansson, S. (2003) Gene expression in Autumn leaves. Plant Physiol., 131: 430-442.

Bindi, M., Hacour, A., Vandermeiren, K., Craigon, J., Ojanperä, K., Selldén, G., Högy,P., Finnan, J., Fibbi, L. (2002) Chlorophyll concentration of potatoes grown under elevated carbon dioxide and/or ozone concentrations. Eur. J. Agron., 17: 319-335.

Bleecker, A.B. and Patterson, S.E. (1997) Last exit: senescence, abscission, and meristem arrest in Arabidopsis. Plant Cell, 7: 1169-1179.

Boese, S.R., Wolfe, D.W., Melkonian, J.J. (1997) Elevated CO_2 mitigates chilling-induced water stress and photosynthetic reduction during chilling. Plant Cell Environ., 20, 625–632.

Boetsch, J., Chin, J., Ling, M., Croxdale, J. (1996) Elevated carbon dioxide affects the patterning of subsidiary cells in *Tradescantia* stomatal complexes. J. Exp. Bot., 47: 925-931.

Bolstad, B.M., Irizarry, R.A., Astrand, M., Speed, T.P. (2003) A comparison of normalization methods for high density oligonucleotide array data based on bias and variance. Bioinformatics, 19: 185-193.

Bolter, C.J. (1993) Methyl jasmonate induces papain inhibitor(s) in tomato leaves. Plant Physiol., 103: 1347–1353.

Botella, M. A., Xu, Y., Prabha, T.N., Zhao, Y., Narasimhan, M.L., Wilson, K.A., Nielsen, S.S., Bressan, R.A., Hasegawa, P.M. (1996) Differential expression of soybean cysteine protease inhibitor genes during development and in response to wounding and methyl jasmonate. Plant Physiol., 112: 1201-1210.

Boulter, D (1993) Insect pest control by copying nature using genetically engineered crops. Biochemistry 34: 1453-1466.

Bowes, G. (1991) Growth at elevated CO_2: photosynthetic responses mediated through rubisco. Plant Cell Environ., 14: 795-806.

Bowes, G. (1993) Facing the inevitable: plants and increasing atmospheric CO_2. Ann. Rev. Plant Physio. and Plant Mol. Biol., 44: 309-332.

Bowler, C. and Fluhr, R. (2000) The role of calcium and activated oxygens as signals for controlling cross-tolerance. Trends Plant Sci., 5: 241-246.

Bozhkov, P.V., Suarez, M.F., Filonova, L.H., Daniel, G., Zamyatnin, A.A., Jr., Rodriguez-Nieto, S., Zhivotovsky, B., Smertenko, A. (2005) Cysteine protease mcII-Pa executes programmed cell death during plant embryogenesis. Proc. Natl. Acad. Sci. U. S. A,. 102: 14463-14468.

Bradford, M.M. (1976) A rapid and sensitive method for the quantitation of microgram quantities of protein utilizing the principle of protein dye-binding. Anal. Biochem., 72: 248–254.

Budai-Hadrian, O., Davydov, O., Wasternack, C., Fluhr, R. (2006) SAS1 Serpin is at a node of cross-talk between jasmonic and salicylic acid pathways in Arabidopsis. Israel J. Plant Sci., 54: 55 – 86.

Bushnell, T.P., Bushnell, D., Jagendorf, A.T. (1993) A purified zinc protease of pea chloroplast, EP1, degrades the large subunit of ribulose -1,5-bisphosphate carboxylase/oxygenase. Plant Physiol., 103: 585-591.

Callis**,** J. (1995) Regulation of protein degradation. Plant Cell, 7: 845–857.

Callis, J. and Vierstra, R.D. (2000) Protein degradation in signalling. Curr. Opin. Plant Biol., 3: 381-386.

Campbell, W.J., Allen, L.H., Bowes, G. (1988) Effects of CO_2 concentration on rubisco activity, amount, and photosynthesis in soybean leaves. Plant Physiol., 88: 1310-1316.

Carlson, R.W. and Bazzaz, F.A. (1981) Photosynthetic and growth response to fumigation with SO_2 at elevated CO_2 for C_3 and C_4 plants. Oecologia, 54: 50-54.

Cercos, M., Urbez, C., Carbonell, J. (2003) A serine carboxypeptidase gene (PsCP), expressed in early steps of reproductive and vegetative development in Pisum sativum, is induced by gibberellins. Plant Mol. Biol., 51: 165-174.

Chan, P.H. and Wildman, S.G. (1972) Chloroplast DNA codes for the primary structure of the large subunit of fraction I protein. Biochim. Biophys. Acta, 277: 677-680.

Chaves, M.M. and Pereira, J.M. (1992) Water stress, $C0_2$ and climate change. J. Exp. Bot., 43: 1131-1139.

Chen, T.H.H. and Murata, N. (2002) Enhancement of tolerance of abiotic stress by metabolic engineering of betaines and other compatible solutes. Curr. Opin. Plant Biol., 5: 250-257.

Cheng, S-H., Moore, B.D., Seemann, J.R. (1998) Effects of short- and long-term treatments at elevated CO_2 on the expression of Rubisco genes and leaf carbohydrate accumulation in *Arabidopsis thaliana* (L.) Henyh. Plant Physiol., 116: 715-723.

Chenna, R., Sugawara, H., Koike, T., Lopez, R., Gibson, T.J., Higgins, D.G., Thompson, J.D. (2003) Multiple sequence alignment with the Clustal series of programs. Nucleic Acids Res., 31: 3497-3500.

Cheong, Y.H., Chang, H.-S., Gupta, R., Wang, X., Zhu, T., Luan, S. (2002) Transcriptional profiling reveals novel interactions between wounding, pathogen, abiotic stress, and hormonal responses in Arabidopsis. Plant Physiol., 129: 1-17.

Chiang, C.-H., Wang, J.J., Jan, F.-J., Yeh, S.-D., and Gonsalves, D. (2001) Comparative reactions of recombinant papaya ringspot viruses with chimeric coat protein (CP) genes and wild-type viruses on CP-transgenic papaya. J. Gen. Virol., 82: 2827-2836.

Chiba, A., Ishida, H., Nishizawa, N.K., Makino, A., Mae, T. (2003) Exclusion of ribulose-1,5-bisphosphate carboxylase/oxygenase from chloroplasts by specific bodies in naturally senescing leaves of wheat. Plant Cell Physiol., 44: 914–921.

Chinnusamy, V., Schumaker, K., Zhu, J.-K. (2004) Molecular genetic perspectives on cross-talk and specificity in abiotic stress signalling in plants. J. Exp. Bot., 55: 225-236.

Chrispeels, M.J. and Herman, E.M. (2000) Endoplasmic reticulum-derived compartments function in storage and as mediators of vacuolar remodelling via a new type of organelle, precursor protease vesicles. Plant Physiol., 123: 1227-1233.

Christou, P., Capell, T., Kohli, A., Gatehouse, J.A., Gatehouse, A.M.R. (2006) Recent developments and future prospects in insect pest control in transgenic crops. Trends Plant Sci., 11: 302-308.

Clemente, T.E., LaVallee, B.J., Howe, A.R., Conner-Ward, D., Rozman, R.J., Hunter, P.E., Broyles, D.L., Kasten, D.S., Hinchee, M.A. (2000) Progeny analysis of glyphosate selected transgenic soybeans derived from *Agrobacterium*-mediated transformation. Crop Sci., 40: 797-803.

Colfalonieri, M., Allegro, G., Balestrazzi, A., Fogher, C., and Delledonne, M. (1998) Regeneration of *Populus nigra* transgenic plants expressing a Kunitz protease inhibitor (Kti3) gene. Mol. Breed., 4: 137-145.

Conley, M.M., Kimball, B.A., Brooks, T.J., Pinter, Jr., P.J., Hunsaker, D.J., Wall, G.W., Adam, N.R., LaMorte, R.L., Matthias, A.D., Thompson, T.L., Leavitt, S.W., Ottman, M.J., Cousins, A.B., Triggs, J.M. (2001). CO_2 enrichment increases water-use efficiency in sorghum. New Phytol., 151, 407-412.

Cooper, B., Eckert, D., Andon, N.L., Yates, J.R., Haynes, P.A. (2003) Investigative proteomics: identification of an unknown plant virus from infected plants using mass spectrometry. J. Am. Soc .Mass Spectrom., 14: 736–741.

Coupe, S.A., Palmer, B.G., Lake, J.A., Overy, S.A., Oxborough, K., Woodward, F.I., Gray, J.E., Quick, W.P. (2006) Systemic signalling of environmental cues in *Arabidopsis* leaves. J. Exp. Bot., 57: 329-341.

Cousins, A.B., Adam, N.R., Wall, G.W., Kimball, B.A., Pinter, Jr., P.J., Leavitt, S.W., LaMorte, R.L., Matthias, A.D., Ottman, M.J., Thompson, T.L., Webber, A.N. (2001) Reduced photorespiration and increased energy-use efficiency in young CO2-enriched sorghum leaves. New Phytol., 150: 275-284.

Crafts-Brandner, S.J. and Salvucci, M.E. (2000) Rubisco activase constrains the photosynthetic potential of leaves at high temperature and CO_2. P. Natl. Acad. Sci. USA, 97: 13430-13435.

Croxdale, J. (1998) Stomatal patterning in monocotyledons: *Tradescantia* as a model system. J. Exp. Bot., 49: 279–292.

Dal Degan, F., Rocher, A., Cameron-Mills, V., Von Wettstein, D. (1994) The expression of serine carboxypeptidases during maturation and germination of the barley grain. P. Natl. Acad. Sci. USA, 91: 8209–8213.

Dani, V., Simon, W.J., Duranti, M., Croy, R.R.D. (2005) Changes in the tobacco leaf apoplast proteome in response to salt stress. Proteomics, 5: 737-745.

Dean, C., Dunsmuir, P., Bedbrook, J. (1989) Structure, evolution, and regulation of *rbcS* genes in higher plants. Ann. Rev. Plant Phys., 40: 415-439.

De Block, M., Verduyn, C., De Brouwer, D., Cornelissen, M. (2005) Poly(ADP-ribose) polymerase in plants affects energy homeostasis, cell death and stress tolerance. Plant J., 41: 95-106.

De Las Rivas, J., Andersson, B., Barber, J. (1992) Two sites of primary degradation of the D1-protein induced by acceptor or donor side photo-inhibition in photosystem II core complexes. FEBS Lett., 301: 246-52.

De Leo, F., Bonadé-Bottino, M., Ceci, L.R., Gallerani, R., Jouanin, L. (2001) Effects of a mustard trypsin inhibitor expressed in different plants on three lepidopteran pests. Insect Biochem. Molec., 31: 593-602.

Del Pozo, O. and Lam, E. (1998) Caspases and programmed cell death in the hypersensitive response of plants to pathogens. Curr. Biol., 8: 1129–1132.

Deng, X. and Woodward, F.I. (1998) The growth and yield responses of *Fragaria ananassa* to elevated CO_2 and N supply. Ann Bot – London, 81: 67-71.

Desimone, M., Henke, A., Wagner, E. (1996) Oxidative stress induces partial degradation of the large subunit of ribulose 1,5- bisphosphate carboxylase/oxygenase in isolated chloroplasts of barley. Plant Physiol., 111: 789-796

Diop, N.N., Kidric, M., Repellin, A., Gareil, M., d'Arcy-Lameta, A., Pham Thi, A.T. and Zuily-Fodil, Y. (2004) A multicystatin is induced by drought-stress in cowpea (*Vigna unguiculata* (L.) Walp.) leaves. FEBS Lett., 577: 545-550.

Domínguez, F. and Cejudo, F.J. (1998) Germination-related genes encoding proteolytic enzymes are expressed in the nucellus of developing wheat grains. Plant J., 15: 569-574.

Domínguez, F., González, M., Cejudo, F.J. (2002) A germination-related gene encoding a serine carboxypeptidase is expressed during the differentiation of the vascular tissue in wheat grains and seedlings. Planta, 215: 727-734.

Drake, B.G., Gonzalez-Meler, M.A., Long, S.P. (1997) More efficient plants: A consequence of rising atmospheric CO_2? Ann. Rev. Plant Phys., 48, 609-639.

Driscoll, S.P., Prins, A., Olmos, E., Kunert, K.J., Foyer, C.H. (2006). Specification of adaxial and abaxial stomata, epidermal structure and photosynthesis to CO_2 enrichment in maize leaves. J. Exp. Bot., 57: 381-390.

Dreher, K. and Callis, J. (2007) Ubiquitin, hormones and biotic stress in plants. Ann. Bot.-London, 99: 787-822.

Duan, X.L., Li, X.G., Xue, Q.Z., Aboelsaad, M., Xu, D.P., and Wu, R. (1996) Transgenic rice plants harboring an introduced potato protease inhibitor II gene are insect resistant. Nat. Biotechnol., 14: 494-498.

Eason, J.R., Ryan, D.J., Pinkney, T.T., and O'Donoghue, E.M. (2002) Programmed cell death during flower senescence: isolation and characterization of cysteine proteases from *Sandersonia aurantiaca*. Funct. Plant Biol., 29: 1055–1064.

Edmonds, H.S., Gatehouse, L.N., Hilder, V.A., Gatehouse, J.A. (1996) The inhibitory effects of the cysteine protein protease inhibitor, oryzacystatin, on digestive proteases and on larval survival and development of the southern corn rootworm (*Diabrotica undecimpunctata howardi*). Entomol. Exp. Appl., 78: 83-94.

Edwards, G. and Walker, D. (1983) C_3, C_4: mechanisms, and cellular and environmental regulation of photosynthesis. Blackwell Science Publishers, London, UK.

Elbaz, M., Avni, A., Weil, M. (2002) Constitutive caspase-like machinery executes programmed cell death in plant cells. Cell Death Differ., 9: 726-733.

Ellis, R.J. (1981). Chloroplast proteins: synthesis, transport and assembly. Ann. Rev. Plant Physio. 32, 111-137.

Emanuelsson, O., Nielsen, H., Brunak, R., Von Heijne, G. (2000) Predicting subcellular localization of proteins based on their N-terminal amino acid sequence. J. Mol. Biol., 300: 1005-1016.

Fan, S-G. and Wu, G-J. (2005) Characteristics of plant protease inhibitors and their applications in combating phytophagous insects. Bot. Bull. Acad. Sinica, 46: 273-292.

Farrar, J.F. and Williams, M.L. (1991) The effects of increased atmospheric carbon-dioxide and temperature on carbon partitioning, source-sink relations and respiration. Plant Cell Environ., 14: 819-830.

Feller, U. Anders, I., Mae, T. (2007) Rubiscolytics: fate of Rubisco after its enzymatic function in a cell is terminated. J. Exp. Bot., doi:10.1093/jxb/erm242

Ferris, R., Long, L., Bunn, S.M., Robinson, K.M., Bradshaw, H.D., Rae, A.M., Taylor, G. (2002) Leaf stomatal and epidermal cell development: Identification of putative quantitative trait loci in relation to elevated carbon dioxide concentration in poplar. Tree Physiol., 22: 633–640.

Ferry, N., Edwards, M.G., Gatehouse, J.A., Gatehouse, A.M.R. (2004) Plant-insect interactions: molecular approaches to insect resistance. Curr. Opin. Biotech., 15: 155-161.

Finkelstein, R.R. and Gibson, S.I. (2002) ABA and sugar interactions regulating development: cross–talk or voices in a crowd? Curr. Opin. Plant Biol., 5: 26–32.

Finkelstein, R.R. and Lynch, T.J. (2000) Abscisic acid inhibition of radicle emergence but not seedling growth is suppressed by sugars. Plant Physiol., 122: 1179–1186.

Fisher, A. and Feller, U. (1994) Senescence and protein degradation in leaf segments of young winter wheat: influence of leaf age. J. Exp. Bot., 45: 103-109.

Fischhoff, D.A., Bowdish, K.S., Perlak, F.J., Marrone, P.G., McCormick, S.H., Niedermeyer, J.G., Dean, D.A., Kusano-Kretzmer, K., Mayer, E.J., Rochester, D.E., Rogers, S.G., Fraley, R.T. (1987) Insect tolerant transgenic tomato plants. Bio/Technol., 5: 807–813.

Flowers, T.J., and Yeo, A.R. (1995) Breeding for salinity resistance in crop plants: where next? Aust. J. Plant Physiol., 22: 875-884.

Flowers, T.J. (2004) Improving crop salt tolerance. J. Exp. Bot., 55: 307-319.

Foyer, C.H. and Noctor, G. (2003) Redox sensing and signaling associated with reactive oxygen in chloroplasts, peroxisomes and mitochondria. Physiol. Plantarum, 119: 355–364.

Foyer, C.H. and Noctor, G. (2007) Shape-shifters building bridges? Stromules, matrixules and metabolite channelling in photorespiration. Trends Plant Sci., 12: 381-383.

Franceschetti, M., Perry, B., Thompson, B., Hanfrey, C., Michael, A.J. (2004) Expression proteomics identifies biochemical adaptations and defense responses in transgenic plants with perturbed polyamine metabolism. FEBS Lett, 576: 477-480.

Frugis, G. and Chua, N.-H. (2002) Ubiquitin-mediated proteolysis in plant hormone signal transduction. Trends Cell Biol., 12: 308-311.

Fuentes-Prior, P. and Salvesen, G.S. (2004) The protein structures that shape caspase activity, specificity, activation and inhibition. Biochem. J., 384: 201–232.

Fujita, M., Fujita, Y., Noutoshi, Y., Takahashi, F., Narusaka, Y., Yamaguchi-Shinozaki, K., Shinozaki, K. (2006) Crosstalk between abiotic and biotic stress responses: a current view from the points of convergence in the stress signaling networks. Curr. Opin. Plant Biol., 9: 436-442.

Furbank, R.T. and Taylor, W.C. (1995) Regulation of photosynthesis in C3 and C4 Plants: A molecular approach. Plant Cell, 7: 797-807.

Gaddour K, Vicente-Carbajosa J, Lara P, Isabel-Lamoneda I, Díaz I, Carbonero P. (2001) A constitutive cystatin-encoding gene from barley (*Icy*) responds differentially to abiotic stimuli. Plant Mol. Biol., 45: 599–608.

Garcia-Ferris, C. and Moreno, J. (1994) Oxidative modification and breakdown of ribulose-1,5-bisphosphate carboxylase oxygenase induced in *Euglena gracilis* by nitrogen starvation. Planta, 193: 208-215.

Gasteiger, E., Hoogland, C., Gattiker, A., Duvaud, S., Wilkins,M.R., Appel, R.D., Bairoch, A. (2005) In: The Proteomics Protocols Handbook (Walker, J.M., ed) pp. 571-607. Humana Press.

Gepstein, S., Sabehi, G., Carp, M.-J., Hajouj, T., Nesher, M.F.O., Yariv, I., Dor, C., Bassani, M. (2003) Large-scale identification of leaf senescence-associated genes. Plant J., 36: 629–642.

Gesch, R.W., Boote, K.J., Vu, J.C.V., Allen, H. Jr., Bowes, G. (1998) Changes in growth CO_2 result in rapid adjustments of ribulose-1,5-bisphosphate carboxylase/oxygenase small subunit gene expression in expanding and mature leaves of rice. Plant Physiol., 118: 521-529.

Ghannoum, O., Von Caemmerer, S., Barlow, E.W.R., Conroy, J.P. (1997) The effect of CO_2 enrichment and irradiance on the growth, morphology and gas-exchange of a C_3 (*Panicum laxum*) and a C_4 (*Panicum antidotale*) grass. Aust. J. Plant Physiol., **24**: 227–237.

Ghannoum, O., Von Caemmerer, S., Conroy, J.P. (2001) Plant water use efficiency of 17 Australian NAD-ME and NADP-ME C_4 grasses at ambient and elevated CO_2 partial pressure. Austr. J. Plant Physiol., 28: 1207–1217.

Gietl, C. and Schmid, M. (2001) Ricinosomes: an organelle for developmentally regulated programmed cell death in senescing plant tissues. Naturwissenschaften, 88: 49-58.

Gish, W. and States, D. J. (1993). Identification of protein coding regions by database similarity search. Nat. Genet., 3: 266-72.

Giri, A.P., Wünsche, H., Mitra, S., Zavala, J.A., Muck, A., Svatoš, A., Baldwin, I.T. (2006) Molecular interactions between the specialist herbivore *Manduca sexta* (Lepidoptera, Sphingidae) and its natural host, *Nicotiana attenuata*. VII. Changes in the plant's proteome. Plant Physiol., 142: 1621-1641.

Glickman, M.H. (2000) Getting in and out of the proteasome. Semin. Cell Dev. Biol., 11: 149-158.

Gong, Z., Lee, H., Xiong, L., Jagendorf, A., Stevenson, B., Zhu, J.-K. (2002) RNA helicase-like protein as an early regulator of transcription factors for plant chilling and freezing tolerance. P. Natl. Acad. Sci. USA, 99: 11507-11512.

Granat, S.J., Wilson, K.A., Tan-Wilson, A.L. (2003) New serine carboxypeptidases in mung bean seedling cotyledons. J. Exp. Bot., 160: 1263–1266.

Granell A, Cercos M, Carbonell J**.** (1998) Plant cysteine proteases in germination and senescence. In: *The Handbook of Proteolytic Enzymes* (Barrett, A.J., Rawlings, N.D. and Woessner, J.F., eds), pp. 578-583. San Diego: Academic Press.

Gray, J.E., Holroyd, G.H., Van Der Lee, F.M., Bahrami, A.R., Sijmons, P.C., Woodward, F.I., Schuch, W., Hetherington, A.M. (2000) The HIC signalling pathway links CO_2 perception to stomatal development. Nature, 408: 713-716.

Grbić, V. (2003) SAG2 and SAG12 protein expression in senescing *Arabidopsis* plants. Physiol. Plantarum**,** 119**:**263–269.

Greer, D.H., Laing, W.A., Campbell, B.D. (1995) Photosynthetic responses of thirteen pasture species to elevated CO_2 and temperature. Aust. J. Plant Physiol., 22: 713–722.

Griffin, K.L. and Seemann, J.R. (1996) Plants, CO_2 and photosynthesis in the 21st century. Chem. Biol., 3: 245-254.

Grime, J.P. (1989) Whole-plant responses to stress in natural and agricultural systems. In: H. Jones, T.J. Flowers, M.B. Jones (Eds.), Plants Under Stress, Cambridge University Press, Cambridge. Pp. 31-46.

Grover, A., Sahi, C., Sanan, N., and Grover, A. (1999) Taming abiotic stresses in plants through genetic engineering: current strategies and perspective. Plant Sci., 143: 101-111.

Grover, A., Agarwal, M., Katiyar-Agarwal, S., Sahi, C., Agarwal, S. (2000) Production of high temperature tolerant transgenic plants through manipulation of membrane lipids. Curr. Sci. India, 79: 557-559.

Grover, A., Aggarwal, P.K., Kapoor, A., Katiyar-Agarwal, S., Agarwal, M., Chandramouli, A. (2003) Addressing abiotic stresses in agriculture through transgenic technology. Curr. Sci. India, 84: 355-367.

Gruis, D.F., Selinger, D.A., Curran, J.M., Jung, R. (2002) Redundant proteolytic mechanisms process seed storage proteins in the absence of seed-type members of the vacuolar processing enzyme family of cysteine proteases. Plant Cell, Vol. 14, 2863-2882.

Gunning, B.E.S. (2005) Plastid stromules: video microscopy of their outgrowth, retraction, tensioning, anchoring, branching, bridging, and tip-shedding. Protoplasma, 225: 33-42.

Gutiérrez-Campos, R., Torres-Acosta, J.A., Pérez-Martínez, J.D.J. and Gómez-Lim, M.A. (2001) Pleiotropic effects in transgenic tobacco plants expressing oryzacystatin I gene. HortScience, 36: 118–119.

Guy, C.L., Huber, J.L.A., Huber, S.C. (1992). Sucrose phosphate synthase and sucrose accumulation at low temperature. Plant Physiol., 100: 502-508.

Hara-Nishimura, I., Inoue, K., Nishimura**,** M. (1991) A unique vacuolar processing enzyme responsible for conversion of several proprotein precursors into the mature forms. FEBS Lett., 294: 89-93.

Hara-Nishimura, I., Takeuchi, Y., Nishimura, M. (1993) Molecular characterization of a vacuolar processing enzyme related to a putative cysteine protease of *Schistosoma mansoni*. Plant Cell, 5: 1651-1659.

Hara-Nishimura, I., Kinoshita, T., Hiraiwa, N., Nishimura, M. (1998) Vacuolar processing enzymes in protein-storage vacuoles and lytic vacuoles. J. Plant Physiol., 152: 668-674.

Harrak, H., Azelmat, S., Baker, E.N. and Tabaeizadeh, Z**.** (2001) Isolation and characterization of gene encoding a drought-induced cysteine protease in tomato (*Lycopersicon esculentum*). Genome, 44: 368-374.

Hatch, M.D. (1992) C_4 Photosynthesis: An unlikely process full of surprises. Plant Cell Physiol., 33: 333-342.

Hayashi, H., Alia Mustardy, L., Deshnium, P., Ida, M., Murata, N. (1997) Transformation of *Arabidopsis thaliana* with the codA gene for choline oxidase: accumulation of glycinebetaine and enhanced tolerance to salt and cold stress. Plant J., 12: 133-142.

Hayashi, Y., Yamada, K., Shimada, T., Matsushima, R., Nishizawa, N.K., Nishimura, M., Hara-Nishimura, I. (2001). A protease-storing body that prepares for cell death or stresses in the epidermal cells of Arabidopsis. Plant Cell Physiol., 42: 894-899.

Heagle, A.S., Miller, J.E., Sherrill, D.E., Rawlings, J.O. (1993) Effects of ozone and carbon dioxide mixtures on two clones of white clover/ New Phytol., 123: 751-762.

Hellman, H. and Estelle, M. (2002) Plant development: regulation by protein degradation. Science, 297: 793–797.

Hensel, L.L., Grbic, V., Baumgarten, D.A., Bleecker, A.B. **(**1993) Developmental and age-related processes that influence the longevity and senescence of photosynthetic tissues in *Arabidoposis* Plant Cell, 5: 553-64.

Herman, E. and Schmidt, M. (2004) Endoplasmic reticulum to vacuole trafficking of endoplasmic reticulum bodies provides an alternative pathway for protein transfer to the vacuole. Plant Physiol., 136: 3440-3446.

Herrick, J.D. and Thomas, R.B. (2003) Leaf senescence and late-season net photosynthesis of sun and shade leaves of overstorysweetgum *(Liquidambar styraciflua*) grown in elevated and ambient carbon dioxide concentrations. Tree Physiol., 23: 109-118.

Hetherington, A.M. and Woodward, F.I. (2003) The role of stomata in sensing and driving environmental change. Nature, 424: 901-908.

Hilder, V.A., Gatehouse, A.M.R., Sheerman, S.E., Baker, R.F., and Boulter, D. (1987) A novel mechanism of insect resistance engineered into tobacco. Nature, 330: 160-163.

Hilder, V.A. and Boulter, D. (1999) Genetic engineering of crop plants for insect resistance – a critical review. Crop Prot., 18: 177-191.

Hiraiwa, N., Takeuchi, Y., Nishimura, M. and Hara-Nishimura, I. (1993) A vacuolar processing enzyme in maturing and germinating seed: its distribution and associated changes during development. Plant Cell Physiol., 34: 1197-1204.

Hochstrasser, M. (1995) Ubiquitin, proteasomes, and the regulation of intracellular protein degradation. Curr. Opin. Cell Biol., 7: 215–223.

Hoeberichts, F.A., Ten Have, A., Woltering, E.J. (2003) A tomato metacaspase gene is upregulated during programmed cell death in *Botrytis cinerea*-infected leaves. Planta, 217: 517-522.

Hopkins, M., Taylor, C., Liu, Z., Ma, F., McNamara, L., Wang, T.-W., Thompson, J.E. (2007) Regulation and execution of molecular disassembly and catabolism during senescence. New Phytol., 175: 201–214.

Horsch, R.B., Fry, J.E., Hoffman, N.L., Wallroth, M., Eichholtz, D., Rogers, S.G., and Frailey, R.T. (1985) A simple and general method for transferring genes into plants. Science, 227: 1229-1231.

Hörtensteiner, S. and Feller, U. (2002) Nitrogen metabolism and remobilization during senescence. J. Exp. Bot., 53: 927-937.

Hsiao, T.C. and Jackson, R.B. (1999) Interactive effects of water stress and elevated CO_2 on growth, photosynthesis, and water use efficiency. In: Luo, Y. and Mooney, H.A. (eds). Carbon Dioxide and Evironmental Stress. Academic Press. Pp. 3-26.

Huber, S.C. and Huber, J.L. (1992) Role of sucrose-phosphate synthase in sucrose metabolism in leaves. Plant Physiol., 4: 1275-1278.

Huber, S.C. and Huber, J.L. (1996) Role and regulation of sucrose-phosphate synthase in higher plants. Annu. Rev. Plant Phys., 47: 431-444.

Huffaker, R.C. (1990) Proteolytic activity during senescence of plants. New Phytol., 116: 199–231.

Humbeck, K., Quast, S. and Krupinska, K. (1996) Functional and molecular changes in the photosynthetic apparatus during senescence of flag leaves from field-grown barley plants. Plant Cell Environ., 19: 337–344.

Hymus, G.J., Baker, N.R., Long, S.P. (2001) Growth in elevated CO_2 can both increase and decrease photochemistry and photoinhibition of photosynthesis in a predictable manner. *dactylis glomerata* grown in two levels of nitrogen nutrition· Plant Physiol., 127: 1204–1211.

Iba, K. (2002) Acclimative response to temperature stress in higher plants: Approaches of gene engineering for temperature tolerance. Annu. Rev. Plant Biol., 53: 225-245.

Idso, S.B., Kimball, B.A., Pettit, G.R., Garner, L.C., Pettit, G.R., Backhaus, R.A. (2000) Effects of atmospheric CO_2 enrichment on the growth and development of *Hymenocallis littoralis* (Amaryllidaceae) and the concentrations of several antineoplastic and antiviral constituents of its bulbs. Am. J. Bot., 87: 769-773.

Inoue, K., Motozaki, A., Takeuchi, Y., Nishimura, M. and Hara-Nishimura, I. (1995) Molecular characterization of proteins in protein-body membrane that disappear most rapidly during transformation of protein bodies into vacuoles. Plant J., 7: 235-243.

Irie, K., Hosoyama, H., Akeuchi, T., Iwabuchi, K., Watanabe, H., Abe, M., Abe, K., Arai, S. (1996) Transgenic rice established to express corn cystatin exhibits strong inhibitory activity against insect gut proteases. Plant Mol. Biol., 30: 149-157.

Irving, L.J, and Robinson, D. (2006) A dynamic model of RuBisCO turnover in cereal leaves. New Phytol., 169: 493-504.

Ishida, H., Nishimori, Y., Sugisawa, M., Makino, A., Mae, T. (1997) The large subunit of ribulose-1,5-bisphosphate carboxylase/oxygen- ase is fragmented into 37-kDa and 16-kDa

polypeptides by active oxygen in the lysates of chloroplasts from primary leaves of wheat. Plant Cell Physiol., 38: 471-479.

Ishida, H., Shimizu, S., Makino, A., Mae, T. (1998) Light-dependent fragmentation of the large subunit of ribulose-1,5-bisphosphate carboxylase/oxygenase in chloroplasts isolated from wheat leaves. Planta, 204: 305-309.

Ishida, H., Yoshimoto, K., Reisen, D., Makino, A., Ohsumi, Y., Hanson, M., Mae, T. (2007) Visulaisation of RuBisCO-containing bodies derived from chloroplasts in living cells of Arabidopsis. Photosynthesis Res., 91:275-276.

Jablonski, L.M., Wang, X., Curtis, P.S. (2002) Plant reproduction under elevated CO_2 conditions: a meta-analysis of reports on 79 crop and wild species. New Phytol., 156: 9–26.

Jacob, J., Greitner, C., Drake, B.G. (1995) Acclimation of photosynthesis in relation to Rubisco and non-structural carbohydrate contents and in situ carboxylase activity in *Scirpus olneyi* grown at elevated CO_2 in the field. Plant Cell Environ., 18: 875-884.

Jain, R.K., and Selvaraj, G. (1997) Molecular genetic improvement of salt tolerance in plants. Biotechnol. Annu. Rev., 3: 245-267.

Jang, J.C. and Sheen, J. (1994) Sugar sensing in higher plants. Plant Cell, 6: 1665–79.

Janska, H. (2005) ATP-dependent proteases in plant mitochondria: what do we know about them today? Physiol. Plant, 123: 399–405.

Jiang, M. and Zhang, J. (2003) Cross-talk between calcium and reactive oxygen species originated from NADPH oxidase in abscisic acid-induced antioxidant defence in leaves of maize seedlings. Plant Cell Environ., 26: 929-939.

Johnson, R., and Ryan, C.A. (1990). Wound-inducible potato inhibitor II genes: Enhancement of expression by sucrose. Plant Mol. Biol., 14: 527-536.

Johansson, E., Olsson, O., Nystrom, T. (2004) Progression and specificity of protein oxidation in the life cycle of Arabidopsis thaliana. J. Biol. Chem., 279: 22204-22208.

Jones, A.M. and Dangl, J.L. (1996) Logjam at the Styx: programmed cell death in plants. Trends Plant Sci., 1: 114-119.

Jones, M.G.K., Outlaw, Jr. W.H., Lowry, O.H. (1977). Enzymic assay of 10^{-7} to 10^{-14} moles of sucrose in plant tissues. Plant Physiol., 60: 379-383.

Juarez, M.T., Twigg, R.W., Timmerman,s M.C.P. (2004) Specification of adaxial cell fate during maize leaf development. Development, 131: 4533–4544.

Kardailsky, I.V. and Brewin, N.J. (1996) Expression of cysteine protease genes in pea nodule development and senescence. Mol. Plant. Microbe Interact., 8: 689-695.

Kato, H. and Minamikawa, T. (1996) Identification and characterization of a rice cysteine endopeptidase that digests glutelin. Eur. J. Biochem., 239: 310-316.

Kavi Kishor, P.B., Hong, Z., Miao, G., Hu, C.A., and Verma, D.P.S. (1995) Overexpression of △-pirroline-5-carboxylate synthetase increases proline production and confers osmotolerance in transgenic plants. Plant Physiol 108: 1387-1394.

Keith, C.S., Hoang, D.O., Barrett, B.M., Feigelman, B., Nelson, M.C., Thai, H., and Baysdorfer, C. (1993) Partial sequence analysis of 130 randomly selected maize cDNA clones. Plant Physiol., 101:329-332.

Keys, A.J. and Parry, M.A.J. (1990) Ribulose bisphosphate carboxylase/oxygenase and carbonic anhydrase. Meth. Plant Biochem., 3: 1-15.

Khan, S., Andralojc, P.J., Lea, P.J. and Parry, M.A.J. (1999) 2-carboxy-D-arabinitol 1-phosphate protects ribulose 1,5-bisphosphate carboxylase/oxygenase against proteolytic breakdown. Eur. J. Biochem., 266: 840–847.

Khanna-Chopra, R., and Sinha, S.K. (1998) Prospects of success of biotechnological approaches for improving tolerance to drought stress in crop plants. Curr. Sci., 74: 25-34.

Kingston-Smith, A.H. and Foyer, C.H. (2000) Overexpression of Mn-superoxide dismutase in maize leaves leads to increased monodehydroascorbate reductase, dehydroascorbate reductase and glutathione reductase activities. J. Exp. Bot., 51: 1867-1877.

Kinoshita, T., Nishimura, M., Hara-Nishimura, I. (1995) Homologues of a vacuolar processing enzyme that are expressed in different organs in *Arabidopsis thaliana*. Plant Mol. Biol., 29: 81-89.

Kinoshita, T., Yamada, K., Hiraiwa, N., Kondo, M., Nishimura, M., Hara-Nishimura, I. (1999) Vacuolar processing enzyme is up-regulated in the lytic vacuoles of vegetative tissues during senescence and under various stressed conditions. Plant J., 19: 43-53.

Kloetzel, P. M. (2001) Antigen processing by the proteasome. Nat. Rev. Mol. Cell Biol., 2: 179-187.

Knight, H. and Knight, M.R. (2001) Abiotic stress signalling pathways: specificity and cross-talk. Trends Plant Sci., 6: 262-267.

Kobayashi, T., Kobayashi, E., Sato, S., Hotta, Y., Miyajima, N., Tanaka, A. and Tabata, S. (1994) Characterization of cDNAs induced in meiotic prophase in lily microsporocytes. DNA Res., 1: 15-26.

Koiwa, K., Shade, R.E., Zhu-Salzman, K., Subramanian, L., Murdock, L.L., Nielsen, S.S., Bressan, R.A., Hasegawa, P.M. (1998) Phage display selection can differentiate insecticidal activity of soybean cystatins. Plant J., 14: 371-379.

Koizumi, M., Yamaguchi-Shinozaki, K., Tsuji, H. and Shinozaki, K. (1993) Structure and expression of two genes that encode distinct drought-inducible cysteine proteases in *Arabidopsis thaliana.* Gene, 29: 175-182.

Kondo H, Abe K, Nishimura I, Watanabe H, Emori Y, Arai S. (1990) Two distinct cystatin species in rice seeds with different specificities against cysteine proteases. J. Biol. Chem., 265: 15832–15837.

Kondo, H., Abe, K., Emori, Y. and Arai, S. (1991) Gene organization of oryzacystatin-II, a new cystatin super family member of plant origin, is closely related to that of oryzacystatin-I but different from those of the animal cystatins. FEBS Lett. 278: 87-90.

Konno, K., Hirayama, C., Nakamura, M., Tateishi, K., Tamura, Y., Hattori, M., Kohno, K. (2004) Papain protects papaya trees from herbivorous insects: role of cysteine proteases in latex. Plant J., 37:370–378.

Kreps, J.A., Wu, Y., Chang, H.S., Zhu, T., Wang, X., Harper, J.F. (2002) Transcriptome changes for *Arabidopsis* in response to salt, osmotic, and cold stress. Plant Physiol., 130: 2129–2141.

Kruger, N.J. (1990) Carbohydrate synthesis and degradation. In *Plant Physiology, Biochemistry and Molecular Biology* (Dennis, D.T. and Turpin, D.M., eds), pp. 59–76. Longman, Harlow, UK.

Krüger, J., Thomas, C.M., Golstein, C., Dixon, M.S., Smoker, M., Tang, S., Mulder, L., Jones, J.D.G. (2002) A tomato cysteine protease required for *Cf*-2-dependent disease resistance and suppression of autonecrosis. Science, 296: 744–747.

Krupinska, K. (2006) Fate and Activities of Plastids During Leaf Senescence. In: Advances in Photosynthesis and Respiration. Wise, R.R. and Hoober, J.K. (eds), vol. 23: The Structure and Function of Plastids. Springer, Netherlands. Pp. 433-449.

Kuroda, M., Ishimoto, M., Suzuki, K., Kondo, H., Abe, K., Kitamura, K., Arai, S. (1996) Oryzacystatins exhibit growth-inhibitory and lethal effects on different species of bean insect pests, *Callosobruchus chinensis* (Coleoptera) and *Riptortus clavatus* (Hemiptera). Biosci. Biotech. Bioch., 60: 209-212.

Kuroda M, Kiyosaki T, Matsumoto I, Misaka T, Arai S, Abe K. (2001) Molecular cloning, characterization, and expression of wheat cystatins. Biosci. Biotech. Bioch., 65: 22–28.

Lai, L.B., Nadeau, J.A., Lucas, J., Lee, E.-K., Nakagawa, T., Zhao, L., Geisler, M., Sack, F.D. (2005) The Arabidopsis R2R3 MYB proteins FOURLIPS andMYB88 restrict divisions late in the stomatal cell lineage. Plant Cell, 17: 2754–2767.

Lake, J.A., Quick, W.P., Beerling, D.J., Woodward, F.I. (2001) Plant development-signals from mature to new leaves. Nature, 411: 154-154.

Lake, J.A., Woodward, F.I., Quick, W.P. (2002) Long distance CO_2 signalling in plants. J. Exp. Bot., 53: 183-193.

Langridge, P., Paltridge, N., Fincher, G. (2006) Functional genomics of abiotic stress tolerance in cereals. Brief. Funct. Genomic. Proteomic., 4: 343-354.

Larkin, J.C., Marks, M.D., Nadeau, J., Sack, F. (1997) Epidermal cell fate and patterning in leaves. Plant Cell, 9: 1109–1120.

Laukens, K., Deckers, P., Esmans, E., Van Onckelen, H., Witters, E. (2004) Construction of a two-dimensional gel electrophoresis protein database for the Nicotiana tabacum cv. Bright Yellow-2 cell suspension culture. Proteomics, 4: 720-727.

Lawson, T., Craigon, J., Tulloch, A-M., Black, C.R., Colls, J.J., Landon, G. (2001) Photosynthetic responses to elevated CO_2 and O_3 in field-grown potato (*Solanum tuberosum*). J. Plant Physiol., 158**,** 309–323.

Leakey, A.D.B., Bernacchi, C.J., Dohleman, F.G., Ort, D.R., Long, S.P. (2004) Will photosynthesis of maize (Zea mays) in the US Corn Belt increase in future [CO_2] rich atmospheres? An analysis of diurnal courses of CO_2 uptake under free-air concentration enrichment (FACE). Glob. Change Biol., 10: 951–962.

Leakey, A.D.B., Uribelarrea, M., Ainsworth, E.A., Naidu, S.L., Rogers, A., Ort, D.R., Long, S.P. (2006) Photosynthesis, productivity, and yield of maize are not affected by

open-air elevation of CO2 concentration in the absence of drought. Plant Physiol., 140: 779-790.

Le Cain, D.R. and Morgan, J.A. (1998) Growth, gas exchange, leaf nitrogen and carbohydrate concentrations in NAD-ME and NADP-ME C_4 grasses grown in elevated CO_2. Physiol. Plantarum, 102: 297–306.

Lee, J.S. and Ellis, B.E. (2007) *Arabidopsis* MAPK Phosphatase 2 (MKP2) positively regulates oxidative stress tolerance and inactivates the MPK3 and MPK6 MAPKs. J. Biol. Chem., 282: 25020-25029.

León, P. and Sheen, J. (2003) Sugar and hormone connections. Trends Plant Sci., 8: 110-116.

Leple, J.C., Bonadebottino, M., Augustin, S., Pilate, G., Letan, V.D. Delplanque, A. Cornu D., Jouanin, L. (1995) Toxicity to *Chrysomela tremulae* (Coleoptera, Chrysomelidae) of transgenic poplars expressing a cysteine protease inhibitor, Mol. Breeding, 1: 319–328.

Lewis, C.E., Noctor, G., Causton, D., Foyer, C.H. (2000) Regulation of assimilate partitioning in leaves. Aust. J. Plant Physiol., 27: 507–517.

Lewis, C.E., Peratoner, G., Cairns, A.J., Causton, D.R., Foyer, C.H. (1999) Acclimation of the summer annual species, *Lolium temulentum*, toCO_2 enrichment. Planta, 210: 104–114.

Li, Z., Sommer, A., Dingermann, T., Noe, C.R. (1996) Molecular cloning and sequence analysis of a cDNA encoding a cysteine protease inhibitor from Sorghum bicolor seedlings. Mol. Gen. Genet., 251: 499–502.

Li, J., Lease, K.A., Tax, F.E., Walker, J.C. (2001) BRS1, a serine carboxypeptidase, regulates BRI1 signaling in *Arabidopsis thaliana*. P. Natl. Acad. Sci. USA, 98: 5916-5921.

Liang, C., Brookhart, G., Feng, G.H., Reeck, G.R., Kramer, K.J. (1991) Inhibition of digestive proteases of stored grain coleopteran by oryzacystatin, a ceysteine proteainse inhibitor from rice seed. FEBS Lett., 278: 139-142.

Lichtenhaler, H.K. and Wellburn, A.R. (1983) Determination of total carotenoids and chlorophylls a and b of leaf extracts in different solvents. Biochem. Soc. T., 11: 591–592.

Lin, J., Jach, M. E., Ceulemans, R. (2001) Stomatal density and needle anatomy of Scots pine (Pinus sylvestris) are affected by elevated CO_2. New Phytol., 150: 665–674.

Lin, J.S. and Wu, S.H. (2004) Molecular events in senescing Arabidopsis leaves. Plant J, 39: 612–628.

Ling, J., Kojima, T., Shiraiwa, M., Takahara, H. (2003) Cloning of two cysteine proteases genes, CysP1 and CysP2, from soybean cotyledons by cDNA representational difference analysis. Biochim Biophys Acta, 1627: 129–139.

Linthorst, H.J.M., Vanderdoes, C., Brederode, F.T. and Bol, J.F. (1993) Circadian expression and induction by wounding of tobacco genes for cysteine protease. Plant Mol. Biol., 21: 685-694.

Lipke, H., Fraenkel, G.S., Liener, I.E. (1954) Effects of soybean inhibitors on growth of *Tribolium confusum*. J. Agr. Food Chem., 2: 410-415.

Liu, Q., Kasuga, M., Sakuma, Y., Abe, H., Miura, S., Yamaguchi-Shinozaki, K., and Shinozaki, K. (1998) Two transcription factors, DREB1 and DREB2, with an EREBP/AP2 DNA binding domain separate two cellular signal transduction pathways in drought- and low-temperature-responsive gene expression, respectively, in Arabidopsis. Plant Cell, 10: 1391-1406.

Liu, J. and Zhu, J-K (1998) A calcium sensor homolog required for plant salt tolerance. Science, 280: 1943-1945.

Lohman, K.N., Gan, S., John, M.C., Amasino, R.M. (1994) Molecular analysis of natural leaf senescence in *Arabidopsis thaliana*. Physiol. Plantarum, 92: 322-328.

Long, S.P., Ainsworth, E.A., Alistair, R., Ort, D.R. (2004) Rising atmospheric carbon dioxide: plants FACE the future. Ann Rev Plant Biol., 55: 591-628.

Long, S.P. and Drake, B.G. (1992) Photosynthetic CO_2 assimilation and rising atmospheric CO_2 concentrations. In: Baker NR and Thomas H (eds) Crop Photosynthesis: Spatial and Temporal Determinants, pp 69–95. Elsevier Science Publishers, Amsterdam.

Long, S.P., Zhu, X.-G., Naidu, S.L., Ort, D.R. (2006) Can improvement in photosynthesis increase crop yields? Plant Cell Environ., 29: 315-330.

Lorimer, G.H. (1981) The carboxylation and oxygenation of ribulose-1,5-bisphosphate: The primary events in photosynthesis and photorespiration. Ann. Rev. Plant Physio., 32: 349-382.

Ludewig, F. and Sonnewald, U. (2000) High CO_2-mediated down-regulation of photosynthetic gene transcripts is caused by accelerated leaf senescence rather than sugar accumulation. FEBS Lett., 479: 19-24.

MacIntosh, S.C., Kishore, G.M., Perlak, F.J., Marrone, P.G., Stone, T.B., Sims, S.R., Fuchs, R.L. (1990) Potentation of *Bacillus thuringiensis* insecticidal activity by serine protease inhibitors. J. Agr. Food Chem., 38: 50-58.

Mae, T., Kai, N., Makino, A. and Ohira, K. (1984) Relationship between ribulose bisphosphate carboxylase content and chloroplast number in naturally senescing primary leaves of wheat. Plant Cell Physiol., 25: 333-336.

Maestre, F.T., Valladres, F., Reynolds, J.F. (2005) Is the change of plant–plant interactions with abiotic stress predictable? A meta-analysis of field results in arid environments. J. Ecol., 93: 748-757.

Majeau, N. and Coleman, J.R. (1996) Effect of CO_2 concentration on carbonic anhydrase and ribulose-1,5-carboxylase/oxygenase expression in pea. Plant Physiol., 112: 569-574.

Makino, A., Sakuma, H., Sudo, E., Mae, T. (2003) Differences between maize and rice in N-use efficiency for photosynthesis and protein allocation. Plant Cell Physiol., 44:952–956.

Manzara, T. and Gruissem, W. (1988) Organization and expression of the genes encoding ribulose-1,5-bisphosphate carboxylase in higher plants. Photosynth. Res., 16: 117-139.

Margis R., Reis E.M., Villeret V. 1998. Structural and phylogenetic relationships among plant and animal cystatins. Arch. Biochem. Biophysics, 359: 24–30.

Marín-Navarro, J. and Moreno, J. (2006) Cysteines 449 and 459 modulate the reduction–oxidation conformational changes of ribulose 1·5-bisphosphate carboxylase/oxygenase and the translocation of the enzyme to membranes during stress Plant Cell Environ., 29: 898–908.

Maroco, J.P., Edwards, G.E., Ku, M.S.B. (1999) Photosynthetic acclimation of maize to growth under elevated levels of carbon dioxide. Planta, 210: 115-125.

Martin, C. and Glover, B.J. (2007) Functional aspects of cell patterning in aerial epidermis. Curr. Opin. Plant Biol., 10: 70–82.

Martínez, M., Rubio-Somoza, I., Carbonero, P., and Díaz, I. (2002) A cathepsin B-like cysteine protease gene from *Hordeum vulgare* (gene *CatB*) induced by GA in aleurone cells is under circadian control in leaves. J. Exp. Bot., 54: 951-959.

Masle, J. (2000) The effects of elevated CO_2 concentrations on cell division rates, growth patterns, and blade anatomy in young wheat plants are modulated by factors related to leaf position, vernalization, and genotype. Plant Physiol., 122: 1399–1415.

Masoud, S.A., Johnson, L.B., White, F.F. and Reeck, G.R. (1993) Expression of a cysteine protease inhibitor (oryzacystatin-I) in transgenic tobacco plants. Plant Mol. Biol, 21: 655–663.

Matros, A., Amme, S., Kettig, B., Buck-Sorlin, G-H., Sonnewald, U., Mock, H-P. (2006) Growth at elevated CO_2 concentrations leads to modified profiles of secondary metabolites in tobacco cv. SamsunNN and to increased resistance against infection with *potato virus Y*. Plant Cell Environ., 29: 126-137.

Matsumoto, I., Watanabe, H., Abe, K., Arai, S., Emori, Y. (1995) A putative digestive cysteine protease from *Drosophila melanogaster* is predominantly expressed in the embryonic and larval midgut. Eur. J. Biochem., 227: 582-587.

Matsumoto, I., Emori, Y., Abe, K., Arai, S. (1997) Characterization of a gene family encoding cysteine proteases of *Sitophilus zeamais* (maize weevil) and analysis of the protein distribution in various tissues including alimentary tracts and germ cells. J. Biochem., 121: 464-476.

Matsumoto, I., Abe, K., Arai, S., Emori, Y. (1998) Functional expression and enzymatic properties of two *Sitophilus zeamais* cysteine proteases showing different antolytic processing profiles in vitro. J. Biochem., 123: 693-700.

Mayers, P.R., Kearns, P., McIntyre, K. E., Eastwood, J. A. (2002) Case study: canola tolerant of Roundup herbicide. An assessment of its substantial equivalence compared to non-modified canola. Genetically modified crops: assessing safety. Atherton, K. T. (ed). Taylor & Francis

McCouch, S. (2005) Diversifying selection in plant breeding. PLoS Biology, 2: e347.

McGrath, M.E. (1999) The lysosomal cysteine proteases. Annu. Rev. Biophys. Biomol. Struct., 28: 181– 204.

McKee, I.F. and Woodward, F.I. (1994) CO_2 enrichment responses of wheat: interactions with temperature, nitrate and phosphate. New Phytol., 127: 447–453.

McKersie, B.D., Bowley, S.R., Jones, K.S. (1999) Winter survival of transgenic alfalfa overexpressing superoxide dismutase. Plant Physiol., 119: 839–848.

McKersie, B.D., Murnaghan, J., Jones, K.S., Bowley, S.R. (2000) Iron-superoxide dismutase expression in transgenic alfalfa increases winter survival without a detectable increase in photosynthetic oxidative stress tolerance. Plant Physiol., 122: 1427-1438.

Mello, M.O., Tanaka, A.S., Silva-Filho, M.C. (2003) Molecular evolution of Bowman–Birk type proteinase inhibitors in flowering plants. Mol. Phylogenet. Evol., 27: 103-112.

Michaud, D., Faye, L., Yelle, S. (1993a) Electrophoretic analysis of plant cysteine and serine proteases using gelatin-containing polyacrilamide gels and class-specific protease inhibitors. Electrophoresis, 14: 94-98.

Michaud, D., Nguyen-Quoc, B., Yelle, S. (1993b) Selective inhibition of Colorado potato beetle cathepsin H by oryzacystatins I and II. FEBS Lett., 331: 173-176.

Michaud, D., Cantin, L., Vrain, T.C. (1995) Carboxy-terminal truncation of oryzacystatin II by oryzacystatin-insensitive insect digestive proteases. Arch. Biochem. Biophys., 322: 469-472.

Mickel, C.E. and Standish, J. (1974) Susceptibility of processed soy flour and soy grits in storage to attack by *Tribolium castaneum.* University of Minnesota Agricultural Experimental Station Technical Bulletin: 178: 1-20.

Millenium Ecosystem Assessment 2005. Ecosystems and human well-being: Synthesis. Island Press, Washington, D.C., U.S.A. http://www.maweb.org/proxy/Document.356.aspx

Miller, J.E., Heagle, A.S., Pursley, W.A. (1998) Influence of ozone stress on soybean response to carbon dioxide enrichment: II. Biomass and development. Crop Sci., 38: 122-128.

Minamikawa, T., Toyooka, K., Okamoto, T., Hara-Nishimura, I. and Nishimura, M. (2001) Degradation of ribulose-bisphosphate carboxylase by vacuolar enzymes of senescing French bean leaves: immunocytochemical and ultrastructural observations. Protoplasma, 218: 144–153.

Mitsuhashi, W., Crafts-Brandner, S.J., Feller, U. (1992) Ribulose-1,5-bisphosphate carboxylase/oxygenase degradation in isolated pea chloroplasts incubated in the light or in the dark. J. Plant Physiol., 139: 653-658.

Mitsuhasi, W. and Oaks, A. (1994) Development of endopeptidase activities in maize (Zea mays L.) endosperms. Plant Physiol., 104: 401-407.

Miyazawa, S.I., Livingston, N.J., Turpin, D.H. (2006) Stomatal development in new leaves is related to the stomatal conductance of mature leaves in poplar (*Populus trichocarpa* × *P. deltoides*). J. Exp. Bot., 57: 373–380.

Mochizuki, A., Nishizawa, Y., Onodera, H., Tabei, Y., Toki, S., Habu, Y., Ugaki, M., and Ohashi, Y. (1999) Transgenic rice plants expressing trypsin inhibitor are resistant against rice stem borers, *Chilo suppressalis.* Entomol. Exp. Appl., 93: 173-178.

Moons, A., Bauw, G., Prinsen, E., Montagu, M.V., and Straeten, D.V.D. (1995) Molecular and physiological responses to abscisic acid and salts in the roots and salt-sensitive and salt-tolerant indica rice varieties. Plant Physiol., 107: 177-186.

Moore, B.D., Cheng, S-H., Rice, J., Seemann, J.R. (1998) Sucrose cycling, rubisco expression and prediction of photosynthesic acclimation to elevated atmospheric CO_2. Plant Cell Environ., 21: 905-915.

Moore, B.D., Cheng, S-H., Sims, D., Seemann, J.R. (1999) The biochemical and molecular basis for photosynthetic acclimation to elevated atmospheric CO_2. Plant Cell Environ., 22: 567-582.

Moore, B., Zhou, L., Rolland, F., Hall, Q., Cheng, W.H., Liu, Y.-X., Hwang, I., Jones, T., Sheen, J. (2003) Role of the Arabidopsis glucose sensor HXK1 in nutrient, light, and hormonal signaling. Science, 300: 332–36.

Morgan, J.M. (1984) Osmoregulation and water stress in higher plants. Annu. Rev. Plant Physiol., 299-319.

Mott, K.A., Cardon, Z.G., Berry, J.A. (1993) Assymetric patchy stomatal closure for two surfaces of *Xanthium strumarium* L. leaves at low humidity. Plant Cell Environ., 16: 25–34.

Mott, K.A., Gibson, A.C., O'Leary, J.W. (1982) The adaptive significance of amphistomatic leaves. Plant Cell Environ., 5: 455–460.

Mott, K.A. and Michaelson, O. (1991) Amphistomaty as an adaptation to high light intensity in *Ambrosia cordifolia* (compositae). Am. J. Bot., 78: 76–79.

Mott, K.A. and O'Leary, J.W. (1984) Stomatal behaviour and CO_2 exchange characteristics in amphistomatous leaves. PlantPhysiol., 74: 47–51.

Moura, D.S., Bergey, D.R., Ryan, C.A. (2001) Characterization and localization of a wound-inducible type I serine-carboxypeptidase from leaves of tomato plants (*Lycopersicon esculentum* Mill.) Planta, 212: 222-230.

Mulholland, B.J., Craigon, J., Black, C.R., Colls, J.J., Atherton, J., Landon, G. (1997) Impact of elevated atmospheric CO_2 and O_3 on gas exchange and chlorophyll content in spring wheat (*Triticum aestivum* L.). J. Exp. Bot., 48: 1853-1863.

Murata, N., Ishizaki-Nishizawa, O., Higashi, S., Hayashi, H., Tasaka, Y., Nishida, I. (1992) Genetically engineered alteration in the chilling sensitivity of plants. Nature, 356: 710-713.

Nagata, K., Kudo, N., Abe, K., Arai, S., Tanokura, M. (2000) Three-dimensional solution structure of oryzacystatin-I, a cysteine protease inhibitor of the rice, *Oryza sativa* L. *japonica*. Biochemistry-US, 39: 14753-14760.

Nakagawa, T. and Yuan, J. (2000) Cross-talk between two cysteine protease families: activation of caspase-12 by calpain in apoptosis. J. Cell Biol., 150: 887-894.

Nelson, J.M., Lane, B., Freeling, M. (2002) Expression of a mutant maize gene in ventral leaf epidermis is sufficient to signal a switch of the leaf's dorsoventral axis. Development, 129: 4581–4589.

Nguyen, H.T., Babu, R.C., and Blum, A. (1997) Breeding for drought resistance in rice: physiology and molecular genetics considerations. Crop Sci., 37: 1426-1434.

Nicklin, M.J.H. and Barrett, A.J. (1984). Inhibition of cysteine proteases and dipeptidyl peptidase I by egg-white cystatin. Biochem. J., 223: 245-253.

Nie, G., Hendrix, D.L., Webber, A.N., Kimball, B.A., Long, S.P. (1995) Increased accumulation of carbohydrates and decreased photosynthetic gene transcript levels in wheat grown at an elevated CO_2 concentration in the field. Plant Physiol., 108: 975-983.

Novitskaya, L., Trevanion, S., Driscoll, S.P., Foyer, C.H., Noctor, G. (2002) How does photorespiration modulate leaf amino acid contents? A dual approach through modelling and metabolite analysis. Plant Cell Environ., 25: 821–836.

Nowak, R. S., Ellsworth, D. S., Smith, S. D (2004) Functional responses of plants to elevated atmospheric CO_2 - do photosynthetic and productivity data from FACE experiments support early predictions? New Phytol., 162: 253-280.

Okamoto, T., Shimada, T., Hara-Nishimura, I., Nishimura, M., Minamikawa, T. (2003) C-terminal KDEL sequence of a KDEL-tailed cysteine protease (sulfhydryl-endopeptidase) is involved in formation of KDEL vesicle and in efficient vacuolar transport of sulfhydryl-endopeptidase. Plant Physiol., 132: 1892–1900.

Ono, K., Hashimoto, H. and Katoh, S. (1995) Changes in the number and size of chloroplasts during senescence of primary leaves of wheat grown under different conditions. Plant Cell Physiol., 36: 9-17.

Padgette, S.R., N.B. Taylor, D.L. Nida, M.R. Bailey, J. MacDonald, L.R. Holden, and Fuchs, R.L. (1996) The composition of glyphosate-tolerant soybean seeds is equivalent to that of conventionalsoybeans. J. Nutr., 126:702-716.

Pannetier, C., Giband, M., Couzi, P., Letan, V., Mazier, M., Tourneur, J., Hau, B. (1997) Introduction of new traits into cotton through genetic engineering: insect resistance as an example. Euphytica 96: 163-166.

Pareek, A., Singla, S.L., and Khush, A.K. (1997) Short term salinity and high temperature stress-associated ultrastructural alterations in young leaf cells of *Oryza sativa* L. Ann. Bot., 80: 629-639.

Parry, M.A.J., Andralojc, P.J., Parmar, S., Keys, A.J., Habash, D., Paul, M.J., Alred, R., Quick, W.P., and Servaites, J.C. (1997) Regulation of Rubisco by inhibitors in the light. Plant Cell Environ., 20: 528–534.

Paul, M.J. and Pellny, T.K. (2003) Carbon metabolite feedback regulation of leaf photosynthesis and development. J. Exp. Bot., 54: 539-547.

Paul, M. and Stitt, M. (1993). Effects of nitrogen and phosphate deficiencies on levels of carbohydrates, respiratory enzymes, and metabolites in seedlings of tobacco, and their response to exogenous sucrose. Plant Cell Environ., 16: 1047-1057.

Pechan, T., Ye, L., Chang, Y.-M, Mitra, A., Lin, L., Davis, F.M. Williams, W.P., Luthe, D.S. (2000) A unique 33-kD cysteine protease accumulates in response to larval feeding in maize genotypes resistant to fall armyworm and other Lepidoptera. Plant Cell, 12: 1031–1041.

Peet, M.M., Huber, S.C., Patterson, D.T. (1986) Acclimation to high carbon dioxide in monoecious cucumbers (*Cucumis sativus*): II. Carbon exchange rates, enzyme activities, and starch and nutrient concentrations. Plant Physiol., 80: 63 67.

Pellegrineschi, A., Reynolds, M., Pacheco, M., Brito, R.M., Almeraya, R., Yamaguchi-Shinozaki, K., Hoisington, D. (2004) Stress-induced expression in wheat of the *Arabidopsis thaliana* DREB1A gene delays water stress symptoms under greenhouse conditions. Genome, 47: 493-500.

Penuelas, J. and Matamala, R. (1990) Changes in N and S leaf content, stomatal density and specific leaf area of 14 plant species during the last three centuries of CO_2 increase. J. Exp. Bot., 41: 1119-1124.

Perlak, F.J., Deaton, R.W., Armstrong, T.A., Fuchs, R.L., Sims, S.R., Greenplate, J.T., Fischhoff, D.A. (1990) Insect resistant cotton plants. Bio/Technol., 8: 939–943.

Perlak, F.J., Stone, T.B., Muskopf, Y.M., Petersen, L.J., Parker, G.B., McPherson, S.A., Wyman, J., Love, S., Reed, G., Biever (1993) Genetically improved potatoes: protection from damage by Colorado potato beetles. Plant Mol. Biol., 22: 313–321.

Pernas, M., Sánchez-Monge, R., Salcedo, G. (2000) Biotic and abiotic stress can induce cystatin expression in chestnut. FEBS Lett., 467: 206-210.

Peterson, L.W., Kleinkopf, G.E., Huffaker, R.C. (1973) Evidence for lack of turnover of ribulose-1,5-diphosphate carboxylase in barley leaves. Plant Physiol., 51: 1042–1045.

Pickart, C.M. (2001) Mechanisms underlying ubiquitination. Annu. Rev. Biochem., 70: 503-533.

Pingali, P.L. (ed.). 2001. CIMMYT 1999–2000 World maize facts and trends. meeting world maize needs: technological opportunities and priorities for the public sector. Mexico, D.F.: CIMMYT

Pino, M.-T., Skiner, J.S., Park, E.-J., Jeknić, Z., Hayes, P.M., Tomashow, M.F. Chen, T.H.H. (2007) Use of a stress inducible promoter to drive ectopic *AtCBF* expression improves potato freezing tolerance while minimizing negative effects on tuber yield. Plant Biotech. J., 5: 591-604.

Pons, L. (2003) Pumping iron into western Africa's corn. Agricultural Research (USDA). http://www.ars.usda.gov/is/AR/archive/apr03/iron0403.pdf

Pontius, J.U., Wagner, L., Schuler, G.D. (2003) UniGene: a unified view of the transcriptome. In: The NCBI Handbook. Bethesda (MD): National Center for Biotechnology Information. 11pp.

Poorter, H. and Navas, M.-L. (2003) Plant growth and competition at elevated CO_2: on winners, losers and functional groups. New Phytol., 157: 175–198.

Porter, M.A. and Grodzinski, B. (1984) Acclimation to high CO_2 in bean. Carbonic anhydrase and ribulose *bis*phosphate carboxylase. Plant Physiol., 74: 413-416.

Portis, A.R. Jr. (2003) Rubisco activase – Rubisco's catalytic chaperone. Photosynth. Res., 75: 11-27.

Puntervoll, P., Linding, R., Gemund, C., Chabanis-Davidson, S., Mattingsdal, M., Cameron, S., Martin, D. M., Ausiello, G., Brannetti, B., Costantini, A. Ferrè, F., Maselli, V., Via, A., Cesareni, G., Diella, F., Superti-Furga, G., Wyrwicz, L., Ramu, C., McGuigan, C., Gudavalli, R., Letunic, I., Bork, P., Rychlewski, L., Küster, B., Helmer-Citterich, M., Hunter, W.N., Aasland, R., Gibson, T.J. (2003). ELM server: A new resource for investigating short functional sites in modular eukaryotic proteins. Nucleic Acids Res., 31: 3625-3630.

Quirino, B.F., Normanly, J. and Amasino, R.M. (1999) Diverse range of gene activity during *Arabidopsis thaliana* leaf senescence includes pathogen-independent induction of defense-related genes. Plant Mol. Biol., 40: 267-278.

Raines, C.A., Horsnell, P.R., Holder, C., Lloyd, J.C. (1992) Arabidopsis thaliana carbonic anhydrase: cDNA sequence and effect of CO_2 on mRNA levels. Plant Mol. Biol., 20:1143–1148.

Ramagli, L.S. (1999) Quantifying protein in 2-D PAGE solubilization buffers. In: Methods in Molecular Biology, 112: 99-103, Link, A.J. (ed), Humana Press Inc, Totowa, NJ.

Reichard, U., Cole, G.T., Hill, T.W., Ruchel, R., Monod, M. Molecular characterization and influence on fungal development of ALP2, a novel serine proteinase from *Aspergillus fumigatus* (2000) Int. J. Med. Microbiol**.,** 290: 549-558.

Repellin, A., Baga, M., Jauhar, P.P., Chibbar, R.N. (2001) Genetic enrichment of cereal crops via alien gene transfer: New challenges. Plant Cell Tiss. Org., 64: 159-183.

Rintamäki, E., Keys, A.J. and Parry, M.A.J. (1988) Comparison of the specific activity of ribulose-1,5-bisphosphate carboxylase-oxygenase from some C3 and C4 plants. Physiol. Plant., 74: 326–331.

Rivard, D., Anguenot, R., Brunelle, F., Le, V.Q., Vézina, L-P., Trépanier, S., Michaud, D. (2006). An in-built protease inhibitor system for the protection of recombinant proteins recovered from transgenic plants. Plant Biotech. J, 4, 359-368.

Robertson, E.J. and Leech, R.M. (1995) Significant changes in cell and chloroplast development in young wheat leaves (*Triticum aestivum* cv. Hereward) grown in elevated CO_2. Plant Physiol., 107: 63–71.

Robertson, E.J., Williams, M., Harwood, J.L., Lindsay, J.G., Leaver, C.J., Leech, R.M. (1995) Mitochondria increase three-fold and mitochondrial proteins and lipid change dramatically in post-meristematic cells in young wheat leaves grown at elevated CO_2. Plant Physiol., 108: 469–474.

Rodermel, S. (1999) Subunit control of Rubisco biosynthesis – a relic of an endosymbiotic past? Photosynth. Res., 59: 105-123.

Rogers, A., Ellsworth, D.S., Humphries, S.W. (2001) Possible explanation of the disparity between the *in vitro* and *in vivo* measurements of Rubisco activity: a study in loblolly pine grown in elevated pCO_2. J. Exp. Bot., 52: 1555-1561.

Rogers, H.H., Runion, G.B., Krupa, S.V. (1994) Plant responses to atmospheric CO_2 enrichment with emphasis on roots and the rhizosphere. Environ. Pollution, 83: 155-189.

Roitsch, T., Balibrea, M.E., Hofmann, M., Proels, R., Sinha, A. K. (2003) Extracellular invertase: key metabolic enzyme and PR protein. J. Exp. Bot., 54: 513-524.

Rojo, E., Martín, R., Carter, C., Zouhar, J., Pan, S., Plotnikova, J., Jin, H., Paneque, M., Sánchez-Serrano, J.J., Baker, B., Ausubel, F.M., Raikhel, N.V. (2004) VPE exhibits a caspase-like activity that contributes to defense against pathogens. Curr. Biol., 14: 1897-1906.

Romeis, J., Meissle, M., Bigler, F. (2006) Transgenic crops expressing *Bacillus thuringiensis* toxins and biological control. Nat. Biotechnol., 24: 63-71.

Romero, C., Belles, J.M., Vayá, J.L., Serrano, R., Culiañez-Maciá, F.A. (1997) Expression of the yeast trealose-6-phosphate synthase gene in transgenic tobacco plants: pleiotropic phenotypes include drought tolerance. Planta 201: 293-297.

Roulin, S. and Feller, U. (1998) Light-independent degradation of stromal proteins in intact chloroplasts isolated from *Pisum sativum* L. leaves: requirement for divalent cations. Planta, 205: 297-304.

Rouquié, D., Peltier, J.B., Marquis-Mansion, M., Tournaire, C., Doumas, P., Rossignol, M. (1997) Construction of a directory of tobacco plasma membrane proteins by combined two-dimensional gel electrophoresis and protein sequencing. Electrophoresis, 18: 654–660.

Rowland-Bamford, A.J., Baker, J.T., Allen, L.H.J., Bowes, G. (1991) Acclimation of rice to changing atmospheric carbon dioxide concentration. Plant Cell Environ., 14: 577–583.

Ryan, C.A. (1989) Insect-induced chemical signals regulating natural plant protection responses. In: Denno, R.F. and McClure, M.S., eds. *Variable plats and herbivores in natural and managed systems.* New York, Academic Press, pp.43-60.

Ryan, C.A. (1990) Protease inhibitors in plants: genes for improving defenses against insects and pathogens. Annu. Rev. Phytopathol., 28: 425-449.

Sage, R.F., Pearcy, R.W., Seemann, J.R. (1987) The nitrogen use efficiency of C_3 and C_4 plants. III. Leaf nitrogen effects on the activity of carboxylating enzymes in *Chenopodium album* (L.) and *Amaranthus retroflexus* (L.). Plant Physiol., 85: 355–359.

Sage, R.F., Sharkey, T.D., Seeman, J.R. (1988) The *in vivo* response of the ribulose-1,5-bissphosphate carboxylase activation state and the pool sizes of photosynthetic metabolites to elevated CO_2 in *Phaseolus vulgaris* L. Planta, 174**:** 407-16.

Sage, R.F., Sharkey, T.D., Seeman, J.R. (1989) Acclimation of photosynthesis to elevated CO_2 in five C_3 species. Plant Physiol., 89, 590-596.

Sage, R.F. (1994) Acclimation of photosynthesis to increasing atmospheric CO2: The gas exchange perspective. Photosynth. Res., 39: 351-368.

Sage, R. F. (2004) The evolution of C_4 photosynthesis. New Phytol., Vol. 161: 341-370.

Sakamoto, W. (2006) Protein degradation machineries in plastids. Annu Rev. Plant Biol., 57: 599-621.

Salisbury, E.J. (1927) On the causes and ecological significance on stomatal frequency with special reference to woodland flora. Philos. T. R. Soc. B, 216: 1–65.

Salvucci, M.E. and Ogren, W.L. (1996) The mechanism of Rubisco activase: Insights from studies of the properties and structure of the enzyme. Photosynth. Res., 47: 1-11.

Sambrook, J., Fritsch, E.F., Maniatis, T. (1989) Molecular Cloning, 2nd edn. Cold Spring Harbor Laboratory Press, New York.

Sanmartín, M., Jaroszewski, L., Raikhel, N.V., Rojo, E. (2005) Caspases. Regulating death since the origin of life. Plant Physiol., 137: 841-847.

Schaffer, M.A. and Fischer, R.L. (1988) Analysis of mRNAs that accumulates in response to low temperature identifies a thiol protease gene in tomato. Plant Physiol., 87: 431-436.

Schaller, A. (2004) A cut above the rest: the regulatory function of plant proteases. Planta, 220: 183-197.

Schmid, M., Simpson, D, and Gietl, C. (1999) Programmed cell death in castor bean endosperm is associated with the accumulation and release of a cysteine endopeptidase from ricinosomes. P. Natl. Acad. Sci. USA, 96: 14159–14164.

Schmidt, G.W. and Mishkind, M.L. (1983) Rapid degradation of unassembled ribulose 1,5-biphosphate carboxylase small subunits in chloroplasts. P. Natl. Acad. Sci. USA, 80: 2632–2636.

Schwanz, P. and Polle, A. (2001) Differential stress responses of antioxidative systems to drought in pendunculate oak (*Quercus robur*) and maritime pine (*Pinus pinaster*) grown under high CO_2 concentrations. J. Exp. Bot., 52: 133-143.

Sharma, H.C., Sharma, K.K., Crouch, J.H. (2004) Genetic transformation of crops for insect resistance: potential and limitations. Crit. Rev. Plant Sci., 23: 47-72.

Shen, B., Jensen, R.G., and Bohnert, H.J. (1997) Increased resistance to oxidative stress in transgenic plants by targeting mannitol biosynthesis to chloroplasts. Plant Physiol., 113: 1177-1183.

Shi, Y. (2002) Mechanisms of caspase activation and inhibition during apoptosis. Mol. Cell, 9: 459-470.

Shimada, T., Hiraiwa, N., Nishimura, M. and Hara-Nishimura, I. (1994) Vacuolar processing enzyme of soybean that converts proproteins to the corresponding mature forms. Plant Cell Physiol., 35: 713-718.

Shinozaki, K. and Yamaguchi-Shinozaki, K. (2000) Molecular responses to dehydration and low temperature: differences and cross-talk between two stress signaling pathways. Curr. Opin. Plant Biol, 3: 217-223.

Sicher, R.C., Kremer, D.F., Rodermel, S.R. (1994) Photosynthetic acclimation to elevated CO_2 occurs in transformed tobacco with decreased ribulose-1,5-bisphosphate carboxylase/oxygenase content. Plant Physiol., 104: 409–415.

Sims, D.A. and Gamon, J.A. (2002) Relationships between leaf pigment content and spectral reflectance across a wide range of species, leaf structures and developmental stages. Remote Sens. Environ., 81: 337-354.

Smart, D.R., Chatterton, N.J., Bugbee, B. (1994) The influence of elevated CO_2 on non-structural carbohydrate distribution and fructan accumulation in wheat canopies. Plant Cell Environ., 17: 435–442.

Soares, A.S., Driscoll, S.P., Olmos, E., Harbinson, J., Arrabaça, M.C., Foyer, C.H. (2008) Adaxial/abaxial specification in the regulation of photosynthesis and stomatal opening with respect to light orientation and growth with CO_2 enrichment in the C_4 species Paspalum dilatatum. New Phytol., 177: 186-198.

Solomon, M., Belenghi, B., Delledonne, M., Menachem, E., Levine, A. (1999) The involvement of cysteine proteases and protease inhibitor genes in the regulation of programmed cell death in plants. Plant Cell, 11: 431-443.

Spreitzer, R.J. and Salvucci, M.E. (2002) Rubisco: structure, regulatory interactions, and possibilities for a better enzyme. Annu. Rev. Plant Biol., 53: 449-475.

Stitt, M. (1991) Rising CO_2 levels and their potential significance for carbon flow in photosynthetic cells. Plant Cell Environ., 14: 741-762.

Strauss, S.H., Knowe, S.A., and Jenkins, J.J. (1997) Benefits and risk of transgenic, Roundup Ready® cottonwoods. J. For., 95: 12–19.

Sugiyama, T., Mizuno, M., Hayashi, M (1984) Partitioning of nitrogen among ribulose-1,5-bisphosphate carboxylase/oxygenase, phosphoenolpyruvate carboxylase, and pyruvate orthophosphate dikinase as related to biomass productivity in maize seedlings. Plant Physiol., 75:665–669.

Sullivan, J.A., Shirasu, K., Deng, X.W. (2003) The diverse roles of ubiquitin and the 26S proteasome in the life of plants. Nat. Rev. Genet., 4: 948-958.

Sun, J., Gibson, K.M., Kiirats, O., Okita, T.W., Edwards, G.E. (2002) Interactions of nitrate and CO_2 enrichment on growth, carbohydrates, and Rubisco in Arabidopsis starch mutants. Significance of starch and hexose. Plant Physiol., 130: 1573–1583.

Swidzinski, J.A., Sweetlove, L.J. and Leaver, C.J. (2002) A custom microarray analysis of gene expression during programmed cell death in *Arabidopsis thaliana*. Plant J., 30: 431–446.

Tajima, H. and Koizumi, N. (2006) Induction of BiP by sugar independent of a *cis*-element for the unfolded protein response in *Arabidopsis thaliana*. Biochem. Biophys. Res. Co., 346: 926-930.

Tanaka, H., Onouchi, H., Kondo, M., Hara-Nishimura, I., Nishimura, M., Machida, C., Machida, Y. (2001) A subtilisin-like serine protease is required for epidermal surface formation in *Arabidopsis* embryos and juvenile plants. Development, 128: 4681-4689.

Tarczynski, M.C., Jensen, R.G., and Bohnert, H.J. (1993) Stress protection of transgenic tobacco by production of osmolyte mannitol. Science, 259: 508-510.

Taylor, G., Ranasinghe, S., Bosac, C., Gardner, S.D.L., Ferris, R. (1994) Elevated CO_2 and plant growth: cellular mechanisms and responses of whole plants. J. Exp. Bot., 45: 1761–1774.

Taylor,, G., Tallis, M.J., Giardina, C.P.Percy, K.E., Miglietta, F., Gupta, P.S., Gioli, B., Calfapietra, C., Gielen, B., Kubiske, M.E., Scarascia-Mugnozza, G.E., Kets, K., Long, S.P., Karnosky, D.F. (2008) Future atmospheric CO_2 leads to delayed autumnal senescence. Global Change Biol., 14: 264–275.

Tissue, D.T., Thomas, R.B., Strain, B.R. **(**1993) Long-term effects of elevated CO_2 and nutrients on photosynthesis and rubisco in loblolly pine seedlings. Plant Cell Environ., 16: 859-865.

Toyooka, K., Okamoto, T., Minamikawa, T. (2000) Mass transport of proform of a KDEL-tailed cysteine protease (SH-EP) to protein storage vacuoles by endoplasmic reticulum–derived vesicle is involved in protein mobilization in germinating seeds. J. Cell Biol., 148: 453-464.

Trobacher, C.P., Senatore, A., Greenwood, J.S. (2006) Masterminds or minions? Cysteine proteinases in plant programmed cell death. Can. J. Bot., 84: 651-667.

Tuba, Z., Szente, K., Kock, J. (1994) Response of photosynthesis, stomatal conductance,water use efficiency and production to long-term elevated CO_2 in winter wheat. J. Plant Physiol., 144: 661–668.

Turk, V., Turk, B., Turk, D. (2001) Lysosomal cysteine proteases: facts and opportunities. EMBO J. 20: 4629–4633.

Ueda, T., Seo, S., Ohashi, Y. and Hashimoto, J. (2000) Circadian and senescence-enhanced expression of a tobacco cysteine protease gene. Plant Mol. Biol., 44: 649–657.

Uren, A.G., O'Rourke, K., Aravind, L., Pisabarro, M.T., Seshagiri, S., Koonin, E.V., Dixit, V.M. (2000) Identification of paracaspases and metacaspases two ancient families of caspase-like proteins, one of which plays a key role in MALT lymphoma. Mol. Cell, 6: 961-967.

Urwin, P.E., Atkinson, H.J., Waller, D.A., McPherson, M.J. (1995) Engineered oryzacystatin-I expressed in transgenic hairy roots confers resistance to *Globodera pallida*. Plant J., 8: 121-131.

Urwin, P.E., Lilley, C.J., McPherson, M.J., Atkinson, H.J. (1997) Resistance to both cyst and rootnot nematodes conferred by transgenic *Arabidopsis* expressing a modified plant cystatin. Plant J. 12: 455-461.

Ussuf, K.K., Laxmi, N.H., Mitra, R. (2001) Protease inhibitors: Plant-derived genes of insecticidal protein for developing insect-resistant transgenic plants. Curr. Sci., 80: 847-853.

Vain, P., Worland, B., Clarke, M.C., Richard, G., Beavis, M., Liu, H., Kohli, A., Leech, M., Snape, J., Christou, P. (1998) Expression of an engineered cysteine protease inhibitor (Oryzacystatin-I delta D86) for nematode resistance in transgenic rice plants. Theor. Appl. Genet., 96: 266-271.

Van Breusegem, F., Slooten, L., Stassart, J.-M., Moens, T., Botterman, J., Van Montagu, M., Inzé, D. (1999) Overproduction of *Arabidopsis thaliana* FeSOD confers oxidative stress tolerance to transgenic maize. Plant Cell Physiol., 40: 515-523.

Vanderauwera, S., De Block, M., Van de Steene, N., Van de Cotte, B., Metzlaff, M., Van Breusegem, F. (2007) Silencing of poly(ADP-ribose) polymerase in plants alters abiotic stress signal transduction. P. Natl. Acad. Sci. USA, 104: 15150-15155.

Van der Vyver, C., Schneidereit, J., Driscoll, S., Turner, J., Kunert, K., and Foyer, C.H. (2003) Oryzacystatin I expression in transformed tobacco produces a conditional growth phenotype and enhances chilling tolerance. Plant Biotech. J., 1: 101-112.

Van Doorn, W.G. and Woltering, E.J. (2005) Many ways to exit? Cell death categories in plants. Trends Plant Sci., 10: 117-122.

Van Heerden, P.D.R., Krüger, G.G.J., Loveland, J.E., Parry, M.A.J., Foyer, C.H. (2003) Dark chilling imposes metabolic restrictions on photosynthesis in soybean. Plant Cell Environ., 26: 323–337.

Van Oosten, J-J. and Besford, R.T. (1996) Acclimation of photosynthesis to elevated CO_2 through feedback regulation of gene expression: Climate of opinion. Photosynth. Res., 48: 353-365.

Van Oosten, J-J., Wilkins, D., Besford, R.T. (1994) Regulation of the expression of photosynthetic nuclear genes by high CO_2 is mimicked by carbohydrates: a mechanism for the acclimation of photosynthesis to high CO_2. Plant Cell Environ., 17: 913-923.

Vercammen, D., Belenghi, B., Van de Cotte, B., Beunens, T., Gavigan, J.-A., De Rycke, R., Brackenier, A., Inzé, D., Hariies, J.L., Van Breusegem, F. (2006) Serpin 1 of Arabidopsis thaliana is a suicide inhibitor for metacaspase 9. J. Mol. Biol., 364: 625-636.

Vernon, L.P. (1960). Spectrophotometer determination of chlorophylls and pheophytins in plant extracts. Anal. Chem. 32: 1144–1150.

Vernon, D.M., Tarczynski, M.C., Jensen, R.G., Bohnert, H.J. (1993) Cyclitol production in transgenic tobacco. Plant J., 4: 199-205.

Vierstra, R.D. (1996) Proteolysis in plants: mechanisms and functions. Plant Mol. Biol., 32: 275-302.

Vierstra, R.D. (2003) The ubiquitin/26S proteasome pathway, the complex last chapter in the life of many plant proteins. Trends Plant Sci., 8, 135-142.

Vinocur, B. and Altman, A. (2005) Recent advances in engineering plant tolerance to abiotic stress: achievements and limitations. Curr. Opin. Biotech., 16: 123-132.

Virgin, I., Salter, A.H., Ghanotakis, D.F., Andersson, B. (1991) Light-induced D1 protein degradation is catalyzed by a serine type protease**.** FEBS Lett., 281: 125 128.

Vitale, A. and Pedrazzini, E. (2005) Recombinant pharmaceuticals from plants: the plant endomembrane system as bioreactor. Mol. Interv., 5: 216-225.

Voges, D., Zwickl, P., Baumeister, W. (1999) The 26S proteasome: A molecular machine designed for controlled proteolysis. Annu. Rev. Biochem., 68: 1015-1068.

Von Caemmerer, S. and Farquhar, G.D. (1981) Some relationships between the biochemistry of photosynthesis and the gas exchange of leaves. Planta, 153: 376-387.

Von Caemmerer, S., Ghannoum, O., Conroy, J.P., Clark, H., Newton, P.C.D. (2001) Photosynthetic responses of temperate species to free air CO_2 enrichment (FACE) in a grazed New Zealand pasture. Aust. J. Plant Physiol., 28: 439–450.

Vu, C.V., Allen, L.H. Jr., Bowes, G. (1983) Effects of light and elevated atmospheric CO_2 on the ribulose bisphosphate carboxylase activity and ribulose bisphosphate level of soybean leaves. Plant Physiol., 73: 729-734.

Vu, J.C.V., Allen Jr., L.H., Bowes, G. (1989) Leaf ultrastructure, carbohydrates and protein of soybeans grown under CO_2 enrichment. Environ. Exp. Bot,. 29: 141–147.

Wagstaff, C., Leverentz, M.K., Griffiths, G., Thomas, B., Chanasut, U., Stead, A.D., Rogers, H.J. (2002) Cysteine protease gene expression and proteolytic activity during senescence of *Alstroemeria* petals. J. Exp. Bot., 53: 233-240.

Walker-Simmons, M. and Ryan, C.A. (1980) Isolation and properties of carboxypeptidase from leaves of wounded tomato plants. Phytochemistry, 19: 43-47.

Walting, J.R. and Press, M.C. (1997) How is the relationship between the C_4 cereal *Sorghum bicolour* and the C_3 root hemi-parasites *Striga hermonthica* and *Striga asiatica* affected by elevated CO_2? Plant Cell Environ., 20: 1292–1300.

Wand, S.J.E., Midgley, G.F., Jones, M.H., Curtis, P.S. (1999) Responses of wild C_4 and C_3 grass (*Poaceae*) species to elevated CO_2 concentration: a meta-analytic test of current theories and perceptions. Glob. Change Biol., 5: 723–741.

Wand, S.J.E., Midgley, G.F., Stock, W.D. (2001) Growth responses to elevated CO_2 in NADP-ME, NAD-ME and PCK C_4 grasses and a C_3 grass from South Africa. Aust. J. Plant Physiol., 28: 13–25.

Ward J.K., Tissue D.T., Thomas R.B., Strain B.R. (1999) Comparative responses of model C3 and C4 plants to drought in low and elevated CO_2. Glob. Change Biol., 5: 857-867.

Watanabe, N. and Lam, E. (2004) Recent advance in the study of caspase-like proteases and Bax inhibitor-1 in plants: their possible roles as regulator of programmed cell death.

Watling, J.R., Press, M.C., Quick, W.P. (2000) Elevated CO_2 induces biochemical and ultrastructural changes in leaves of the C_4 cereal sorghum. Plant Physiol., 123: 1143–1152.

Webber, A.N., Nie, G.-Y., Long, S.P. (1994) Acclimation of photosynthetic proteins to rising atmospheric CO2. Photosynth. Res., 39: 413-425.

Werneke, J.M, Chatfield, J.M. and Ogren, W.L. (1989) Alternative mRNA splicing generates the two ribulosebisphosphate carboxylase/oxygenase activase polypeptides in spinach and Arabidopsis. Plant Cell, 1: 815-825.

Winder, T.L., Anderson, J.C., Spalding, M.H. (1992) Translational regulation of the large and small subunits of ribulose bisphosphate carboxylase/oxygenase during induction of the CO_2 concentrating mechanism in *Chlamydomonas reinhardtii*. Plant Physiol. 98: 1409–1414.

Wingler, A., Purdy, S., MacLean, J.A., Pourtau, N. (2006) The role of sugars in integrating environmental signals during the regulation of leaf senescence. J. Exp. Bot., 57: 391-399.

Winzeler, M., Dubois, D., Nosberger, J. (1990) Absence of fructan degradation during fructan accumulation in wheat stems. J. Plant Physiol., 136: 324–329.

Woltering. E.J., Van der Bent, A., Hoeberichts, F.A. (2002) Do plant caspases exist? Plant Physiol., 130: 1764-1769.

Woodward, F.I. (1987) Stomatal numbers are sensitive to increases in CO_2 from pre-industrial levels. Nature, 327: 617-18.

Woodward, F.I. (2002) Potential impacts of global elevated CO_2 concentrations on plants. Curr. Opin. Plant Biol., 5: 207–211.

Woodward, F.I. and Kelly, C.K. (1995) The effect of CO_2 concentration on stomatal density. New Phytol., 131, 311-327.

Woodward, F. I J., Lake, A, Quick, W. P. (2002) Stomatal development and CO_2: ecological consequences. New Phytol., 153: 477–484.

Wullschleger, S. D., Norby, R. J. Gunderson, C. A. (1992) Growth and maintenance respiration in leaves of *liriodendron tulipifera* L. exposed to long-term carbon dioxide enrichment in the field. New Phytol., 121: 515-523.

Xiong, Y., Contento, A.L., Nguyen, P.Q., Bassham, D.C. (2007) Degradation of oxidised proteins by autophagy during oxidative stress in Arabidopsis. Plant Physiol., 143: 291–299.

Xu, X-F. and Chye, L-M. (1999) Expression of cysteine protease during developmental events associated with programmed cell death in brinjal. Plant J., 17: 321-328.

Yamada, T., Ohta, H., Shinohara, A., Iwamatsu, A., Shimada, H., Tsuchiya, T., Masuda, T., and Takamiya, K. (2000) A cysteine protease from maize isolated in a complex with cystatin. Plant Cell Physiol. 41: 185-191.

Yamauchi, M., Aguilar, A.M., and Vaughan, D.A. (1993) Seshu, Rice (*Oryza sativa* L.) germplasm suitable for direct sowing under flooded soil surface. Euphytica, 67: 177-184.

Yancey, P.H., Clark, M.E., Hand, S.C., Bowlus, R.D., and Somero, G.N. (1982) Living with water stress: evolution of osmolyte systems. Science, 217: 1214-1222.

Yang, D.-H., Webster, J., Adam, Z., Lindahl, M., Andersson, B. (1998) Induction of acclimative proteolysis of the light-harvesting chlorophyll a/b protein of photosystem ii in response to elevated light intensities. Plant Physiol., 118: 827-834.

Ye, G.-N., Hajdukiewicz, P.T.J., Broyles, D., Rodriguez, D., Xu, C.W., Nehra, N., Staub, J.M. (2001) Plastid-expressed 5-enolpyruvylshikimate-3-phosphate synthase genes provide high level glyphosate tolerance in tobacco. Plant J., 25: 261–270.

Yoshida, T. and Minamikawa, T. (1996) Successive amino-terminal proteolysis of the large subunit of ribulose 1,5-bisphosphate carboxylase/oxygenase by vacuolar enzymes from french bean leaves. Eur. J. Biochem., 238: 317–324.

Zhang, N., Kallis, R.P., Ewy, R.G., Portis, Jr., A.R. (2002) Light modulation of RuBisCO in Arabidopsis requires a capacity for redox regulation of the larger RuBisCO activase isoform. P. Natl. Acad. Sci. USA, 99: 3330-3334.

Zhang, H. and Nobel, P.S. (1996) Photosynthesis and carbohydrate partitioning for the C_3 desert shrub *Encelia farinosa* under current and doubled CO_2 concentrations. Plant Physiol., 110: 1361-1366.

Zhao, Y., Botella, M.A., Subramanian, L., Niu, X., Nielsen, S.S., Bressan, R.A. Hasegawa, P.M. (1996). Two wound-inducible soybean cysteine protease inhibitors have greater insect digestive protease inhibitory activities than a constitutive homologue. Plant Physiol., 111: 1299- 1306.

Zhu, J., Goldstein, G., Bartholomew, D.P. (1999) Gas exchange and carbon isotope composition of Ananas comosus in response to elevated CO2 and temperature. Plant Cell Environ., 22: 999-1007.

Zimmermann, P., Hirsch-Hoffmann, M., Hennig, L., Gruissem, W. (2004) GENEVESTIGATOR. Arabidopsis microarray database and analysis toolbox. Plant Physiol., 136: 2621-2632.

Ziska, L.H. and Bunce, J.A. (1999) Effect of elevated carbon dioxide concentration at night on the growth and gas exchange of selected C4 species. Aust. J. Plant Physiol., 26: 71-77.